

2018

Xenobiotic effects on male mouse reproductive system and hepatic gene expression and epigenetics: studies with bisphenol A and TCPOBOP

<https://hdl.handle.net/2144/31677>

"Downloaded from OpenBU. Boston University's institutional repository."

BOSTON UNIVERSITY
GRADUATE SCHOOL OF ARTS AND SCIENCES

Dissertation

**XENOBIOTIC EFFECTS ON MALE MOUSE REPRODUCTIVE
SYSTEM AND HEPATIC GENE EXPRESSION AND EPIGENETICS:
STUDIES WITH BISPHENOL A AND TCPOBOP**

by

NICHOLAS J. LODATO

B.S., Widener University, 2007

Submitted in partial fulfillment of the
requirements for the degree of
Doctor of Philosophy

2018

© Copyright by NICHOLAS J. LODATO 2018

All rights reserved, except Chapter 3, Copyright 2017 Toxicological Sciences

Approved by

First Reader _____

David Waxman, Ph.D.

Professor of Biology, Medicine, and Biomedical Engineering; Program in
Bioinformatics

Second Reader _____

John Celenza, Ph.D.

Associate Professor of Biology

DEDICATION PAGE

To my wife Sarah and my daughter Lillian, without whom I would have likely finished
this dissertation years earlier.

ACKNOWLEDGEMENTS

I would like to thank my advisor, Dr. David Waxman, for his years of mentoring and guidance throughout my graduate career. I also want to thank the members of my committee, past and present, including Drs. Kim McCall, Chip Celenza, Tom Gilmore, Trevor Siggers, Frank Naya, Gloria Callard, and Cyndi Bradham for their continued support and advice. I will always remember the many members of the Waxman Lab that not only made an impact in shaping my research but whom I can truly call my friends, including Cindy Marmol, Dr. Marie Jordan, Dr. Mona Connerney, Dr. Sasha Suvorov, Dr. Tara Conforto, Dr. Aarathi Sugathan, Dr. Christina Hao, Dr. Dana Lau-Corona, George Steinhardt, Bryan Matthews, Aram Shin, Dr. Eugene Manley, Tom Woo and the many, many others in the lab and throughout the BU community with whom I had the pleasure to interact with regularly. I thank old friends from New Jersey and newer friends from Boston, including Dr. Patrick Migliorini, Cristian Laltoo, Eitan Goldenberg, Chelsea Gavitt, Dr. Tristan Lubinski, and Rebecca Meyer for always being there despite the large distances measured in either miles or football team affiliations. I also want to thank my parents, Michael and Nancy Lodato, for their constant encouragement and my brother and sister, Dr. Michael Lodato and Dr. Lauren Lodato, for being regular sources of inspiration. Lastly, I would have never realized my dreams of achieving a PhD without the constant love, support, and source of laughs and smiles from my wonderful wife Sarah and my amazing daughter Lillian.

**XENOBIOTIC EFFECTS ON MALE MOUSE REPRODUCTIVE
SYSTEM AND HEPATIC GENE EXPRESSION AND EPIGENETICS:
STUDIES WITH BISPHENOL A AND TCPOBOP**

NICHOLAS J. LODATO

Boston University Graduate School of Arts and Sciences, 2018

Major Professor: David J. Waxman, Ph.D. Professor of Biology, Medicine, and
Biomedical Engineering; Program in Bioinformatics

ABSTRACT

The nuclear receptor superfamily is a large group of related receptors that bind steroid hormones, signaling molecules, or xenobiotic chemicals and are expressed across many mammalian tissues. The impact of nuclear receptor activation using two different mouse model systems is explored in this thesis: (1) *in utero* exposure of the environmental xenoestrogen and proposed endocrine disruptor bisphenol A (BPA) and (2) short adult exposures to the mouse constitutive androstane receptor (CAR) specific agonist ligand 1,4-bis-[2-(3,5-dichloropyridyloxy)]benzene (TCPOBOP). First, experiments involving the impact of *in utero* BPA exposure on the male mouse reproductive tract are described. Minimal changes to long-term mouse testis morphology and function were observed as mice treated with BPA *in utero* did not show significant changes in spermatozoa production or testis histopathology. Microarray analysis showed few persistently dysregulated genes, none of which were validated using qPCR due to high variability among biological

replicates. Next, nuclear RNA-seq was used to characterize global changes in the mouse liver transcriptome following exposure to TCPOBOP, including changes in novel long non-coding RNAs that may contribute to xenobiotic-induced pathophysiology. Dysregulated protein coding genes were associated with a striking male-biased pro-tumor response, including activation of pro-tumor upstream regulators such as cyclin D1 and inhibition of tumor suppressors such as p21 and p53, consistent with the reported male-biased susceptibility to CAR-dependent mouse liver tumorigenesis. Novel long non-coding RNAs were identified in livers of mice exposed to TCPOBOP, including lncRNAs proximal to the CAR target genes like *Cyp2b10*. Then, DNase-seq was used to identify DHS in male and female mouse liver that open or close following TCPOBOP treatment proximal to CAR responsive coding and non-coding genes. Finally, a series of ChIP-seq experiments targeting the activating histone modifications H3K4me1, H3K4me3 and H3K27ac, and the repressive chromatin modification H3K27me3 were performed in male mice to characterize the corresponding changes in local chromatin environment around DHS and responsive genes. Using a combination of DNase-seq and ChIP-seq, several classes of DNA regulatory elements have been identified, including active enhancers and promoter regions that may play a function role in regulating nearby CAR-responsive protein-coding and lncRNA genes.

TABLE OF CONTENTS

TITLE PAGE	i
READER'S APPROVAL PAGE	iii
DEDICATION	iv
ACKNOWLEDGEMENTS	v
ABSTRACT	vi
LIST OF TABLES.....	xv
LIST OF FIGURES.....	xvii
LIST OF ABBREVIATIONS.....	xx
CHAPTER 1- Introduction.....	1
1.1 Abstract.....	1
1.2 Endocrine disrupting compounds (EDC).....	2
1.2.1 Diethylstilbestrol (DES) and methoxychlor (MXC).....	3
1.2.2 Bisphenol A (BPA).....	4
1.2.3 Testis physiology	7
1.3 Nuclear receptors: xenobiotic sensing receptor CAR.....	10

1.3.1	CAR protein structure	12
1.3.2	Regulation of gene expression	17
1.3.3	CAR target genes	17
1.3.4	Role of CAR in hepatocellular carcinoma (HCC)	22
1.3.5	Long non-coding RNA (lncRNA)	23
1.3.6	Regulation of gene expression	24
1.4	Thesis goals and hypotheses	31
CHAPTER 2- Impact of Prenatal Bisphenol A Exposure on the Young Adult		
Male Mouse Reproductive System.....		
		41
2.1	Abstract.....	41
2.1	Introduction.....	42
2.3	Methods	46
2.3.1	Animals.....	46
2.3.2	Anatomical measurements and organ weights.....	47
2.3.3	Mature spermatozoa counts	47
2.3.4	Histology.....	47
2.3.5	qPCR and Microarray	48
2.3.6	Statistical Analysis.....	49

2.4	Results.....	50
2.4.1	Litter size is not impacted by BPA or DES	50
2.4.2	Anatomical markers show minimal impact of BPA or DES exposure	50
2.4.3	Testis histology is unchanged by BPA or DES	52
2.4.4	Assessing sperm production in mice exposed to BPA or DES <i>in utero</i>	52
2.4.5	Global transcriptional responses to <i>in utero</i> BPA or DES exposure-.....	53
2.4.6	KEGG pathway analysis of regulated genes.....	54
2.4.7	qPCR validation of gene responses measured by microarray.....	54
2.5	Discussion	55

CHAPTER 3- Male-biased response of tumor promotion-associated genes and dysregulation of novel long non-coding RNAs in constitutive androstane receptor-activated mouse liver..... 74

3.1	Abstract.....	74
3.2	Introduction	75
3.3	Materials and Methods	79
3.3.1	Animals.....	79
3.3.2	Tissue fixation, cyrosectioning and CAR immunostaining	80

3.3.3	Nuclear extraction and RNA purification	81
3.3.4	qPCR analysis	81
3.3.5	High throughput RNA sequencing (RNA-seq) analysis.....	82
3.3.6	Pathway and upstream regulator analysis	84
3.3.7	Statistics	85
3.4	Results.....	85
3.4.1	Nuclear RNA analysis to assess short-term responses to CAR	85
3.4.2	Global transcriptomic responses to CAR and PXR activation	87
3.4.3	KEGG pathway analysis	88
3.4.4	Identification of upstream regulators of CAR gene responses	89
3.4.5	Impact of TCPOBOP and PCN on non-coding transcriptome	92
3.4.6	LncRNAs proximal to regulated RefSeq genes are responsive to TC	94
3.4.7	LncRNAs distal to regulated RefSeq genes also respond to TC	96
3.5	Discussion	97

CHAPTER 4- Modulation of the mouse liver epigenome following

TCPOBOP exposure	141	
4.1	Introduction	142
4.2	Materials and Methods	145

4.2.1	Animal procedures and tissue extraction	145
4.2.2	Sonication of liver chromatin and ChIP analysis.....	146
4.2.3	Chromatin Immunoprecipitation (ChIP) assay	149
4.2.4	DNase-I hypersensitivity assay.....	150
4.2.5	DNase-seq and ChIP-seq libraries, sequencing and data analysis	151
4.2.6	Peak normalization.....	154
4.2.7	TAD definitions and grouping.....	155
4.2.8	TCPOBOP-responsive gene sets.....	156
4.2.9	DHS and K27ac peak mapping.....	156
4.2.10	DHS and K4me3 clustering	157
4.2.11	Statistics	158
4.3	Results.....	158
4.3.1	TAD boundaries separate up and down regulated genes	158
4.3.2	DHS cluster in TADs with co-responsive genes.....	159
4.3.3	Δ DHS responses precede changes in gene expression	160
4.3.4	Δ DHS are enriched nearby TCPOBOP-responsive genes	162
4.3.5	Δ DHS Open and Close nearby TCPOBOP-responsive HCC genes.....	163
4.3.6	Chromatin marks flanking Δ DHS.....	163

4.3.7	Activated enhancers map to responsive genes.....	165
4.3.8	Genes regulated after 3 h TC exposure precede enhancer activation	167
4.4	Discussion	168
4.4.1	Regulated genes cluster in TADs.....	169
4.4.2	Δ DHS as positive regulators of gene expression	171
4.4.3	Active enhancers target <i>Cyp2b10</i> and other induced genes.....	173
4.4.4	Conclusions.....	174
CHAPTER 5 Thesis summary and future directions		197
5.1	Chapter 2: <i>In utero</i> exposure to BPA does not permanently impact mouse testis function.....	197
5.1.1	Chapter 2 summary	197
5.1.2	Chapter 2 discussion and future directions	198
5.2	Chapter 3: Male-based response of tumor promotion-associated genes and dysregulation of novel long non-coding RNAs in constitutive androstane receptor-activated mice	200
5.2.1	Chapter 3 summary	200
5.2.2	Chapter 3 discussion and future directions	201

5.3	Chapter 4: Regulation of chromatin accessibility and histone modifications by activated CAR in male mouse liver	205
5.3.1	Chapter 4 summary	205
5.3.2	Chapter 4 discussion and future directions	206
	APPENDIX	208
	REFERENCES	223
	CURRICULUM VITAE	267

LIST OF TABLES

Table 2.1	KEGG pathway analysis of genes regulated by BPA or DES.....	70
Table 2.2	Regulation of select genes measured by microarray.....	71
Table 2.3	Primer sequences used for qPCR.....	73
Table 3.1	Primer sequences used for qPCR analysis.....	134
Table 3.2	Regulation of RefSeq genes by TCPOBOP or PCN in mouse liver.....	135
Table 3.3	Output from IPA upstream regulator analysis.....	136
Table 3.5	Mono-exonic and multi-exonic lncRNAs that respond to TCPOBOP or PCN at $ \text{fold-change} > 2$ and $\text{FDR} < 0.05$	137
Table 3.6	TCPOBOP and PCN responsive multi-exonic lncRNAs and their relationship to co-regulated RefSeq genes.....	139
Table 4.1	Sequencing reads obtained and peaks called	187
Table 4.2	Genes cluster in TADs.....	189
Table 4.3	Δ DHS map to responsive genes.....	190
Table 4.4	Highly active TDS.....	192
Table 4.5	Δ DHS that respond in multiple data sets.....	193
Table 4.6	Enrichment scores	194
Table 4.7	Common gene targets.....	195

Table 4.8	Results from ChIP-Seq	196
-----------	-----------------------------	-----

LIST OF FIGURES

Fig 1.1	Non-monotonic dose-response.....	33
Fig. 1.2	Chemical structures.....	34
Fig. 1.3	Testis development	35
Fig. 1.4	Male germ cell	36
Fig. 1.5	Chemical structures of CAR.....	37
Fig. 1.6	Overview of CAR binding via dimeration with RXR	38
Fig. 1.7	Indirection activation of CAR.....	39
Fig. 1.8	Agonists, antagonists and inverse agonist	40
Fig 2.1	Schematic overview of experimental design	61
Fig 2.2	Litter size following BPA or DES treatment	62
Fig 2.3	Adolescent and young adult anatomical measures following BPA or DES treatment	63
Fig 2.4	Histology of mature mouse testis following BPA or DES exposure.....	64
Fig 2.5	Mature spermatozoa counts in the adult male mouse. Histology of mature mouse testis following BPA or DES exposure.	65
Fig 2.6	Microarray analysis of testis exposed to BPA or DES.	65
Fig 2.7	qPCR validation of microarray results.....	68

Fig 2.8	Expression of <i>Star</i> measured via qPCR.	69
Fig. 3.1	I.P injection of TCPOBOP stimulates CAR nuclear localization in mouse liver within 3 h.	104
Fig. 3.2	TCPOBOP induces the expression of <i>Cyp2b10</i> and <i>Cyp2c55</i> while PCN represses the expression of <i>Hsd3b</i> and <i>Apol7a</i>	105
Fig. 3.3	TCPOBOP induces <i>Cyp2b10</i> , <i>Cyp2c55</i> , and <i>Akr1b7</i> in male and female	107
Fig. 3.4	Nuclear RNA-Seq identifies RefSeq genes responsive to activators of CAR or PXR.	109
Fig. 3.5	Sex differences in TCPOBOP gene responses identified by nuclear RNA.	111
Fig. 3.6	Genes that respond to TCPOBOP in males and females are more highly induced in females	113
Fig. 3.7	KEGG pathways enriched in sets of RefSeq genes responding to TCPOBOP or PCN.	115
Fig. 3.8	Upstream regulator analysis of TCPOBOP and PCN responsive.	117
Fig. 3.9	Mechanistic networks related to CAR-mediated HCC are found in TCPOBOP treated males but not females.	119
Fig. 3.10	Gene targets of 10 factors involved in CAR-mediated HCC.	121

Fig. 3.11	Genes regulated by TCPOBOP in males only are enriched for the CAR-mediated HCC pathway.	122
Fig. 3.12	The Nf-kB pathway is active in PCN treated males and TCPOBOP treated females but not TCPOBOP treated males.	124
Fig. 3.13	TCPOBOP responsive mouse liver lncRNAs.	125
Fig. 3.14	Liver-expressed lncRNAs responsive to TCPOBOP or PCN that are proximal to regulated RefSeq genes.	126
Fig. 3.15	lncRNA_4655 may negatively related Por.	128
Fig. 3.16	Two regulated lncRNAs are anti-sense to <i>Cyp2c37</i> and <i>Cyp2c50</i>	130
Fig. 3.17	lncRNAs responsive to TCPOBOP or PCN that are not proximal to the nearest regulated RefSeq gene.	132
Fig. 4.1	TCPOBOP-responsive genes cluster in TADs	175
Fig. 4.2	Δ DHS respond to TCPOBOP in mouse liver	176
Fig. 4.3	Promoter-like and Enhancer-like Δ DHS.	178
Fig. 4.4	Distance from Δ DHS to the nearest TSS	180
Fig 4.5	Stable active regions and dynamic active enhancers	181
Fig. 4.6	Dynamic active enhancers near <i>Cyp2b10</i> and <i>Cyp3a11</i>	183
Fig. 4.7	Gene induction precedes dynamic active enhancer formation	185

LIST OF ABBREVIATIONS

Δ DHS	Delta DHS
Δ K27ac	Delta K27ac
5C	Chromosome conformation capture carbon copy
Å	Angstrom
A2	A2 spermatogonia
A3	A3 spermatogonia
A4	A4 spermatogonia
A _{aligned} or A1	A _{aligned} spermatogonia
AF2	Activating function domain 2
AGD	Anogenital distance
Akr1b7	Aldo-keto reductase family 1, member B7
Alas1	5'-Aminolevulinate synthase 1
Alb	Albumin
Aldh	Aldehyde dehydrogenases
Amh	Anti-mullerian hormone
AMPK	AMP-activated protein kinase
ANCOVA	Analysis of covariance
ANOVA	Analysis of variance

Apoc3	Apolipoprotein C-III
Apol7a	Apolipoprotein 7a
A _{pr}	A _{paired} spermatogonia
AR	Androgen receptor
BPA	Bisphenol A
BW or bw	Body weight
C	Celcius
CAR	Constitutive androstane receptor
CCRP	Cytoplasmic CAR retention protein
CD	Compact disk
CDC	Centers for Disease Control
cDNA	Complementary DNA
CEBP α or CEBP β	CCAAT/enhancer binding protein alpha or beta
Ces2a	Carboxylesterase 2A
ChIA-PET	Chromatin interaction analysis with paired-end tag sequencing
ChIP	Chromatin immunoprecipitation
ChIP-sea	Chromatin immunoprecipitation with sequencing
Chr	Chromosome number
CHUK	Conserved helix-loop-helix ubiquitous kinase

CITCO	6-(4-Chlorophenyl)imidazo[2,1-b][1,3]thiazole-5-carbaldehyde O-(3,4-dichlorobenzyl)oxime
CRISPR	Clustered regularly interspaces short palindromic repeats
CSF2	Colony stimulating factor 2
CTNNB1	Catenin beta 1
Cyp	Cytochrome P450
Cyp11	Cytochrome P450, family 11
Cyp17	Cytochrome P450, family 17
Cyp19	Cytochrome P450, family 19
Cyp2b10	Cytochrome P450, family 2, subfamily b, polypeptide 10
CYP2B6	Cytochrome P450, family 2, subfamily B, polypeptide 6
Cyp2c37	Cytochrome P450, family 2, subfamily c, polypeptide 37
Cyp2c50	Cytochrome P450, family 2, subfamily c, polypeptide 50
Cyp2c53-ps	Cytochrome P450, family 2, subfamily c, polypeptide 53 pseudogene
Cyp2c55	Cytochrome P450, family 2, subfamily c, polypeptide 55
D	Diplotene
DAB	3,3'-Diaminobenzidine
DAVID	Database of Annotation, Visualization and Integrated Discovery

DBD	DNA binding domain
DDT	Dichlorodiphenyltrichloroethane
DEHP	diethylhexyl phthalate
DEN	Diethylnitrosomine
DES	Diethylstilbestrol
DHS	DNase-I hypersensitive site
DME	Drug metabolizing enzymes
DMEM	Dulbecco's Modified Eagle's medium
DMSO	Dimethyl sulfoxide
DNA	Deoxyribonucleic acid
DNase-seq	DNase-I hypersensitivity assay with sequencing
dpc	days post coitus
DR	Direct repeat
DR4	Direct repeat 4
DR5	Direct repeat 5
DTT	Dithiothreitol
DVD	Digital video disk
E	Embryonic day
E10.5	Embryonic day 10.5
E14.5	Embryonic day 14.9

E18	Embryonic day 18
E2	Estradiol
E2f	E2 transcription factor
E7.5	Embryonic day 7.5
E9	Embryonic day 9
E9.5	Embryonic day 9.5
EDC	Endocrine disrupting compound
EDTA	Ethylenediaminetetraacetic acid
EGFR	Epidermal growth factor receptor
EGTA	Ethylene glycol-bis(β -aminoethyl ether)-N,N,N',N'-tetraacetic acid
ENCODE	Encyclopedia of DNA elements
EPA	Environmental Protection Agency
ER	Everted repeat
ER or ER α or ER β	Estrogen receptor, estrogen receptor alpha, estrogen receptor beta
ER6	Everted repeat 6
ErbB	Erythroblastic leukemia viral oncogene
ERK	Extracellular signal-regulated kinase
ERR γ	Estrogen-related receptor gamma

ES	Elongated spermatids
F	Female
FC	Fold change
FDR	False discovery rate
Fig	Figure
Foxa1	Forkhead Box A1
FoxM1	Forkhead Box M1
FoxO1	Forkhead Box O1
FPKM	Fragments per kilobase per million reads
g	gram
GATA-4	GATA binding protein 4
GCY	Gonocytes
GEO	Gene Expression Omnibus
Ggt	Glutathione transferase
Ginm1	Glycoprotein integral membrane 1
Gjb4	Gap junction protein beta 4
GR	Glucocorticoid receptor
GR	Genital ridge
GRIP1	Glutamate receptor Interacting protein 1
h	hour

H12	Helix 12
H3	Helix 3
H3K26me3 or K27me3	Histone 3, lysine 27 trimethylation
H3K27ac or K27ac	Histone 3, lysine 27 acetylation
H3K36me2	Histone 3, lysine 36 dimethylation
H3K36me3	Histone 3, lysine 36 trimethylation
H3K4me1 or K4me1	Histone 3, lysine 4 monomethylation
H3K4me3 or K4me3	Histone 3, lysine 4 trimethylation
H3K9me3	Histone 3, lysine 9 trimethylation
H4	Helix 4
HCC	Hepatocellular carcinoma
HCl	Hydrochloric acid
Hdac9	Histone deacetylase 9
HEPES	4-(2-hydroxyethyl)-1-piperazineethanesulfonic acid
HGF	Hepatocyte growth factor
HNF3	Hepatocyte nuclear factor 3
Hsd3b	Hydroxy-delta-5-steroid dehydrogenase, 3 beta
HSP90	Heat shock protein 90
Hx	Helix x

I	Isoleucine
ID2	Inhibitor of DNA binding 2
IgG	Immunoglobulin G
IKBKB	Inhibitor Of nuclear factor kappa B kinase subunit beta
In	
Inhbb	Inhibin beta B
IPA	Ingenuity Pathway Analysis
IR	Inverted repeat
KCl	Potassium chloride
KEGG	Kyoto encyclopedia of genes and genomes
kg	Kilogram
Klf4	Kruppel likefactor 4
Klhdc7a	Kelch domain containing 7A
KO	Knockout
L	Leucine
L	Leptotene
LBD	Ligand binding domain
lncRNA	Long non-coding RNA
LOEL	Lowest observed effect level
M	Male

MA	Mitotic arrest
MAPK	Mitogen-activated protein kinase
MEK	MAPK/ERK Kinase
mg	Milligram
min	minute
mL	Milliliter
mM	millimolar
mRNA	messenger RNA
Mrp	Multi-drug resistant-associated transporter
MXR	Methoxychlor
Mycor c-Myc	Avian Myelocytomatosis Viral Oncogene Homolog
NF κ B, Nf-kB	Nuclear factor kappa-light-chain-enhancer of activated B cells
NIEHS	National Institute of Environmental Health Sciences
NLS	Nuclear localization signal
NMDR	Non-monotonic dose responses
NR	Nuclear receptor
NTP	National Toxicology Program
Oct3/4	Octamer-binding transcription factor 3/4
P	Pachytene

P1	Preleptotene
p21	protein 21 kilodaltons, cyclin-dependent kinase inhibitor 1
p38	protein 38 kilodaltons
p53 or Tp53	Protein 53 kilodaltons, tumor protein p53, tumor suppressor p53
Padi4	Peptidyl arginine deiminase 4
PB	Phenobarbital
PBREM	Phenobarbital responsive enhancer module
PBS	Phosphate buffered saline
PCN	Pregnenolone 16- α carbonitrile
PCR	Polymerase chain reaction
PGC	Primordial germ cells
PGC-1	Peroxisome proliferator activated receptor gamma coactivator 1
PM	Peritubular myoid
PMSF	Phenylmethane sulfonyl fluoride
PND	Postnatal day
Por	Cytochrome P450 Oxidoreductase
PP2a	Protein phosphatase 2a

PPAR γ	Peroxisome proliferator-activated receptor gamma
ppb	Parts per billion
Prss22	Protease, serine 22
PXR	Pregnane X receptor
qPCR	Quantitative PCR
RABL6	RAB, Member RAS Oncogene Family Like 6
RACK	Receptor for activated C-kinase
Rb	Retinoblastoma protein
RefSeq	NCBI Reference Sequence Database
RIN	RNA integrity number
RIPA	Radioimmunoprecipitation assay
RNA	Ribonucleic acid
RNAPII	RNA polymerase II
RNA-seq	Ribonucleic acid with sequencing
RPKM	Reads per kilobase per million reads
rpm	Revolutions per minute
Rspo1	R-spondin 1
RXR	Retinoid X receptor
SBG	Spermatogonia type B
SCC	Spermatogenic stem cell

SCO	Sertoli cell only
Sfl	Steroidogenic factor 1
SGA	Spermatogonia type A
Slc15a1	Solute carrier family 15 member 1
Sox2	Sry-box 4
Sox9	Sry-related HMG box 9
SR	Self-renew
SRC1	Steroid receptor coactivator 1
Sry	Sex-determining region of Y
Star	Steroidogenic acute regulatory protein
Sult	Sulfotransferase
Sult3a1	Sulfotransferase family 3A, member 1
SWI/SNF	SWItch/Sucrose Non-Fermentable
TAD	Topologically associated domain
TBX2	T-box 2
TCPO	TCPOBOP
TCPOBOP	1,4-Bis-[2-(3,5-dichloropyridyloxy)]benzene
TE	Tris-EDTA buffer
TF	Transcription factor
Thr-38	Threonine 38

TNF	Tumor necrosis factor
TP	Transition proteins
TSS	Transcription start site
UDP	Uridine diphosphate
Ugt	UDP-glucuronyltransferase
US	United States
v/v	volume to volume percentage
VEGF	Vascular endothelial growth factor
WA	White adipose
Wnt4	Wingless-related integration site 4
XE	Xenoestrogen
Xist	X-inactive specific transcrip
Yap	Yes associated protein
Z	Zygotene
μg or ug	Microgram
μL or uL	Microliter
μM or uM	Micrometer, micron

CHAPTER 1- Introduction

1.1 Abstract

Environmental chemicals define a broad class of molecules that are found in the soil, air, water supplies or food as a result of pollution or in consumer products as a result of the manufacturing process. Some chemicals, such as the heavy metals mercury, lead, cadmium and arsenic, are found at US Environmental Protection Agency Superfund cleanup sites due to pollution from oil spills, toxic waste dumps and natural disasters. Other chemicals, such as bisphenol A (BPA), are monomers used as a building block for generating hard polycarbonate plastics used in water bottles, baby bottles and toys, interior linings for canned foods, dental fillings, consumer electronics and various other applications. Additionally, chemicals such as dichlorodiphenyltrichloroethane (DDT) and methoxychlor were used as chemical pesticides and insecticides for commercial farming. Together, these environmental chemicals pose a health risk to humans and wildlife through their multitude of exposure routes, near ubiquitous presences and, for many chemicals, poorly understood impact and mechanism of action following exposure. One proposed mechanism of action for some of these chemicals in mammals is through the direct binding to nuclear receptors primarily found in liver, gonads and other endocrine tissues. The nuclear receptor superfamily contains several receptors, including constitutive androstane receptor (CAR) that act as a so-called xenobiotic sensor and steroid hormone receptors like estrogen

receptor (ER) which is involved in hormone and endocrine signaling. CAR binds a broad set of xenobiotic chemicals and induces several numbers of Phase I and Phase II drug metabolizing enzymes, especially the cytochrome P450 (Cyp) gene superfamily to rapidly metabolize and clear foreign compounds. ER is closely involved in hormone signaling and development of several tissues *in utero*, in particular the gonads. While most ER ligands are endogenous steroid hormones, it has been shown to bind exogenous estrogen-like compounds, known as xenoestrogens.

In my thesis work, I have explored the potential impact of environmental chemical exposure using two separate and distinct models. In the first model, designed to assess the impact of a single environmental chemical, I exposed male mice *in utero* to doses of the proposed xenoestrogen and endocrine disruptor BPA that were designed to mimic the average human exposure and measured reproductive health in adulthood. The second model, in contrast, was designed to assess the impact of a broad set of chemicals by inducing CAR with its potent, receptor-specific ligand, TCPOBOP, in order to characterize the impact on the mouse liver transcriptome and epigenome.

1.2 Endocrine disrupting compounds (EDC)

The first section of my thesis (Chapter 2) focuses on the effects of exposure to a single environmental chemical, and proposed endocrine disruptor, on the developing male mouse reproductive system. The endocrine disruption field was established by Theo Colburn in

1991 when a group of 21 scientists met at the Wingspread Conference Center in Wisconsin to discuss the harmful side effects of exposure to industrial chemical in wildlife. Endocrine disrupting compounds (EDCs) are broadly defined as compounds that have the ability to interfere with endogenous hormone signaling. Furthermore these compounds can sometimes induce linear dose responses but often induce nonmonotonic dose responses (NMDR), giving U-shaped or inverted U-shaped plots typical of endogenous steroid hormones (Fig 1.1) (Vandenberg et al. 2009). A specific subclass of EDCs, xenoestrogens (XEs), have the capacity to bind to and activate the nuclear receptor estrogen receptor α (ER α) or ER β or estrogen-related receptor γ (ERR γ) due to their structural similarities to endogenous estrogens, such as estradiol. Three of these compounds - methoxychlor (MXC), diethylstilbestrol (DES), and bisphenol A (BPA) - are the focus of this section (Fig. 1.2).

1.2.1 Diethylstilbestrol (DES) and methoxychlor (MXC)

Diethylstilbestrol (DES) and methoxychlor (MXC) are potent xenoestrogens. DES was actively prescribed in the US to pregnant women to help prevent miscarriages beginning in 1938 and ending in 1971, when it was finally banned. As a result, the CDC estimates that 5-10 million American children were exposed *in utero* to this potent XE, the effects of which are increased incidence of vaginal and cervical cancer in exposed daughters (Rubin 2011). MXC is an insecticide developed as an alternative to DDT, which was banned in the US in 1971 when it was discovered to be an EDC capable of reducing the egg shell

strength of many bird species. The US EPA later banned MXC as well as it was found to lower fertility in both male and female rodents. MXC was still in use for thirty-two years, however, leaving countless exposed.

1.2.2 Bisphenol A (BPA)

BPA was first synthesized in 1936 as an alternative to natural estrogen for hormone replacement (Umweltbundesamt 2010). While it was never prescribed and it was replaced by better hormone mimics, it was found to be useful as plasticizer and roughly 6-8 billion pounds of it are produced globally each year (Kang et al. 2011). Polycarbonate plastics synthesized from BPA polymers are ubiquitous and found in a wide range of products including CD/DVDs, eyeglasses, plastic water coolers and baby bottles (Umweltbundesamt 2010). BPA epoxy resins are used as dental sealants and also coat the interiors of canned food (Umweltbundesamt 2010). A lowest observed effect level (LOEL) of 50 mg/kg bw/day was established in 1988 based on rodent models (Rubin 2011). The CDC set the human reference dose at 50 µg/kg body weight/day using and a uncertainty factor of 1000 based on an assumed linear dose response (Rubin 2011). While this method to determine a safe limit for human exposures is not ideal and may not reflect the toxicology of this compound, it is still used in food safety evaluations today.

1.2.2.1 Controversy surrounding BPA in literature

The effects of exposure to XEs are controversial and are an active area of research. Initial studies performed by vom Saal et al. in 1998 identified bisphenol A as an endocrine disruptor in male and female mouse reproduction (vom Saal et al. 1998) and early work corroborated this conclusion. Several studies found either adult or developmental exposures to BPA altered testicular histology (Fisher et al. 1999, Atanassova 2000, Chitra et al. 2003, Takahashi and Oishi 2003, Naciff et al. 2005) or sperm physiology (vom Saal et al. 1998, Sakaue et al. 2001, Al-Hiyasat et al. 2002, Chitra et al. 2003, Takahashi and Oishi 2003, Toyama and Yuasa 2004) in rodents. Soon after the initial classification of BPA as an EDC, there was significant pushback from some groups that reported no clear evidence of endocrine disruption by bisphenol A. Gray (Gray et al. 2010), Ryan (Ryan et al. 2010) and Tyl (Tyl et al. 2002, Tyl et al. 2008, Tyl 2009), reported no significant effects of BPA in rodents using both *in utero* and adult exposure models. However, vom Saal and others pointed out major flaws in their experiments which have led to a misinterpretation of their results (vom Saal et al. 2010). These studies used the estrogen insensitive Long-Evens rat strain which then lead them to use inappropriately low doses of both BPA and their positive control ethinylestradiol, due to their insensitivity to estrogens. Additionally, polycarbonate cages were used to house the rats, which themselves are made from BPA, and thus all rats in the experiment were exposed to an unknown level of BPA (vom Saal et al. 2010). Outside of these studies, there have been other reports in the literature that show little to no long term effects of early BPA exposure on the male mouse reproductive tract,

despite closely following the standard practices described by vom Saal and others. LaRocca (LaRocca et al. 2011) exposed C57/Bl6 mice, an estrogen sensitive mouse strain (Wadia et al. 2007), to 50 μg BPA/kg body weight/day and 1000 μg BPA/kg body weight/day and found little effects the male reproductive tract. Conversely, recent publications on BPA again suggest it is an EDC capable of altering meiosis and spermatogenesis in rodents (Vrooman et al. 2015, Wisniewski et al. 2015, Li et al. 2016, Xie et al. 2016, Ahbab et al. 2017). Exposure to BPA has also been correlated with reduced sperm quality in men (Goldstone et al. 2015, Vitku et al. 2016) as well as obesity in elderly women (Lee et al. 2015). Given the conflicting reports in the literature about the exact impact on BPA on overall male reproductive health, additional research is clearly needed. Absent in the literature is a consensus about mouse exposures to BPA at human relevant doses during specific windows of development to identify clear critical time points of vulnerability. The window we have chosen to study is embryonic days 9 through 18, which represents a critical period in testis organogenesis and establishment of cells required for proper spermatogenesis in adult animals. Doses chosen represents conditions at and around the human reference dose to avoid missing relevant findings due to known nonmonotonic dose responses observed with BPA (Fig. 1.1). To understand how perturbations in endocrine signaling during development through xenoestrogen exposure affects testicular function and morphology, however, we first need to understand how the mouse testis is developed and functions in normal, healthy mice.

1.2.3 Testis physiology

Proper testis organogenesis and development is critical for androgen biosynthesis throughout life as well as post-pubertal spermatogenesis. In this section, I will review testis organogenesis in male mice in the context of the embryonic development timeline as a justification for our dosing window. Additionally, I will review the process of spermatogenesis in adult mice as a foundation for understanding testis pathophysiology and any subsequent perturbations in sperm count.

1.2.3.1 Testis organogenesis and development

Testis organogenesis in mice is initiated by the migration of primordial germ cells (PGCs) and somatic cells (Sertoli cell precursors in males) into the genital ridge of the embryo at E9.5 (Sekido and Lovell-Badge 2009). This early structure is known as the bipotential gonad as it is capable of differentiating into either a testis or an ovary given the correct internal and external cues. In both sexes at E10.5, the transcription factor *Sox9* is expressed at a basal level in both sexes. A second transcription factor, steroidogenic factor 1 (*Sf1*), is also expressed and has the potential to activate sex-determining region of Y (*Sry*) located on the Y-chromosome; thus *Sf1* can only induce *Sry* in males as females lack this locus. In males, *Sry* and *Sf1* work in concert to boost *Sox9* expression until a critical threshold is reached when it can be maintained by auto-regulation (Wilhelm et al. 2007, Sekido and Lovell-Badge 2009). In the females, *Sry* is not expressed and β -catenin begins to accumulate in response to Wnt4 signaling (Sekido and Lovell-Badge 2009). This sets up a

system where gonads destined to be testes express high levels of *Sox9* and low levels of β -catenin whereas gonads destined to become ovaries express high levels of β -catenin and low levels of *Sox9* (Fig. 1.3). *Sox9* expression is entirely responsible for the development of the organ as a whole as well as differentiation of all of the associated cell types. *Sox9* promotes the differentiation of Sertoli cells, Wolffian ducts (precursors of the epididymides and vas deferens), peritubular myoid (PM) cells and Leydig cells, the major androgen producing cell type in the male (Wilhelm et al. 2007). During organogenesis, PM cells surround the Sertoli cells and PGCs to form sex cords which will eventually develop into seminiferous tubules. By E14.5, clear construction of seminiferous tubules with PM cells encompassing Sertoli cells and germ cell masses are established with Leydig cells forming within the interstitial space (Wilhelm et al. 2007). From E14.5 until birth, seminiferous tubules and interstitial Leydig cells continue to grow under the control of *Sox9*. Thus, the window between E9 and birth (~E20) represents a critical window where outside influences can cause permanent deleterious alterations in testis development.

1.2.3.2 Spermatogenesis

The adult mammalian testis is a heterogeneous organ and is the site of spermatogenesis as well as the major source of androgen biosynthesis. As discussed above, adult exposure to BPA disrupts both androgen biosynthesis and spermatogenesis in rodents (vom Saal et al. 1998, Fisher et al. 1999, Atanassova 2000, Takahashi and Oishi 2000, Sakaue et al. 2001, Al-Hiyasat et al. 2002, Chitra et al. 2003, Takahashi and Oishi 2003, Naciff et al. 2005,

vom Saal and Hughes 2005, Salian et al. 2009, Nakamura et al. 2010, Salian et al. 2011, Xi et al. 2011). Spermatogenesis occurs in seminiferous tubules where a spermatogenic stem cell (SCC) divides and eventually gives rise to many differentiated spermatozoa. Broadly, the process is comprised of three major types of cells: spermatogonia, spermatocytes, and spermatids. Each of these groups can be further divided into many subtypes.

Type A_s spermatogonia (the SCC) lay on the basal lateral epithelium of seminiferous tubules. Once stimulated to divide, they give rise to A_{pr} (A_{paired}) spermatogonia followed by A_{al} ($A_{aligned}$) spermatogonia which are so-called as their orientation is parallel to the epithelium (de Rooij 2009, Godmann et al. 2009). A_{al} , also known as A1, spermatogonia can continue to divide and create chains up to 16 cells long (de Rooij 2009, Godmann et al. 2009). A1 spermatogonia progressively divide five times by mitosis and are known as A2, A3, A4, In, and type B spermatogonia after each division (de Rooij 2009, Godmann et al. 2009). A sixth round of mitosis then yields resting primary spermatocytes. A resting primary spermatocyte, also known as pre-leptotene spermatocytes, enters meiosis I and marks the beginning of the leptotene primary spermatocyte stage (Rousseaux et al. 2005, Godmann et al. 2009). These cells then differentiate through zygotene and pachytene primary spermatocyte stages where crossing over and recombination occurs before finally arriving in the diplotene primary spermatocyte stage. Once at this stage meiosis division I yields type II secondary spermatocytes. These cells rapidly enter meiotic division II to

form haploid round spermatids (Rousseaux et al. 2005). The remaining process of a round spermatid (stage 1) maturing into a spermatozoon (stage 16) is known as spermiogenesis. The three major cell types (spermatogonia, spermatocytes, and spermatids) can be visually distinguished from each other by morphology and nuclei staining patterns in histological hematoxylin and eosin staining. The process of spermatogenesis is tightly controlled by Sertoli cells and Leydig cells in the SSC niche. The SSC niche is thought to be a unique milieu within the seminiferous tubule and also among other stem cell niches (de Rooij 2009). This is because the topography of a testis cross-section reveals several different environments that lay adjacent to A_s spermatogonia and their surrounding Sertoli cells (Fig. 1.4). The true niche is believed to be located where Sertoli cells are neighboring large, diverse, and complex interstitial spaces (de Rooij 2009). Any perturbations to the niche identified by histology can be attributed to stem cell loss and ultimately to sub- or infertility. In Chapter 2, I explored the potential impact on in utero BPA or DES exposure on proper testis organogenesis. To do this, I present data on anatomical structures present or absent in mice exposure to BPA or DES. I then measured sperm count as a metric for overall reproductive health of the animals exposed to BPA or DES. Lastly, I present global gene expression profiles of mice exposed to BPA or DES compared to unexposed animals.

1.3 Nuclear receptors: xenobiotic sensing receptor CAR

In contrast to the previous section which focused on a single chemical exposure and the impact on multiple endpoints through undefined, presumed multiple, receptors, the next

section of my thesis (Chapter 3 and 4) aims to establish coding and non-coding transcriptomic and epigenomic signatures when a single nuclear receptor is activated in mouse liver. To achieve this, we have chosen the nuclear receptor CAR (constitutive androstane receptor) and its potent and receptor-specific ligand TCPOBOP (Fig. 1.5). CAR is one of the so-called xenobiotic sensing receptors found in the mammalian genome. Once thought to be an orphan receptor with no known endogenous ligands or functions, it is now known to directly bind several steroid hormones (Kawamoto et al. 2000, Hernandez et al. 2009) and regulate bile acid (Lickteig et al. 2016), glucose and lipid homeostasis (Kodama et al. 2004, Konno et al. 2008, Moreau et al. 2008, Wada et al. 2009, Gao and Xie 2010) in liver. The main function of CAR is thought to be clearance of xenobiotics through direct binding of the chemical in its large ligand binding pocket (Suino et al. 2004, Xu et al. 2004), or indirect activation through EGFR signaling (Meyer and Jirtle 2013, Yang and Wang 2014, Kobayashi et al. 2015), and induction of genes involved in drug metabolism (Sueyoshi et al. 1999, Ueda et al. 2002, Chen et al. 2003, Kodama et al. 2004, Timsit and Negishi 2007). In addition to the positive physiological benefits to activated CAR (i.e. xenobiotic clearance and homeostasis), several negative effects have been associated with prolonged CAR activation. Recently, activated CAR has been linked to induction of liver steatosis (Mellor et al. 2016) and tumor promotion (Yamamoto et al. 2004). In this section, I will review the protein structure of CAR that allows both its constitutive activity in the absence of ligand and its ability to bind a diverse set of compounds, the protein sequence conservation of CAR between mouse and human, the known physiological roles of CAR

in mouse and human liver, sex differences in the expression of CAR in mouse liver and the impact of steroid hormones on CAR activity.

1.3.1 CAR protein structure

CAR contains two domains essential to its function as a ligand activated transcription factor; a DNA binding domain (DBD) and a c-terminal ligand binding domain (LBD). Additionally, CAR has an activating function domain (AF2) at the c-terminus that is the site of co-activator or co-repressor binding in the nucleus. The crystal structure of mouse CAR bound to its potent, synthetic ligand TCPOBOP and in a heterodimer with RXR was resolved in 2004 (Suino et al. 2004) and the same year, human CAR bound to its specific ligand, CITCO, and complexed with RXR and other coactivators was published (Xu et al. 2004), providing great insight into its structure and species similarities in mice and humans. In this section, I will describe the protein structure of CAR and how its physical properties lead to its known functions.

1.3.1.1 DNA binding domain (DBD)

The DBD of CAR is well conserved between mouse and humans with 88% homology between the two species (Timsit and Negishi 2007), thus allowing CAR to bind to homologous sequences in the mouse and human genome. Additionally, the DBD of NRs in a given species is highly homologous and as such, most NRs can recognize and bind to identical sequences in the genome. The core recognition sequence for NRs is a non-

palindromic repeat of a half-site of 3'-AGGTAC-5', found in either a direct repeat (DR), inverted repeat (IR) or everted repeat (ER) with a given number of spacer sequence in between the two half-sites (Waxman 1999, Claessens and Gewirth 2004). NRs can be classified by their preference for binding to specific repeat orientations, with CAR preferentially binding to DR containing 4 or 5 nucleotide spacers (DR4; DR5) or an ER6 motif (Fig. 1.6).

1.3.1.2 Ligand binding domain (LBD)

In contrast to the DBD, the LBD in CAR is more variable across mammalian species and between NRs in a given species. The mouse CAR LBD is only 72% homologous to human CAR (Timsit and Negishi 2007) which leads to differences in ligand binding efficiency between the two species. For example, the potent mouse CAR direct agonist 1,4-Bis-[2-(3,5-dichloropyridyloxy)]benzene (TCPOBOP) is specific for mouse CAR while 6-(4-Chlorophenyl)imidazo[2,1-b][1,3]thiazole-5-carbaldehyde O-(3,4-dichlorobenzyl)oxime (CITCO) is a potent and specific ligand for human CAR (Fig. 1.5). X-Ray crystallography of the mouse CAR LBD followed by a sequence alignment of mouse CAR to human CAR shows that 10 out of 31 residues responsible for TCPOBOP docking in the mouse CAR LBD are different between species (Suino et al. 2004).

Structurally, the LBD of most NRs, including CAR, contains 12 α -helices which form a hydrophilic binding pocket suitable for binding small molecules (Huang et al. 2010). The

size of the binding pocket formed by these 12 helices vary across NRs and can contribute to their function. For example, ER, while capable of binding xenoestrogens as discussed earlier, can only bind a narrow range of chemicals that have estrogen-like structures and derivatives due to its moderately sized ligand binding pocket (450 \AA^3) (Huang et al. 2010). In contrast, CAR and PXR have larger binding pockets that are capable of binding structurally diverse compounds. In addition to TCPOBOP, mouse CAR can bind steroid hormones such as androstanol and androstenol (Forman et al. 1998), environmental estrogens such as ethinyl estradiol (Repo et al. 2008) and nonylphenol (Hernandez et al. 2007), phthalates such as DEHP (Eveillard et al. 2009) and statins such as cerivastatin (Kobayashi et al. 2005) due primarily to its 525 \AA^3 binding pocket (675 \AA^3 in human CAR) that can expand to accommodate larger molecules (Suino et al. 2004). A summary of known CAR agonists, antagonist and inverse agonists can be found in Table 1.1. The binding pocket of mouse PXR is 1200 \AA^3 , allowing it to not only bind structurally diverse compounds such as the steroid hormone derivative pregnolone 16- α carbonitrile and the plant derived sulforaphane but also the extremely large, bacteria derived, antibiotic rifampicin (Timsit and Negishi 2007). The ability to bind such a broad class of molecules is what allows both CAR and PXR to function as xenobiotic sensors in the cell.

1.3.1.3 Helix 12, AF2 domain

Contained within the LDB of CAR and other NRs, at the c-terminal end, is helix 12 (H12), also known as the activating function 2 (AF2) domain. The AF2 domain is the site of

coactivator or corepressor binding through LXXLL motifs found in coactivator proteins or LXXXIXXXL found in corepressor proteins (Suino et al. 2004). Binding sites for either coactivators or corepressors can be revealed depending on the orientation of the AF2 domain relative to the other helices in the LDB, specifically H3 and H4 (Huang et al. 2010). For most NRs, the AF2 domain is fixed in an inactive state in the absence of bound ligand and does not contain a binding site for either coactivators or corepressors. When an agonist ligand binds to the LBD, the AF2 domain undergoes a conformational change which reveals a small binding site for coactivator LXXLL motifs. If the ligand is an antagonist, the conformation change the AF2 domain undergoes reveals a larger binding site that allows for corepressor binding through a LXXXIXXXL motif (Suino et al. 2004). In contrast to other NRs, the AF2 domain in the CAR protein is fixed in the active orientation, allowing for binding of coactivators in the absence of ligand and thus giving CAR its constitutive activity. The ligand-independent active orientation of AF2 is due to three distinct structural aspects unique to CAR among all NRs. First, the length of the linker sequence separating H11 (named Hx in CAR) and H12 is shorter than in other NRs, making the relative orientation between these two helices less flexible. Second, the CAR H12 helix is itself truncated when compared to other NRs and the c-terminal carboxylate group forms a hydrogen bond with H4, stabilizing the H12 in the active orientation. Lastly, H2 is extended in CAR which stabilizes the H3 helix by shifting its position (Suino et al. 2004). Although beyond the scope of this thesis, CAR's ability to bind a structurally diverse set of chemicals is critical to its underlying biology.

1.3.1.4 Consequences of constitutive activity

One of the defining characteristics of CAR among all NRs is its constitutive activity in the absence of ligand. A consequence of activity in the absence of direct binding is CAR is able to be activated by indirect mechanisms. Indeed, the classic CAR activator phenobarbital (PB) works through an indirect mechanism and is mediated by EGFR (Fig. 1.7) (Meyer and Jirtle 2013, Yang and Wang 2014, Kobayashi et al. 2015). Due to its constitutive activity, the cell needs to sequester CAR in the cytoplasm to prevent persistent and aberrant activity and it achieves this sequestering by complexing CAR with heat shock proteins 90 (HSP90) and by a tetratricopeptide repeat protein termed the cytoplasmic CAR retention protein (CCRP) (Kobayashi et al. 2003, Timsit and Negishi 2014) and by phosphorylating CAR at Thr-38 (Osabe and Negishi 2011). Direct binding of ligands causes conformational changes that free CAR from the protein complex with HSP90 and CCRP, leads to the dephosphorylation of Thr-38 by PP2a and exposes a nuclear localization signal (NLS) (Kanno et al. 2005). However, when an indirect activator like PB is present, CAR is dephosphorylated at Thr-38 by PP2A through RACK and MEK/ERK signaling (Yang and Wang 2014).

In addition to the ability of CAR to be activated by direct and indirect ligands, the activity of CAR can also be reduced by an inverse agonist due to its constitutive activity in the absence of ligand (Hanania et al. 2010). Unlike a true antagonist, which prevents activation

of a receptor (i.e. the receptor is kept in its basal state), an inverse agonist reduces the activity of a receptor and lowers its constitutive activity below its basal state (Fig. 1.8). For example, if CAR was activated by an indirect activator like PB, the simultaneous presence of an antagonist would have no effect on the activated CAR's activity (i.e. it will remain fully active). However, if CAR was activated by an indirect activator like PB, the simultaneous presence of an inverse agonist would reduce the activated CAR's activity (i.e. it would be less active). Indeed, androstanol and androstenol, two of the few known endogenous ligands of CAR, are inverse agonists of the receptor (Forman et al. 1998, Suino et al. 2004).

1.3.2 Regulation of gene expression

Once activated by exogenous xenobiotics or endogenous steroid hormones in the cytoplasm, CAR translocates to the nucleus and regulates the transcription of protein coding genes involved in drug metabolism and excretion, thus playing a central role in xenobiotic sensing and clearance. In this section, I will review known direct gene targets of CAR as well as transcriptome wide gene regulation in mouse liver by CAR.

1.3.3 CAR target genes

1.3.3.1 Protein coding genes

Cytochrome P450 genes are well known protein coding targets of CAR regulation in liver. Some of the earliest work on the effects of phenobarbital or TCPOBOP on liver as early as

1959 identified cytochrome P450s as being highly induced following drug treatment long before CAR was known to be the receptor and transcription factor intermediate (Remmer 1959, Orrenius and Ericsson 1966, Poland et al. 1980, Poland et al. 1981, Waxman and Azaroff 1992, Waxman 1999). Since then, the *Cyp2* family has been extensively studied for their robust response to CAR ligands in both mouse and humans, notably *Cyp2b10* in mice and its human orthologue *CYP2B6* (Kawamoto et al. 1999, Sueyoshi et al. 1999, Kawamoto et al. 2000, Blizard et al. 2001, Ueda et al. 2002, Chen et al. 2003, Kobayashi et al. 2003, Tian et al. 2011, Kobayashi et al. 2015). Additionally, there has been increasing evidence that CAR regulates *Cyp2* genes by directly binding to response elements upstream of mouse *Cyp2b10* or human *CYP2B6* (Park et al. 1996, Sueyoshi et al. 1999, Tian et al. 2011). In earlier experiments, it was shown that a 5' flanking region 2kb upstream (-2318 to -2155) of the human *CYP2B1* promotor was required for transactivation of the gene by phenobarbital in transfected rat primary hepatocytes and was therefore termed the phenobarbital responsive element (PBRE) (Park et al. 1996). That specific region was found to be conserved in mouse, rat and human and the core 51 bp sequence containing two nuclear receptor binding sites was all that was required for recruitment of CAR and activation of *Cyp2b10* gene expression in mice (Honkakoski et al. 1998). The 51 bp core sequence was named the phenobarbital responsive enhancer module (PBREM) and contains two DR4 motifs. Other *Cyp2* family members that have been identified as CAR-inducible include *Cyp2c39* and *Cyp2c55* (Jackson et al. 2006). In addition to *Cyp210*, other known CAR-inducible genes have PBREM in close proximity to their proximal promoters

including the UDP-glucuronyltransferase *Ugt1a1* (Kuno et al. 2008). To date, however, genome wide mapping of CAR binding to determine how many gene targets CAR potentially regulates directly has not been performed due to the lack of a commercially available ChIP-Seq quality antibody.

1.3.3.2 Transcriptomic data currently available

To date, a number of groups have attempted to understand genome wide transcriptional regulation in liver by activated CAR. In 2002, Ueda et al. published a microarray analysis of the mouse liver transcriptome following phenobarbital injection in wild type and CAR-null mice (Ueda et al. 2002). In their experiment, the 10 out of 22 genes upregulated in a CAR dependent manner were enzymes known to be involved in drug metabolism, including *Cyp2b10*. However, a major limitation of their study was it was done on a relatively narrow microarray platform that contained 8,736 cDNA probes and used phenobarbital as the CAR agonist, which is now known to activate other NRs including PXR. Also, despite probes against seven other cytochrome P450 genes, surprisingly, no other cyp genes were found to be regulated by CAR. In 2012, Aleksunes and Klaassen used a panel of arrays to determine the transcriptome profile of wild type and CAR-null mice exposed to TCPOBOP and focused on the regulation of drug metabolizing enzymes. In addition to *Cyp2b10*, genes encoding many other drug metabolizing were induced following CAR activation. These genes included cytochrome P450 families 1 (*Cyp1a2*) and 3 (*Cyp3a11*), *Aldh* family 1 enzymes (*Aldh1a1*, *Aldh1a7*), *Ugt1* family enzymes

(*Ugt1a1*, *Ugt1a9*), *Ugt2* (*Ugt2b35*), sulfotransferases (*Sult1e1*, *Sult2a2*, *Sult3a1* and *Sult5a1*), glutathione transferases (*Gsta1*, *Gsta4*, *Gstt1*, *Gstm1*, *Gstm2*, *Gstm3*, *Gstm4*) and the multidrug resistant-associated transporters (*Mrp2*, *Mrp3*, *Mrp4*) (Aleksunes and Klaassen 2012). More recently, Li et al. published an RNA-Seq based study characterizing the changes in gene expression in the human hepatocellular carcinoma derived HepRG following exposure to the human CAR specific ligand CITCO or phenobarbital (Li et al. 2015). In addition to the classic responding genes such as *CYP2B6* and *CYP3A4* (the human orthologue to mouse *Cyp3a11*), they found a number of metabolism related KEGG pathways enriched for induced genes in their data set. Such pathways included 1) metabolism of xenobiotics by cytochrome P450 2) two separate drug metabolism pathways and 3) amino acid metabolic pathways such as valine, leucine and isoleucine degradation and glycine, serine and threonine metabolism. KEGG pathways down regulated include several related to cancer including 1) p53 signaling 2) cell cycle and 3) pathways in cancer.

1.3.3.3 Sex dependent sensitivity to CAR ligands

Our laboratory has published several studies on sex differences in the basal expression of drug metabolizing enzymes (Waxman et al. 1991, Wauthier and Waxman 2008, Waxman and Holloway 2009, Conforto and Waxman 2012). Members of the *Cyp2b* family (*Cyp2b9*, *Cyp2b10*, *Cyp2b13*) and *Cyp3a* family (*Cyp3a1*, *Cyp3a44*), among other DME genes, have been shown to be highly female specific (Waxman and Holloway 2009). Many of these genes are known CAR targets leading to the hypotheses that basal CAR activity is higher

in female liver and that responsiveness to CAR agonist ligands could show sex biasness. One gene that appears to be differentially regulated basally is the gene for CAR itself, *Nr1i3*. On the gene expression level, CAR is more highly expressed in untreated female mouse liver than in untreated males (Petrick and Klaassen 2007, Lu et al. 2013), which may account for some sex differences in target gene expression in the absence of ligands. However a confounding factor is the role endogenous steroid hormones play in modulating CAR activity in liver. As discussed above, the androgens androstenol and androstanol are known inverse agonists of CAR and can lower the efficacy of agonists simultaneously present, including the very potent agonist TCPOBOP (Ledda-Columbano et al. 2003). Additionally, several steroid hormones that are highly abundant in females including 17 β -estradiol and estrone can activate CAR while progesterone can inhibit CAR activity (Kawamoto et al. 2000). Sex differences in responsiveness to activated CAR at select loci in mouse liver have been studied, however analysis of genome wide transcription regulation via RNA-Seq in male and female mice has not been performed, thus limiting our understanding to a narrow field. In the 2012 study by Aleksunes and Klaassen discussed above, they found the sulfotransferase *Sult3a1* to be induced by TCPOBOP in female liver but not male liver and while *Sult2a2* was induced in both males and females, it was more highly induced in females (Aleksunes and Klaassen 2012). The multidrug resistance-associated gene *Mrp4* was also induced in both sexes but to a much higher extent in females, despite being equally expressed in both sexes basally. Interestingly, several genes in their study showed a male bias in responsiveness. The UDP-

glucuronyltransferases *Ugt2b34* and *Ugt2b35* and the aldehyde dehydrogenase *Aldh1a7* were all more highly induced in males (Aleksunes and Klaassen 2012). There also appears to be some physiological outcomes from prolonged CAR activation that are sex dependent. In 2013, Saito et al measured higher cell proliferation in female mouse livers exposed to TCPOBOP than their male counterparts and differences were partially ablated when females were treated with TCPOBOP and androstanol simultaneously (Saito et al. 2013). Given the apparent sex biasness measured at select loci, an in depth, RNA-Seq based analysis is needed to fully understand global biasness in response to activated CAR in mouse liver.

1.3.4 Role of CAR in hepatocellular carcinoma (HCC)

Men are more susceptible than women to hepatocellular carcinoma (HCC), the fifth most common form of cancer world-wide (El-Serag and Kanwal 2014). This sex bias cannot be explained by life style differences between the sexes, such as alcohol consumption and obesity (El-Serag and Kanwal 2014). Sex bias in HCC incidence is also seen in mice where females are more resistant to chemically induced HCC than males (Kalra et al. 2008), a trait that may be partially explained by sex hormones and *Foxa1/a2* (Li et al. 2012). Typical regimens for chemical induction of HCC in mice include long term treatment with a DNA-damaging carcinogen or tumor initiator, such as DEN (diethylnitrosamine), plus a non-genotoxic tumor promotor, such as phenobarbital or TCPOBOP to activate CAR (Yamamoto et al. 2004, Heindryckx et al. 2009, Li et al. 2012). HCC is not induced when

the same treatments are given to CAR-deficient mice (Yamamoto et al. 2004). In female mice, high levels of estrogens activate the estrogen receptor (ER). Foxa1-ER complexes directly regulate genes associated with tumor formation through binding in upstream enhancer regions, including the suppression of the oncogene *Myc* (Li et al. 2012). In male liver, high levels of androgen activate the androgen receptor (AR), which like ER, can also directly interact with Foxa1 (Li et al. 2012). However, unlike Foxa1-ER complexes, Foxa1-AR directly bind to DNA-replication and cell cycle related genes and elicit a pro-tumor response (Li et al. 2012). In this way, Foxa1 has both tumor protective and tumor promotion properties, depending on which steroid hormones are present. When TCPOBOP+DEN was administered to Foxa1-KO mice, female-KO mice showed a dramatic increase in tumor formation while male-KO mice showed a dramatic decrease in tumors (Li et al. 2012).

1.3.5 Long non-coding RNA (lncRNA)

Long non-coding RNAs (lncRNAs) are a class of transcribed genes that are not translated into functional protein in the cell. These transcripts are retained in the nucleus to carry out various functions as RNAs. The most well-known and characterized lncRNA, Xist, for example, is involved in establishing and spreading chromatin marks during X-inactivation. These transcripts, however, perform many functions in the cell and as many as 15,000 lncRNAs have been discovered in the human genome. Recently, our lab has published a comprehensive list of ~5,000 liver expressed lncRNAs in mice (Melia et al. 2016). However a detailed analysis of which liver expressed lncRNAs are CAR targets has been

not performed. Given many of these lncRNAs act in cis to influence the expression of genes in close proximity, it is important to understand where the CAR-responsive lncRNA transcripts are in the genome in relation to CAR-responsive protein coding transcripts. To that end, CAR-responsive lncRNAs will be assessed in both male and female mice for not only their responsiveness but also their location in the genome relative to protein coding genes.

1.3.6 Regulation of gene expression

In addition to knowing what genes are regulated by CAR in mouse liver, I am also interested in understanding how these genes are regulated. To this end, while the epigenome has been well established as playing a critical role in regulating gene expression in the cell, lncRNAs are emerging as potential candidates that help establish the epigenome. To study the dynamic changes to the epigenome, I am interested in how DNase-I hypersensitive sites (DHS) and covalent modifications to the tail region of histone H3 change in response to CAR activation in mouse liver.

DNase-I hypersensitivity sites are one of the fundamental epigenomic marks used by the cell. These areas of open chromatin are defined by their increased sensitivity to endonuclease activity due to the lack of protective histone proteins. Being devoid of histone proteins allows for the binding of transcription factors directly to specific DNA sequences which then influence expression of nearby genes, either by increasing or decreasing the

expression, or overall chromatin structure. In this way, the DHS itself can be thought of as a blank canvas for the cell to dot with transcription factors or to decorate flanking histone tails with covalent modifications to drive or halt transcription of a target gene. In this section, I will review how the cells modulate the accessibility of DHS to open a site, how we can measure their accessibility in mouse liver and the role they play in epigenetic regulation of gene expression.

1.3.6.1 Opening the genome

Chromatin is organized into tightly compacted, nearly inaccessible and transcriptionally silent heterochromatin and relatively open, accessible and transcriptionally active euchromatin. However, chromatin structure is dynamic and specific regions of the genome may rapidly switch from dense heterochromatin to open euchromatin, or vice-versa, during development or in response to stimuli if genes in those regions are needed by the cell. How the cell rapidly alters chromatin structure will be the focus of this subsection.

1.3.6.1.1 Pioneer factors

A model for opening closed chromatin is through the action of a pioneer transcription factor. Even though heterochromatin is dense and inaccessible to most DNA binding proteins like transcription factors, a sub-set of TFs can in fact bind to these regions. These factors are known collectively as pioneer factors for their ability to bind dense heterochromatin and facilitate chromatin opening to allow for other TFs to subsequently bind in neighboring

regions. Some pioneer factors, when expressed ectopically, can trigger massive rearrangement of chromatin structure which leads to a change in the cell lineage identity. In 2006, Takahashi and Yamanaka famously identified four such pioneer factors, Oct3/4, Sox2, c-Myc and Klf4 which, when overexpressed in adult fibroblast cells, can induce reprogramming of the fibroblasts into an embryonic stem cell-like state (Takahashi and Yamanaka 2006). It was later determined that this reprogramming is driven by changes in chromatin structure and in particular the rearrangement of chromatin from heterochromatin to euchromatin near genes required for maintenance of a pluripotent state and thus allowing them to be expressed (Meshorer and Misteli 2006, Gaspar-Maia et al. 2011, Iwafuchi-Doi and Zaret 2014, Soufi et al. 2015).

Several transcription factors expressed in mouse liver are known pioneer factors. Such factors include CCAAT/enhancer binding protein α (CEBP α) and β (CEBP β) (Grontved et al. 2013, Madsen et al. 2014), forkhead box A, also known as hepatocyte nuclear factor 3, (FoxA/HNF3) and GATA-4 (Cirillo et al. 2002). HNF3 and GATA-4 are factors critical in the development of fetal mouse liver as they bind to closed upstream regions of the albumin gene (Alb) and drive the opening of chromatin to facilitate expression of Alb (Cirillo et al. 2002). In adult livers, HNF3 is highly expressed and is involved in maintaining an open chromatin state at target sites (Zaret and Carroll 2011).

CEBP α and CEBP β are also highly expressed in adult mouse liver. These receptors share a common DNA binding motif and can be found at an overlapping set of binding sites in the mouse genome. Functionally, CEBP α has been shown to act as a pioneer factor in mouse adipocytes (Madsen et al. 2014) while CEBP β is required to maintain open chromatin in mouse liver (Grontved et al. 2013). CEBP α and CEBP β have been reported to interact with the nuclear receptors peroxisome proliferator-activated receptor γ (PPAR γ) and glucocorticoid receptor (GR), respectively, to facilitate NR binding to adjacent and newly accessible DHS (Grontved et al. 2013, Madsen et al. 2014). Interestingly, some ligand activated nuclear receptors themselves also show some abilities to act as pioneer factors. Activation of GR, for example, has been shown to synergistically increase the binding of ER to a nearby site by utilizing a proposed “assisted loading” mechanism, whereby rapid GR binding, recruitment of remodeling complexes and dissociation allows for subsequent binding of ER (Voss et al. 2011). However, despite the high overlap of DNA binding motifs among nuclear receptors, not all nuclear receptors appear to share pioneer factor properties. In the same study that identified GR as a pioneer factor, ER was unable to bind to closed DHS without GR first remodeling the target site and was only able to bind opened DHS (Voss et al. 2011). In this example, and in the CEBP α /PPAR γ example discussed above, pioneer factors enhance nuclear receptor binding capacity and may be critical for their full activity.

Mechanistically, pioneer factors appear to begin to facilitate the opening of closed DHS by their unique ability to bind motif half-sites found on DNA at the surface of histones (Soufi et al. 2015). In contrast, most transcription factors do not have this ability and motifs found at the surface of a histone are functionally inaccessible. Once bound, nearby chromatin is opened by the recruitment of chromatin remodeling complexes. To that end, CEBP α and GR have been shown to directly interact with the well characterized histone remodeling complex SWI/SNF, and recruit it to specific sites in the genome (Nagaich et al. 2004, Madsen et al. 2014).

1.3.6.2 Measuring DNase I hypersensitivity

One way to assess the DHS map genome wide is through a technique called DNase-Seq (Song and Crawford 2010). DNase-Seq involved digesting intact nuclei with the endonuclease DNase-I under tightly controlled conditions such that cutting by the enzyme only occurs in sites that are hypersensitive. If two such cuts are made in a region of hypersensitivity, a short DNA fragment is released and can be used to assemble a library for sequencing. Mapping sequenced reads back to the genome will then result in read pileups that correspond to the regions of hypersensitivity. However this technique does have limitations as precise digestion conditions are needed to map true DHS. If the nuclei are over digested, long DNA fragments resulting from cutting outside of a DHS will be released. Subsequent mapping of these long fragments leads to a lawn of reads that may dampen the signal coming from true DHS. Under digestion, however, can be equally

problematic as the chances of having two cut sites in a single DHS is reduced and thus long fragments spanning at least one nucleosome are also produced.

1.3.6.3 DHS mark DNA regulatory elements

In 2012, the human ENCODE consortium published a study that attempted to map all DHS in the human genome by performing DNase-Seq across 125 human derived cell lines (Thurman et al. 2012). They reported close to 3 million DHS were found in at least one cell line and close to 2 million of those were found in at least two lines while only ~3,000 were ubiquitously found in all cell lines. The authors determined that while promoters for a given gene were highly accessible across many cell types, accessibility at distant enhancers were cell line specific (Thurman et al. 2012). This suggests that many genes are primed for transcription with open TSS regions and are waiting for the correct cues from distal enhancers to be transcribed. The authors of the human ENCODE study also mapped DHS to their target genes by chromosome conformation capture carbon copy (5C) and chromatin interaction analysis with paired-end tag sequencing (ChIA-PET). They found regulation of target genes by DHS is incredibly complex; 37% of promoters interacted with 20 or more distal DHS and 52% of DHS interact with 2 or more distal promoters (Thurman et al. 2012).

1.3.6.4 Chromatin marks

Promoters, enhancers and other distinct DNA regulator elements can be identified by the combination of histone marks and DHS present at a given loci and the given loci's proximity to the nearest gene. For example, promoters are located directly upstream of a genes TSS and are marked by H3K4me3 (Sugathan and Waxman 2013, Shlyueva et al. 2014). An active promotor, or a gene that is actively being transcribed, is associated with the acquisition of H3K27ac and is marked by the combination of H3K4me3, H3K27ac and DHS. Similarly, the acquisition of H3K27me3 at the promotor and the combination of H3K4me3 and H3K27me3 without a DHS or with a DHS mark inactive or poised promoters, respectively (Sugathan and Waxman 2013, Shlyueva et al. 2014). Distal regulatory elements such as enhancers can also be characterized by the histone modifications present at H3K4 and H3K27. Inactive enhancers are generally marked with H3K4me1 and do not contain a DHS. Activation of such enhancers is associated with acquisition of H3K27ac and subsequent opening of a DHS to facilitate transcription factor binding (Shlyueva et al. 2014). Poised and latent enhancers are two additional classes of enhancers that have been recently characterized. Poised enhancers tend to have both activating (H3K4me1) and repressive (H3K27me3) marks and acquire DHS and H3K27ac and lose H3K27me3 when activated (Creyghton et al. 2010, Sugathan and Waxman 2013, Shlyueva et al. 2014). Latent enhancers lack any histone mark at H3K4 or H3K27 (Ostuni et al. 2013). When activated by a stimulus, these loci slowly acquire H3K4me1, H3K27ac and a DHS. Interesting, when the stimuli is removed, the H3K4me1 mark is retained while

H3K27ac is lost and the DHS is closed, marking the site as an inactive enhancer. When re-challenged with the same stimulus, the acquisition of H3K27ac and activation of the enhancer is more rapid, indicating a short-term memory is established by the persistent presence of H3K4me1 (Ostuni et al. 2013). By assaying for the global changes to H3K4me, H3K27ac, H3K27me3 and DHS following CAR activation, we can characterize the dynamics of many of these types of DNA regulatory elements in mouse liver. By then mapping these regulatory elements to their presumed gene targets (protein coding or non-coding) we can get a better understanding of how these target genes are regulated.

1.4 Thesis goals and hypotheses

This thesis contains three major goals and hypotheses that are novel and will advance the fields of endocrine disruption by xenoestrogens and epigenetic regulation of coding and non-coding RNAs by nuclear receptors. In Chapter 2, I characterize the impact of BPA on the developing male mouse reproductive system. To achieve this, male mice have been exposed to BPA during embryonic development and markers of male reproductive health were assayed for during their postnatal lives. In Chapter 3, I determine the sex dependent regulation of coding and non-coding genes in mouse liver by CAR. To achieve this, male and female mice were exposed to TCPOBOP for 3 or 27h and liver RNA was collected and sequenced. Expression of coding and non-coding RNAs in the presence or absence of TCPOBOP in these mice was then measured. In Chapter 4, I determine the regulation of mouse liver chromatin accessibility, histone modifications and associated early gene

responses by CAR. To achieve this, male mice were exposed to TCPOBOP for 3h and livers were collected. Chromatin accessibility in these livers was measured by DNase-Seq and global maps of histone modifications and transcription factor binding was determined by ChIP-Seq. These changes to the mouse liver epigenome were then associated with gene expression changes measured in Chapter 3.

Fig. 1.1 Non-monotonic dose-response. A non-monotonic dose-response is seen in GH3/B6/F10 pituitary tumor cells exposed to a wide range of BPA. Strong ERK phosphorylation (activation) peaks at two different dose ranges separated by a period of no ERK activation by BPA. Figure adapted from Watson et al (2010).

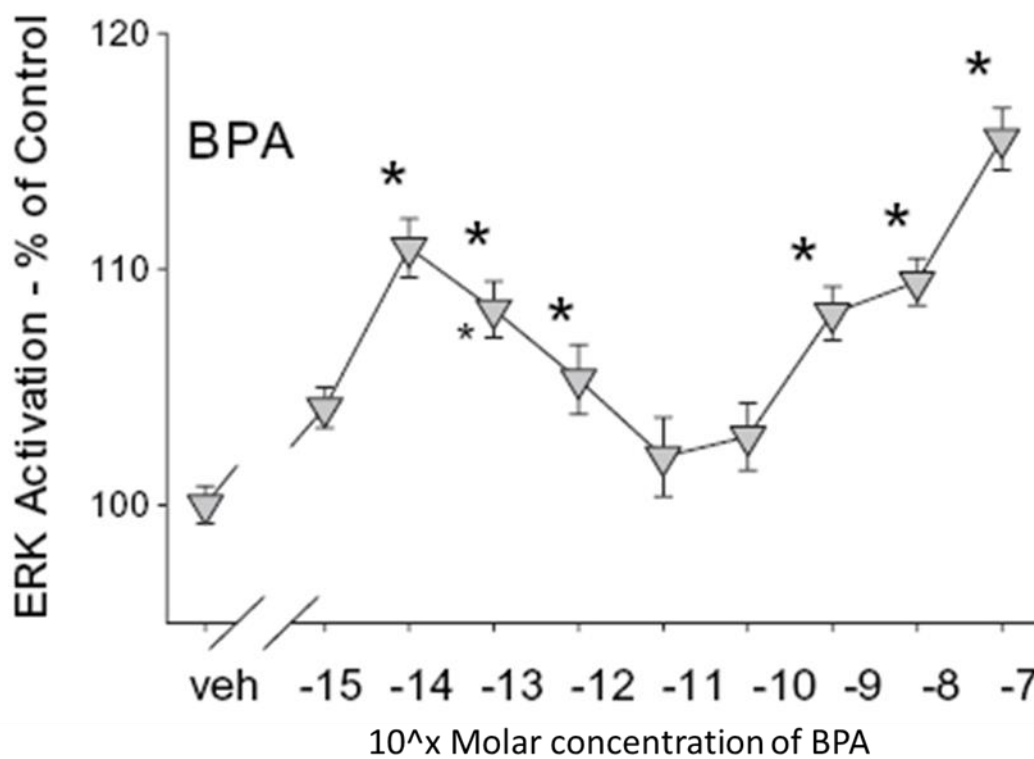
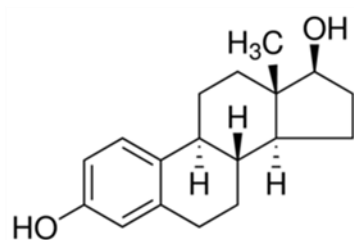
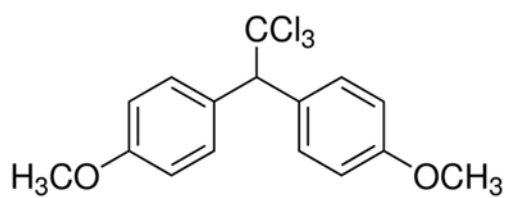
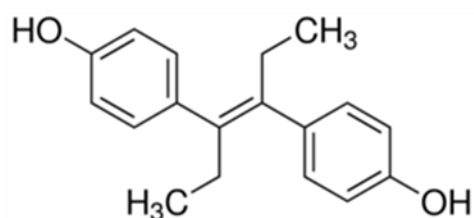


Fig. 1.2 Chemical structures. Chemical structures of estradiol (E2), diethylstilbestrol (DES), methoxychlor (MXC) and bisphenol A (BPA).

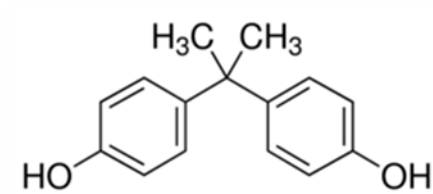
Estradiol (E2)



Diethylstilbestrol (DES)



Methoxychlor (MXC)



Bisphenol A (BPA)

Fig. 1.3 Testis development. Development of a testis in male mice is driven by SF1, SRY and SOX9 during a critical window around embryonic days 10-12. Adapted from Sekido et al (2009)(Sekido and Lovell-Badge 2009)

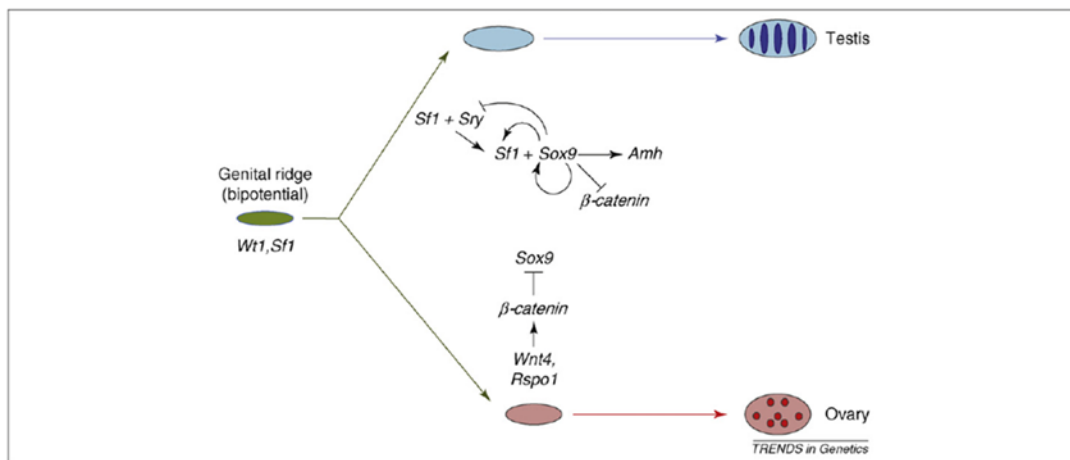
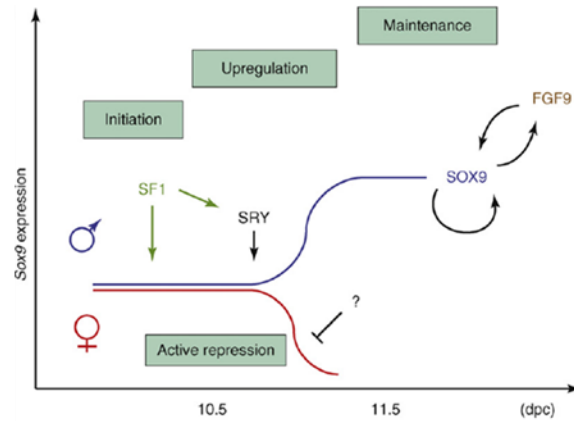


Fig. 1.4 Male germ cell development. Primordial Germ Cells (PGC) are first specified (GC spec) by embryonic day 7.5 (E7.5) in the mouse and they migrate (GC MI) to the genital ridge (GR) soon after. PGCs mature into gonocytes (GCY) and enter mitotic arrest (MA) during the last stages of development before birth. During embryonic development, a massive reprogramming of their epigenome occurs. In the adult, spermatogenesis begins with spermatogonia type A (SGA) cells, which themselves have many subtypes. Spermatogonia stem cells (SSCs; A_s) self-renew (SR), and through mitosis produce Apaired cells (A_{pr}), Aaligned (A_{a14} and A_{a18}), A_1 - A_4 , Intermediate (Int) and type B (SGB). Meiosis I yields spermatocytes, which going through multiple cell stages, including: Preleptotene cells (PI), leptotene (L), zygotene (Z), pachytene (P), and diplotene (D). Meiosis II yields haploid round spermatids (RS) and development from this point forward is exclusively called spermiogenesis. During spermiogenesis, nucleosomes are replaced by transition proteins (TP) and protamines resulting in an ultra-compact nucleus by the elongated spermatid (ES) stage. Adapted from Godmann et al (2009).

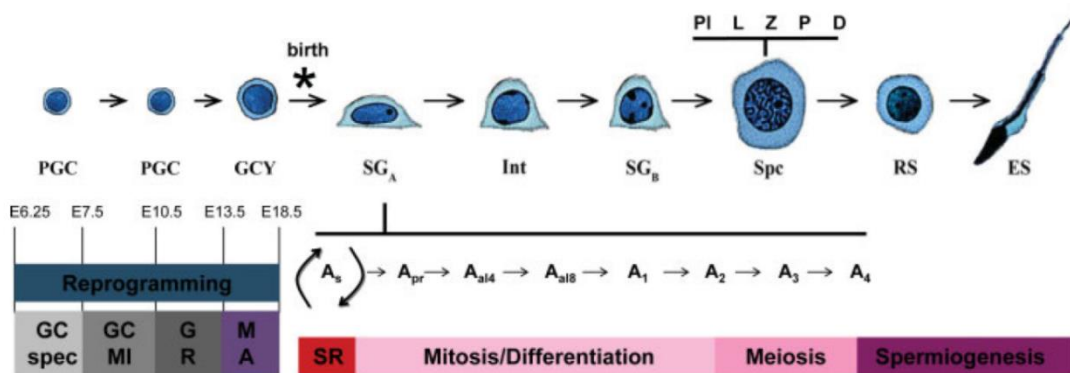


Fig. 1.5 Chemical structures of CAR agonists. Chemical structures of CAR agonists TCPOBOP, CITCO, phenobarbital and inverse agonists androstanol and androstenol.

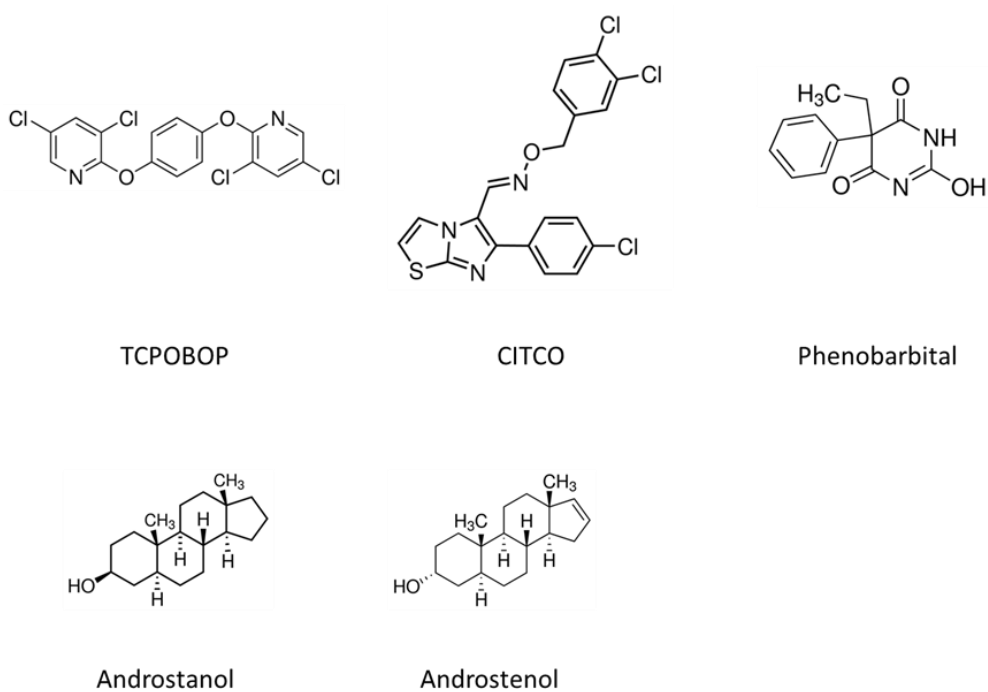


Fig. 1.7 Indirection activation of CAR. Indirect activation of CAR by phenobarbital vs direct activation of CAR by TCPOBOP. Figure adapted from Yang et al (2014) (Yang and Wang 2014)

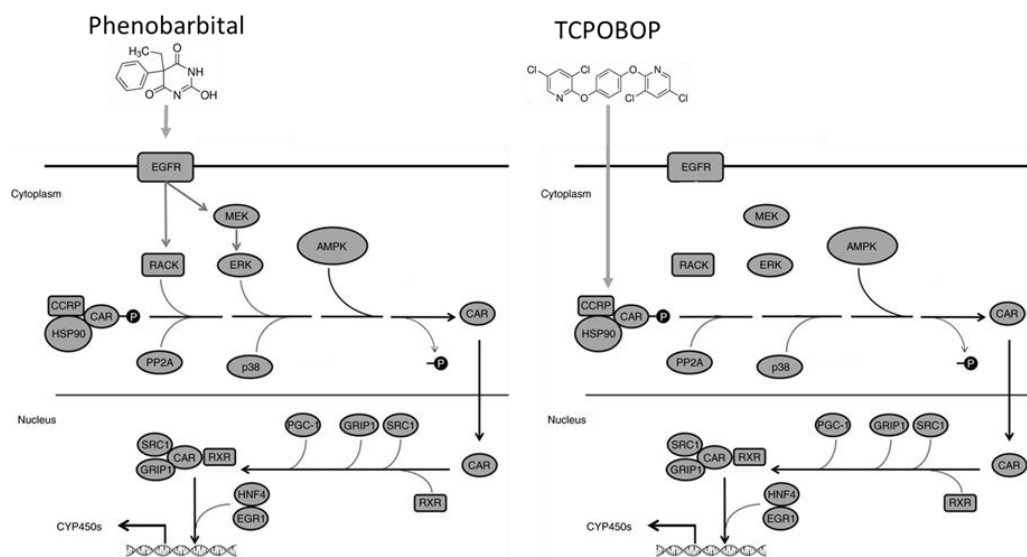
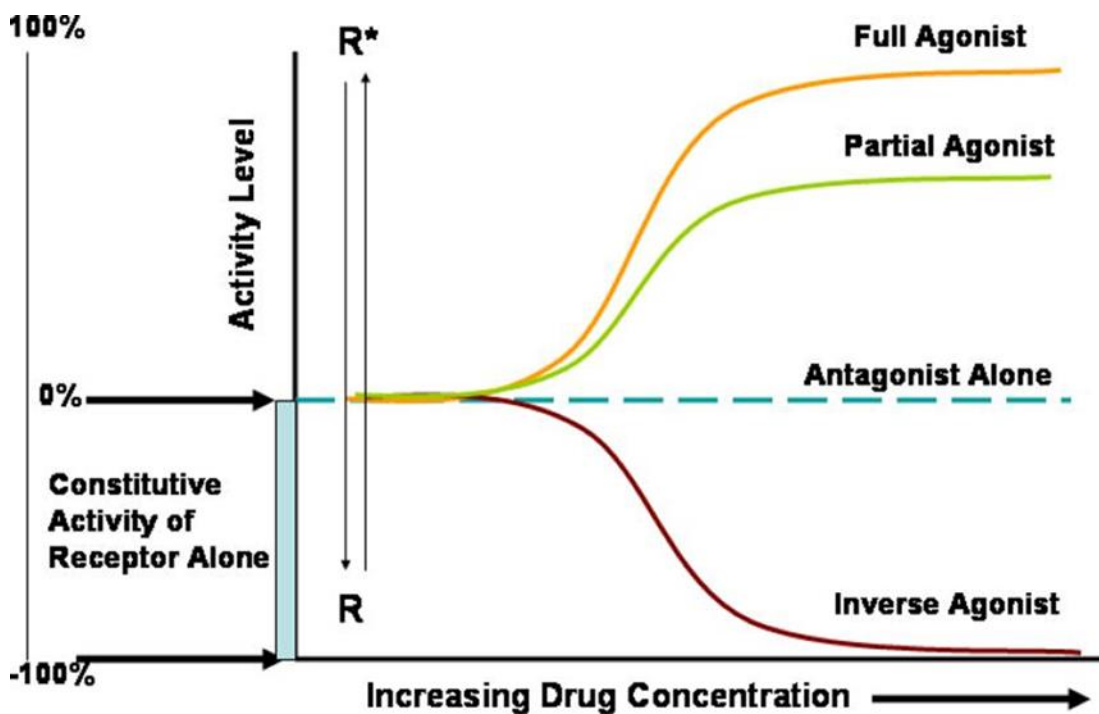


Fig. 1.8 Agonists, antagonists and inverse agonist. Schematic view of how agonist, antagonists or inverse agonist can modulate the activity of a receptor that is constitutive active, like CAR. Adapted from Hanania et al (2010) (Hanania et al. 2010).



CHAPTER 2- Impact of Prenatal Bisphenol A Exposure on the Young Adult Male Mouse Reproductive System

2.1 Abstract

During male mouse embryogenesis, critical events occur which convert the bipotential gonads into testes. The gonads are particularly vulnerable to environmental chemical exposure during this developmental period, which could lead to long-term, deleterious effects on the reproductive system. In this chapter, we investigated whether changes to the anatomy, testis histology, or gene expression occur in young adult male CD-1 mice following *in utero* exposure to BPA. Mice were exposed from day E9-E18, inclusive, at doses of 5, 50 and 500 μg BPA (dissolved in corn oil)/kg dam body weight/day *via* oral bolus. Other groups of mice were exposed to 5 μg diethylstilbestrol (DES)/kg dam body weight/day as a positive control or to corn oil only, as a vehicle control. Mice were euthanized on PND28 or PND49 for gene expression analysis and anatomical measurements and on PND49 or between PND63 and PND80 for sperm counts. Modest anatomical changes were seen in the xenoestrogen-exposed offspring. Anogenital distance decreased in PND49 mice exposed to BPA (500 $\mu\text{g}/\text{kg}$ dose) compared to unexposed controls. No decrease in sperm count or change in testis histology was seen in any of the exposed groups at any age tested. Microarray analysis performed on pooled whole testis tissue RNA identified candidate genes that respond to xenoestrogen exposure, however,

none of the genes tested were validated by qPCR due to high individual variation within control and xenoestrogen-exposed pools. In conclusion we found little to no long-term effect of a short, *in utero* BPA exposure to the male mouse reproductive system during gonadogenesis at the doses of BPA tested.

2.1 Introduction

Endocrine disrupting compounds (EDCs) are broadly defined as compounds that have the ability to interfere with endogenous hormone signaling. Determining the long-term effects of an exposure to low doses of an EDC is vital to human risk assessment as EDCs often do not show immediate adverse effects and exhibit nonmonotonic dose response (NMDR) pharmacokinetics, particularly if the compound sufficiently mimics a natural hormone in its structure and activity (Vandenberg et al. 2009). Therefore, studying EDCs by classical methods which include exposing adult animals to high doses and measuring immediate effects such as cytotoxicity and carcinogenicity may mask activities of EDCs manifested at much lower doses. A specific class of EDCs, known as xenoestrogens (XEs), are synthetic chemicals that mimic endogenous estrogens and as such have the capacity to bind to and activate estrogen receptor (ER) α or ER β , or estrogen-related receptor (ERR) γ (Montes-Grajales and Olivero-Verbel 2013, La Rosa et al. 2014, Yiu et al. 2014).

Bisphenol A (BPA) is a synthetic chemical that has been used in the production of strong, clear polycarbonate plastics and epoxy polymers since the 1950's. Polycarbonate plastics

synthesized from BPA are ubiquitous and found in a wide range of products including CD/DVDs, eyeglasses, plastic water coolers and baby bottles while BPA epoxy resins are used as dental sealants and also coat the interiors of canned food (source: CDC.gov; NIH.gov). Due its durability and broad applications, BPA plastics are in very high demand and thus 6+ billion pounds of bisphenol A (BPA) is produced globally each year (Kang et al. 2011, Manfo et al. 2014). BPA is currently thought of as a potential XE and EDC and is an active area of research. The current human reference dose of BPA (i.e. the dose that is considered safe for human exposure) was established using traditional linear pharmacokinetics without considering possible endocrine disrupting and natural hormone mimic behaviors (vom Saal and Welshons 2006). Studies conducted by the National Toxicology Program (NTP) in 1982 indicated that BPA was not carcinogenic at 50 mg/kg bw/day in a rat chronic oral exposure via food bioassay (Vogel 2009), and the US Environmental Protection Agency subsequently applied an uncertainty factor of 1000 to the lowest observed effect level of 50 mg/kg bw/day and established the human reference dose as 50 µg/kg bw/day (vom Saal and Welshons 2006).

The effects of exposure to BPA in rodent models are controversial. BPA was originally identified as an EDC in male and female mouse reproduction (vom Saal et al. 1998) but other reports conflict with that finding (Myers et al. 2009, Gray et al. 2010, vom Saal et al. 2010). Gray (Gray et al. 2010), Ryan (Ryan et al. 2010) and Tyl (Tyl et al. 2002, Tyl et al. 2008, Tyl 2009) report no significant effects of BPA in rodents using both *in utero* and

adult exposure models. However, these results may be due to the use of the estrogen-insensitive Long-Evans rat which then lead them to use inappropriately low doses of both BPA and their positive control ethinylestradiol (vom Saal et al. 2010). Additionally, polycarbonate cages, which are made from BPA plastics, were used to house the rats used in the experiment and thus are a source of uncontrolled contamination (vom Saal et al. 2010). LaRocca (LaRocca et al. 2011) exposed C57/Bl6 mice, an estrogen sensitive mouse strain (Wadia et al. 2007), to 50 µg BPA/kg body weight/day and 1000 µg BPA/kg body weight/day and found little effects on the male reproductive tract. However, other animal models and exposure windows have found an impact of BPA on the male reproductive tract. Several recent studies found BPA exposure altered testicular histology (Fisher et al. 1999, Atanassova 2000, Chitra et al. 2003, Takahashi and Oishi 2003, Naciff et al. 2005), sperm physiology (vom Saal et al. 1998, Sakaue et al. 2001, Al-Hiyasat et al. 2002, Chitra et al. 2003, Takahashi and Oishi 2003, Toyama and Yuasa 2004) highlighting a need for further research in this field.

Diethylstilbestrol (DES) is a potent XE and was commonly prescribed to pregnant women in the United States and Europe from the 1941 to the 1970 to prevent miscarriages and premature births (Rubin 2007). However, after DES exposure was found to be associated with cervical and vaginal cancers in women prescribed the drug, the FDA banned the use of DES in 1971 (Rubin 2007). Male and female children exposed *in utero* to DES showed high incidences of infertility as adults as well as reproductive tract cancers (Newbold et al.

1985, Palmlund 1996, Nikaido et al. 2004, Newbold et al. 2007, Vandenberg et al. 2009). Studies using rodent models have linked these deleterious effects to a critical window of gonadal development in which exposure to DES can permanently disrupt tissue development and overall reproductive success of the organism (Colborn et al. 1993, Gupta 2000, Nikaido et al. 2004, Rubin 2007, Soto et al. 2013).

Embryonic day 9 (E9) through E18 is a critical window of gonadal development as the bipotential gonads develop into either the testes in male mice or ovaries in female mice. Exposure to EDCs during this window can lead to reduced reproductive success due to subfertility (Salian et al. 2009), altered steroid hormone biosynthesis capacity (Naciff et al. 2005, Ikeda et al. 2008), and external genitalia malformation (Gupta 2000, Honma et al. 2002, Golub et al. 2010).

First, we aimed to determine the long term, persistent changes to the anatomy and physiology of young adult mice following *in utero* exposure to BPA during a critical period of embryogenesis. Second, we aimed to measure changes in testis gene expression in young adult male mice following XE exposure using the same model. The window of exposure chosen for these experiments, E9 through E18, inclusively, fully encompasses the period of sex determination and embryonic gonadogenesis. We found minimal changes in whole mouse body weight (BW), abundance of epididymal white adipose tissue (WA), anogenital distance (AGD), and sperm count following BPA or DES exposure while no changes in

gene expression were consistently measured using global microarray analysis or targeted quantitative real time PCR (qPCR).

2.3 Methods

2.3.1 Animals

CD-1 mice were purchased from Charles River and housed in polysulfone cages with polysulfone water bottles and metal food containers. Mice were subject to a 12 hour light: 12 hour dark cycle and fed a controlled phytoestrogen diet. Harlan Teklan (Madison, WI) 2920x low phytoestrogen feed (<20 ppb and ≤ 20 mg total phytoestrogen per kg feed) and drinking water prepared using an APEC Water (Industry, CA) RO-90 Ultra Reverse Osmosis system were provided *ad libitum*. Prior to breeding, body weight measurements were recorded for seven days to establish a baseline and used as a secondary indicator of pregnancy following copulation. Pairings were set up in the evening and the presence of a vaginal plug was checked early the next morning. Presence of a plug denoted embryonic day 1 (E1). Body weight was monitored daily throughout pregnancy and weight data from E1 though E9 was used as a secondary indicator of pregnancy. BPA obtained from the NIEHS and DES obtained from Sigma-Aldrich were dissolved in tocopherol stripped corn oil at concentrations of 5 μg , 50 μg , or 500 μg BPA/mL and 5 μg DES/mL. BPA or DES solutions, or corn oil alone (vehicle control), were administered via oral bolus at a volume of 1 μl /gram body weight, from E9 though E18 daily, for a final dose of 5 μg , 50 μg , or

500 µg BPA/kg dam body weight/day and 5 µg DES/kg dam body weight /day. Day of delivery was denoted PND1 and pups were weaned and separated by sex at PND21.

2.3.2 Anatomical measurements and organ weights

Male pups were sacrificed by cervical dislocation at PND28 and PND49. Body weight (BW) was measured at time of sacrifice and anogenital distance (ADG) was measured with a digital caliper (Fisher Scientific). Epididymal white adipose (WA) tissue was removed and weighed. Paired testes were removed, weighed and placed in *RNAlater* before flash frozen in liquid nitrogen and stored at -80°C prior to RNA isolation.

2.3.3 Mature spermatozoa counts

Paired caudal epididymes were removed, placed in DMEM media pre-heated to 37°C, and weighed. The tissue was scored several times with a razor blade before being placed in a 15 mL conical tube with media and incubated in a 37°C water bath for 10 minutes. The tube was inverted three times and the media containing sperm was removed. Media containing live spermatozoa was diluted 1:5 in sperm fixation solution (5% Sodium bicarbonate, 0.3% paraformaldehyde) and counted on a hemocytometer.

2.3.4 Histology

In select litters, the left testis was removed and placed in modified Davidsons Fixation solution (Latendresse et al. 2002) at 4°C overnight. The tissue was rinsed with PBS and

placed in 70% ethanol at 4°C prior to paraffin wax embedding. 5 µM longitudinal sections were made on a Leica (model) microtome and stained with hematoxylin and eosin Y using a BioGenex i6000 Autostainer (Fremont, CA) for histological analysis.

2.3.5 qPCR and Microarray

Whole right testes were homogenized in TRIzol reagent (Life Technologies) and RNA was extracted according to the manufacturer's protocol. RNA was quantified using a NanoDrop (ND-1000) instrument. Approximately 500 ng of total RNA were loaded on to an Agilent RNA 6000 Nano chip and run on a Bioanalyzer 2600 (Agilent Technologies) to measure the RNA Integrity Number (RIN). Samples with a RIN ≥ 8.0 were considered good quality with minimal degradation and used in microarray analysis. Samples were pooled into two biological replicate pools per age group per exposure. Pools contained between 5 and 14 individuals representing between 2 and 4 litters. Dye labeling (Alexa 55 and Alexa 647), microarray hybridization (Agilent Whole Mouse Microarray, 44k v1 platform), chip scanning, and data extraction were performed at Wayne State University. A dye swap strategy was implemented to eliminate dye bias. Rosetta resolver was used to generate fold change and p-values. A threshold of absolute fold change ≥ 2 and $p > 0.005$ was used to identify regulated genes.

Quantitative real time PCR (qPCR) was used to validate the results of the microarrays. Primer Express v2.0 (Applied Biosystems) was used to design primers against target genes.

cDNA was synthesized from an aliquot of RNA pools submitted for microarray analysis. Power SYBR Green PCR Master Mix reagent (Applied Biosystems) and an Applied Biosystems 7900 Real Time, 384 well format PCR instrument was used for qPCR analysis. Ct values were determined using SDS software v3.0 (Applied Biosystems). Primers designed against the 18S RNA were used for normalization and the $\Delta\Delta\text{CT}$ method was used for relative quantification between samples. A t-test was used to determine significance between pairs of exposures. Primer sequences used are listed in Table 2.

2.3.6 Statistical Analysis

All statistical analyses were performed in IBM SPSS Statistics 20. In most experiments, an ANOVA with a Bonferoni post hoc test to correct for multiple comparisons was first performed to determine if there was a significant change between the vehicle control group and any exposure, as well as changes between any two given exposures. An ANCOVA was performed to determine if there was a change in body weight between exposure groups. Litter size was factored into the analysis as a covariate, given the inverse relationship between litter size and body weight. A Bonferoni post hoc test was used to correct for multiple comparisons with a p-value cut off set to 0.05.

2.4 Results

2.4.1 Litter size is not impacted by BPA or DES

We first evaluated the effects of *in utero* BPA or DES exposure on overall litter size. Dams were exposed to BPA (5, 50, or 500 μg BPA/kg dam body weight) or DES (5 μg DES/kg dam body weight) daily via oral bolas from E9 through E18, inclusively. A schematic overview of the experimental design is outlined in Fig. 2.1. Male pups per litter, as well as total litter size, were counted at time of weaning to insure accuracy in sex determination. Results are presented in Fig. 2.2. No significant difference was measured in either total litter size or number of male pups per litter, as determined by ANOVA. Vehicle control treated litters had 12.2 pups on average with 5.8 males per litter while BPA treated litters ranged between 11.5-12.2 pups per litter with 6.2-7.3 males per litter for the three exposures. Litter sizes from the DES treated dams averaged 11.8 pups with 6.2 males per litter.

2.4.2 Anatomical markers show minimal impact following BPA or DES exposure

To assess changes to the general anatomy of male pups exposed to XEs, we examined several endpoints known to be affected by endocrine disruption, including total body weight, anogenital distance (AGD), which is controlled by androgen signaling during embryonic development and puberty and is commonly used as a marker of reproductive health in males (Thankamony et al. 2016), and abundance of epididymal white adipose tissue, which is controlled by estrogen signaling (Cooke et al. 2001, Cooke and Naaz 2004,

Pallottini et al. 2008). Anatomical measurements were taken at PND28 to represent adolescent stage while PND49 to represent sexually mature, young adult mice. At PND28, mice exposed *in utero* to 50 μg BPA were on average 2.4 grams heavier than unexposed controls of the same age. The mean body weight of control mice at PND28 was 22.6 grams (± 2.67 grams; $n=30$) and the average body weight of exposed mice was 25.0 grams (± 2.00 ; $n=18$). Significance was determined by an ANCOVA, which considered litter size as a co-variant, followed by a Bonferoni post hoc test, as body weight and litter size are inversely proportional in young mice. A statistically significant change was only seen in mice exposed to 50 μg BPA but not at a lower dose of 5 μg BPA or a higher dose of 500 μg BPA, indicating a non-monotonic dose response to BPA (Fig. 2.3). At PND28, there was no change to AGD or white adipose tissue accumulation, thus no evidence of endocrine disruption of the estrogen or androgen signaling pathways was observed at this time point.

By PND49, the significant differences in BW between 50 μg BPA and vehicle controls seen at PND28 was abolished. However, there was a significant decrease in the AGD of PND49 mice exposed to the 500 μg dose, although no change was seen at any other dose. Mice exposed to 5 μg DES had on average a shorter AGD at PND49 but the results were not significant. Given these changes were not seen at PND28 and were only manifested in the older animals, this suggests a delay brought on by puberty and potential blockage in the androgen biosynthesis pathway. A significant change in abundance of white adipose tissue in the epididymal fat pad was not measured by either BPA or DES at PND49.

2.4.3 Testis histology is unchanged by BPA or DES

Next, we analyzed the testis morphology and cellular organization of the seminiferous tubules in adolescent and adult male mice to determine if BPA or DES impacted spermatogenesis on the cellular level. Testes from mice exposed *in utero* to BPA or DES at PND28 or PND49 were fixed in modified Davidson's fixative overnight and stored in 70% ethanol. Tissues were embedded in paraffin and 5 μm sections were stained with Harris hematoxylin and eosin Y (Figure 3.4). Tissues were examined visually for changes in gross morphology, including Sertoli cell only (SCO) tubules, empty tubules, sloughing off of germ cell layers, or disruption of Leydig cell. Representative images of the vehicle control group and the BPA treated groups are shown in Fig. 2.4. No changes in morphology or testis histology were evident in any group examined.

2.4.4 Assessing sperm production in male mice exposed to BPA or DES *in utero*

To assay the impact of an *in utero* BPA or DES exposure on male fertility, mature spermatozoa were counted in vehicle control, 500 μg BPA, or 5 μg DES exposed mice at PND49 or at PND63-80. Mice at PND28 are not sexually mature and produce enough mature spermatozoa to count. Mature spermatozoa are stored in the caudal epididymes of male mice, thus the epididymes were excised, scored with a blade, and placed in pre-heated DMEM media. Following a 10 minute incubation, the supernatant was collected, diluted with a fixing solution containing 5% sodium bicarbonate and 0.3% paraformaldehyde, and

fixed spermatozoa counted on a hemocytometer. No changes to spermatozoa count were observed when the data were when normalized to either the paired epididymal weight or to the paired testes weight as a quantification of production efficiency (Fig. 2.5).

2.4.5 Global transcriptional responses to *in utero* BPA or DES exposure-

Microarray analysis was performed to assess the global gene expression changes in the juvenile and young adult mouse testis following *in utero* 50 or 500 μg BPA or 5 μg DES exposure. Genes with $|\text{fold change}| > 2$ with a $p\text{value} < 0.005$ were considered significant. At both PND 28 and PND49, more genes were dysregulated in the 500 μg BPA group (114 and 121 genes, respectively) compared to the 50 μg BPA group (74 and 68 genes, respectively), reflecting the higher dose of drug exposure (Fig. 2.6). However, there is minimal overlap between the two doses of BPA and the two time points (Fig. 2.6A). At PND28, 16 genes are in common between the 74 genes regulated by the 50 μg BPA dose and the 114 genes regulated by the 500 μg BPA dose. Similarly, at PND49, 5 genes are common between the 68 genes regulated by the 50 μg BPA dose and the 121 genes regulated by the 500 μg BPA dose. Additionally, there is little overlap between the two times points of a given dose with only 19 genes in common at the 50 μg BPA dose and 16 genes in common at the 500 μg BPA dose (Fig. 2.6B). Thus, unique sets of genes are regulated in the four BPA treated groups with little overlap between them. As a comparison, gene expression changes were measured following a DES exposure at PND28. A total of 330 genes were regulated by DES, which represents the largest set of genes out of the five

EDC exposure groups. Of these 330 genes, 38 overlap with either dose of BPA at PND28 and 292 are unique to DES (Fig. 2.6A).

2.4.6 KEGG pathway analysis of regulated genes

KEGG pathway analysis was performed using DAVID (david.ncifcrf.gov; version 6.8). Pathways enriched for genes regulated by BPA or DES with a minimum pvalue of 0.05 are presented in Table 2.1. At the 50 µg BPA dose, the cAMP pathway is the only KEGG pathway enriched at PND28 while Insulin secretion and ErbB signaling pathways were enriched at PND49. At the 500 µg BPA dose, Steroid hormone biosynthesis and related pathways involving drug and retinal metabolism were enriched at PND49 while no pathways were identified at PND28. Despite many more genes dysregulated by DES, the pyrimidine metabolism pathway was the only enriched pathway in the DES dysregulated genes.

2.4.7 qPCR validation of gene responses measured by microarray

To validate the results from the microarray experiments, a total of 21 genes were selected from the gene lists for validation by qPCR. Results from *Hdac9* and Apolipoprotein C-III (*Apoc3*) are shown and represent the group of genes tested (Table 2.2; Fig. 2.8). Additional genes of interest were selected based on their importance in steroid hormone biosynthesis (Inhibin beta B; *Inhbb*) or testis organogenesis (GATA Binding Protein 4, Inhibitor of DNA Binding 2; *Gata4*, *Id2*). Representative data are presented in Fig. 2.7. None of the

genes tested by qPCR showed any significant dysregulation by either BPA or DES, as determined by ANOVA followed by a Bonferoni Multiple Comparison post-hoc test. Finally, the expression of steroidogenic acute regulatory protein (*Star*) mRNA was measured in the testes of individual mice at PND28 (Figure 2.8). The individuals used were the same individuals used to construct the pools used in the microarray experiments as well as in previous qPCR experiments. No statistically significant change in expression of *Star* was measured.

2.5 Discussion

The development of plastic is one of the most significant advances of the 21st century and has undoubtedly had a positive impact on many in the developed world. However, the ever expanding use of plastics today comes with increasing exposure to chemicals used in their manufacturing, including BPA. Human exposure to BPA is ubiquitous, with at least 90% of all urine samples and 75% of all nursing mothers breast milk contained detectable amounts of both free and conjugated BPA (Calafat et al. 2005, Meeker et al. 2010, Nahar et al. 2012, Mendonca et al. 2014).

Perhaps related to the ubiquitous present of plastics, obesity in the United States, particularly in children, is on the rise. According to the CDC, as of 2010 upwards of 37% of adults and 17% of children are classified as obese, which puts them at risk of several life threatening diseases (www.cdc.gov). One possible explanation for the rise in obesity is the

increased exposure of the human population to EDCs and XEs. Estrogen and EDCs have a well-established role in regulating body weight and adipose tissue in humans (Cooke and Naaz 2004, Newbold et al. 2007). BPA specifically been shown to lead to obesity in mice (Rubin 2011). We measured total body weight and abundance of white adipose tissue from the epididymal fat pad. At PND28, pup body weight significantly increased after *in utero* exposure to 50 µg BPA/kg from 22.6 grams in controls to 25.0 grams. However, by PND49, although mice from this exposure group are slightly heavier, the increase is not statistically significant. To calculate significance, an ANCOVA followed by a Bonferroni poc hoc test was performed. The ANCOVA was chosen to factor in litter size as a covariant, because pup body weight, particularly in young mice, is inversely proportional to the size of the litter. On a molecular level, the abundance of Apolipoprotein C3 (*Apoc3*) mRNA was measured in our samples at PND28 and PND49. Deletion of *Apoc3* in mice has been shown to induce obesity via an increase in adipose tissue and fatty acid uptake from plasma triglycerides (Duivenvoorden et al. 2005). In this study, we measured no significant change in *Apoc3* mRNA between controls and any exposure group.

The most critical endpoint of the male reproductive system is production of healthy, mature spermatozoa. In 2012 human sperm production worldwide was found to be decreased (Rolland et al. 2013) and could be due to the increasing EDC and XE exposure. The role of BPA in inhibiting spermatogenesis remains controversial. In an early study identifying BPA as an endocrine disruptor, vom Saal established BPA's potential for lowering sperm

count and sperm production in rodents (vom Saal et al. 1998). However in a subsequent study, no change in germ cell apoptosis or testis pathophysiology were measured (Larocca et al. 2011). We examined several male reproductive health endpoints following *in utero* exposure to BPA. Mature spermatozoa from adult mice in this experiment were collected from the caudal epididymis. Mice were grouped into two separate age cohorts. Postnatal day 49 mice represented a cohort that was at the beginnings stages of fertility and PND63-80 represent an age group of mice that are fully mature and fertile. We normalized the sperm counts per gram epididymis as a measure of storage capacity and also per gram paired testes as a measure of production. No change in sperm counts were measured at any age and in any exposure group compared to controls. In addition, seminiferous tubules were examined by cross sectioning mouse testis and staining with hematoxylin and eosin. No gross changes in tubule structure were seen.

In males, anogenital distance is established during embryogenesis and elongation is driven by androgens, particularly 5α -dihydrotestosterone, during puberty and is a marker for male reproductive health (Welsh et al. 2010). Recent studies have linked decreased AGD with decreased circulating serum testosterone levels and testicular dysfunction in humans (Eisenberg et al. 2012). In the male mice, the onset of puberty occurs between PND27 and PND34 (Varney et al. 1991) and in our experiments PND28 mice represent a prepubescent mouse while PND49 mice have already undergone puberty. AGD was measured at the time of euthanasia in all mice included in our experiments. At PND28, no significant change in

AGD was measured in any treatment group relative to controls. However, at PND49 the mice exposed *in utero* to 500 µg BPA/kg body weight had significantly shorter anogenital distances than controls. Additionally, the AGD from these mice was unchanged from their PND28 counterparts indicating a stunting of elongation during puberty which may be due to a disruption of testosterone production. To examine this at a molecular level, we measured testis mRNA levels of several members of the steroid hormone biosynthesis pathway in the testis of exposed mice. The conversion of plasma cholesterol to androgens is achieved by the protein products of three genes, *Star*, *Cyp11a1* and *Cyp17a1* (Hanukoglu 1992). *Star* is responsible for the cellular uptake of cholesterol and is the rate limiting step in the conversion of cholesterol to steroid hormones. The protein product of the *Cyp11a1* gene, cholesterol side-chain cleavage enzyme, converts cholesterol into pregnenolone. 17α -hydroxylase, the protein product of the *Cyp17a1* gene, then converts the pregnenolone or progesterone into their 17α -hydroxy derivatives. 17α -hydroxypregnenolone or 17α -hydroprogesterone can then be further modified by 17α -hydroxylase to the two androgens dehydroepiandrosterone and androstenedione respectively. Steroidogenesis is under the control of a negative feedback loop initiated by inhibin B secretion, coded by the *Inhbb* gene, from steroidogenic Leydig cells. Expression of *Star* and *Cyp11a1* has been shown to be down regulated by BPA in cultured mouse antral follicles cells, resulting in reduced steroid hormone production (Peretz and Flaws 2013), while CYP17A1 activity in human and rat testis microsomes is decreased following BPA exposure (Ye et al. 2011). Inhibin B levels have been shown to be decreased in men associated with urinary BPA concentration

(Meeker et al. 2010). In this chapter, we measured the mRNA expression of *Star*, *Cyp11a1*, *Cyp17a1* and *Inhbb* genes by qPCR at PND28 and PND49. The expression of *Star* was variable among individuals and no clear regulation was seen between the control group and mice exposed to 500 µg BPA/kg body weight. The results are similar for *Cyp11a1*, *Cyp17a1* and *Inhbb*. No change was seen in the expression in *Star*, *Cyp11a1*, *Cyp17a1* or *Inhbb* indicating a functional steroid hormone biosynthesis pathway in male mice exposed *in utero* to BPA at the doses tested.

Two transcription factors important for testis development and reported to be responsive to *in utero* exposure to XEs, *Gata4* and *Id2* (Larocca et al. 2011), were assayed by qPCR for their mRNA expression levels. *Gata4* is critical for steroidogenic Leydig cell formation in the developing mouse testis (Bielinska et al. 2007) and is important for Sertoli cell function in adult mice (Kyronlahti et al. 2011). Conditional knock-out mouse models show the loss of *Gata4* expression in adult Sertoli cells leads to infertility (Kyronlahti et al. 2011). In our experiment, *Gata4* and *Id2* expression were unchanged in prepubescent and adult mice following *in utero* exposure to XEs.

In conclusion, we observed no long-term changes in male mouse reproductive health following *in utero* exposure BPA. The goal of the experiments outlined above was to determine if exposure to doses related to the human reference dose of BPA exclusively during a critical 10 day window of gonadal development was sufficient to permanently

alter testis gene expression, morphology, or function. Exposure to DES during the same period was used for comparison. The experiments were not designed to test the risk of BPA or DES exposure during any period of testis development. We measured no changes in mouse body weight or in sperm production in adult animals but did observe a stunting of AGD after puberty. Using a global gene expression analysis via microarray followed by a more direct and focused method of qPCR, we did not detect permanent changes in mRNA levels of several genes tested.

Fig 2.1 Schematic overview of experimental design. Mice were bred in-house and the evidence of copulation via detection of vaginal plug denoted embryonic day 1 (E1). BPA or DES were dissolved in tocopherol stripped corn oil. Pregnant dams were separated into dosing groups, weighed each day, and administered 1 μ L of XE+corn oil solution per gram body weight via oral bolus to achieve exposure doses of 5, 50, or 500 μ g BPA per kilogram body weight per day or 5 μ g DES per kilogram body weight per day. Control dams were administered 1 μ L of corn oil only per gram body weight to serve as vehicle controls. The exposure window was from E9 through E18, inclusively. After exposure, dams were housed individually and parturition marked postnatal day 1 (PND1). Mice were weaned and separated by sex at PND21. At PND28 and PND49, mice were euthanized, anatomical measurements were taken and testes were either immersed in modified Davidson's fixative for histology or homogenized in TRIzol for RNA extraction. At PND49 or between PND63 and PND80, the caudal epididymes were removed and motile spermatozoa were isolated and counted.

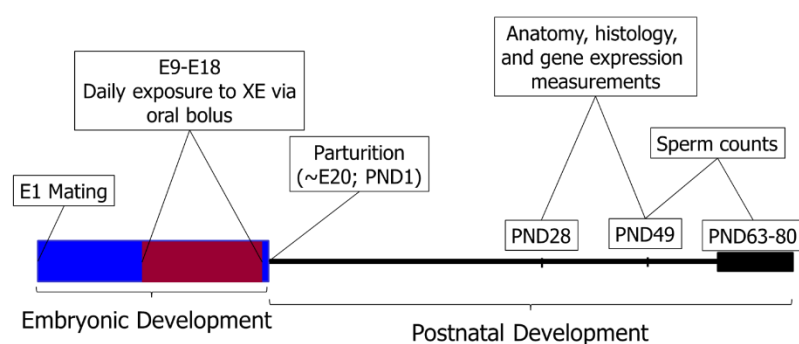


Fig 2.2 Litter size following BPA or DES treatment. Pups were counted and sexed at time of weaning. Litter size and number of male mice per litter are shown

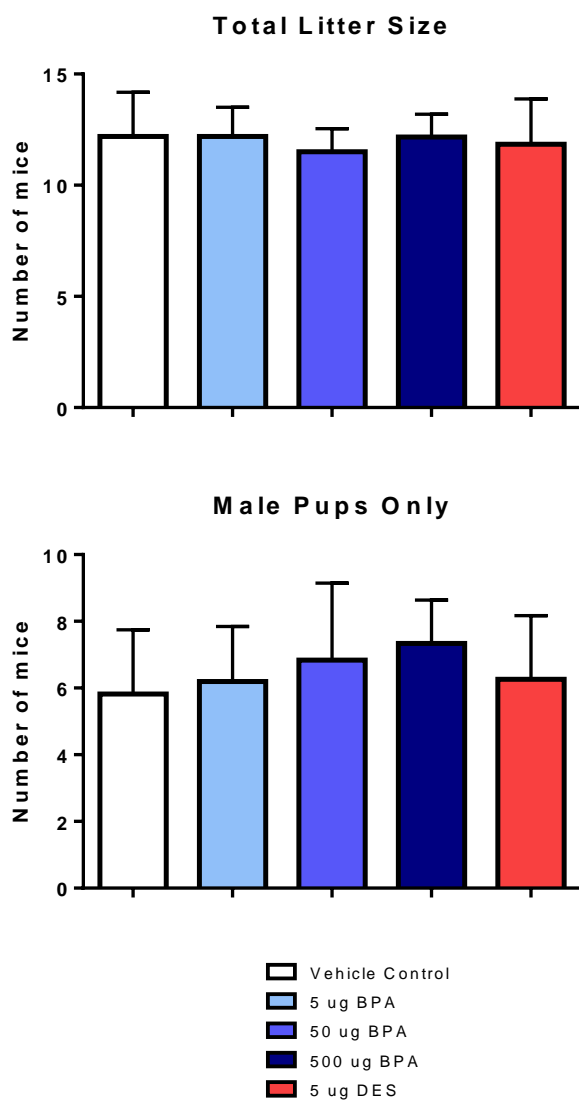


Fig 2.3 Adolescent and young adult anatomical measures following BPA or DES treatment. Body weight (BW), anogenital distance (AGD) normalized to BW, and abundance epididymal white adipose (WA) tissue normalized to BW were quantified at PND28 and PND49 in mice exposed to 5, 50, or 500 μg BPA, 5 μg DES, or vehicle control.

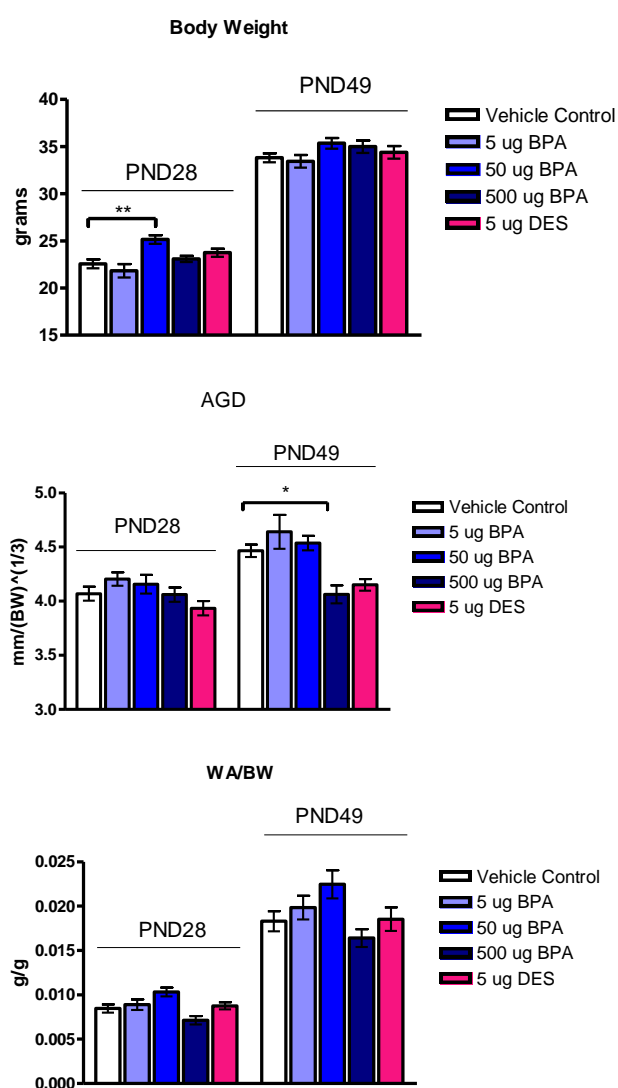
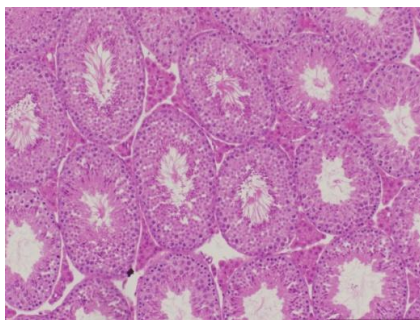
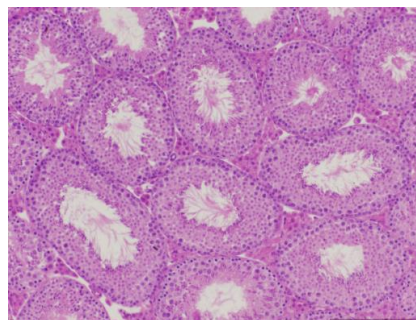


Fig 2.4 Histology of mature mouse testis following BPA or DES exposure.

Testes from PND28 and PND49 mice were fixed in modified davidson's fixative overnight, rinsed with PBS and placed in 70% ethanol. Tissue was embedded in paraffin and 5 μ m cross sectional slices were stained with Harris hematoxylin and eosin Y. Representative images of control mice and XE treated mice are shown. No obvious pathophysiology (i.e. sloughing off of germ cell layers or SCO tubules) was seen at any exposure group and at any time point.



Control
PND49



50 μ g
BPA

Fig 2.5 Mature spermatozoa counts in the adult male mouse. Histology of mature mouse testis following BPA or DES exposure. Mature spermatozoa counts in the adult male mouse. Cauda epididymes were excised from mice at either PND49 to represent a young sexually mature individual or between PND63 and PND80 to represent a fully mature individual. Epididymes were placed in pre-heated DMEM media, scored several times with a razorblade, and incubated at 37°C for 10 minutes. The supernatant was removed, diluted 1:5 in a sperm fixation solution, and counted on a hemocytometer. A. Spermatozoa counts normalized per gram of paired cauda epididymis removed. No change in count was seen in any exposure group at both time windows tested. B. Spermatozoa counts were also normalized to the paired testes weight and no changes were seen.

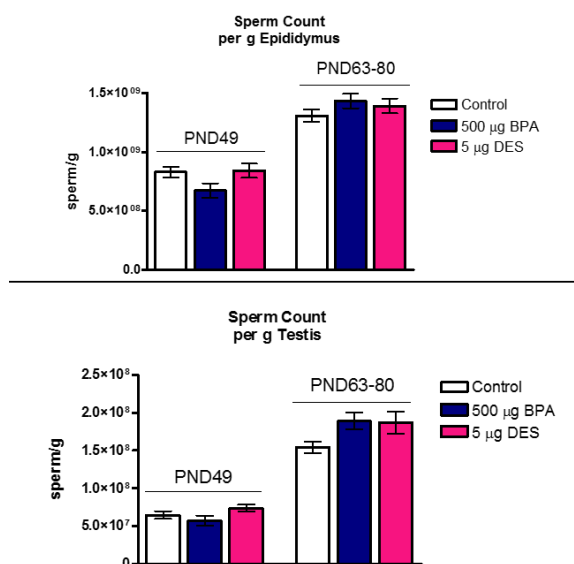


Fig 2.6 Microarray analysis of testis exposed to BPA or DES. A. The number of unique and overlapping genes differentially expressed after in utero exposure to DES or

BPA at PND28 or PND49. Little overlap is seen between the two doses of BPA and DES at PND28 as well as the two doses of BPA at PND49. B. The number of regulated genes at a given exposure that persist from PND28 to PND49. Only 25.5% (19/74) of genes dysregulated by 50 ug BPA at PND28 are still dysregulated by PND49. These 19 genes only represent 27.9% (19/68) of the total genes dysregulated at PND49. Of the 114 genes dysregulated at PND28 in the 500 ug BPA exposure group, only 16 of them (14.0%) are still dysregulated at PND49. These 16 genes only represent 12.9% (16/121) of the total genes dysregulated at PND49.

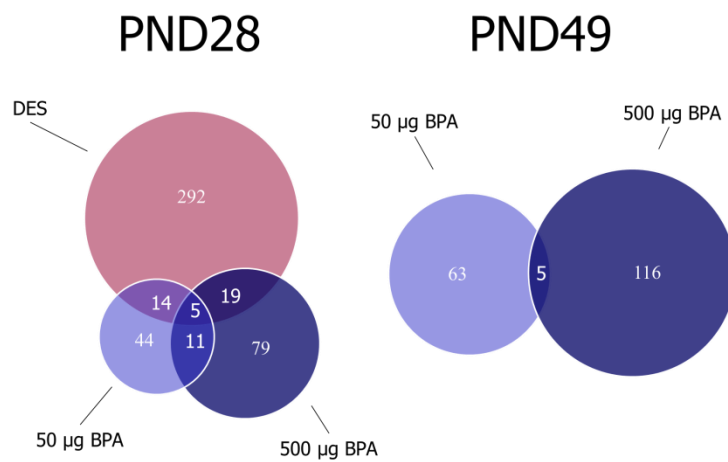
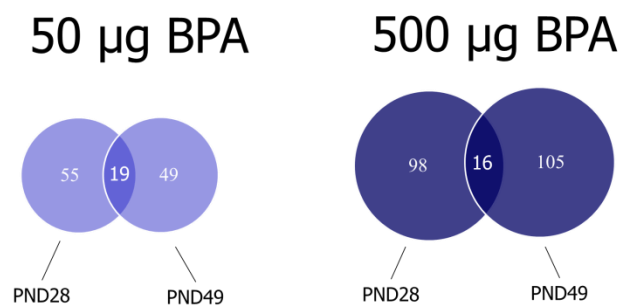
A.**B.**

Fig 2.7 **qPCR validation of microarray results.** qPCR validation of select genes found to be regulated by microarray in the young adult mouse testes following in utero xenoestrogen exposure (*Hdac9* and *Apoc3*). Additional genes shown are markers for normal testis development (*Gata4* and *ID2*) and function (*Inhbb*). Bars represent pools of individuals and are the identical pools to those which were used for microarray. Variability among biological replicates is high in all genes tested and no significant change in the expression of any gene was measured. Statistical significance determined by one way ANOVA followed by Bonferoni post hoc test.

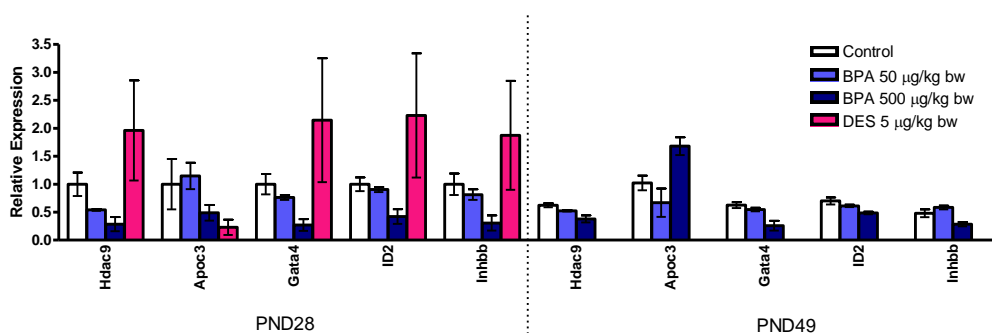


Fig 2.8 **Expression of Star measured via qPCR.** PCR quantification of the expression of *Star* mRNA at PND28. Each bar represents data from an individual mouse used in the experiment. Even among control mice, the expression of *Star* is highly inconsistent. *Star* gene expression is unchanged following in utero exposure to 500 μg BPA/kg. Statistical significance determined by one way ANOVA followed by Bonferoni post hoc test.

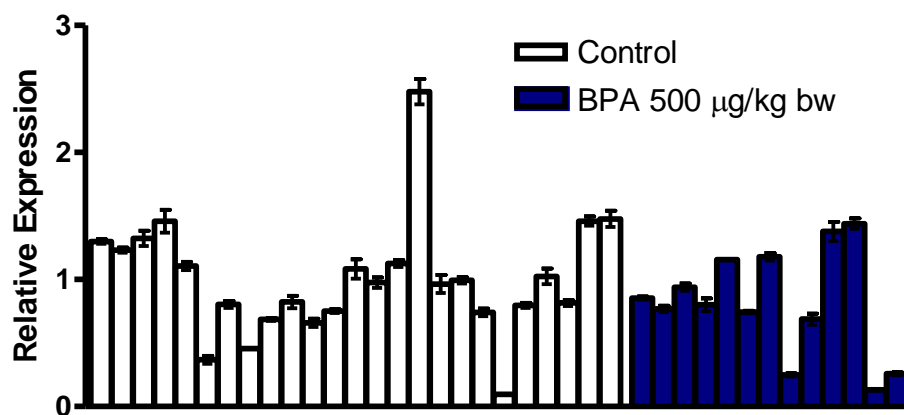


Table 2.1- KEGG pathway analysis of genes regulated by BPA or DES. KEGG functional pathway analysis was performed on sets of genes regulated by 50 µg or 500 µg BPA or 5 µg DES compared to vehicle control at PND28 and 50 µg or 500 µg BPA compared to vehicle control at PND49. Pathways with a pvalue < 0.05 were considered significant and are presented.

Term	Count	PValue	Benjamini
BPA 50 PND28			
mmu04024:cAMP signaling pathway	3	0.0991	0.9964
BPA 50 PND49			
mmu04911:Insulin secretion	3	0.0225	0.7554
mmu04012:ErbB signaling pathway	3	0.0229	0.5131
BPA 500 PND28			
<i>None</i>			
BPA 500 PND49			
mmu05204:Chemical carcinogenesis	6	0.0001	0.0099
mmu00140:Steroid hormone biosynthesis	5	0.0012	0.0457
mmu00830:Retinol metabolism	5	0.0013	0.0334
mmu00591:Linoleic acid metabolism	4	0.0025	0.0463
mmu01100:Metabolic pathways	14	0.0151	0.2093
mmu04975:Fat digestion and absorption	3	0.0179	0.2074
DES			
mmu00240:Pyrimidine metabolism	5	0.0169	0.9219

Table 2.2 Regulation of select genes measured by microarray. Summary of microarray data for 5 genes tested by qPCR. All probes for each given gene are reported with probe sequence. *Apoc3* was downregulated in mice treated with 500 ug BPA at PND49. Similar fold change and p-values were reported with both probes against this gene. One probe for *Hdac9* reported significant up regulation in PND28 mice treated with DES while no significant change was reported by all other *Hdac9* probes at all exposure groups and time points.

Table 2.3 Primer sequences used for qPCR. Sequences used for qPCR validation of select genes identified by microarray or in the literature as important markers of testis development and function.

Gene Symbol	Gene Name	Primer Pair
Hdac9	Histone deacetylase	F- AAGCACAACTCCAGGAGCACAT R- AAGCACAACTCCAGGAGCACAT
Apoc3	Apolipoprotein C-III	F- CGTGCAGGAGTCCGATATAGC R- CCAGTAGCCTTTCAGGGATCT
Gata4	GATA Binding Protein 4	F- ACCCTGGAAGACACCCCAAT R- CTGCCTTCTGAGAAATCATCAAAC
ID2	Inhibitor of DNA Binding 2	F- GAACACGGACATCAGCATCCT R- CATAAGCTCAGAAGGGAATTCAGAT
Inhbb	Inhibin beta B	F- CCGAGATCATCAGCTTTGCA R- GGTTGCCTTCATTAGAGACGAAGA
StAR	Steroidogenic acute regulatory protein	F- AACCAACCAGGAAGGCTGGAA R- CCCACATCTGGCACCATCTT

CHAPTER 3- Male-biased response of tumor promotion-associated genes and dysregulation of novel long non-coding RNAs in constitutive androstane receptor-activated mouse liver

3.1 Abstract

Xenobiotic agonists of constitutive androstane receptor (CAR) induce many hepatic drug metabolizing enzymes, but following prolonged exposure, promote hepatocellular carcinoma, most notably in male mouse liver. Here, we used nuclear RNA-seq to characterize global changes in the mouse liver transcriptome following exposure to the CAR-specific agonist ligand 1,4-bis-[2-(3,5-dichloropyridyloxy)]benzene (TCPOBOP), including changes in novel long non-coding RNAs that may contribute to xenobiotic-induced pathophysiology. Protein-coding genes dysregulated by 3h TCPOBOP exposure were strongly enriched in KEGG pathways of xenobiotic and drug metabolism, with stronger and more extensive gene responses observed in female than male liver. After 27h TCPOBOP exposure, the number of responsive genes increased >8-fold in males, where the top enriched pathways and their upstream regulators expanded to include factors implicated in cell cycle dysregulation and hepatocellular carcinoma progression (cyclin-D1, oncogenes E2f, Yap, Rb, Myc, and proto-oncogenes β -catenin, FoxM1, FoxO1, all predicted to be activated by TCPOBOP in male but not female liver; and tumor suppressors p21 and p53, both predicted to be inhibited). Upstream regulators uniquely associated with

3h TCPOBOP-exposed females include TNF/Nf- κ B pathway members, which negatively regulate CAR-dependent proliferative responses and may contribute to the relative resistance of female liver to TCPOBOP-induced tumor promotion. Many novel long non-coding RNAs were identified in livers of mice exposed to TCPOBOP or to a pregnane-X-receptor agonist, including lncRNAs proximal to the CAR target genes *Cyp2b10*, *Por* and *Alas1*. These data provide a comprehensive view of the CAR-regulated transcriptome and give insight into the mechanism of sex-biased susceptibility to CAR-dependent mouse liver tumorigenesis.

3.2 Introduction

Many foreign chemicals, including industrial chemicals, environmental pollutants and pharmaceuticals alter gene expression through receptor-based mechanisms involving ligand-activated transcription factors, such as the nuclear receptors CAR (constitutive androstane receptor; NR1I3) and PXR (pregnane X receptor; NR1I2) (Chang and Waxman 2006, Cherian et al. 2015). CAR and PXR are expressed at highest levels in mammalian liver, where they act as xenobiotic sensors that detect and respond to foreign chemicals. Some chemicals bind directly to the large and promiscuous ligand binding pockets of CAR and PXR (Cherian et al. 2015), while others activate cell signaling pathways linked to nuclear receptor activation, as exemplified by the activation of CAR by phenobarbital (Hori et al. 2016). Activated CAR and PXR rapidly translocate to the nucleus, where they form

heterodimers with retinoid X receptor (NR2B1), bind DNA, and trans-activate many genes (Kobayashi et al. 2015).

CAR and PXR induce overlapping sets of genes in liver, including many drug metabolizing enzyme members of the cytochrome P450 (Cyp) gene superfamily, as well as phase II conjugation enzymes and drug transporters (Timsit and Negishi 2007, Cui and Klaassen 2016). Thus, activation of either CAR or PXR may increase the metabolism and clearance of xenobiotics sensed by these receptors. CAR also regulates the expression of genes that impact diverse physiological pathways, including lipid metabolism, glucose homeostasis, inflammation, and hepatogenesis (Moreau et al. 2008, Yan et al. 2015). While some effects of CAR activation are beneficial, others are deleterious. TCPOBOP and other foreign chemical CAR activators can increase the hepatotoxicity of alcohol and drugs (Chen et al. 2011, Yamazaki et al. 2011), hepatomegaly, liver tumor promotion and hepatocarcinogenesis (Kazantseva et al. 2016). Activators of CAR can also induce non-alcoholic steatohepatitis (Takizawa et al. 2011) and increase serum triglycerides in diabetes and liver disease (Maglich et al. 2009). CAR activators can thus dysregulate a wide range of metabolic and other physiological processes in the liver.

CAR regulates several genes that show female-bias in expression in liver, including *Cyp2b10*, suggesting that CAR may impact gene expression in a sex-biased manner. The greater abundance of CAR in female compared to male mouse liver (Hernandez et al. 2009,

Lu et al. 2013) further suggests female mice may be more sensitive than males to CAR activators. While liver sex differences and their impact on expression of drug-metabolizing enzymes and many other genes are well-studied (Waxman and Holloway 2009), studies of the sex-dependent effects of CAR are limited to CAR-regulated Cyps (Hernandez et al. 2009) and a few other genes (Ledda-Columbano et al. 2003), or use phenobarbital, which activates both CAR and PXR (Geter et al. 2014). Furthermore, many genome-wide studies of CAR transcriptional responses are limited by their use of microarray technology (Ross et al. 2009, Tojima et al. 2012, Oshida et al. 2015), which cannot reliably distinguish closely related genes within a family or superfamily. RNA-seq technology does address this concern, however, to date, RNA-seq analysis of CAR transcriptional responses has been limited to male liver (Selwyn et al. 2015, Cui and Klaassen 2016). Further, several studies employ exposures lasting days or even weeks (Ross et al. 2009, Luisier et al. 2014, Cui and Klaassen 2016), which do not elucidate early, and potentially transient, effects CAR on the transcriptome, and stimulate a complex array of responses, including both primary and secondary consequences of CAR activation. A further limitation is that current studies of CAR activation only investigate protein-coding genes; however, it is becoming increasingly clear that non-coding RNAs, in particular long non-coding RNAs (lncRNAs), play vital roles in regulating protein-coding genes both in cis and trans (Goff and Rinn 2015, Sun and Kraus 2015). Based on our recent work, at least 5,000 lncRNAs are expressed in mouse liver, many of which show strong tissue-specific expression, and a subset of which have homologs in other species, including humans (Melia et al.

2016). The responsiveness of such liver-expressed lncRNAs to activators of CAR and other nuclear receptors is unknown.

Here, we use RNA-seq to characterize in a comprehensive manner early responses of the mouse liver transcriptome to a short, 3 h exposure of male and female mice to the CAR agonist ligand TCPOBOP (Tzamelis et al. 2000), including changes in expression of protein-coding and non-coding genes. Results are compared to the short-term effects of PXR activation in male liver. We also assess transcriptional responses 27 h after initiation of TCPOBOP exposure, to identify persistent changes in gene expression, and to capture delayed primary gene responses as well as secondary responses. We report striking sex differences in gene responses to CAR activation, including stronger initial responses in female liver, as well as important qualitative differences after 27 h TCPOBOP exposure, including more extensive dysregulation of many key cell cycle control genes linked to liver tumor promotion in male compared to female mouse liver. We also identify 530 liver-expressed lncRNAs that show strong (>4-fold) changes in expression induced by activators of CAR or PXR, in some cases in association with activation of nearby, co-regulated protein-coding genes, including *Cyp2b10* and other drug metabolizing enzyme genes.

3.3 Materials and Methods

3.3.1 Animals

All mouse work was carried out in compliance with procedures approved by the Boston University Institutional Animal Care and Use Committee. Male and female CD-1 mice, 7 wk old, were purchased from Charles River Laboratories (Wilmington, MA) and kept on a 12-hour light cycle (7:30 AM – 7:30 PM). 1,4-Bis-[2-(3,5-dichloropyridyloxy)]benzene (TCPOBOP) and pregnenolone 16 α -carbonitrile (PCN), purchased from Sigma-Aldrich (St. Louis, MO), were dissolved in a 1% DMSO solution in corn oil (vehicle) to give 0.15 mg/mL TCPOBOP or 2.5 mg/mL PCN. Mice were administered each chemical, or vehicle control, by i.p. injection of 20 μ L/g body weight, resulting in a final dose of 3 mg/kg TCPOBOP or 50 mg/kg PCN. Injections were given at a fixed time of day (between 8:00 AM and 8:45 AM of treatment day 1) to control for circadian effects on liver gene expression (Kettner et al. 2016). Mice were euthanized between 11:00 AM and 11:45 AM on day 1 (3 h treatment and control groups) or between 11:00 AM and 11:45 AM on day 2 (27 h treatment and control groups) to give either a 3 h or 27 h exposure (+/- 5 min) for each individual mouse. A small piece of each liver was snap frozen in liquid nitrogen for whole tissue RNA extraction (total RNA). The remainder of the liver was fixed for immunohistochemistry (see below) or was used to isolate nuclei for nuclear RNA analysis.

3.3.2 Tissue fixation, cryosectioning and CAR immunostaining

Fresh mouse livers were each placed in ~20 mL isopentane in a stainless-steel beaker on dry ice until frozen. Livers were then removed and stored at -80°C. Each liver was later mounted on metal chucks in a Leica Cryostat (CM1950) and embedded in OCT compound at -20°C, and 5 μ M sections were prepared. Liver sections were adhered to slides and stored at -80°C. Sections were fixed in 100% methanol at -20°C for 15 min. Following fixation, tissue was rinsed with cold PBS three times. Hydrogen peroxide (0.3%) was added to the slides for 30 min at room temperature followed by a PBS rinse. Slides were blocked for 30 min with avidin solution (30 μ L goat serum + 4 drops avidin block (Vector Avidin/Biotin Blocking Kit, Vector Laboratories, cat. #SP-2001) in 1 mL of PBS) at room temperature, then rinsed with PBS. Slides were then blocked for 30 min with biotin solution (30 μ L goat serum + 4 drops biotin block (Vector Avidin/Biotin Blocking Kit) in 1 mL of PBS) at room temperature, then rinsed with PBS. Slides were stained overnight at 4°C with antibodies against mouse CAR (30 μ L goat serum in 1 mL PBS + 1:150 dilution of antibody sc-50462) (Santa-Cruz Biotechnology) or with IgG as a negative control. Slides were rinsed with PBS and incubated for 1 h at 4°C with secondary antibody (30 μ L goat serum in 1 mL PBS + 1:200 dilution of goat-anti-rabbit secondary antibody). Slides were developed with Vectastain ABC Elite reagent (5 mL PBS + 2 drops of reagent A + 2 drops of reagent B) for 30 min at room temperature and rinsed with PBS. DAB color reagent was prepared by adding 2 drops of buffer stock to 15 mL of distilled water, followed by 4 drops of Vector Peroxidase Substrate Kit DAB (Vector Laboratories, cat. #SK-4100) and 2 drops

of hydrogen peroxide solution, with thorough mixing. DAB solution was added to each slide and color allowed to develop for 2 to 10 min at room temperature. Slides were flushed with distilled water to stop the reaction and photographed.

3.3.3 Nuclear extraction and RNA purification

Livers were homogenized on ice in a Potter-Elvehjem homogenizer in 8 mL of homogenization buffer (10 mM HEPES buffer (pH 7.9) containing 10% (v/v) glycerol, 2 M sucrose, 25 mM KCl, 0.15 mM spermine, 0.5 mM spermidine trihydrochloride and 1 mM EDTA). The homogenate was layered onto 3 mL of fresh homogenization buffer and spun in a Thermo Fisher TH-641 ultracentrifuge rotor at 25,000 rpm for 35 min. The pellet (intact nuclei) was resuspended in 20 mM Tris HCl buffer (pH 8.0) containing 75 mM NaCl, 0.5 mM EDTA, 50% (v/v) glycerol, 0.85 mM DTT and 0.125 mM PMSF, then aliquoted and stored at -80°C. TRIzol LS reagent was used according to the manufacturer's protocol (Life Technologies) to purify liver nuclear RNA from ~25% of the nuclei in a mouse liver.

3.3.4 qPCR analysis

cDNA synthesis reactions were performed using either liver total RNA or liver nuclear RNA (1 µg) after digestion with DNase I to eliminate genomic DNA contaminants. Reverse transcription and cDNA synthesis were performed using the Applied Biosystems High Fidelity RT kit (ThermoFisher). Primers specific for *Cyp2b10*, *Cyp2c55* and other genes

of interest were designed using Primer Express software. Primer pairs were placed in adjacent exons of target genes with amplicons spanning long introns to decrease the possibility of having genomic DNA contamination contribute to the qPCR signal, and are detailed in Table 3.1. Quantitative real time PCR (qPCR) was performed using Power SYBR Green PCR Master Mix (ThermoFisher) in 384 well plates and read on an ABI 7900 Real Time PCR system. Fold change values were calculated using the $\Delta\Delta C_t$ method, using the expression of 18S ribosomal RNA as the background C_t value for normalization between samples.

3.3.5 High throughput RNA sequencing (RNA-seq) and differential expression analysis

Nuclear RNA-seq was performed using two or three biological replicate pools for each treatment group, with each pool representing liver nuclear RNA from $n=3-4$ individual mouse livers. Sequencing libraries were prepared from 1 μg of pooled liver nuclear RNA by poly(A) selection using the NEBNext Poly(A) mRNA Magnetic Isolation Module, followed by processing with the NEBNext Ultra Directional RNA Sequencing for Illumina kit (New England Biolabs). Sequencing was performed at the New York Genome Center (New York, New York) on an Illumina HiSeq2500 instrument and 50 bp paired-end sequence reads were obtained. Data were analyzed using a custom RNA-seq analysis pipeline described elsewhere (Connerney et al. 2017). Briefly, sequence reads were mapped to the mouse genome (release mm9) using TopHat (v2.0.13). Genomic regions

that contain exonic sequence in at least one isoform of a gene (exon collapsed regions; (Connerney et al. 2017)) were defined for each RefSeq gene and for each lncRNA gene. HTSeq (0.6.1p1) was then used to obtain read counts for exon collapsed regions of RefSeq genes, and featureCounts (1.4.6-p5) was used to obtain read counts for exon collapsed regions of lncRNAs. A set of 15,558 liver-expressed lncRNA transcripts was considered for differential expression analysis. These lncRNAs are based on the set of intergenic liver lncRNAs that we defined earlier (Melia et al. 2016), 2016) which we updated by including lncRNAs that are anti-sense or intragenic with respect to RefSeq genes, and by increasing the number of mouse liver RNA-seq datasets used for lncRNA discovery from 45 to 186. RefSeq and lncRNA genes that showed significant differential expression following exposure to TCPOBOP or PCN were identified by EdgeR as outlined elsewhere (Melia et al. 2016). RefSeq genes dysregulated with an expression fold-change (i.e., either up regulation or down regulation) > 1.5 and a false discovery rate (FDR), i.e., an adjusted p-value < 0.001 were considered significant and are shown in Table S3.2. 530 liver-expressed lncRNAs responded to either TCPOBOP or PCN exposure with an expression fold-change > 4 at FDR < 0.05 and were considered significant. 252 of the 530 lncRNAs (48%) are multi-exonic-exonic and 278 are mono-exonic. A fold-change > 2 at FDR < 0.05 was then applied to the 530 lncRNAs to determine significant regulation in each of the five data sets for downstream analysis, as shown in Table S3.3. Of the 530 lncRNAs, 22 have RefSeq NR designations; 18 of these (17 multi-exonic and 1 mono-exonic) are also included in the

listings of responsive RefSeq genes in Table S3.2. Raw and processed RNA-seq data are available at GEO (<https://www.ncbi.nlm.nih.gov/gds>) accession number GSE95685.

3.3.6 Pathway and upstream regulator analysis

RefSeq genes showing differential expression following exposure to TCPOBOP or PCN were submitted to DAVID Bioinformatics Resources (<https://david.ncifcrf.gov/>) for KEGG pathway analysis. Separate gene lists were submitted for each of the 5 mouse liver RNA-seq data sets (TCPOBOP exposure of males and females, for both 3 h and at 27 h, and PCN exposure of males for 3 h). 26 unique KEGG pathways were considered significant at FDR <0.05 (as controlled by the Benjamini-Hochberg method) in at least one of the 5 data sets (Table S3.4). Pathways were categorized as broadly related to either drug/xenobiotic metabolism or cell cycle/DNA replication/cancer by inspection of the lists of differentially regulated genes associated with each pathway. In separate analyses, data for the full set of 24,197 RefSeq genes for each of the 5 data sets was uploaded to Ingenuity Pathway Analysis (IPA; <https://www.qiagenbioinformatics.com/products/ingenuity-pathway-analysis/>) and Upstream Regulator analysis was performed on genes showing significant differential expression, as defined above. Upstream regulators with p-value of overlap < 0.001 and |activation z-score| > 2 and a minimum of 5 target genes were considered significant and are listed in Table S3.5, ranked based on p-value of overlap. Upstream regulators identified by IPA as molecular type ‘chemical’ or ‘biologic drug’ were excluded, as were redundant terms. Upstream regulators were categorized as follows:

Nuclear receptor-related, factors broadly related to either drug/xenobiotic or lipid metabolism; factors that are key regulators of CAR-mediated hepatocarcinogenesis (Kazantseva et al. 2016); factors related to TNF and Nf- κ B signaling; and factors related to non-liver cancers. Cancer-related regulators were further categorized as pro-tumor or anti-tumor, based on their activation state, as predicted by IPA Upstream Regulator analysis, and their known function (e.g. activation of a tumor promotor is pro-tumor and activation of a tumor suppressor is anti-tumor, etc.).

3.3.7 Statistics

Student t-test implemented using Prism 6 (Graphpad) was used to assess statistical significance for all qPCR analysis and for comparing RNA-Seq induction values between male and female livers. An exact binomial test implemented in the statistical analysis package R was used to determine statistical significance of liver cancer pathway enrichments in male and female liver, and to evaluate the enrichment of multi-exonic lncRNAs in the induced gene sets.

3.4 Results

3.4.1 Nuclear RNA analysis to assess short-term responses to CAR and PXR agonists

We first verified by immunohistochemistry that CAR protein was present in a large fraction of the hepatocytes in mouse liver and translocated to the nucleus within 3 h of i.p. injection

of the CAR-specific agonist ligand TCPOBOP (Fig. 3.1). Next, we evaluated the effects of 3 h TCPOBOP exposure on gene expression by qPCR analysis of liver nuclear RNA to capture early transcriptional changes. Results were compared to analysis of total (unfractionated) liver RNA. Much stronger induction (stronger up regulation) of the CAR target genes *Cyp2b10* and *Cyp2c55* was observed in the nuclear RNA fraction (65-fold and 70-fold, increases, respectively; Fig. 3.2A) as compared to total liver RNA (15-fold and 6-fold increases, respectively). Similarly, the PXR activator PCN, after a 3 h exposure, repressed the expression of *Hsd5b* and *Apol7a* to a greater extent in the liver nuclear RNA fraction than in total liver RNA: 2.4-fold and 4.8-fold repression, respectively, in nuclear RNA vs. only 1.4-fold and 1.5-fold repression, respectively, in total RNA (Fig. 3.2A). All four genes showed lower basal expression in the nuclear than in the total RNA fraction (Fig. 3.2B), which contributes to the greater sensitivity of the nuclear RNA fraction to a change in transcription rate induced by activators of CAR and PXR.

Next, we examined the effect of TCPOBOP exposure for either 3 h or 27 h on liver nuclear levels of CAR target genes *Cyp2b10*, *Cyp2c55* and *Akr1b7* in both male and female mice. These time points were set 24 h apart to fix the time of day for all treatment groups and thereby control for circadian effects on CAR-dependent gene expression (Lu et al. 2013). TCPOBOP induction of all three genes was not detectable at 30 min and 1 h (data not shown) but was readily apparent after 3 h (Fig. 3.3). *Cyp2b10* induction was near maximal at 3 h in both males and females, whereas *Cyp2c55* was sub-maximally induced at 3 h (50-

70-fold increases) compared to 27 h (375-400-fold increases) in both sexes. *Akr1b7* also showed a delayed response to TCPOBOP. This delay was more pronounced in male liver, resulting in a sex difference in induction at 3 h: 3-fold increase in *Akr1b7* in male liver vs. 14-fold increase in female liver.

3.4.2 Global transcriptomic responses to CAR and PXR activation

Nuclear RNA-seq analysis was carried out to identify on a global scale TCPOBOP-stimulated RNA responses in both male and female mouse liver. Responses of male liver to 3 h PCN exposure were also examined. In 3 h TCPOBOP-exposed mice, many more RefSeq genes showed significant changes in expression in female liver (206 genes) than in male liver (105 genes) (Table 3.2), as detailed in Table S3.2. This result is consistent with the higher levels of CAR expression reported in female liver (Lu et al. 2013). 968 genes responded to PCN exposure in male liver, of which 121 genes responded in the same manner (i.e. induction or repression) following TCPOBOP exposure in either male or female liver (Fig. 3.4A). In all five exposure groups, more genes were up regulated than down regulated (Table 3.2). While 63 genes showed a common response to 3 h TCPOBOP exposure in males and in females, many other genes were responsive in only one sex: 41 genes were uniquely responsive to 3 h TCPOBOP in male liver and 142 genes were uniquely responsive in female liver (Fig. 3.5A). These sex differences are not an artifact of the threshold values (fold-change and FDR) used to identify significant response genes, as many of the genes showed strong responses to TCPOBOP in the responsive sex but were

marginally, if at all, responsive in the opposite sex. Examples include *Slc15a2* and *Prss22* in male liver and *Akr1b7* in female liver (Fig. 3.5A).

Many more genes were responsive to TCPOBOP exposure after 27 h as compared to 3 h (Fig. 3.4B), with more genes responding in male liver (871 genes) than in female liver (558 genes), in contrast to the 3 h results (Table 3.2). 344 of the genes that responded at 27 h were regulated in common in both sexes (Fig. 3.5B), with 119 genes down regulated and 225 genes up regulated. Although fewer genes responded to TCPOBOP in females than in males at 27 h, the magnitude of the response for the up regulated male-female common genes was significantly greater in females at both time points (Fig. 3.6A). Similar results were apparent when all of the common response genes were examined individually (Fig. 3.6B). Furthermore, a majority of all genes that showed a common response to TCPOBOP in both sexes were more strongly induced, or were more strongly repressed, in female compared to male liver (Fig. 3.6C). Individual examples are highlighted in Fig. 3.5A and Fig. 3.5B (*center panels*).

3.4.3 KEGG pathway analysis

KEGG pathway analysis of the gene sets responsive to 3 h TCPOBOP identified 12 significant pathways in male liver and 11 in female liver (Fig. 3.7). Nine of these pathways were common between the two 3 h data sets. These pathways all relate to xenobiotic and lipid metabolism and related metabolic processes, consistent with the known role of CAR

as a xenobiotic sensor. The KEGG pathway cell cycle showed significant, albeit weak enrichment in the male but not the female gene set at 3 h. Many more KEGG pathways were identified at 27 h than at 3 h, in both males and females (Fig. 3.7), consistent with the expanded list of responsive genes at 27 h (Table 3.2). Whereas xenobiotic and lipid metabolism and related terms were prominent on the list of enriched KEGG pathways at 27 h in both males and females, cell cycle and DNA replication showed significant enrichment in male liver only. Further, many more cell cycle pathway genes were dysregulated in male liver at 27 h (30 genes; FDR $<E-10$) than at 3 h (5 genes, FDR = 0.04). PCN dysregulated close to 1,000 genes at 3 h (Table 3.2), but only 10 enriched KEGG pathways were identified, with biosynthesis of antibiotics being the only pathway not related to drug and lipid metabolism (Fig. 3.7).

3.4.4 Identification of upstream regulators of CAR gene responses

IPA Upstream Regulator analysis identified CAR and PXR as top upstream regulators of the genes that respond to TCPOBOP or PCN in all five data sets (Fig. 3.8). This finding reflects the commonality of the gene responses to TCPOBOP and PCN, described here, with those reported previously for various activators of CAR and PXR, which populate the gene-gene regulator association database queried by IPA. Many unique upstream regulators apparently unrelated to the primary CAR-induced xenobiotic and lipid metabolism responses were identified in male but not female liver after 27 h TCPOBOP exposure. Included are 10 key regulatory factors linked to cell cycle dysregulation and

hepatocellular carcinoma progression (Ledda-Columbano et al. 2000, Zhang et al. 2009) that are specifically associated with CAR activation (Kazantseva et al. 2016), namely, the cyclin-dependent kinase inhibitor CCND1/cyclin D1, the oncogenes E2f, Yap and Rb, and proto oncogenes CTNNB1/ β -catenin, Myc, FoxM1 and FoxO1, all of which were predicted to be activated by TCPOBOP, and the tumor suppressors p21 and p53, which both were predicted to be inhibited (Fig. 3.8). Mechanistic networks involving these factors, and their prevalence in TCPOBOP-exposed male but not female liver are shown in Fig. 3.9. Overall, the predicted activation states of these regulatory factors of CAR-induced hepatocarcinogenesis indicate that TCPOBOP stimulates a prominent pro-tumor response in male liver, insofar as oncogenic factors are predicted to be activated and tumor suppressors are predicted to be inhibited by TCPOBOP exposure. Other pro-tumor factors identified as activated upstream regulators for the male 27 h TCPOBOP dataset included TBX2, a cell cycle regulator and direct repressor of p21, RABL6 (RBEL1A), a negative regulator of p53, and growth factors CSF2, VEGF, and HGF (Fig. 3.8). Of note, for each of the 10 hepatocarcinogenesis-associated upstream regulators, the number of target genes that responded to 3 h TCPOBOP exposure was greater in female than in male liver, consistent with the greater hepatoproliferative responses reported for short-term TCPOBOP-treated female mouse liver (Ledda-Columbano et al. 2003); however, by the 27 h time point, many more target genes of these regulators responded to TCPOBOP in male than in female liver (Fig. 3.10). Indeed, the number of up regulated liver cancer pathway-associated genes (i.e., genes downstream of these 10 upstream regulators) unique

to 27 h-TCPOBOP male liver (153 genes) as compared to 27 h-TCPOBOP female liver (26 genes) was significantly greater ($p=0.002$ by exact binomial test) than the corresponding numbers of total genes up regulated in each sex (349 in males vs. 93 in females; Fig. 3.11). Thus, there is a significantly stronger enrichment in male compared to female liver for TCPOBOP-responsive liver cancer pathway genes as compared to TCPOBOP-responsive genes in other pathways. Consistent with these findings, while 3 of the 10 factors linked to CAR-dependent hepatocarcinogenesis were identified as upstream regulators of female liver responses to TCPOBOP at the 3 h time point (FoxM1, E2F1 and CTNNB1/ β -catenin), the p -values of overlap for their target genes were much weaker in female than in male liver (Table 3.3). FGF19, which was specifically associated with female liver responses to TCPOBOP at 27 h (Fig. 3.8) induces hepatocellular carcinoma in human liver but not mouse liver (Zhou et al. 2017).

Next, we considered whether any of the upstream regulators activated in female liver might lessen the hepatocarcinogenic potential of TCPOBOP in females. We identified 13 upstream regulators that were specific to 3 h TCPOBOP-exposed female liver, and were also common to 3 h PCN-exposed male liver, neither of which show the strong hepatocarcinogenic responses to TCPOBOP exposure seen in male liver (Shizu et al. 2013) (Fig. 3.8). Strikingly, five of the 13 upstream regulators found only in these two exposure models (TNF, Nf-kB, RELA, IKBKB, CHUK (IKBKA) are linked to TNF/NF κ B signaling, indicating that this pathway is preferentially activated by both exposures (Fig. 3.12). The

TNF/NF κ B pathway exerts negative cross-talk to CAR gene responses (Van Ess et al. 2002) and to the hepatoproliferative response to TCPOBOP (Columbano et al. 2005), suggesting that these five upstream regulators contribute to the relative resistance of female liver to TCPOBOP hepatocarcinogenesis. Consistent with this, the Nf- κ B inhibitor NFKBIA was identified as a much stronger activated upstream regulator in 27 h-TCPOBOP male liver than in 3 h-TCPOBOP-female liver (Table 3.3).

3.4.5 Impact of TCPOBOP and PCN on non-coding transcriptome

Given the increasing recognition that many non-coding RNAs regulate gene expression via epigenetic and other mechanisms, we used the five RNA-seq datasets described above to investigate the impact of TCPOBOP and PCN exposure on 15,558 non-coding RNA transcripts identified in mouse liver (see Methods). These transcripts include long non-coding RNAs (lncRNAs) that are intergenic, intragenic, or antisense with respect to protein coding genes. A total of 530 liver-expressed lncRNAs showed significant responses to either TCPOBOP or PCN, with at least a 4-fold change in expression in one of the 5 datasets at FDR <0.05 (Table 3.4). 80 of 402 TCPOBOP-responsive lncRNAs also responded to PCN treatment, while an additional 118 lncRNAs were uniquely responsive to PCN, a majority of which were down regulated (73 of 118 lncRNAs; Table 3.5). The overall set of 530 responsive lncRNAs was significantly enriched for multi-exonic lncRNA genes, which are more likely to be functional than mono-exonic lncRNAs (Liu et al. 2017). Thus, 252 of the 530 responsive lncRNAs (47.5%) are multi-exonic as compared to only

20.2% of the overall set of 15,558 liver-expressed lncRNAs (2.35-fold enrichment; $p < E-15$, exact binomial test). 30 lncRNAs were induced by TCPOBOP early (3 h) and persisted at 27 h in both sexes (Table 3.5), with inductions as high as ~400-fold seen for lncRNA_5998, which is which is upstream of *Cyp2b10* (see below). 15 of these 30 lncRNAs were also induced by PCN. Early gene responses – both induction and repression – characterized many other lncRNAs, a subset of which showed sex-specificity in their response to TCPOBOP (Table 3.5). Some of these early lncRNAs could contribute to the late (secondary) changes in expression of TCPOBOP-responsive protein coding genes. Other lncRNAs showed a delayed response to TCPOBOP (i.e., lncRNA induction not seen until 27 h): 67 such late lncRNAs responded to TCPOBOP in both male and female liver, 94 responded in male liver only, and 117 responded in female liver only (Table 3.5, Fig. 3.13). The sex-specificity of the late lncRNA responses is intriguing, given the striking sex differences in late protein coding gene responses in male liver associated with liver tumor promotion, described above. Considering only multi-exonic lncRNAs, 3 h TCPOBOP exposure altered the expression of 52 and 62 lncRNAs in male and female liver, respectively, a majority of which were up regulated (Table 3.6). After 27 h TCPOBOP exposure, 112 multi-exonic lncRNAs were dysregulated in male liver and 131 multi-exonic lncRNAs were dysregulated in female liver; again, a majority (72-76%) were up regulated (Table 3.6). Examples of multi-exonic lncRNAs responsive to TCPOBOP are shown in Fig. 3.14, Fig. 3.15, Fig. 3.16, and Fig. 3.17. 126 multi-exonic lncRNAs were responsive to PCN, 57% of which were down regulated (Table 3.6). This is consistent with the greater

proportion of protein coding genes down regulated by PCN as compared to TCPOBOP (Fig. 3.4).

3.4.6 LncRNAs proximal to regulated RefSeq genes are responsive to TCPOBOP

LncRNAs are frequently co-expressed with nearby protein-coding genes, and often regulate expression of protein-coding genes in *cis* (Engreitz et al. 2016). Accordingly, we examined the proximity of the lncRNAs responsive to TCPOBOP or PCN to the nearest regulated protein-coding gene. Across the five RNA-seq data sets, a total of 129 responsive multi-exonic lncRNAs overlapped or were within the same genomic topologically associating domain (TAD) (Vietri Rudan et al. 2015) as a co-responsive RefSeq gene (*cis* co-expression, 45-58% of the responsive multi-exonic lncRNAs; Table 3.6). 21 other multi-exonic lncRNAs (2-8%) were *cis* to RefSeq genes showing the opposite response to TCPOBOP or PCN in one or more datasets (Table 3.6). Since gene regulatory elements are largely contained within TADs, whose boundaries form looped, insulated domains (Hnisz et al. 2016), these lncRNAs have the potential to regulate their nearest responsive RefSeq gene through a *cis* mechanism, involving either positive regulation (129 *cis* co-expressed gene pairs) or negative regulation (21 *cis* opposite gene pairs).

The *cis* co-expressed lncRNAs comprise four classes of orientation relative to their nearest co-regulated RefSeq genes: **1)** lncRNAs upstream of and transcribed from the opposite strand as the RefSeq gene. Two examples are lncRNA_5998, which is 5.2 kb upstream of

Cyp2b10 (Fig. 3.14A), and lncRNA_8301, which is 15.6 kb upstream of *Alas1* (Fig. 3.14A). *Cyp2b10* and *Alas1* are well known CAR and PXR targets and are highly induced in all five data sets, as are their adjacent co-regulated lncRNAs (Fig. 3.14D, Fig. 3.14E). **2)** lncRNAs characterized by anti-sense transcription starting within the first intron of the co-regulated RefSeq gene. Examples include lncRNA_8460, which is anti-sense to *Ginm1* (Fig. 3.14C) and lncRNA_4655, which is anti-sense to *Por* (Fig. 3.15A). lncRNA_4655 is expressed at a low level, but is induced in all five data sets (Table S3.3), as is *Por* (Fig. 3.15B). Conversely, lncRNA_8460 is highly expressed and rapidly induced in all five data sets, while the overlapping RefSeq gene, *Ginm1*, is expressed at a low level and not induced by TCPOBOP until 27 h in both males and females (Fig. 3.15C, Fig. 3.15F). **3)** lncRNAs found within an intron of a highly expressed RefSeq gene and often spanning multiple genes. Examples include two lncRNAs in the *Cyp2c* locus that span the genomic region from *Cyp2c37* through *Cyp2c50*. lncRNA_15011 originates in intron 5 of *Cyp2c37* and ends in intron 4 of *Cyp2c50* (isoform 2), while lncRNA_15014 originates in intron 7 of *Cyp2c37* and ends in intron 6 of *Cyp2c50* (isoform 2) (Fig. 3.16A). Both lncRNAs are highly expressed and are induced in all five datasets (Fig. 3.16B), as are *Cyp2c37* and *Cyp2c50* (Fig. 3.16C). **4)** lncRNAs that are within the same TAD as a regulated RefSeq gene, but are distant in terms of linear chromosome distance. The DNA loop that anchors the TAD structure has been shown to bring these linearly distant sequences into close 3-dimensional proximity and allow for *cis* regulation (Hnisz et al. 2016). An example is lncRNA_3779, which is highly induced in TCPOBOP-exposed male and female liver at

27 h (Fig. 3.17A, Fig. 3.17C). In male liver, the TCPOBOP-responsive RefSeq protein coding gene closest to lncRNA_3779 is *Klhdc7a*, which is ~455 kb away, while in female liver the nearest responsive RefSeq gene is *Padi4*, which is ~313 kb away. lncRNA_3779, *Klhdc7a* and *Padi4* are all located within the same TAD. Interestingly, lncRNA_3779 is upregulated in both data sets while *Klhdc7a* is down regulated in both and *Padi4* is upregulated in TCPOBOP-treated females at 27 h but not males (Fig. 3.17C).

3.4.7 LncRNAs distal to regulated RefSeq genes also respond to TCPOBOP

In addition to the above lncRNAs, which are *cis* to TCPOBOP or PCN responsive protein coding genes, we identified ~100 other lncRNAs – some highly expressed – whose nearest regulated RefSeq gene is not in the same TAD. These distal lncRNAs comprise 35-51% of the responsive multi-exonic lncRNAs in each data set (Table 3.6). One example is lncRNA_8767 (Fig. 3.17B, Fig. 3.17D). The distant location of this TCPOBOP-induced lncRNA relative to the nearest responsive protein coding gene, and its complex gene structure (4 multi-exonic isoforms; Fig. 3.17B) indicates this lncRNA – and many others in this class – is specifically targeted for transcription and is not a spurious by-product of the very active transcription of a highly expressed nearby protein coding gene. Since *cis* gene–gene regulatory element interactions are largely contained within TADs (Hnisz et al. 2016), these lncRNAs are unlikely to regulate TCPOBOP or responsive protein coding genes by a *cis* mechanism, but rather, may utilize one of the *trans* regulatory mechanisms described for lncRNAs (Sun and Kraus 2015).

3.5 Discussion

The impact of the CAR-specific agonist ligand TCPOBOP on the mouse transcriptome has been investigated after exposures lasting several days or weeks (Ross et al. 2009, Luisier et al. 2014, Cui and Klaassen 2016), which gives insights into the long-term effects of CAR activation, but does not inform about early transcriptional responses, including early events associated with hepatocyte proliferation linked to tumor promotion. Here we identify genes induced or repressed after exposure to TCPOBOP for either 3 h (presumed primary response genes) or 27 h (primary + secondary response genes). The set of genes dysregulated in 3 h TCPOBOP-treated mouse liver is enriched for xenobiotic and lipid metabolism, and includes *Cyp2b10* and other established primary targets of CAR. Many more genes were dysregulated by TCPOBOP at 27 h, likely reflecting secondary transcriptional responses. Moreover, at 27 h, CAR responses in male but not female liver showed strong enrichment for genes functionally linked to CAR-dependent hepatocyte proliferation and hepatic tumor promotion (Kazantseva et al. 2016) and for their upstream regulators. These regulators include cyclin D1, which was predicted to be activated, and p53 and p21, which were predicted to be inhibited (Kazantseva et al. 2014). These findings are consistent with the greater susceptibility of male mice to CAR-dependent tumor promotion (Li et al. 2012) and suggest that the molecular events that lead to hepatic tumor promotion are initiated early (within 27 h) following CAR activation.

It is unclear what triggers the broadening of TCPOBOP gene responses in male liver from the narrow focus on genes of xenobiotic and lipid metabolism seen at 3 h, to genes linked to cell cycle dysregulation and liver hepatocellular carcinoma promotion seen at 27 h. This striking change in gene responses at 27 h to encompass genes active in liver tumor promotion was not seen in female liver, which may in part be due to the robust early activation of TNF and Nf- κ B signaling pathways that we observed in TCPOBOP-treated female but not male liver. Importantly, TNF/NF κ B signaling exerts negative cross-talk on CAR-dependent gene responses (Van Ess et al. 2002) and suppresses the hepatoproliferative effects of TCPOBOP exposure (Columbano et al. 2005), suggesting that TNF-activated Nf- κ B contributes to the partial resistance of female liver to the hepatoproliferative response to TCPOBOP. TNF/NF κ B signaling was also predicted to be activated in 3 h PCN-exposed male liver, which also does not exhibit the strong hepatocarcinogenic responses associated with male liver TCPOBOP exposure (Shizu et al. 2013). Additional mechanisms for male-biased liver tumor promotion may involve the pro-tumor actions of androgen receptor-FoxA1 complexes and the anti-tumor effects of estrogen receptor-FoxA1 complexes, via the inhibition of *Myc* (Li et al. 2012). Of note, *Foxa1* was induced 2-fold in our 27 h TCPOBOP data sets, in both male and female liver.

We detected TCPOBOP-induced changes in gene expression with increased sensitivity by RNA-seq analysis of liver nuclear RNA, rather than by analysis of total (unfractionated) liver RNA. The increased sensitivity provided by the nuclear fraction likely reflects a

buffering of the induction response by the comparatively stable pool of transcripts found in the cytoplasm. Nuclear RNA was also more sensitive for detection of gene down regulation, where the buffering effect of preexisting mature cytoplasmic mRNA can mask a decrease in gene transcription, especially for mature mRNAs that are relatively stable and when the analysis is carried out at an early time point, i.e., before a new steady state level of cytoplasmic mRNA is established. The use of nuclear RNA-seq also increased the sensitivity for detecting changes in expression of lncRNAs, a large majority of which show strong nuclear localization (Melia et al. 2016).

Female mice were more responsive than males to TCPOBOP-induced changes in gene expression, as indicated by the ~2-fold greater number of responsive genes at 3 h in females than in males, and by the greater magnitude of gene responses in females both 3 h and 27 h after initiating TCPOBOP exposure. This is consistent with earlier reports that CAR is more highly expressed and more active in female than male mouse liver (Hernandez et al. 2009, Lu et al. 2013), and with the finding that the androgens androstanol and androstenedione are inverse agonists of CAR activity (Kawamoto et al. 2000, Kohalmy et al. 2007) that can compete with exogenous CAR agonists for CAR binding in male liver. In addition, estradiol and estrone act as agonists of CAR (Kawamoto et al. 2000) that stimulate basal CAR activation in female liver (Koh et al. 2012). Despite this intrinsic female bias in CAR responsiveness, a male-biased gene response pattern emerged 27 h after TCPOBOP exposure, when many genes involved in cell cycle control and

hepatocellular carcinoma progression were preferentially dysregulated in male liver, as discussed above.

Female mice are more resistant to hepatocellular carcinoma induced by the tumor initiator diethylnitrosamine when combined with a non-genotoxic tumor promotor, such TCPOBOP or phenobarbital (Kalra et al. 2008). However, exposure to TCPOBOP alone induces hepatocyte proliferation more frequently in female than in male liver (Ledda-Columbano et al. 2003). There are several possible explanations for the apparent disparity between those findings and our findings here. First, the reported female bias in hepatocyte proliferation is limited to TCPOBOP exposures up to 36 h, as there is no apparent sex bias after 48 h (Ledda-Columbano et al. 2003). This is consistent with our finding of an early female bias in cell proliferation gene expression (Fig. 3.10). Conceivably, the reversal of the sex bias in expression of cell cycle control genes by 27 h in our dataset may account for the loss of sex bias in hepatic proliferation at 48 h (Ledda-Columbano et al. 2003). Second, given our finding of a strong enrichment for key mediators of CAR-dependent liver tumor promotion in 27 h-TCPOBOP-treated male but not female liver, as well as the early activation in female liver of TNF/NF κ B signaling, which is associated with inhibition of hepatoproliferative response to TCPOBOP (Columbano et al. 2005), the transcriptional environment in male liver may be poised for stronger and more rapid liver tumor progression than female liver, despite lower overall cell proliferation rates. Indeed, acute activation of CAR can lead to increased cell proliferation but not liver tumor formation

(Dong et al. 2015). Thus, early measurements of cell proliferation alone may not be sufficient to predict the hepatocellular promotion effects of TCPOBOP and perhaps other CAR agonists.

Cyclin D1 regulates cell cycle progression from G1 to S phase, as well double-strand break repair by homozygous recombination (Bartek and Lukas 2011, Jirawatnotai et al. 2011). Overexpression or dysregulation of cyclin D1 drives tumor formation in many tissues, including liver (Deane et al. 2001, Bartek and Lukas 2011, Jirawatnotai et al. 2011, Kazantseva et al. 2014). Cyclin D1 (*Ccnd1* gene) is induced in TCPOBOP-exposed mouse liver and is a key mediator of CAR-dependent increases in hepatocyte proliferation (Ledda-Columbano et al. 2003, Kazantseva et al. 2014). We observed early induction of cyclin D1 in female but not male liver, consistent with prior reports (Ledda-Columbano et al. 2003), followed by strong up regulation of cyclin D1 in both sexes at 27 h. However, we also found that cyclin D1 is a highly significant upstream regulator of downstream TCPOBOP responses in male but not in female liver, with 52 cyclin D1 target genes being responsive to TCPOBOP in males compared to only 11 target genes in females at 27 h. The increase in hepatocyte proliferation within 24 h of TCPOBOP treatment (Ledda-Columbano et al. 2000, Li et al. 2012) is reduced in cyclin D1-deficient mice (Ledda-Columbano et al. 2000, Ledda-Columbano et al. 2002), consistent with our finding that liver cyclin D1 induction is an early response to TCPOBOP exposure. However, longer exposures to TCPOBOP (≥ 36 h) in the same cyclin D1-deficient mice showed no difference in hepatocyte

proliferation, apparently due to compensatory effects of cyclin E (Ledda-Columbano et al. 2002). Thus, while cyclin D1 is not strictly necessary for long-term TCPOBOP mediated hepatocyte proliferation, it is required for the initial response.

Other key factors in cell cycle control that are disrupted by TCPOBOP in a CAR-dependent manner include the tumor suppressor p53 and its target gene p21 (Ledda-Columbano et al. 2002, Kazantseva et al. 2014). In healthy cells, p53 induces p21, and p21, in turn, inhibits cyclin D1 signaling to trigger cell cycle arrest (Xiong et al. 1993). Disruption of either p53 or p21 signaling is linked to liver cancer progression (Deane et al. 2001, Zhang et al. 2009). Here, we show that p21 and p53 are upstream regulators of TCPOBOP gene responses whose activity is inhibited by TCPOBOP in male but not female liver. Interestingly, 151 of the 217 male liver TCPOBOP-responsive genes that are downstream of either p53, p21 or cyclin D1 are unique to only one of these three regulators, suggesting these regulators may in part act independently of the canonical p53 → p21 → cyclin D1 pathway that connects them.

Our comprehensive characterization of the non-coding liver transcriptome led to the discovery of 530 lncRNAs, including 252 multi-exonic lncRNAs, whose expression is either induced or repressed following exposure to TCPOBOP or PCN. lncRNAs have diverse actions, which include tethering to their site of transcription (Werner and Ruthenburg 2015), which enables them to recruit activating or repressive histone mark

writers to nearby target genes in *cis*, as well as distal actions by epigenetic and other mechanisms that operate in *trans* (Goff and Rinn 2015, Sun and Kraus 2015). 150 of the 252 multi-exonic lncRNAs are encoded by genes that are either proximal to, or are found within the same genomic TAD (Hnisz et al. 2016) as a TCPOBOP or PCN responsive protein coding gene, with 129 of these lncRNAs showing co-expression and 21 showing the opposite response to TCPOBOP or PCN as the associated protein coding gene. Examples include lncRNA_5998, which is upstream and antisense to *Cyp2b10*, is proximal to an enhancer that binds CAR and contributes to *Cyp2b10* induction (Honkakoski and Negishi 1997), and is induced to similar levels as *Cyp2b10* (Fig. 6). Other examples include lncRNAs transcribed anti-sense to an overlapping, responsive protein coding gene that they may regulate. This regulation may involve anti-sense mechanisms (Pelechano and Steinmetz 2013) that lead to decreased sense transcription by RNA polymerase II (Hobson et al. 2012), recruitment of histone modifiers to silence the genomic region (Rinn et al. 2007), or other mechanisms. Examples include lncRNA_8450, which is induced by TCPOBOP to very high levels (~100 FPKM) and is transcribed anti-sense to the weakly induced overlapping protein-coding gene *Ginm1* (Fig. 3.14 C), suggesting lncRNA_8450 may actively interfere with *Ginm1* expression. Many other TCPOBOP or PCN responsive lncRNAs are distant from other TCPOBOP or PCN responsive genes and some of these may operate through *trans* regulatory mechanisms. Further study is required to elucidate the functions of the CAR and PXR-responsive lncRNAs described here and their impact on CAR and PXR dependent physiological and pathophysiological processes.

Fig. 3.1 **I.P injection of TCPOBOP stimulates CAR nuclear localization in mouse liver within 3 h.** Immunohistochemical analysis of male mouse liver showing CAR localized to the cytoplasm in the absence of TCPOBOP (vehicle control) but translocated to the nucleus after 3 h TCPOBOP exposure. Male mice were injected with TCPOBOP (3 mg/kg body weight) at 8 am. Liver was collected and fixed in ~20 mL isopentane in a stainless-steel beaker on dry ice until frozen. Tissue was sectioned at 5 μ M, adhered to slides and stained with antibody against CAR or IgG.

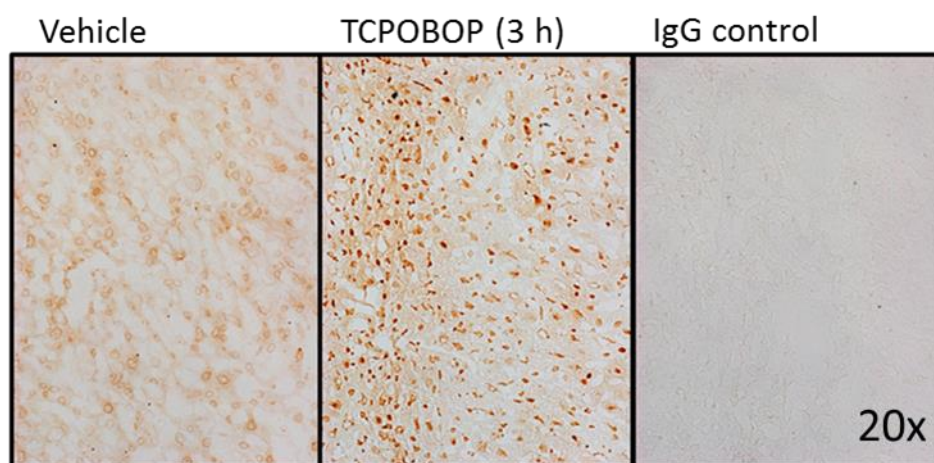


Fig. 3.2 TCPOBOP induces the expression of *Cyp2b10* and *Cyp2c55* while PCN represses the expression of *Hsd3b* and *Apol7a*. A. Induction of *Cyp2b10* and *Cyp2c55* by TCPOBOP (3 h) and suppression of *Hsd3b5* and *Apol7a* expression by PCN (3 h) in male mouse liver, as measured by qPCR. RNA isolated from whole liver tissue ('Total') shows modest induction of *Cyp2b10* and *Cyp2c55* by TCPOBOP (t-test: *, P<0.05; **, P<0.01; ***, P<0.001 vs. vehicle controls), while RNA purified from liver nuclei ('Nuclear') shows much strong induction (higher fold change) for both genes (t-test: +, P<0.05; ++, P<0.01; +++, P<0.001 for difference in induction between Total and Nuclear). Down regulation of *Hsd3b5* and *Apol7a* is also significantly stronger in nuclear RNA compared to total RNA. B. Expression levels measured by qPCR analysis of total liver RNA is higher than for the corresponding nuclear liver RNA samples, all from vehicle control livers, for the four genes shown.

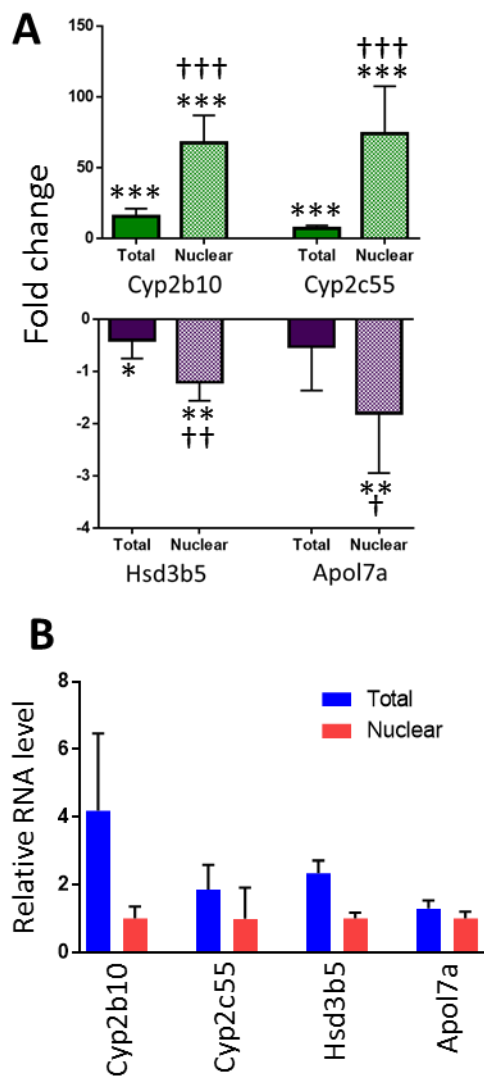


Fig. 3.3 TCPOBOP induces *Cyp2b10*, *Cyp2c55*, and *Akr1b7* in male and female mice. Induction of *Cyp2b10*, *Cyp2c55* and *Akr1b7* in livers of mice treated with TCPOBOP or PCN in males (M) or females (F) for 3 h (3) or for 27 h (27), as indicated at the bottom. Expression level for the male 3 h vehicle control samples was set to 1. Strong and statistically significant (ANOVA; t-test, $P < 0.05$, not marked) induction of all 3 genes was seen in both male and female livers after 3 h. A significantly greater increase in expression at 27 h compared to 3 h is seen in males for all three genes, and in females for *Cyp2c55* and *Ark1b7* (ANOVA; t-test; ‡, $P < 0.05$; ‡‡‡, $P < 0.001$). A significant sex bias was found for the induction of all three genes, with females showing a stronger induction of *Cyp2b10* and *Akr1b7* than males at 3 h, and stronger induction of *Cyp2c55* at 3 h and 27 h than males (ANOVA; t-test; ^, $P < 0.05$; ^^, $P < 0.01$). For panels B, C and D, n=5-12 individual livers per group.

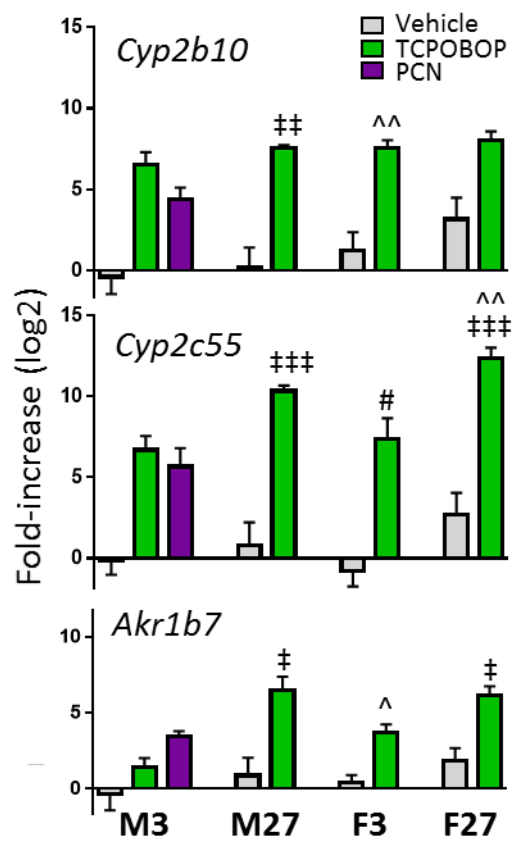


Fig. 3.4 Nuclear RNA-Seq identifies RefSeq genes responsive to activators of CAR or PXR. Overlap between sets of genes responsive at 3 h in males and females treated with TCPOBOP (TCPO) and in males treated with PCN. C. Overlap of genes responsive to TCPOBOP in males (top) and in females (bottom) at 3 h vs. 27 h. Genes that were responsive in multiple data sets, but in opposite directions, were omitted from these analyses. See Table S3.2 for full details on all genes responsive to TCPOBOP or PCN.

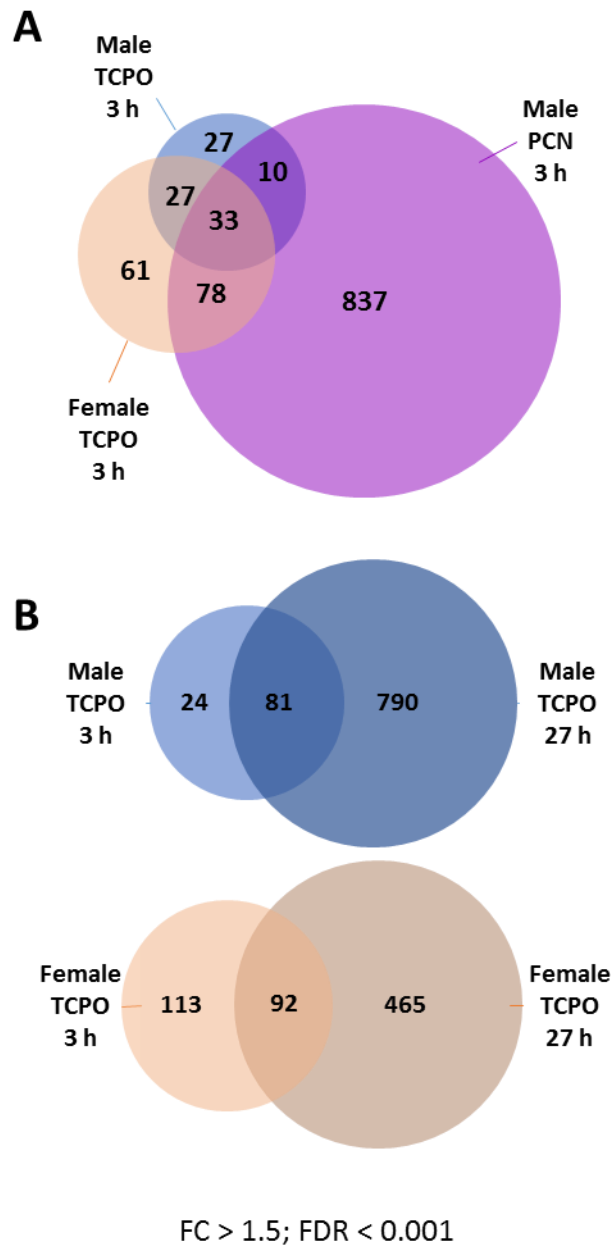


Fig. 3.5 **Sex differences in TCPOBOP gene responses identified by nuclear RNA-seq.** A and B. Top – Overlap of genes responsive to TCPOBOP (TCPO) exposure in male vs female liver after 3 h (A) or after 27 h (B) at $|\text{fold change}| > 1.5$ and $\text{FDR} < 0.001$. Omitted are 3 genes that responded in the opposite direction in males vs females at 27 h. Bottom – Plot of FC (fold-change) values for genes responsive to TCPOBOP in male liver only, female liver only or in both sexes, which each individual gene shown as a separate data point. Genes that did not meet the fold change and FDR cutoff values are in the two outmost groups (gray dots). Dashed horizontal lines indicate a fold-change of 1.5. Examples of genes showing a strong sex bias in their response include *Slc15a1* and *Prss22* (3 h male only), *Akr1b7* (3 h female only), *Gjb4* and *Sult3a1* (27 h male only) and *Gm16432* (27 h female only), as marked. Many genes that respond to TCPOBOP in common in both sexes are more strongly induced in females, as highlighted by *Ces2a* (3 h) *Cyp2c55* and *Cyp2c53-ps* (3 and 27 h).

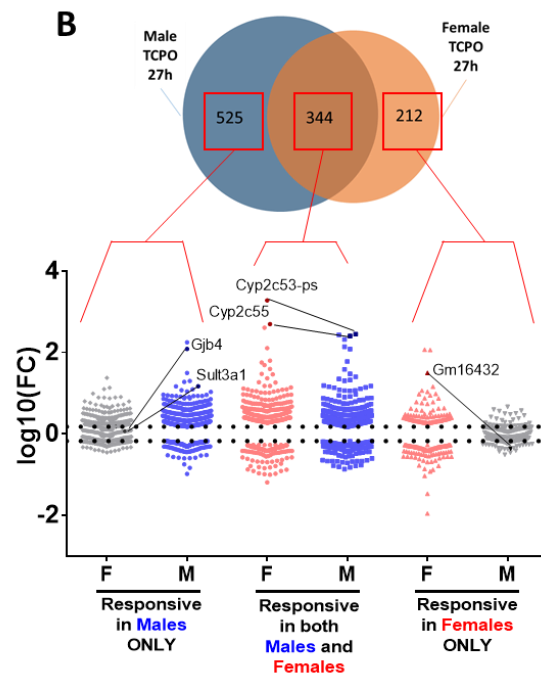
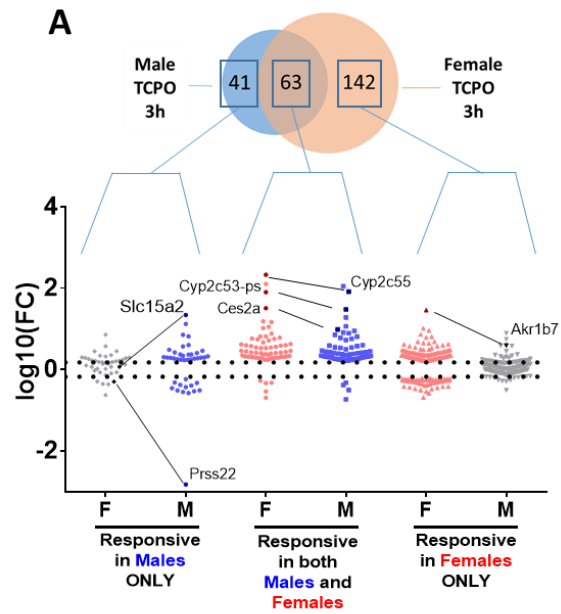


Fig. 3.6 Genes that respond to TCPOBOP in males and females are more highly induced in females. A. Box plot of log₂ fold-change values showing that genes up regulated by TCPOBOP in both sexes, after either 3 h (top) or 27 h (bottom), are significantly more strongly induced in female liver (t-test; **, P< 0.01). B. Fold change values of individual TCPOBOP common response genes in male (blue) and female liver (red), as marked, ranked by decreasing fold change in female mice. C. Numbers of TCPOBOP common response genes whose |fold change| is larger in male liver or in female liver, as indicated.

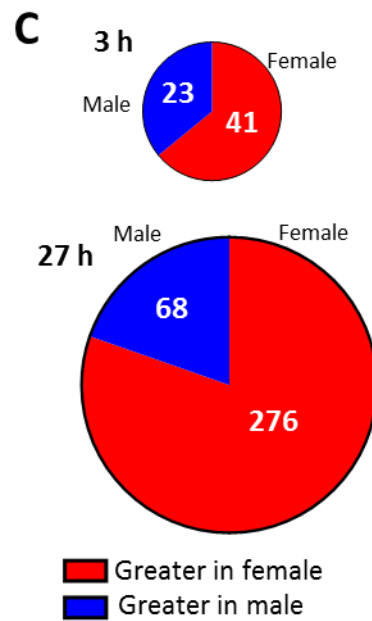
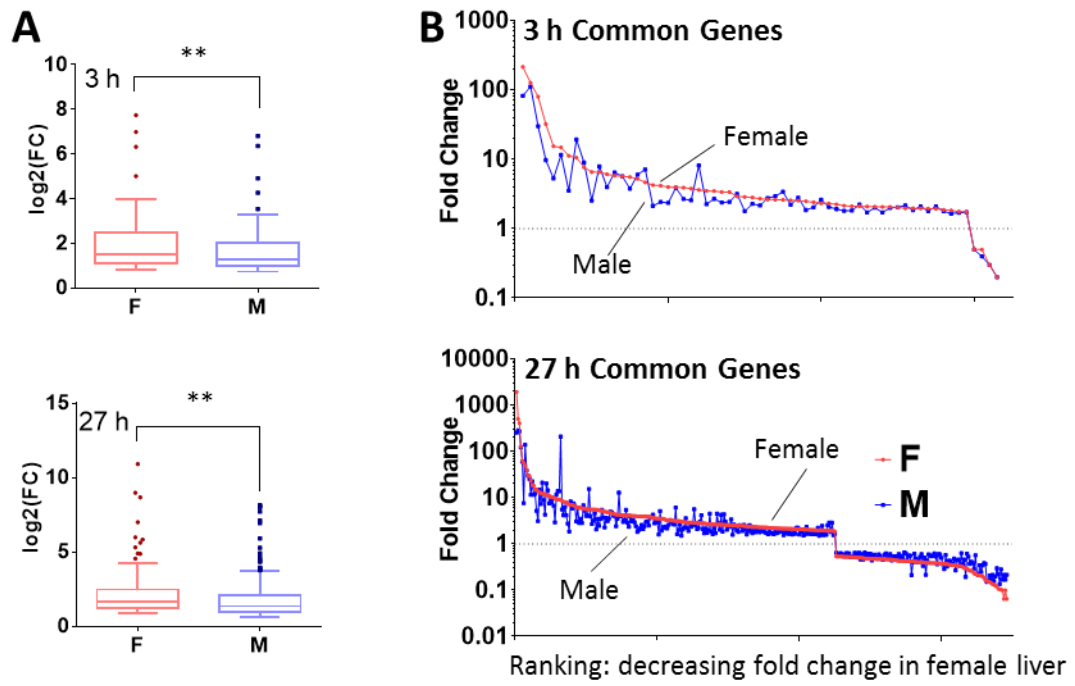


Fig. 3.7 **KEGG pathways enriched in sets of RefSeq genes responding to TCPOBOP or PCN.** Shown are gene numbers and Benjamini p-values for KEGG pathways enriched in responsive genes ($|\text{FC}| > 1.5$ and $\text{FDR} < 0.001$) in each of the indicated five RNA-seq data sets, based on DAVID analysis. Pathways not directly related to metabolism are shown in lighter color (red). Pathways related to drug metabolism or other liver metabolic processes are found in all data sets, while pathways related to cell cycle and DNA replication are found exclusively in TCPOBOP exposed males at 27 h. Horizontal dashed red lines: $\text{FDR} = 0.05$. See Table S3.4 for full details of KEGG pathway analysis.

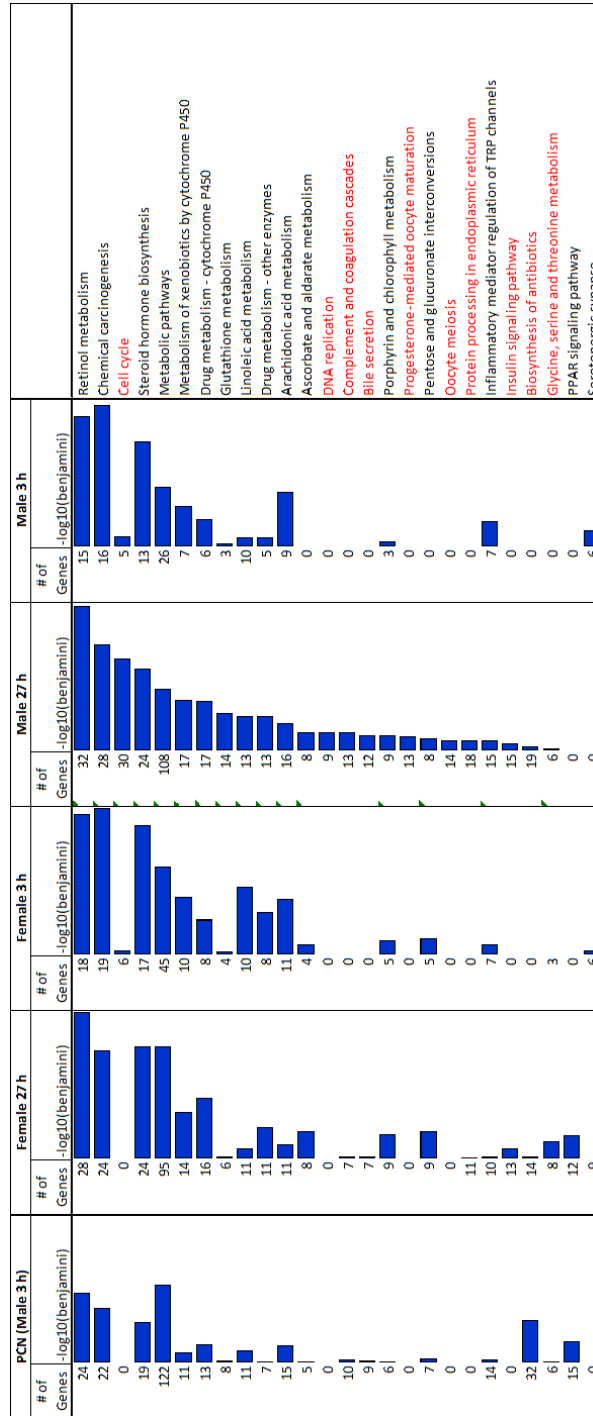


Fig. 3.8 Upstream regulator analysis of TCPOBOP and PCN responsive genes.

Shown are up to the top 10 upstream regulators identified in each RNA-seq data set by IPA. Green bars identify upstream regulators related to activation CAR or other nuclear receptors (NR). Orange bars identify upstream regulators associated with a pro-tumor response, and purple bars identify upstream regulators associated with an anti-tumor response based on their known biological functions and direction of the activated z-score calculated by IPA. Blue arrow heads mark upstream regulators known to be involved in CAR-dependent liver tumor promotion, and gray arrow heads mark TNF/NF κ B pathway related regulators

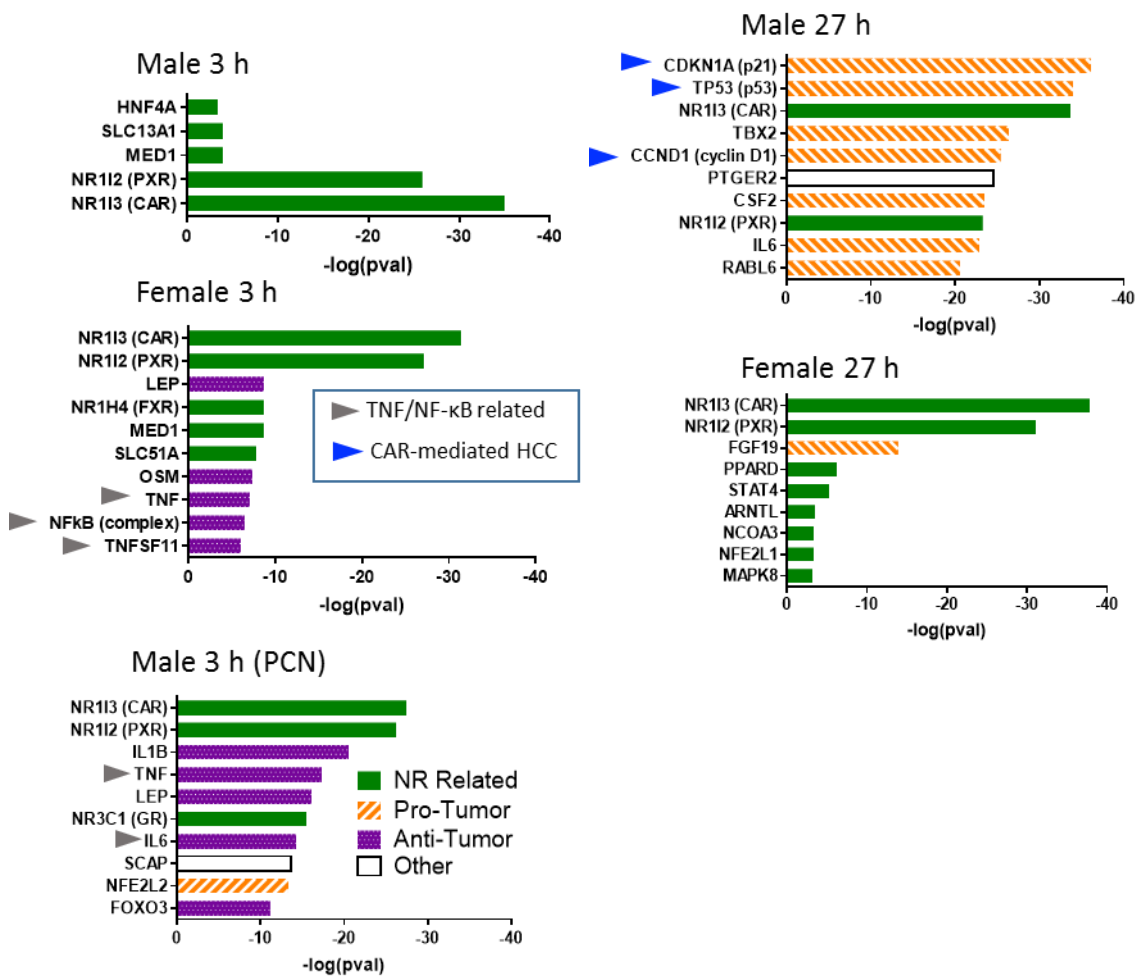
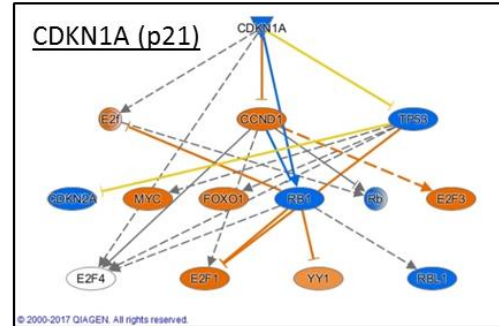
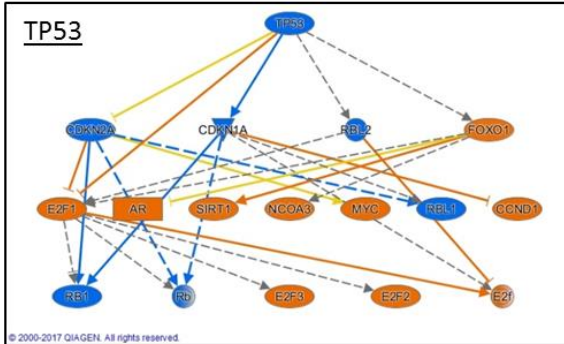
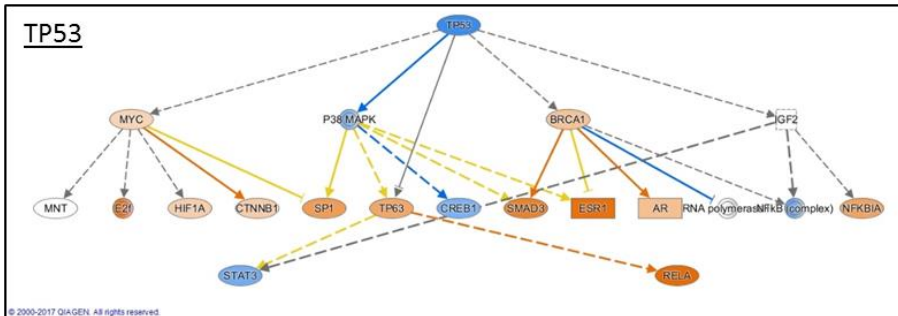


Fig. 3.9 Mechanistic networks related to CAR-mediated HCC are found in TCPOBOP treated males but not females. IPA upstream regulator mechanistic networks relating to CAR-dependent liver tumor promotion. Orange color indicates activation of the upstream regulator while blue color indicates inhibition. The intensity of color indicates strength of activation or inhibition. Strong activation of pathways related to TP53 and CDKN1A (p21) are seen in TCPOBOP-treated males at 27 h, while minimal activation of TP53 is seen in TCPOBOP-treated females at 27 h. 16 out of the 17 upstream regulators identified in the TP53 mechanistic network in male liver show strong activation/strong inhibition, while 12 out of 14 upstream regulators in the p21 network also showed strong activation/strong inhibition. In contrast, although IPA identified a mechanistic network for TP53 in females, 0 out of the 20 upstream regulators showed either strong activation or strong inhibition. A mechanistic network related to CDKN1A (p21) in 27 h TCPOBOP-treated female liver was not reported by IPA.

27 h TCPOBOP - Male



27 h TCPOBOP - Female



Prediction Legend

more extreme in dataset less
 Increased measurement (red circle)
 Decreased measurement (green circle)

more confidence less
 Predicted activation (orange circle)
 Predicted inhibition (blue circle)

Glow Indicates activity when opposite of measurement

Predicted Relationships
 Leads to activation (orange arrow)
 Leads to inhibition (blue arrow)
 Findings inconsistent with state of downstream molecule (yellow arrow)
 Effect not predicted (grey arrow)

Fig. 3.10 Gene targets of 10 factors involved in CAR-mediated HCC. Gene targets were identified by IPA for each of the 10 indicated pro-tumor upstream regulators identified in male liver at 27 h (see Table S3.5). Shown is the number of gene targets for each upstream regulator that are responsive at $|FC|>1.5$ and $FDR<0.001$ in each of the five exposure groups.

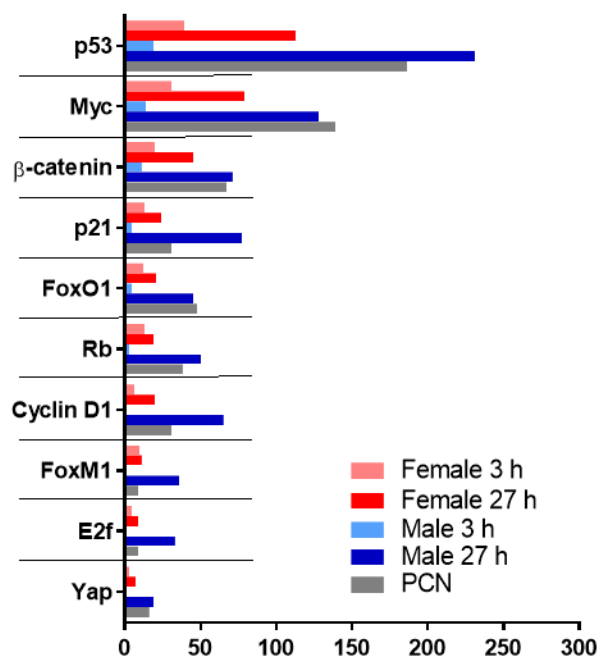
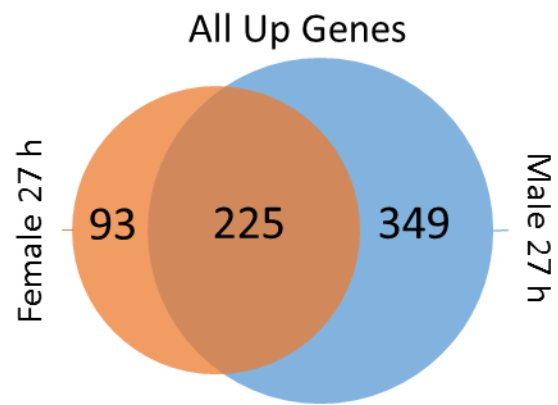
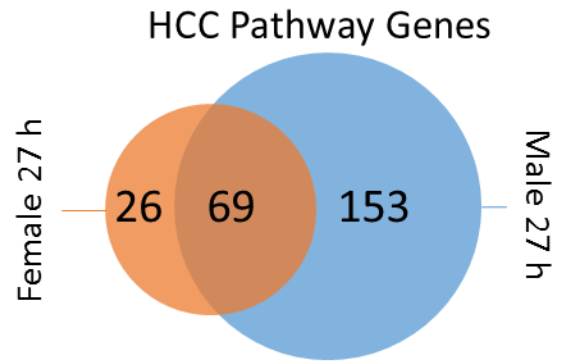


Fig. 3.11 Genes regulated by TCPOBOP in males only are enriched for the CAR-mediated HCC pathway. A single gene list was obtained from the union of all 27 h TCPOBOP-responsive gene targets of the 10 pro-tumor upstream regulators (HCC pathway gene targets) in male and female liver (Table S3.4). Shown is the overlap of the HCC gene pathway gene targets that are up regulated by TCPOBOP at 27 h in male vs. female liver (top), and the overlap of all genes up regulated by TCPOBOP at 27 hr in male vs. female liver (bottom). These patterns of overlap differ at $p=0.002$ (exact binomial test) (see text).



$p=0.002$

Fig. 3.12 The Nf-κB pathway is active in PCN treated males and TCPOBOP treated females but not TCPOBOP treated males. IPA upstream regulator mechanistic network related to Nf-κB. Results are shown for 3h TCPOBOP exposed male and female liver, and for 3 h PCN exposed male liver. It is apparent that activation of Nf-κB along with its downstream gene targets occurs in TCPOBOP exposed females and PCN exposed males, and that minimal-to-no activation of this pathway occurs in TCPOBOP exposed males.

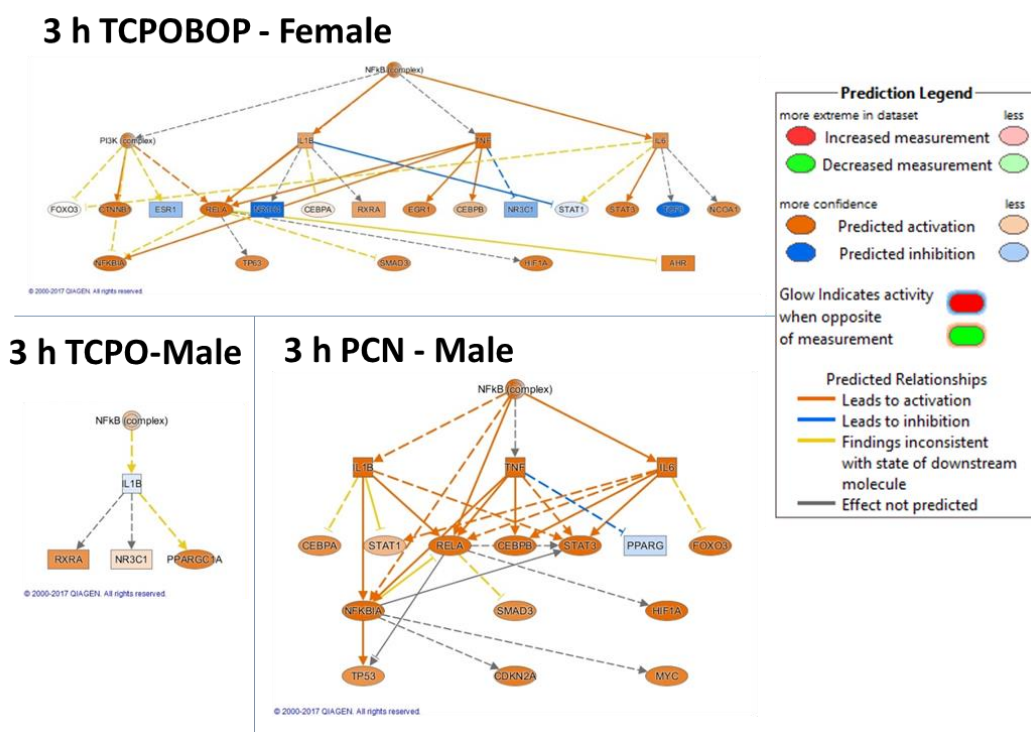


Fig. 3.13 TCPOBOP responsive mouse liver lncRNAs. Venn diagram showing overlap within the set of 402 TCPOBOP responsive mouse liver lncRNAs across 4 RNA-seq data sets (251 up regulated, 151 down regulated; Table 1). lncRNAs that were responsive to TCPOBOP in multiple datasets but in opposite directions were excluded from this analysis. For example, 3 lncRNAs that were down regulated in female liver at 3 h but were up regulated in female liver at 27 h were not included in the list of 5 lncRNAs shown here to overlap between those two groups.

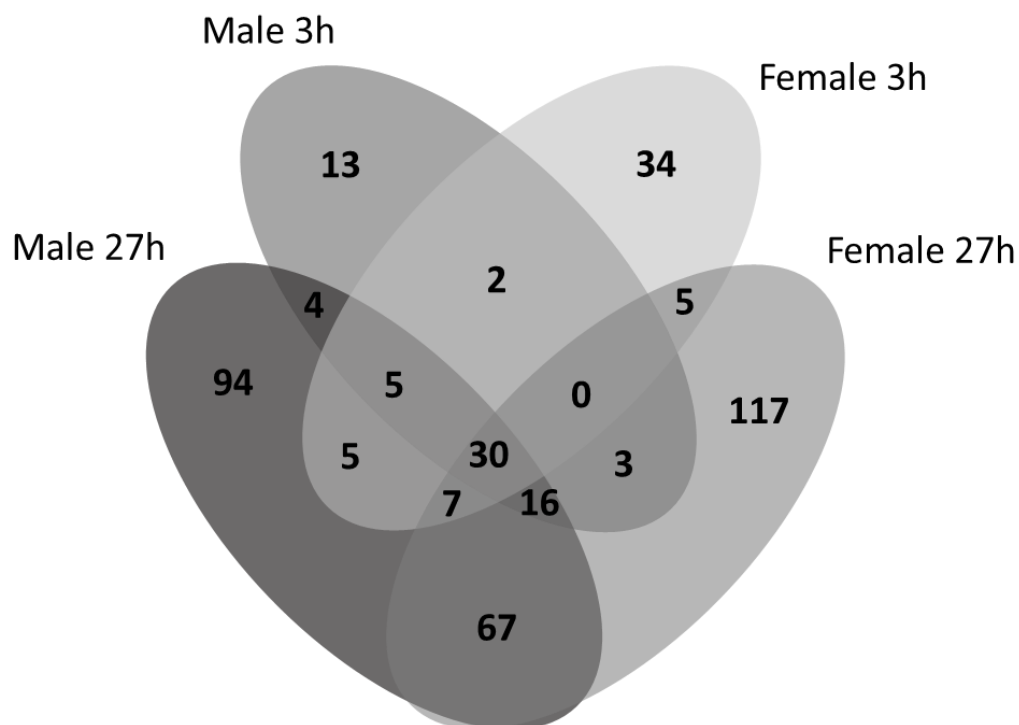


Fig. 3.14 **Liver-expressed lncRNAs responsive to TCPOBOP or PCN that are proximal to regulated RefSeq genes.** A-C, Structure and relative position of select regulated multi-exonic lncRNAs that are in close proximity to, or overlapping, a responsive RefSeq gene. Shown are RNA-seq read densities for male liver after 3 h and 27 h TCPOBOP treatment, as well as vehicle control tracks. D-F, Relative expression (FPKM, fragments per kilobase per million sequence reads) for each lncRNA and its nearby responsive RefSeq gene, as measured by RNA-Seq. The mean expression level (FPKM) of each transcript in the vehicle control samples was as follows: Cyp2b10, 1.2; lncRNA_5998, 0.1; Glnm1, 6.3; lncRNA_8460, 1.4; Alas1, 32.1; and lncRNA_8301, 0.3, and is marked by a horizontal dashed line in each figure.

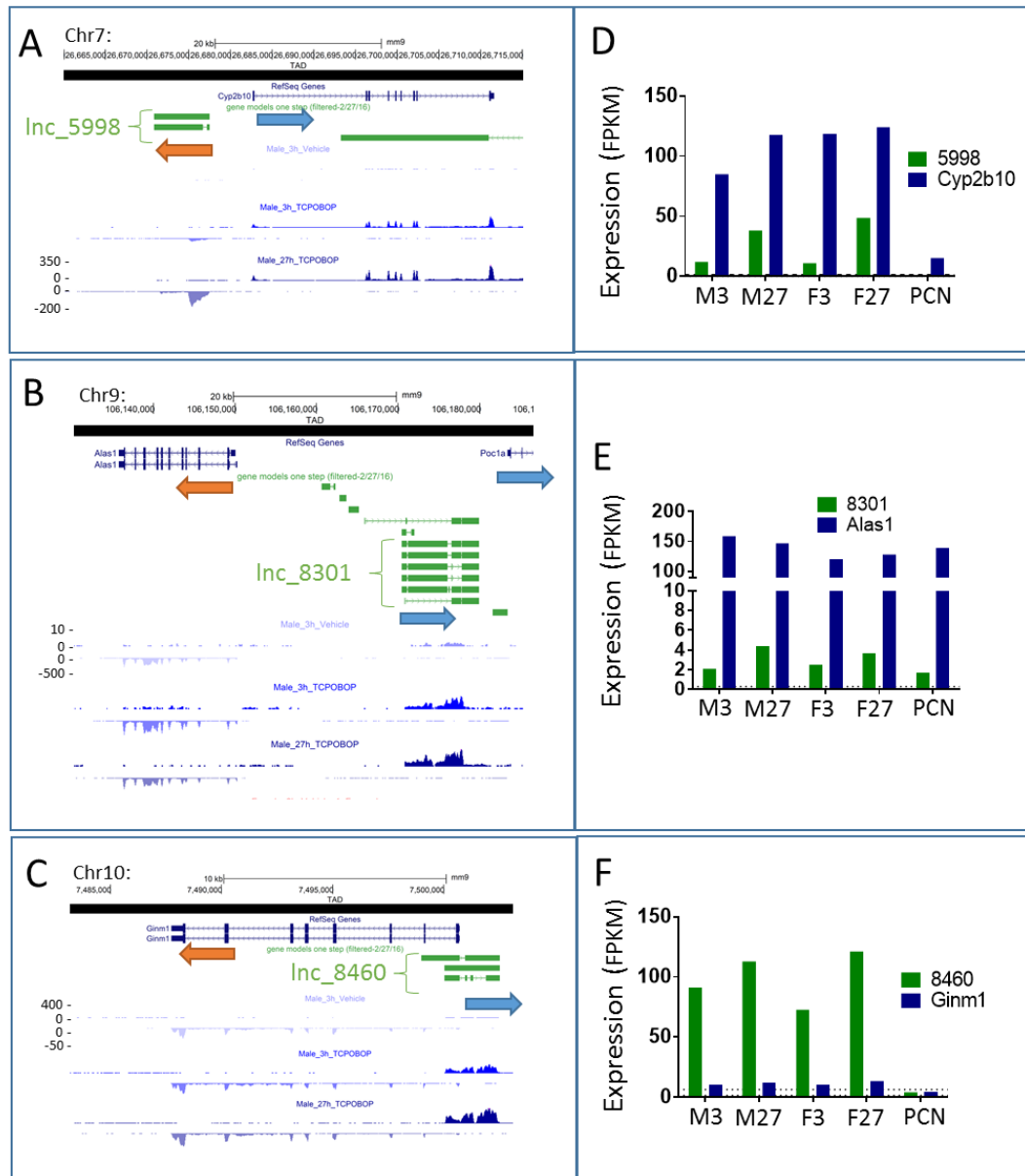
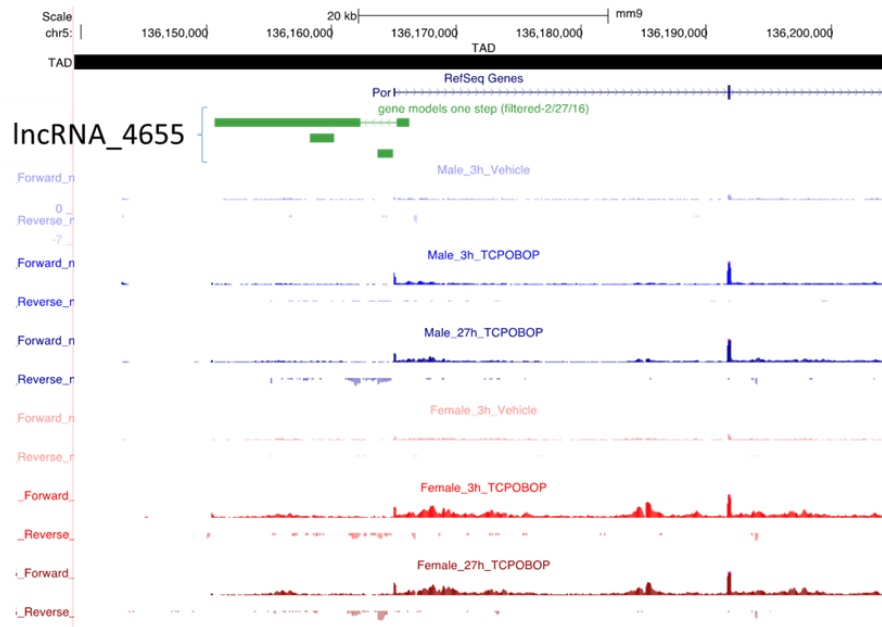


Fig. 3.15 **lncRNA_4655 may negatively related Por.** A. Structure and orientation of lncRNA_4655 and its overlapping RefSeq gene Por. B. Relative expression of lncRNA_4655 and Por. The mean expression level (FPKM) of each transcript in the vehicle control samples was as follows: lncRNA_4655, 0.03; Por, 21.48.

A



B

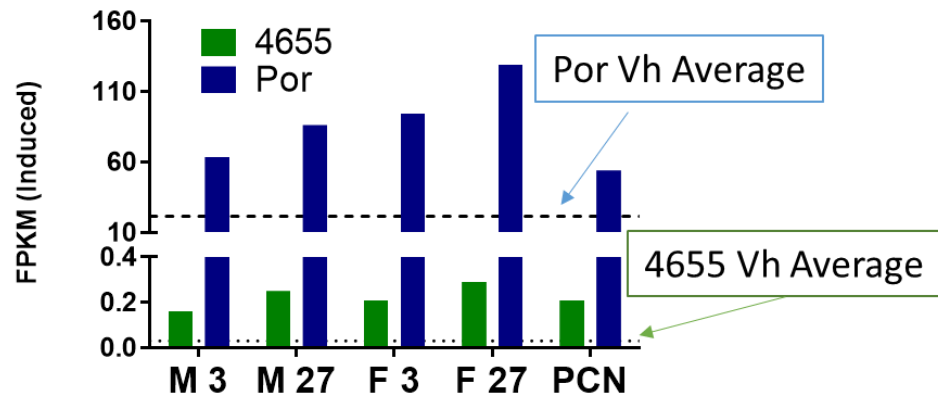
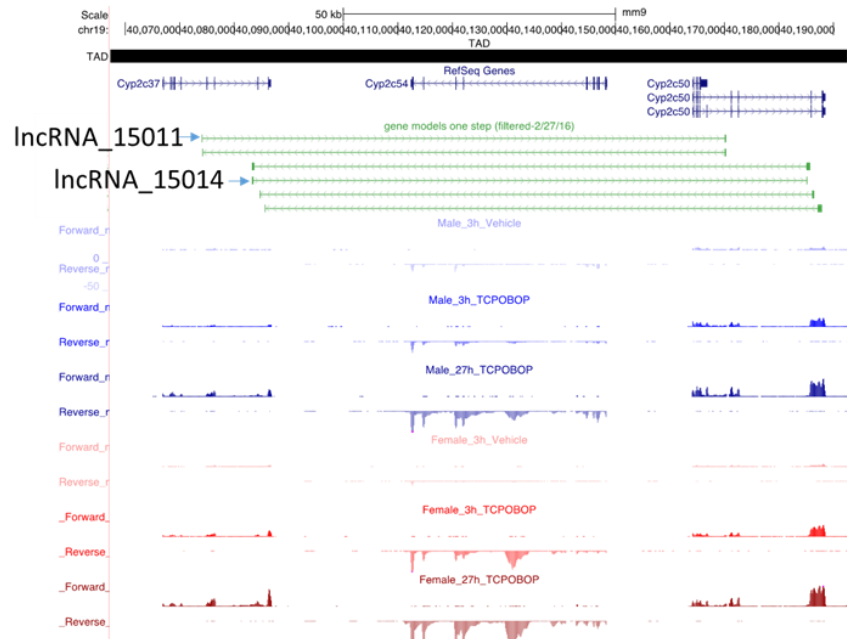
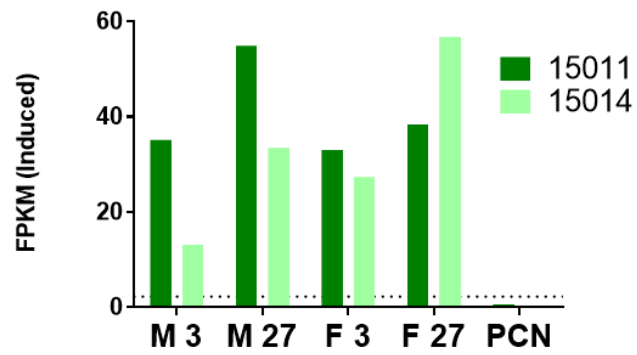


Fig. 3.16 Two regulated lncRNAs are anti-sense to *Cyp2c37* and *Cyp2c50*. A. Structure and relative orientation of two lncRNAs (*lncRNA_15011* and *lncRNA_15014*) and two highly expressed RefSeq genes (*Cyp2c37* and *Cyp2c50*). B. Relative expression of *lncRNA_15011* and *lncRNA_15014*. C. Relative expression of *Cyp2c37* and *Cyp2c50*. The mean expression level (FPKM) of each transcript in the vehicle control samples was as follows: *lncRNA_15011/lncRNA_15014*, 2.3; *Cyp2c37/Cyp2c50*, 6.7.

A



B



C

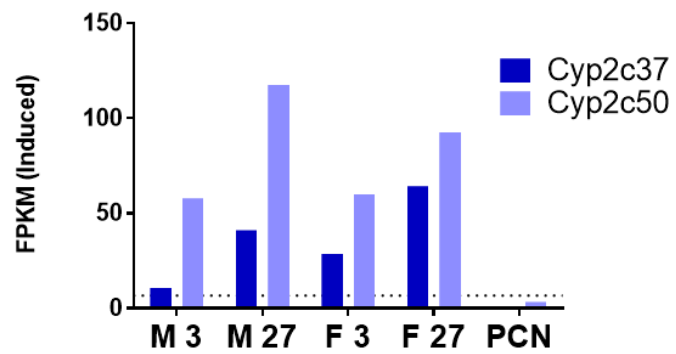


Fig. 3.17 LncRNAs responsive to TCPOBOP or PCN that are not proximal to the nearest regulated RefSeq gene. A, Structure of *lncRNA_3779* and a subset of its isoforms (also see Fig. S4G), which is in the same TAD but > 300 kb away from the closest TCPOBOP responsive transcript (Table S3.6). B, Structure of *lncRNA_8767*, whose nearest TCPOBOP responsive RefSeq gene is in a different TAD (i.e., is distal). Also shown are RNA-seq read densities for male liver after 3 h and 27 h TCPOBOP treatment, as well as vehicle control tracks. C-D, Expression levels (FPKM values) of *lncRNA_3779* and *lncRNA_8767* across the five data sets, as measured by RNA-Seq. The mean expression level (FPKM) of each transcript in the vehicle control samples was as follows: *lncRNA_3779*, 1.6; and *lncRNA_8767*, 0.6, and is indicated by a horizontal dashed line.

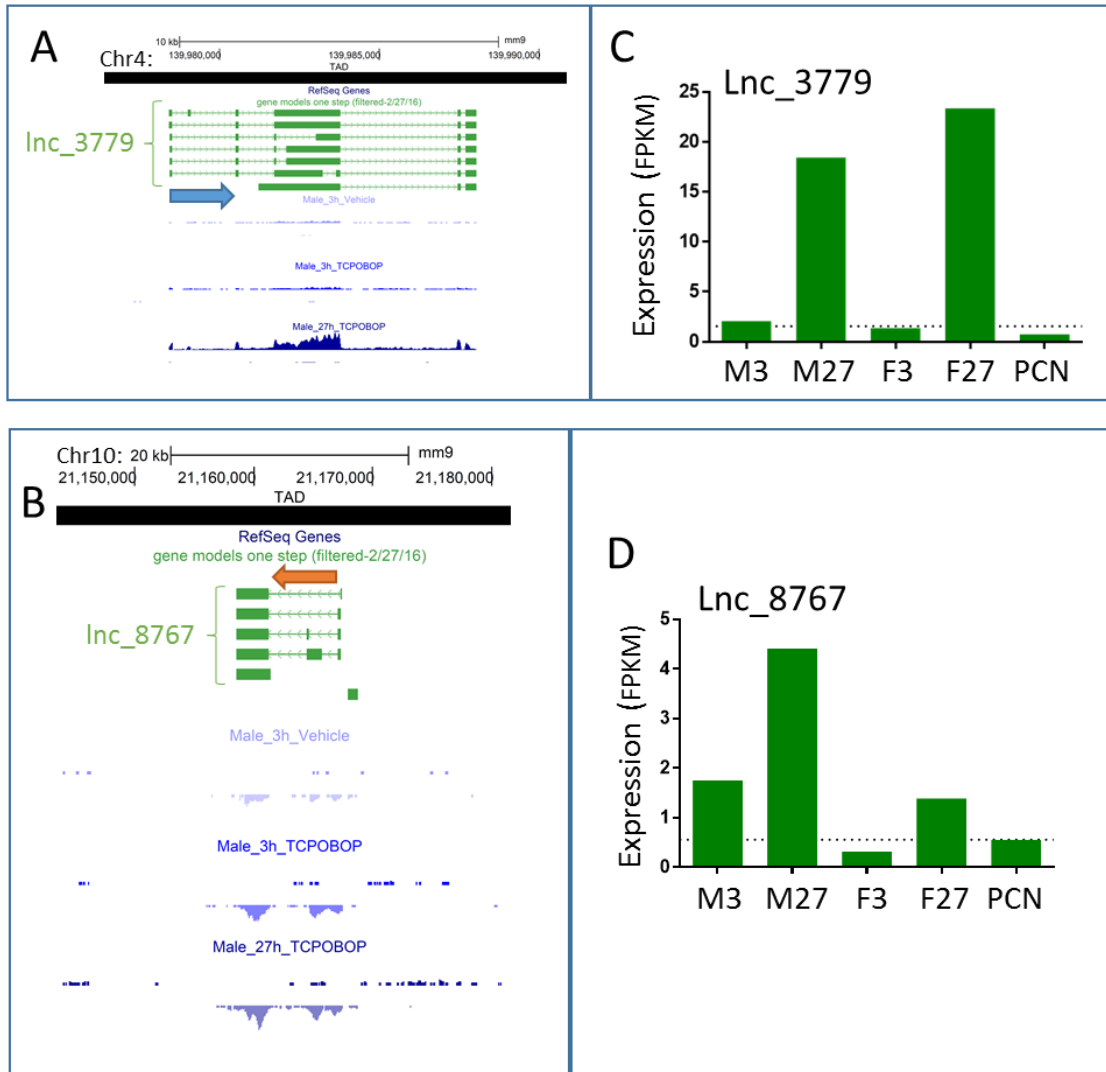


Table 3.1 Primer sequences used for qPCR analysis.

Mouse Gene Target	Forward Primer	Reverse Primer
18S	CGCCGCTAGAGGTGAAATTC	CCAGTCGGCATCGTTTATGG
Cyp2b10	GGAGGAACTGCGGAAATCCC	ATAGAACAGCTCCAGCAGGC
Cyp2c55	AAGAACATCAGCAAATCCTCAAC	CTTTGAACCAAGTACAGAGTGAACA
Hsd3b5	TCGAAAACATGAAGGGAATTGTC	CAGTACTCTCACCTTGGCCTTTGT
Apol7a	GCGGCTCCTGCTGACAGA	TGCAAGGCAGCTTCCTCTTC
Akr1b7	GCTGGACTATCTGGACCTGTATCTG	TTTGCCTTTATTGCTTTGGGTAAT

Table 3.2 Regulation of RefSeq genes by TCPOBOP or PCN in mouse liver.

Differentially expressed genes were identified using edgeR. Numbers of genes that respond to TCPOBOP or PCN treatment in mouse liver at $|\text{fold-change}| > 1.5$ and $\text{FDR} < 0.001$ are reported.

Experiment			Up RefSeq Genes	Down RefSeq Genes	Total Genes
Male	TCPOBOP	3 h	88	17	105
Male	TCPOBOP	27 h	576	295	871
Female	TCPOBOP	3 h	149	57	206
Female	TCPOBOP	27 h	318	240	558
Male	PCN	3 h	542	426	968

Table 3.3 Output from IPA upstream regulator analysis. Shown are select predicted upstream regulators in TCPOBOP treated female mice (3h) and TCPOBOP treated male mice (27) involved in CAR-mediated HCC or Nf-kB signaling.

Upstream Regulator	Molecule Type	TCPOBOP Female 3 h			TCPOBOP Male 27 h		
		Predicted Activation State	Activation z-score	p-value of overlap	Predicted Activation State	Activation z-score	p-value of overlap
FOXM1	transcription regulator	Activated	2.6	1.9E-06	Activated	4.2	1.3E-14
CTNMB1 (beta-catenin)	transcription regulator	Activated	2.3	8.5E-06	Activated	2.1	7.9E-08
E2F1	transcription regulator	Activated	2.1	2.1E-04	Activated	3.5	1.7E-12
NFKBIA	transcription regulator	Activated	2.8	4.9E-05	Activated	2.4	2.2E-08

Table 3.5 Mono-exonic and multi-exonic lncRNAs that respond to TCPOBOP or PCN at $|\text{fold-change}| > 2$ and $\text{FDR} < 0.05$. Shown are: lncRNAs that respond to TCPOBOP in at least one of the four TCPOBOP treatment groups (All TCPOBOP-responsive); lncRNAs that respond in all 4 TCPOBOP datasets and in the same direction (i.e. up in all 4, or down in all 4) (Common responses in all 4); lncRNAs that respond to TCPOBOP at 3 h in males and/or females, as indicated, irrespective of their response to TCPOBOP at 27 h (Early responding); lncRNAs that respond to TCPOBOP at 27 h but not at 3 h (Late responding); and lncRNAs responsive to PCN in male liver at 3 h but that did not respond in any of the four TCPOBOP datasets (Responsive to PCN only). For both early responding and late responding lncRNAs, 'both Male and Female' indicates the lncRNA is either up regulated or down regulated in both sexes. The last column indicates the number of TCPOBOP-responsive lncRNAs in each category that responded in the same direction to 3 h PCN treatment in male liver. Ten lncRNAs whose response to TCPOBOP was discrepant across the four conditions were excluded from this analysis. n/a, not applicable.

TCPOBOP response profile	Up	Down	Also PCN responsive (same direction)
	Number of lncRNAs		
All TCPOBOP-responsive lncRNAs	251	151	80
Common responses in all 4 TCPOBOP datasets	30	0	15
Early responding, both Male and Female	34	3	20
Early responding, Male only	7	10	7
Early responding, Female only	19	20	15
Late responding, both Male and Female	50	17	7
Late responding, Male only	50	44	10
Late responding, Female only	68	49	9
Responsive to PCN only	45	73	n/a

Table 3.6 TCPOBOP and PCN responsive multi-exonic lncRNAs and their relationship to co-regulated RefSeq genes. Shown are responsive multi-exonic lncRNAs ($|\text{FC}|>2$, $\text{FDR}<0.05$) in each data set and their genomic location relative to the nearest responsive RefSeq gene ($|\text{FC}|>1.5$, $\text{FDR}<0.001$). Cis co-expression and cis opposite expression refer to lncRNA-RefSeq gene pairs where both genes respond to TCPOBOP or PCN and either overlap in their genomic coordinates by at least 1 base pair, or are within the same topologically associating domain (TAD), as indicated under Proximity to RefSeq. The lncRNA and RefSeq genes in each pair can either be co-expressed or show opposite expression, as indicated. Distal lncRNAs are those whose nearest regulated RefSeq gene is in a different TAD on the same chromosome.

Multi-exonic lncRNA gene sets	Male	Male	Female	Female	Male	Male
	TCPOBOP 3 h	TCPOBOP 27 h	TCPOBOP 3 h	TCPOBOP 27 h	TCPOBOP 3 h	TCPOBOP 27 h
	Number of lncRNAs					
Responsive lncRNAs						
Up regulated	52	112	62	131	126	126
Down regulated	40	83	39	93	53	53
	12	29	23	38	73	73
Proximity to RefSeq						
Overlaps RefSeq gene	19	31	17	27	26	26
Same TAD as RefSeq gene	7	42	14	37	54	54
Cis vs Distal						
Cis co-expressed lncRNA-RefSeq pairs (%)	26 (50%)	64 (58%)	30 (48%)	59 (45%)	73 (58%)	73 (58%)
Cis opposite lncRNA-RefSeq pairs (%)	0	9 (8%)	1 (2%)	5 (4%)	7 (6%)	7 (6%)
Distal lncRNAs (%)	26 (50%)	39 (35%)	31 (50%)	67 (51%)	46 (37%)	46 (37%)

CHAPTER 4- Modulation of the mouse liver epigenome following TCPOBOP exposure

4.1 Abstract

The impact of activated nuclear receptors on the epigenome has been studied for several nuclear hormone receptors but the genome-wide chromatin remodeling induced by CAR activation has not been investigated. Here, we provide a detailed analysis of the rapid changes to the mouse liver epigenome following short-term exposure to the mouse CAR-specific agonist ligand TCPOBOP for 3 h or 27 h. By using previously characterized mouse liver topologically associating domain (TAD) boundaries, we show that ~50% of TCPOBOP-responsive genes cluster in TAD regions. Next, DNase-seq analysis revealed several thousand genomic regions in mouse liver that respond to TCPOBOP-exposure, which also cluster into highly responsive TADs and map to highly responsive protein coding and non-coding genes. ChIP-seq analysis of three activating histone modifications (K4me1, K4me3, and K27ac) identified enhancer regions that become activated in mouse liver upon TCPOBOP-exposure. Finally, we observed a temporal relationship between gene induction and epigenomic modifications; some Δ DHS that open or close at 3 h map to genes that respond to TCPOBOP only after 27 h while some genes that are induced respond before new enhancers are activated. These studies provide a comprehensive view

of rapidly changing epigenomic modifications in mouse liver following *in vivo* exposure to the mouse CAR agonist ligand, TCPOBOP.

4.2 Introduction

The nuclear receptor (NR) superfamily includes the steroid hormone receptors, such as androgen receptor (AR; *Nr3c4*), glucocorticoid receptor (GR; *Nr3c1*), and estrogen receptor α and β (ER α , ER β ; *Nr3a1*, *Nr3a2*), as well as the xenobiotic sensing receptors constitutive androgen receptor (CAR; *Nr1i3*) and pregnane X receptor (PXR; *Nr1i2*). Following activation of these receptors by steroid hormones, in the case of AR, ER, and GR, or xenobiotic chemicals, in the case of CAR and PXR, NRs translocate to the nucleus where they act as transcription factors that induce or repress target gene expression.

Epigenetic modifications of the genome mark genes that can be rapidly targeted for induction or repression by activated NRs. The genome-wide effects of ER α (Mann et al. 2011, Abdel-Hafiz and Horwitz 2015), AR (Cucchiara et al. 2017), and GR (Nagaich et al. 2004, Burd et al. 2012, Grontved et al. 2013) on epigenomic remodeling of chromatin following activation has been widely studied, but comparatively little is known about the xenobiotic sensing receptors, particularly TCPOBOP-activated CAR. For example, GR induces chromatin opening and closing through direct DNA binding events (Nagaich et al. 2004, Burd et al. 2012), while activation of AR and ER in prostate and breast cancers, respectively, have been associated with widespread changes in histone modifications

(Mann et al. 2011, Abdel-Hafiz and Horwitz 2015, Cucchiara et al. 2017). Previous methods used to characterize epigenetic modifications that influence the induction of CAR target genes, such as *Cyp2b10* (Honkakoski and Negishi 1997, Chen et al. 2012), its human ortholog *CYP2B6* (Inoue and Negishi 2009), and other DME gene targets (Sugatani et al. 2001, Chen et al. 2003, Kuno et al. 2008), have been limited to low throughput techniques focused on a few select genomic regions. However, to date, a genome wide analysis of potential DNA regulatory elements and epigenomic changes that occur following CAR activation in liver has not been performed.

Transcriptional regulatory elements can be identified by analysis of chromatin accessibility, which reflects the presence or absence of nucleosomes at specific loci, and can be determined genome wide by limited DNase-I digestion of isolated nuclei followed by massively parallel sequencing (DNase-Seq) to identify DNase-I hypersensitivity sites (DHS) (Thurman et al. 2012, Ling and Waxman 2013, Ling and Waxman 2013). DNase-seq, in combination with chromatin immunoprecipitation with sequencing (ChIP-seq) for various histone modifications, has been used to identify functional cis-regulatory elements in mammalian cells (Shlyueva et al. 2014), including mouse liver (Sugathan and Waxman 2013, Yue et al. 2014). Recent advances led by the Mouse ENCODE Consortium have identified several hundred thousand putative regulatory elements across many mouse cell lines and tissues, including liver, through a combination of DNase-seq and ChIP-seq for histone proteins and transcription factors (TFs) (Yue et al. 2014). However, by design,

tissue samples analyzed by the ENCODE consortium were derived from mice that were not subjected to any experimental treatments and thus do not identify regulatory elements that may be dynamically activated or repressed following exposures to chemicals that activate TFs such as CAR. Chromatin sites that are DHS and contain the histone modifications H3 lysine 4 monomethylation (K4me1) and H3 lysine 27 acetylation (K27ac), mark active enhancer regions (Creyghton et al. 2010, Shlyueva et al. 2014), while DHS in combination with H3 lysine 4 trimethylation (K4me3) and K27ac is a mark of active promoters (Shlyueva et al. 2014). Thus, using these three chromatin marks in conjunction with DHS data can be effective at identifying major cis-regulatory elements that control gene expression.

Historically, our understanding of how genomes are organized was based on a few select locus control regions (LCRs) that were known to influence the expression of genes within a localized cluster (Fraser and Grosveld 1998), however, recent studies show the mammalian genome is organized into mega-base scale structures by a series of chromatin loops known as topologically associating domains (TADs) (Rao et al. 2014, Bonev and Cavalli 2016). TAD regions are delineated by chromatin boundaries that functionally separate large genomic regions from each other. Thus a refined approach to identifying DNA regulatory elements that influence target gene expression is to limit the interactions to within inter-TAD connections. Additionally, TAD regions provide a series of insulated

regions that may allow for rapid, coordinated gene regulation of gene families within a localized genomic cluster (Le Dily and Beato 2015).

Here, we use DNase-seq to identify DHS in male and female mouse liver that open or close following TCPOBOP treatment. These Δ DHS regions are identified both early (3 h) and late (27 h) after TCPOBOP treatment, and are shown to be enriched proximal to CAR responsive coding and non-coding genes within the same TAD. ChIP-seq experiments targeting the activating histone modifications K4me1, K4me3 and K27ac were performed in male mice to characterize the TCPOBOP-induced changes in local chromatin environment around DHS and responsive genes. ChIP-seq data were used in conjunction with male liver DNase-seq data described above to identify DNA regulatory elements that respond to CAR activation in male mouse liver, including active enhancers and active promoters and their putative gene targets. Through global analysis of DHS and histone marks we present a comprehensive overview of changes to the epigenome that may influence mouse liver gene expression following TCPOBOP exposure.

4.3 Materials and Methods

4.3.1 Animal procedures and tissue extraction

All mouse work was carried out in compliance with procedures approved by the Boston University Institutional Animal Care and Use Committee. Animal handling and treatments were performed as described in Chapter 3. Briefly, male and female mice, 7-weeks old,

were purchased from Charles River Laboratories (Wilmington, MA) and kept on a 12-hour light cycle (7:30 AM – 7:30 PM). Mice were treated with TCPOBOP (Sigma Cat. # T1443) at a dose of 3 mg/kg body weight or with vehicle alone (corn oil with 1% DMSO) by i.p. injection between 8:00 AM and 8:45 AM on day 1. Livers were collected after 3 h, or after 27 h (3 h + 24 h), between 11:00 AM and 11:45 AM on day 1 or day 2, respectively, to control for the strong circadian rhythm effects on gene expression seen in mouse liver (Kettner et al. 2016).

Nuclei were isolated from individual vehicle-treated (control) and TCPOBOP-treated mouse livers as described in Chapter 3. Briefly, fresh liver tissue was homogenized in buffer on ice in a Potter-Elvehjem homogenizer. The homogenate was layered on fresh homogenization buffer and spun at 4°C in an ultracentrifuge for 35 min at 25,000 RPM. For DNase-I hypersensitivity assays (see below), nuclear pellets containing approximately 150 million nuclei were resuspended in 400 µL of nuclei storage buffer and either crosslinked immediately with formaldehyde, as described below, or stored at -80°C for DNase digestion and DNase hypersensitivity analysis.

4.3.2 Sonication of liver chromatin and ChIP analysis

Chromatin immunoprecipitation (ChIP) analysis of histone marks was carried out using sonicated liver chromatin, either prepared by sonication of cross-linked liver nuclei, or by sonication of whole liver tissue that was initially snap-frozen in liquid nitrogen and then

crosslinked with formaldehyde and then sonicated, in experiments carried out by Aram Shin of our laboratory.

To crosslink nuclei, ~100 million nuclei freshly isolated from male mouse livers were resuspended in 1 mL of crosslinking buffer (10 mM HEPES pH 7.6, 25 mM KCl, 0.34 M sucrose, 2 mM MgCl₂, 0.15 mM 2-mercaptoethanol) preheated to 30°C. Formaldehyde (37% stock solution) was added to give a final concentration of 0.8% (v/v), followed by incubation at 30°C for precisely 9 min with periodic mixing to crosslink the nuclei. Glycine was then added to a final concentration of 0.1 M to quench the crosslinking reaction at room temperature. Crosslinked nuclei were layered on 3 mL of fresh homogenization buffer and centrifuged at 4°C for 30 min at 25,000 RPM. Crosslinked nuclear pellets were resuspended in RIPA buffer (50 mM Tris-HCl pH 8.1, 150 mM NaCl, 1% (v/v) NP-40, 0.5% (v/v) deoxycholic acid, Na salt; 0.1% (v/v) sodium dodecyl sulfate, and 1 tablet Roche cOmplete Protease Inhibitor Cocktail™ per 50 mL (Sigma, catalog number 11697498001)). Nuclei were then sonicated in a Bioruptor Twin sonicator on high until chromatin was ~100-300 bp in length (80-100 cycles; 1 cycle = 30 sec on and 30 sec off). Sonicated material from vehicle and 3 h TCPOBOP-treated livers was then used for ChIP for histone marks (see below).

To crosslink whole liver tissue, a third of each liver (previously snap-frozen in liquid nitrogen and stored at -80°C) was retrieved and placed on ice for 5 min, followed by tissue

disruption in a glass Dounce homogenizer with 4 mL of cross-linking buffer (50 mM HEPES [pH 7.5], 100 mM NaCl, 1 mM EDTA, and 0.5 mM EGTA) containing protease inhibitors (Thermo Scientific Pierce Protease Inhibitor Tablets, EDTA-free). The tissue homogenate was passed through a 70-micron cell strainer in a petri dish. Additional cross-linking buffer was added to the homogenizer to rinse out the remaining tissue and passed through the cell strainer. Formaldehyde was added to the homogenate to a final concentration of 1% and mixed rapidly in a conical tube. The mixture was rocked for 10 min at 22°C, followed by the addition of glycine to a final concentration of 0.125 M. The sample was rocked for 2 min at 22°C and then centrifuged at 4°C for 5 min at 2,500g. The pellet was washed twice in 10 mL of PBS, resuspended in 10 mL of lysis buffer 1 (50 mM HEPES [pH 7.5], 140 mM NaCl, 1 mM EDTA, 10% glycerol, 0.5% IGEPAL CA-630, 0.25% Triton X-100, and protease inhibitors) and rocked for 10 min at 4°C. The sample was then centrifuged at 4°C for 5 min at 2,000g, and the resultant pellet was resuspended in 10 mL of lysis buffer 2 (200 mM NaCl, 1 mM EDTA, 0.5 mM EGTA, 10 mM Tris-HCl [pH 8.0], and protease inhibitors) and rocked for 5 min at 4°C. After another centrifugation, the pellet was resuspended in RIPA buffer to a final volume of 2 mL. The sample was transferred to a 15-mL TPX tube (Diagenode) containing 0.3 mL polypropylene beads (Diagenode), and sonicated for 35 cycles (30s on, 30s off) at 4°C using a Bioruptor Pico sonicator (Diagenode). Sonicated material from vehicle-treated and 27 h TCPOBOP-treated livers was then used for ChIP for histone marks (see below).

4.3.3 Chromatin Immunoprecipitation (ChIP) assay

Protein A Dynabeads (Invitrogen #1002D) were used for all ChIP reactions in the 3 h exposure group and Protein A/G Magnetic Beads (Bimake #B23030) were used for in the 27 h exposure group. For K4me1, K4me3, and K27ac, 15 μ L of Dynabeads or 10 μ L of Bimake beads were used. For K27me3, 10 μ L of Dynabeads or 5 μ L of Bimake beads were used. Beads were washed three times with 1 mL of blocking solution (0.5% (w/v) BSA in PBS). 300 μ L of fresh blocking solution was then added to each tube containing beads, followed by antibody specific for histone H3 K4me1 (1.2 μ g, Abcam ab8895), K4me3 (3 μ g, Abcam ab8580), K27ac (1.2 μ g, Abcam ab4729), or K27me3 (2 μ g, Abcam ab6002). Beads and antibody in blocking solution were incubated for 3 h at 4°C with rocking. Beads with bound antibody were washed three times with blocking solution and the following amounts of sonicated chromatin were then added: 10 μ g for K27me3; 15 μ g for K4me1, K4me3, and K27ac. ChIP reactions were incubated overnight at 4°C with rocking. The next day, ChIP samples were centrifuged at 2,000 RPM for 2 min at 4°C and washed with RIPA buffer three times. Next, ChIP samples were washed three times with RIPA containing 0.5 M NaCl, followed by a single wash with TE buffer. After the final wash, 50 μ L elution buffer (50 mM Tris-HCl, pH 8.1, 10 mM EDTA, 1% (v/v) SDS) was added and samples were incubated in a 65°C water bath for 35 min with periodic mixing. The supernatant containing eluted chromatin was adjusted to an NaCl concentration to 0.2 M and then incubated at 65°C to reverse crosslinks. RNase A (ThermoFisher E0531, 10 mg/mL) was then added to a final concentration of 0.12 mg/mL and the samples were

incubated at 37°C for 30 min. Proteinase K (Bioline BIO-37084, 20 mg/mL) was added to a final concentration of 0.39 mg/mL and samples were incubated at 37°C for 2 h. Finally, DNA was purified using QIAprep 2.0 spin columns (Qiagen) according to the manufacturer's manual and eluted in a final volume of 50 μ L TE buffer.

4.3.4 DNase-I hypersensitivity assay

Frozen liver nuclei in nuclei storage buffer, corresponding to \sim 30 million nuclei, were rinsed in ice-cold Buffer A (15 mM Tris-Cl pH 8.0, 15 mM NaCl, 60 mM KCl, 1 mM EDTA pH 8.0, 0.5 mM EGTA pH 8.0, 0.5 mM spermidine, 0.3 mM spermine tetrahydrochloride) three times by adding 500 μ L Buffer A and centrifuging at 1,500 RPM at 4°C for 10 min. Following the final rinse, nuclear pellets were resuspended in Buffer D (Buffer A + 6 mM CaCl₂, 75 mM NaCl) pre-warmed to 37°C, to give a final concentration of 5.88×10^6 nuclei per mL. 32 units of DNase-I enzyme (RQ1 RNase-Free DNase, 1 U/ μ L (Promega, catalog number M610A) was added to 68 μ L of pre-warmed Buffer D in a 2-mL tube and incubated for 30 sec at 37°C. 850 μ L of resuspended nuclei (5×10^6 nuclei) were added to the 2-mL tube and digested with DNase I for precisely 2 min. After 2 min, 950 μ L of Stop Buffer (50 mM Tris-HCl pH 8.0, 100 mM NaCl, 0.1% (v/v) SDS, 100 mM EDTA pH 8.0, 1 mM spermidine, 0.3 mM spermine tetrahydrochloride, 20 μ g/mL RNase A) was added and the sample was immediately placed in a 55°C water bath. DNase-I digestion was done on 30×10^6 total nuclei per mouse, divided into 6 separate tubes, in parallel. Samples were then incubated at 55°C for >15 min. 5 μ L proteinase K was then

added and samples were further incubated at 55°C overnight. The six parallel DNase digestions were pooled and the DNA was isolated by phenol:chloroform extraction. The final supernatant was adjusted to 0.8 M NaCl. Digested material was size-selected by sucrose gradient centrifugation, as follows. First, phenol:chloroform extracted material (11.4 mL) was loaded on a sucrose gradient containing following layers (bottom to top: 12 mL of 20% sucrose buffer (20 mM Tris-HCl pH 8.0, 5 mM EDTA pH 8.0, 1 M NaCl, containing 20% sucrose) and 3 mL each of 17.5%, 15.0%, 12.5%, and 10.0% sucrose buffer, for a total volume of 34.5 mL. The sucrose gradient was then spun in an ultracentrifuge at 25,000 RPM for 24 h at 25°C. Fractions (1.9 mL) were sequentially removed from the top of the gradient, and fractions number 7-11, corresponding to digested material ~100 bp to ~1,000 bp in length, were isolated and pooled. Material from fractions 7-11 was further purified on a QIAprep 2.0 spin column (Qiagen) according to the manufacturer's manual. Agencount AMPure XP bead purification was performed using the manufacturer's protocol with ratios of 0.6x and 1.9x for double sized size-selection to obtain 125-400 bp DNA fragments.

4.3.5 DNase-seq and ChIP-seq libraries, sequencing and data analysis

DNase-seq was performed using two biological replicate pools for each of four treatment groups (males and females, TCPOBOP treatment for 3 h or 27 h, and time-matched vehicle controls). Each replicate pool consisted of DNA fragments released by DNase-I from n=3-5 individual livers; released fragments from each individual liver in a separate DNase

digestion reaction were purified and then pooled and used for library preparation. ChIP-seq was carried out on three biological replicates (chromatin prepared from individual mouse livers) for each ChIP target in male mice (TCPOBOP treatment for 3 h or 27 h and time-matched vehicle controls). Sequencing libraries were prepared from 5 ng of ChIP DNA or 5 ng DNase-I released DNA material using the NEBNext Ultra DNA Library Prep Kit for Illumina (New England Biolabs). Sequencing was performed at the New York Genome Center (New York, New York) on an Illumina HiSeq 2500 instrument. Single end sequence reads, 50 bp in length, were obtained for the DNase-seq samples, and 50 bp paired end reads were obtained for the ChIP-seq samples.

Sequencing data was analyzed using a custom DNase-seq/ChIP-seq pipeline developed by Andy Rampsaud of this laboratory. The pipeline processes raw FASTQ files and outputs various quality control metrics, including FASTQC reports (FASTX-Toolkit v0.0.13.2), confirmation of read length, verification of the absence of read strand bias, quantification of contaminating adapter sequence (Trim_galore v0.4.2), and distributions of insert-size lengths (for paired-end read sequencing), as calculated and visualized using Picard (v1.123). Reads were mapped to the mouse genome (release mm9) using Bowtie2 (v2.2.6) (Langmead et al. 2009). All DNase-seq and ChIP-seq peak sets, discovered as described below, were filtered to remove ENCODE blacklisted regions (Consortium 2012) as well as peaks comprised of >4 identical reads that do not overlap any other read ('straight peaks').

Regions of DNase hypersensitivity (DHS) were discovered as peaks identified by MACS2 (v2.1.0.20150731) (Zhang et al. 2008) run using the options (`--nomodel --shift -100 --extsize 200`), to inhibit read shifting, and (`--keep-dup`), to retain all reads contributing to a peak signal. Peaks were discovered for each of n=4 samples per TCPOBOP treatment condition, i.e. n=2 vehicle-treated and n=2 TCPOBOP-treated DNase-seq samples x 4 conditions (male and female at 3 h and 27 h). The 16 resultant DHS peak lists were merged using mergeBed (BEDtools) to give a single list of 60,739 peaks, based on the union of all DHS peak regions. This DHS set was used for all downstream analysis involving DHS. Genomic regions that were more open or more closed ($|\text{fold-change}| > 2$ and $\text{FDR} < 0.05$ (Benjamini-Hochberg adjusted p-value)) following TCPOBOP treatment were discovered using diffReps (Shen et al. 2013) using the nucleosome option (200 bp window size) and setting (`--frag`) to zero for all comparisons. MACS2 peaks (DHS) that overlapped with a diffReps identified region, as determined by BEDtools (Quinlan and Hall 2010), were annotated as ΔDHS , while MACS2 peaks that did not overlap a diffReps region were designated static DHS. The full listing of DHS regions is reported in [Supplemental Table S.4.1](#).

ChIP-seq peaks were identified for three activating histone H3 marks, K4me1, K4me3, and K27ac, using MACS2 (v2.1.0.20150731) using the option (`--keep-dup`); all other parameters were set to the default option. For each chromatin mark, peak unions were

generated based on the union of peaks called in the n=12 male mouse liver ChIP-seq samples (n=3 vehicle, n=3 TCPOBOP at 3 h, and n=3 vehicle, n=3 TCPOBOP at 27 h). A single list of 78,340 K27ac peaks was generated using this method. Genomic regions that showed significantly differential ChIP-seq signals between vehicle-treated and TCPOBOP-treated samples were discovered separately at 3 h and at 27 h using the nucleosome option (200 bp window) in diffReps and $|\text{fold-change}| > 2$ and $\text{FDR} < 0.05$ (Benjamini-Hochberg adjusted p-value) thresholds. The overlap between K27ac diffReps regions at 3 h or at 27 h and the list of 78,340 MACS2 peaks was determined using BEDTools, and peaks were annotated as differential K27ac peaks based on overlap results. K27ac MACS2 peaks that did not have a corresponding overlapping diffReps region were annotated as static K27ac peaks. K4me1 and K4me3 peaks were annotated using the same method as K27ac. 139,460 K4me1 peaks and 43,120 K4me3 peaks were identified based on the unions of n=12 sequenced samples for each mark. The full listings of all K27ac, K4me1, and K4me3 peak regions with annotations is found in Supplemental Table S4.2 A-C.

4.3.6 Peak normalization

For DHS and ChIP-seq peak visualization in the UCSC genome browser (<https://genome.ucsc.edu/>), peaks were normalized using reads in peak per million mapped sequence reads (RiPPM) as a scaling factor. First, to obtain a comprehensive list of peaks for each data set (termed peak union), FASTQ files from individual replicates were

concatenated to produce combined replicates. For each data set, a vehicle-treated combined sample, TCPOBOP-treated combined sample, and all-replicates (vehicle-treated and TCPOBOP-treated) combined sample was generated. Peak calls from individual and combined samples were concatenated into a single file. BEDtools merge was then used to generate a single peak list. The fraction of reads in peaks for each sample was then calculated to obtain a scaling factor. Raw read counts were divided by the per-million scaling factor to obtain the RiPPM normalized read counts.

4.3.7 TAD definitions and grouping

Topologically associated domains (TADs) were those defined for mouse liver (Vietri Rudan et al. 2015). TAD regions were identified that contained at least one regulated gene whose expression was altered by TCPOBOP in either male or female liver at either time point. The number of genes in each TAD that were up regulated or were down regulated was counted for each condition of TCPOBOP exposure (male and females at each time point), allowing us to separate TADs into three distinct groups for each exposure condition: TADs that contain at least one up regulated gene but no down regulated genes (up-only TAD), TADs that contain at least one down regulated gene but no up regulated genes (down-only TAD), and TADs that contained both up and down regulated genes (mixed TAD). TADs that do not contain any TCPOBOP-responsive genes were not considered further.

4.3.8 TCPOBOP-responsive gene sets

Lists of TCPOBOP-responsive RefSeq and lncRNA genes were generated as described in Chapter 3, based on a gene list comprised of 24,197 RefSeq genes and 3,152 multi-exonic lncRNA genes. This list of candidate gene targets was used for peak mapping (see below). Each gene was mapped to a TAD region based on the location of its transcription start site (TSS). TCPOBOP-responsive lncRNA genes were defined by $|\text{fold change}| > 2$ and adjusted p-value (FDR) < 0.05 ; responsive RefSeq genes were defined by a $|\text{fold change}| > 1.5$ and adjusted p-value (FDR) < 0.001 , the same as in Chapter 3. Additionally, genes that are downstream targets of 10 known CAR-dependent upstream regulators – cyclin D1, p53, p21, FoxO1, FoxM1, Rb, b-catenin, E2f, Yap, Myc – which were previously identified by Ingenuity Pathway Analysis in Chapter 3 (Lodato et al. 2017), were flagged and used for further downstream analysis.

4.3.9 DHS and K27ac peak mapping

Genomic regions that show a TCPOBOP-induced change in chromatin accessibility, i.e., Δ DHS that open or that close following TCPOBOP exposure, as well as static DHS, were mapped to mouse liver TAD regions for each given experiment (male and female, 3 h or 27 h TCPOBOP exposure). For each experiment, we counted the number of up regulated and down regulated genes within each TAD that contained a DHS (an opened Δ DHS, a closed Δ DHS, or a static DHS). DHS were then classified based on their DHS status

(opened, closed, or static) and if they were found within a TAD that also contained a regulated gene, or not.

A single putative gene target was assigned for each DHS, and separately, for each K27ac peak, using BEDtools, to map the above lists of 60,739 DHS peaks and 78,340 K27ac peaks to the nearest gene TSS within the same TAD. Full listing of mapping results can be found in Supplemental Table S4.3.

Regions of interest based on their DHS and K27ac patterns were defined genome wide. First, the overlap of the sets of 60,739 DHS and 78,340 K27ac peaks was determined using BEDtools. Given DHS, by their definition, lack histone proteins, DHS and K27ac regions that were <1000 bp (1 kb) apart were considered overlapping. Overlapping regions that contain both a static DHS and a static K27ac peak following TCPOBOP treatment were termed ‘stable active regions’, while Δ DHS that also overlapped with a Δ K27ac were termed ‘dynamic active enhancers’. Full listing of dynamic active enhancers and stable active regions can be found in Supplemental Table S4.3.

4.3.10 DHS and K4me3 clustering

Δ DHS were grouped by k-means clustering based on K4me3 signal in a 2-kb window centered at the DHS midpoint using deepTools. For 3 h Δ DHS, two clusters (k=2) was used to differentiate regions with low K4me3 signal (putative enhancer regions) from

regions with high K4me3 (putative promoter regions). For 27 h Δ DHS, three clusters (k=3) was used to distinguish low and high K4me3 signal, like 3 h Δ DHS, and an additional cluster with intermediate K4me3 signal. Three clusters was not used for analysis of 3 h Δ DHS due to two subsequent resulting clusters being indistinguishable. Full listing of K4me3 clustering results can be found in Supplemental Table S4.4.

4.3.11 Statistics

Fisher exact test was implemented in the analysis package R to assess the statistical significance of enrichment calculations. Where noted, student t-test was implemented using Prism 7 (Graphpad) to assess pair-wise relationships.

4.4 Results

4.4.1 TAD boundaries separate up and down regulated genes

Mammalian genomes are organized at multiple levels, including functional segmentation into large megabase-scale DNA loops, called topologically associating domains (TADs). TADs function to insulate genomic regions by allowing intra-TAD, but not inter-TAD, interactions (Oti et al. 2016) and provide a context for potential coordinated transcriptional responses to stimuli (Le Dily and Beato 2015). To investigate whether TCPOBOP-responsive genes cluster in TAD regions, we used the ~3,600 sets of TAD boundaries established for mouse liver (Vietri Rudan et al. 2015) to identify TADs that contain genes that respond to TCPOBOP exposure. ~70-80% of TCPOBOP-responsive TADs contain

only a single regulated gene (Fig. 4.1A). The other ~20-30% of responsive TADs contain multiple (2 to 12) responsive genes, encompassing 41-52% of TCPOBOP-responsive genes (Fig. 4.1B, Table 4.2). The TADs that have multiple TCPOBOP-responsive genes were further classified by the concurrence of gene responses within the TAD (Table 4.2). ~64-81% of TADs with multiple responsive genes show concurrent regulation, with 46-77% having genes that are up regulated without any down regulated genes, and 4-30% having genes that are down regulated without any up regulated genes (Table 4.2, Supplemental Table S4.5).

4.4.2 DHS dynamically open and close and cluster in TADs with co-responsive genes

To ascertain whether TCPOBOP treatment alters liver chromatin accessibility, we carried out DNase I hypersensitivity analysis (DNase-seq) to identify open chromatin regions as DHS in liver nuclei harvested from TCPOBOP-treated mice and vehicle-treated controls. Genomic regions that showed statistically significant differences in accessibility to DNase-I cleavage following TCPOBOP treatment (Δ DHS) were identified at two time points (3 h and 27 h) in both male and female mouse liver (Fig. 4.2 A-D and Table 4.3). TCPOBOP induced DHS opening as well as DHS closing, with some Δ DHS regions responding early (3 h) and others responding late (27 h) to TCPOBOP treatment (Table 4.5, Fig. 4.2 A-B) were identified. In both sexes, many more Δ DHS were found in the 27 h TCPOBOP-treated livers, which is consistent with the larger number of genes and greater magnitude of gene

induction responses reported in Chapter 3 for 27 h compared to 3 h TCPOBOP exposure (Fig. 4.2 A-B). Further, a majority Δ DHS were unique to one sex (Fig. 4.2 C-D and Table 4.5), consistent with the sex-differences in gene responses described in Chapter 3.

Δ DHS were grouped based on whether they mapped to a TAD that contains only up regulated genes, only down regulated genes, a mixture of up and down regulated genes, or no regulated gene (Table 4.3, Fig. 4.2 E-F). At both 3 h and 27 h, a majority of Δ DHS are not in a TAD with a regulated gene (Fig. 4.2 E-F, grey). Of the Δ DHS that open after 3 h, and are within a TAD containing a regulated gene(s), 76-90% are associated with up regulated genes (Table 4.3, Group_1A). Many more Δ DHS were identified after 27 h TCPOBOP treatment, and a higher fraction of these Δ DHS (40-45%) mapped to TADs with TCPOBOP-responsive genes (Fig. 4.2 E-F), primarily TADs with up regulated genes in the case of Δ DHS that opened (Table 4.3, Group_1A), and TADs with down regulated genes for Δ DHS that closed (Table 4.3, Group_3B). These findings indicate that TCPOBOP-associated Δ DHS regions are generally associated with positive regulation of gene expression.

4.4.3 Δ DHS responses precede changes in gene expression

Unexpectedly, a majority of the Δ DHS that open following TCPOBOP exposure were found in TADs that do not contain a TCPOBOP-responsive gene (Fig. 4.2 E-F and Table 4.3, Group_2 and Group_4). We considered the possibility that the gene targets of these

Δ DHS (putative enhancers; see below) might respond more slowly to TCPOBOP than their associated Δ DHS regions. Indeed, we found that a substantial fraction of the 3 h Δ DHS without any 3 h TCPOBOP-responsive genes within the same TAD are in TADs that contain one or more TCPOBOP-responsive genes at 27 h (Fig. 4.2 G; 128 out of 366 such Δ DHS in male liver (37.5%), and 102 out of 358 such Δ DHS in female liver (28.5%)). Similarly, a subset of the 3 h-closing Δ DHS within a TAD that do not contain a regulated gene at 3 h acquire one or more responsive genes by 27 h (Fig. 4.2 G; 9 of 62 such Δ DHS (14.5%) in male liver, and 32 of 87 such Δ DHS (37%) in female liver). Thus, gene expression changes lag behind chromatin opening or closing for a subset of 3 h TCPOBOP-responsive Δ DHS. Furthermore, in male liver, 92 of the 128 Δ DHS that open with a delayed gene response were in a TAD that contained an up regulated gene(s), while 3 of the 9 Δ DHS that close with a delayed gene response were in a TAD that contained a down regulated gene(s) (Fig 4.2 H). Similarly, in female liver, 83 of the 102 Δ DHS that open with a delayed gene response were in a TAD that contained an up regulated gene(s), while 22 of the 32 Δ DHS that close with a delayed gene response were in a TAD that contained a down regulated gene(s) (Fig. 4.2 H). Several TADs that contain TCPOBOP-induced DME gene families also contain many Δ DHS, including TAD3479, which contains 9-12 inducible *Cyp2c* genes and up to 38 Δ DHS (Table 4.4, Supplemental Table S4.5). Other highly active TADs that contain DME gene families include TAD110, which contains *Ugt1a* genes; TAD694, which contains *Gstm* genes; TAD1156, which contains *Cyp3a* genes; and TAD1421, which contains *Cyp2b* genes (Table 4.4, Supplemental Table S4.5).

4.4.4 Δ DHS are enriched nearby TCPOBOP-responsive genes

Putative gene targets for each DHS were assigned by mapping the DHS to the nearest gene transcription start site (TSS) within the same TAD, considering both RefSeq genes and liver-expressed multi-exonic lncRNA genes (see Methods, Supplemental Table S4.1). Next, we examined the relationship between changes in chromatin accessibility and gene expression for the set of 121 Δ DHS that open in both sexes at 3 h and remain open at 27 h (i.e., Δ DHS common to all 4 TCPOBOP treatments; Table 4.5, Supplemental Table S4.1). These Δ DHS, whose induced open chromatin state persists for at least 24 h in both sexes, showed an exceptionally strong, 121-fold enrichment ($p < E-43$; Fisher exact test) for genes that showed a common response to TCPOBOP in all four treatments (Table 4.6). 27 of these 121 Δ DHS map to 19 TCPOBOP-responsive genes, including 6 lncRNA genes (Table 4.7). Protein-coding RefSeq genes in this group include *Cyp2b10*, *Cyp3a11* and *Por*, all known targets of TCPOBOP-activated CAR.

Further, in each of the 4 TCPOBOP experiments, we observed a strong enrichment of Δ DHS that open for up regulated genes, as compared to a background set comprised of static DHS (Table 4.6). Similarly, in both sexes, Δ DHS that close were strongly enriched for genes that are down regulated at 27 h. There was also a weak enrichment of Δ DHS that close for genes that are down regulated in at 3 h in females, but not in males (Table 4.6). These findings support the proposal that these sets of TCPOBOP-responsive Δ DHS

encompass regulatory elements (enhancers and promoters) that activate by TCPOBOP treatment and regulate TCPOBOP-stimulated gene responses.

4.4.5 Δ DHS Open and Close nearby TCPOBOP-responsive HCC genes

We previously reported a striking male-bias for TCPOBOP activation of CAR-dependent hepatocellular carcinoma promoting pathways, specifically after 27 h TCPOBOP exposure (Lodato et al. 2017). One hypothesis is that this sexually dimorphic genic response is driven by a corresponding male bias Δ DHS response. To test this hypothesis, we counted the number of Δ DHS that map to downstream gene targets of a set of 10 known CAR-dependent HCC upstream regulators (see Methods and Chapter 3) in both male and female mouse liver (Fig. 4.2 I). Surprisingly, we observe no significant sex bias in the number Δ DHS that map to these genes (enrichment score = 1.0, $p = 0.97$; Fig. 4.2 I, left), even if we restrict the genes to only those HCC downstream targets that are responsive to TCPOBOP (enrichment score = 1.07, $p=0.58$; Fig. 4.2 I, right).

4.4.6 Chromatin marks flanking Δ DHS

To better understand the dynamic changes in the epigenome after TCPOBOP exposure, we performed genome-wide ChIP-seq analysis of TCPOBOP-treated mouse liver chromatin, and vehicle-treated controls, to map three histone-H3 chromatin marks commonly seen at promoters or enhancers flanking DHS (Shlyueva et al. 2014): K4me3, which is commonly found at promoters; K4me1, which marks distal enhancer regions; and K27ac, which marks

active enhancers when found in combination with K4me3, or active promoters when found in combination with K4me1 (Mann et al. 2011, Abdel-Hafiz and Horwitz 2015). We used the K4me3 mark intensities in a 2-kb window surrounding each TCPOBOP-induced Δ DHS region to cluster the sets of Δ DHS found at 3 h and 27 h. Two clusters of Δ DHS were obtained from the 3 h TCPOBOP dataset, one with strong K4me3 marks (promoter-like Δ DHS) and one with weak K4me3 marks (enhancer-like Δ DHS) (Fig. 4.3A). A third cluster (intermediate K4me3 marks; weak promoter-like Δ DHS) was obtained at 27 h (Fig. 4.3B) in addition to strong and weak K4me3 clusters, as was found at 3 h. At 3 h, the median distance from the Δ DHS to the nearest TSS was 0 bp and 16 kb for the strong and weak K4me3-marked Δ DHS clusters (Fig. 4.4), while at 27 h, the median distance was 0 bp, 1 kb, and 25 kb for the weak, intermediate, and strong K4me3 clusters, respectively (Fig 4.4). These results are consistent with the K4me3-marked Δ DHS being promoter-like Δ DHS (Shlyueva et al. 2014). The Δ DHS distal to TSS had the highest K4me1 signals at both time points, consistent with their designation as enhancer-like Δ DHS (Fig. 4.3 A-B). Both Δ DHS classes (i.e. promoter-like and enhancer-like) showed strong K27ac, consistent with their being active promoters and active enhancers, respectively.

Significant changes in K27ac mark intensity (Δ K27ac) were seen in TCPOBOP-exposed liver chromatin, with \sim 1,200 sites showing an increase and \sim 500-600 sites showing a decrease in this mark after 3 h or 27 h (Table 4.8, Supplemental Table S4.2 A). Many fewer K4me1 sites were responsive to TCPOBOP, with only 324 sites showing a significant

change after 3 h, and 366 sites changing at 27 h (Table 4.8, Supplemental Table S4.2 B). K4me3 is the most stable, with only 188 sites at 3 h and 87 sites at 27 h showing significant changes following TCPOBOP exposure (Table 4.8, Supplemental Table S4.2 C). Only a fraction of these Δ K27ac sites were at or nearby (within 1 kb) Δ DHS; many more were at or nearby static DHS at both 3 h and 27 h and about ~50% were not found near any DHS (Fig. 4.5 A). Likewise, a majority of Δ DHS were associated with static K27ac at 3 h or no K27ac at 27 h (Fig. 4.5 B). Since K27ac plus DHS mark active promoters and enhancers, this finding suggests that TCPOBOP activation of liver regulatory elements can be manifested in several ways: by an increase in K27ac marks at DHS that are constitutively open (static DHS), and by chromatin opening (Δ DHS) at genomic regions that in many cases are already marked by K27ac, but in some cases are associated with a further increase in K27ac (Δ K27 in combination with Δ DHS) (Fig. 4.5 A-B).

4.4.7 Activated enhancers map to responsive genes

DHS and K27ac were used in combination with the enhancer DHS definition described above (i.e. DHS with nearby K27ac) to define (1) dynamic enhancers, i.e. genomic regions whose accessibility and K27ac were both induced (Δ DHS and Δ K27ac) following TCPOBOP treatment; and (2) static active enhancers (marked by both a static DHS and a static K27ac mark; see Methods) (Fig. 4.5 C). All active regions, defined by the presence of a DHS and a K27ac peak (i.e. static and Δ DHS in combination with either static or Δ K27ac), were mapped to the all genes within the same TAD. The number of TCPOBOP-

responsive genes that had only static active enhancers within the same TAD, and genes that had both static active regions and dynamic active enhancers were counted and are reported at both 3 h (Fig. 4.5 D) and 27 h (Fig. 4.5 E). There was a strong enrichment, at both 3 h (59-fold; $p < E-14$, Fisher exact test) and 27 h (18-fold; $p < E-141$), of the responding genes for a mapped dynamic enhancer as compared to a static active enhancer when only the single nearest gene target within the TAD was considered (Fig. 4.5 F). There was an equally strong enrichment of the up regulated genes for a mapped dynamic enhancer as compared to inactive regions (i.e. static DHS without a K27ac mark) at 3 h (46-fold; $p < E-27$) and also at 27 h (17-fold; $p < E-134$) (Fig. 4.5 F).

Genes with dynamic enhancer sites within their TADs represent only a small subset of the total number of genes up regulated at each time point (Fig. 4.5 D, brown). Thus, 24 out of the 67 Δ DHS- Δ K27ac dynamic active enhancer sites map to 34 of the 138 genes up regulated at 3 h (Fig. 4.5 D, brown), while 199 out of the 480 Δ DHS- Δ K27ac dynamic active enhancers map to 255 of the 708 genes up regulated at 27 h (Fig. 4.5 E). Genes with associated Δ DHS- Δ K27ac dynamic active enhancers within their TADs, however, were more strongly induced by TCPOBOP than those genes that were targeted by static active enhancers alone (Fig. 4.5 G). Examples of dynamic active enhancers and stable active regions were visualized near three highly TCPOBOP-inducible genes described in Chapter 3, *Cyp2b10*, *lnc_5998* and *Cyp3a11* (Fig. 4.6 A-B). *Cyp2b10* and an induced upstream lncRNA, *lnc_5998*, are found on chromosome 7 within TAD1421, while *Cyp3a11* is found

on chromosome 5 within TAD1156. Six dynamic active enhancers are found upstream of *Cyp2b10*, three of which are within the gene body of *lnc_5998* (Fig. 4.6 A, yellow arrow heads). Two dynamic active enhancers are proximal to the *Cyp3a11* TSS (Fig. 4.6 B, yellow arrow heads) while three static DHS are found upstream (negative strand) of the TSS, two of which are flanked by Δ K27ac (Fig. 4.6 B, purple arrow heads) and one of which is flanked by static K27ac (Fig. 4.6 B, blue arrow heads, stable active region).

4.4.8 Genes responding to 3 h TCPOBOP exposure prior to enhancer activation

As shown above, a minority of TCPOBOP-responsive genes have a dynamic active enhancer in the same TAD at either 3 h or 27 h (Fig. 4.5 D-E, orange). One hypothesis is that the early induction of these genes by TCPOBOP is mediated by static active enhancer regions, and that other enhancer regions become active after longer exposure to TCPOBOP. To test this hypothesis, the 138 genes induced by TCPOBOP at 3 h were mapped to the active regions defined after 27 h of TCPOBOP exposure. Remarkably, 90 out of the 138 genes acquire a dynamic active enhancer within their TAD boundaries by 27 h, representing nearly three times as many genes that had a dynamic active enhancer within their TAD at 3 h (Fig. 4.7 A). An example of this can be seen in TAD2089, located on chromosome 10, which contains the highly induced protein coding gene *Gadd45b* (Fig. 4.7 B). At 3 h, static active enhancer regions, characterized by static DHS and static K27ac, are found ~25-50 kb downstream of *Gadd45b* (Fig 4.7 B, blue arrow heads). Δ DHS regions that respond to TCPOBOP at 3 h are flanked by low, static levels of K27ac at 3 h (Fig. 4.7

B, green arrow heads). At 27 h, however, several dynamic active enhancers are found within this same cluster as the static enhancer regions, and show clear increases in K27ac associated with strong Δ DHS (Fig. 4.7 B, green arrow heads). A promoter-associated Δ DHS (K4me3 cluster 2 at 27 h, see above), was also identified only at 27 h and is flanked by a strong Δ K27ac peak (Fig. 4.7 B, black arrow head). The emergence of delayed dynamic active enhancers within TADs that contain genes regulated early is associated with further induction of the regulated gene at 27 h. 20 out of the 54 genes that respond before dynamic active enhancers appear within their TADs show a further increase in the fold change of their induction at 27 h (>2-fold increase) , including *Gadd45b* (Fig. 4.7 C).

4.5 Discussion

Epigenomic reorganization has been characterized following activation of several nuclear receptors, including estrogen receptor and glucocorticoid receptor (Nagaich et al. 2004, Siersbaek et al. 2011, Voss et al. 2011, Grontved et al. 2013, Abdel-Hafiz and Horwitz 2015, Cucchiara et al. 2017), but the genome-wide chromatin remodeling induced by CAR activation has not been investigated. Here, we provide a detailed analysis of the rapid epigenomic remodeling of mouse liver chromatin following exposure to the mouse CAR specific agonist ligand TCPOBOP for 3 h or 27 h. We found that ~50% of TCPOBOP-responsive genes cluster in TADs (Fig. 4.1 B), and TCPOBOP-induced genes and TCPOBOP-repressed genes were generally found in separate TADs (Table 4.2). DNase-seq analysis identified several thousand genomic regions where TCPOBOP exposure

induces chromatin opening or chromatin closing (Table 4.3, Supplemental Table S4.1). Mapping of these regions to the closest gene within the same TAD revealed a strong enrichment for Δ DHS that open mapping to genes that are induced by TCPOBOP, and Δ DHS that close mapping to genes that are repressed (Table 4.6, Supplemental Table S4.1). We also observed a temporal relationship between DHS opening and closing and gene regulation; some Δ DHS that open or close at 3 h map to genes that respond to TCPOBOP only after 27 h (Fig 4.2 G) while some genes that are induced by TCPOBOP respond before new enhancers are activated (Fig. 4.7). Finally, ChIP-seq analysis of three activating histone modifications (K4me1, K4me3, and K27ac), combined with DNase-seq data, was used to identify active enhancer and promoter regions that respond to CAR activation in association with putative target gene expression (Fig. 4.3, Fig. 4.4). We found that active enhancers cluster in active TADs that contain multiple dysregulated *Cyp* gene family members, including TAD1421, which contains *Cyp2b10* and *Inc_5998*, and TAD1156, which contains several TCPOBOP-responsive *Cyp3a* genes (Fig. 4.6, Table 4.4).

4.5.1 Regulated genes cluster in TADs

We found that ~50% of TCPOBOP-responsive genes cluster with other, similarly responsive genes in TAD regions (Fig 4.1, Table 4.2). TADs function to organize megabase sized sections of the genome into three-dimensional compartments (Dixon et al. 2016), which enable linearly distant chromosomal regions to interact via a series of DNA loops that segment each chromosome (Faure et al. 2012, Rao et al. 2014, Nora et al. 2017). TADs

insulate regulatory elements within a TAD from neighboring genes in adjacent TADs, thereby increasing the specificity of regulatory interactions (Vietri Rudan et al. 2015, Oti et al. 2016). TADs that contain the *Cyp2b*, *Cyp2c* and *Cyp3a* gene families were particularly responsive to the transcriptional and epigenetic stimulatory actions of TCPOBOP, as exemplified by TAD3479, which contains the *Cyp2c* cluster with its 12 TCPOBOP-responsive genes and a total of 38 Δ DHS across the four TCPOBOP exposure conditions we investigated (Table 4.4, Supplemental Table S4.5). Clustering of *Cyps* into TAD regions that can be rapidly activated following xenobiotic exposure may be advantageous from an evolutionary perspective, as it allows for a limited number common regulatory elements to induce multiple but distinct genes within a family, and thereby allow for induction of a broad range of xenobiotic metabolic activities following xenobiotic exposure.

Whereas *Cyp2b10* was highly induced by TCPOBOP along with several Δ DHS within TAD1421, *Cyp2b9* and *Cyp2b13*, also found in TAD1421, did not respond to TCPOBOP, even after 27 h of TCPOBOP exposure (See Chapter 3). Presumably, the latter two *Cyp2b* genes are shielded from the DNA looping that is expected to bring the promoter of *Cyp2b10*, but not promoters of the other, nearby *Cyp2b* genes, in contact with the Δ DHS/putative regulatory elements (see below) that lead to the rapid and robust activation of *Cyp2b10*. Interestingly, others have reported that *Cyp2b9* and *Cyp2b13* become TCPOBOP-inducible after 4 days of exposure (Cui and Klaassen 2016), suggesting a requirement for more

complex epigenetic reprogramming than for *Cyp2b10*, perhaps related to the preferential epigenetic suppression of *Cyp2b9* and *Cyp2b13* (but not *Cyp2b10*) in male as compared to female mouse liver (Sugathan and Waxman 2013). Other DME gene families also show clustered induction patterns. Thus, in the cluster of glutathione S-transferase family *Gstm* genes in chromosome 3/TAD694, *Gstm3* is strongly induced by TCPOBOP by 3 h in both male and female liver, whereas other *Gstm* genes in the same TAD, including *Gstm1*, *Gstm2*, and *Gstm4*, respond at 27 h, while *Gstm6* and *Gstm7*, also found in TAD694, are unresponsive (Table 4.4, Supplemental Table S4.5). It is not certain what factors determine the specificity of TCPOBOP for particular genes within a responsive TAD or cause the delayed induction of a subset of genes within a highly active cluster, but the underlying basal chromatin state may contribute to the time differences in responsiveness, as suggested by other studies of time-dependent responses to hormonal stimuli in the same mouse liver model (Lau-Corona et al. 2017).

4.5.2 Δ DHS as positive regulators of gene expression

TCPOBOP-responsive Δ DHS, like the TCPOBOP induced and repressed genes discussed above, cluster into highly active TAD regions (Supplemental Table S4.5). Mapping of these Δ DHS to TCPOBOP-responsive RefSeq and multi-exonic lncRNA genes in the same TAD, on a per experiment basis (e.g. mapping Δ DHS in males treated with TCPOBOP for 3 h to genes regulated in males treated with TCPOBOP for 3 h, etc.) revealed a strong enrichment of Δ DHS that open for genes that are induced (Table 4.6, Supplemental Table

S4.1). Further, Δ DHS that close were enriched for genes that were repressed by TCPOBOP (Table. 4.6, Supplemental Table S4.1). When examining whole TADs, Δ DHS that open tend to be in TADs with ≥ 1 induced gene but no repressed gene(s), while Δ DHS that close tend to be in TADs with ≥ 1 repressed gene but no induced gene(s) (Table 4.3, Supplemental Table S4.5). Together, these findings suggest these Δ DHS are positive regulators (i.e., promoters and enhancers) of gene expression, and that factors bound to these regions, e.g., TCPOBOP-activated CAR, stimulate increases in gene transcription. Exactly how these chromatin regions open or close chromatin is not yet known, but likely involves the SWI/SNF chromatin remodeling complex (Tang et al. 2010). The rapid opening of Δ DHS within 3 h of TCPOBOP treatment may, in part, be driven by direct CAR binding. Supporting this proposal, TCPOBOP is a highly specific agonist ligand of CAR, and further, there is a well characterized CAR binding motif (DR4, PBREM sequence) centered within the cluster of Δ DHS that open upstream of *Cyp2b10* (Honkakoski and Negishi 1997). Moreover, PXR, a NR closely related to CAR, binds to DR4 motifs upstream of several DME genes that are induced in common by CAR and PXR, such as *Cyp3a11* and *Gstm3* (Cui et al. 2010), where we also found several TCPOBOP-activated Δ DHS. Given the specificity of TCPOBOP for CAR and the short time frame (within 3 h) for the early Δ DHS responses, it seems unlikely that secondary transcriptional responses (i.e. induction of a CAR gene target) contribute to chromatin opening at this time point. Of note, direct binding of other NRs to closed chromatin has been associated with chromatin remodeling, including GR and PPAR (Nagaich et al. 2004, Siersbaek et al. 2011, Voss et al. 2011). The

~1,000 Δ DHS that do not open until after 27 h of TCPOBOP exposure (Table 4.5) may be the result of secondary responses, which could include epigenetic actions by one or more of the few hundred multi-exonic lncRNA genes that are rapidly induced by TCPOBOP in mouse liver (Lodato et al. 2017); these include *lnc_5998* (Fig. 4.6 A).

4.5.3 Active enhancers target *Cyp2b10* and other induced genes

Histone H3 K4me3 is a mark associated with promoters in mammalian tissues while K4me1 and K27ac mark active enhancers (Barski et al. 2007, Sugathan and Waxman 2013, Shlyueva et al. 2014). We used DNase-seq in combination with ChIP-seq targeting K4me3 to define enhancer and promoter regions that become more active (Δ DHS) in mouse liver following TCPOBOP exposure. Static enhancers (static DHS and static K27ac) and dynamic enhancers (Δ DHS and Δ K27ac) were defined using DNase-seq and ChIP-seq targeting K27ac in vehicle and TCPOBOP-treated mouse liver (Fig. 4.5 C, Supplemental Table 4.3). Mapping dynamic enhancer regions and static active enhancers to the nearest gene TSS within the same TAD, we observed a striking enrichment for dynamic enhancers as compared to stable active regions, at both 3 h and 27 h of TCPOBOP exposure (Fig. 4.5 F). Based on a detailed analysis of specific genomic loci, we report several of these dynamic enhancer regions are likely targeting *Cyp2b10* (Fig 4.6 A), *Cyp3a11* (Fig. 4.6 B), and other highly responsive genes. The increased in K27ac at these sites is likely due to the histone acetyl transferase p300 (Pradeepa et al. 2016). Histones surrounding upstream putative enhancer regions of *CYP3A4* were recently shown to be modified following

treatment with the human PXR ligand rifampicin for 48 h, in a PXR-dependent manner, in human-derived LS174T cells (Yan et al. 2017). It was also shown that PXR recruits the histone acetyltransferase p300 and the nuclear receptor co-activator NCOA6 to these sites through protein-protein interactions, and both p300 and NCOA6 are necessary for the observed rifampicin-mediate histone mark remodeling (Yan et al. 2017).

4.5.4 Conclusions

We present a genome-wide view of the dynamic epigenomic changes that occur in mouse liver following short exposures to the mouse CAR agonist ligand TCPOBOP, and we use mouse liver TAD definitions to map changes in epigenetic elements to putative gene targets to discovered DNA regulatory elements that respond to drug treatment. We observe a coordinated regulation of target gene families grouped by TAD and associated DHS that open rapidly. Lastly, we report increases in the activating histone mark K27ac that are associated with Δ DHS at putative promoter regions that likely target several highly responsive DME genes.

Fig. 4.1 TCPOBOP-responsive genes cluster in TADs. A. Percent of topologically associating domains (TADs) that contain either a single TCPOBOP-responsive gene (black) or multiple TCPOBOP-responsive genes (red) in male or female liver treated with TCPOBOP for 3 h or 27h. B. Percent of TCPOBOP-responsive genes found within TADs that contain either a single TCPOBOP-responsive gene (black striped) or multiple TCPOBOP-responsive genes (red striped). Approximately 50% of TCPOBOP-responsive genes cluster in TADs together. See Supplemental Table S4.5 for a full listing of responsive TADs and the corresponding number of up and down regulated genes in each experimental group.

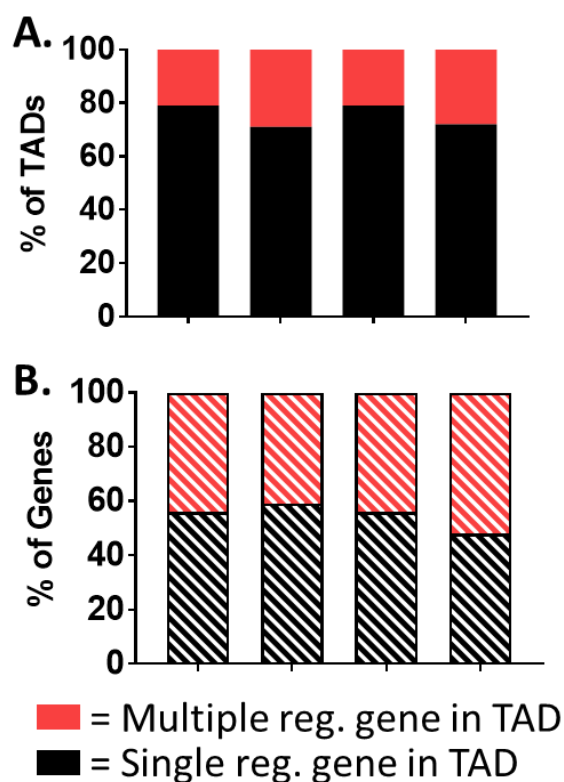


Fig. 4.2 **Δ DHS respond to TCPOBOP in mouse liver.** A-D. Overlap analysis of Δ DHS regions discovered in male and female liver after TCPOBOP treatment for 3 h or 27 h. Δ DHS were determined for each experiment based on the full list of 60,739 DHS (see Methods). Only Δ DHS that responded in the same direction were considered overlapping (e.g. Δ DHS that open in males at 3 h and Δ DHS that open in males at 27 h; Δ DHS that close in males at 3 h and Δ DHS that close in males at 27 h, etc.). E-F. Δ DHS were assigned to TAD regions based on their location in the genome. The number of TCPOBOP-responsive genes within the same TAD was then counted for each Δ DHS. A minority of Δ DHS had a TCPOBOP-responsive gene within the same TAD (black), while the majority did not (grey). G. Number of Δ DHS identified in male and female liver at 3 h that did not have a 3 h TCPOBOP-responsive gene in the same TAD (grey bars in Fig. 4.2 E-F) but that do have one or more responsive genes at 27 h in the same TAD (white). H. Direction of regulation for genes that show a delayed responsive relative to Δ DHS within the same TAD (white bars in Fig. 4.2 G) was analyzed. Genes that responded in the same direction at 27 h as their co-TAD Δ DHS (blue) and genes that responded in the opposite direction (yellow) were counted. I. Δ DHS that map to genes targets of 10 CAR-dependent HCC upstream regulators, as defined in Chapter 3, were counted. Despite dysregulation of these genes showing a strong male-bias, Δ DHS mapped to either all downstream genes (right) or dysregulated downstream genes at the same frequency in both male and female mice. E.S. = Enrichment Score (ratio of number of female Δ DHS that map to HCC gene to all female

DHS divided by ratio of number of male Δ DHS that map to HCC gene compared to all male DHS).

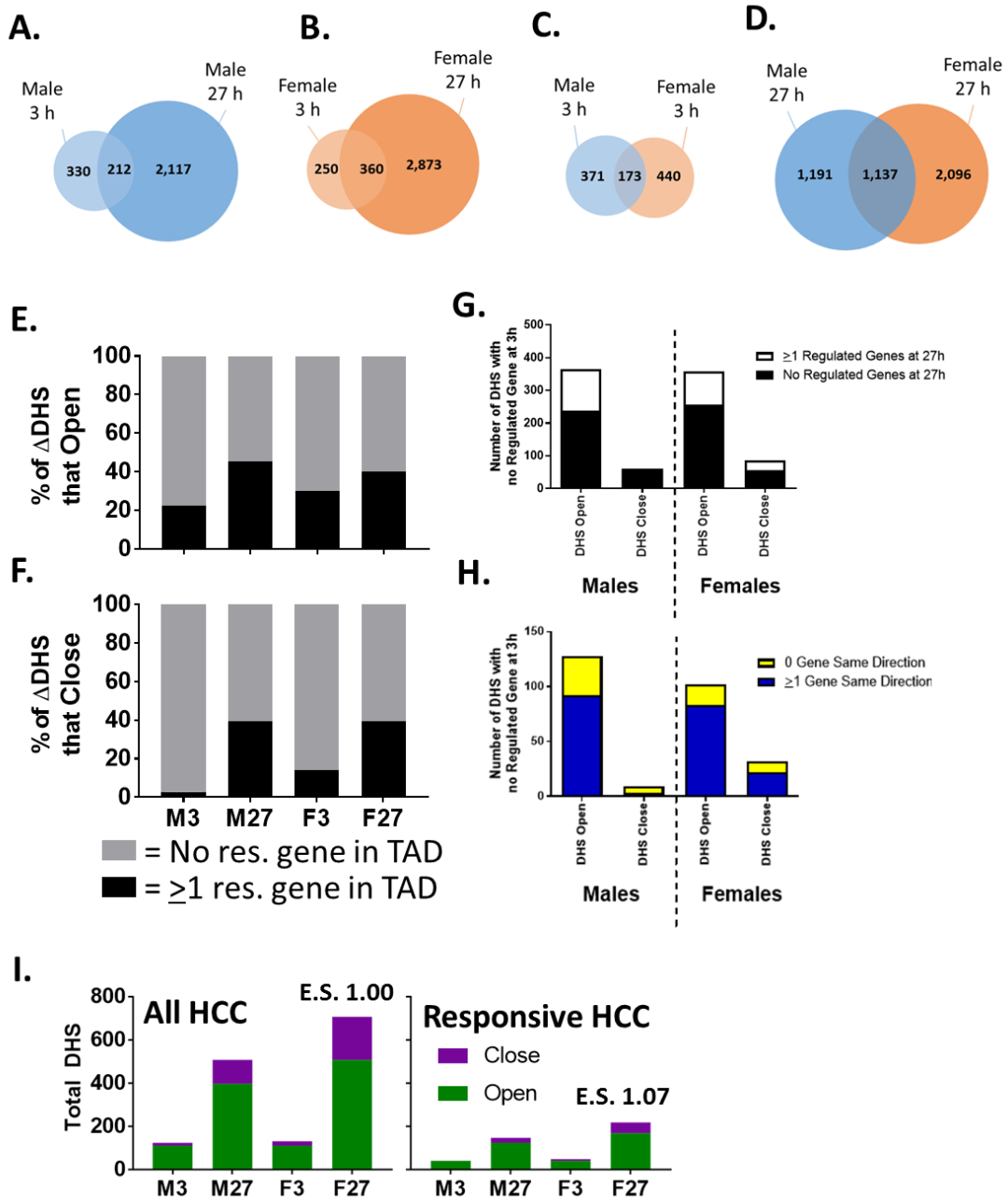


Fig. 4.3 Promoter-like and Enhancer-like Δ DHS. Shown is a heatmap of normalized sequence reads for 3 h male Δ DHS regions (A) and 27 h Δ DHS regions (B). DNase-seq signals (black), and ChIP-seq signal for K4me1 (orange), K4me3 (blue), and K27ac (green) at Δ DHS, in vehicle treated (Vh) and TCPOBOP-treated (TC) liver, were visualized in a 2 kb window centered on the Δ DHS midpoint (+1 kb downstream and -1 kb upstream) using deepTools (see Methods). Δ DHS were clustered by the K4me3 ChIP-seq signal via k-means using deepTools. A. Two clusters were used to separate Δ DHS at 3 h into one promoter-like cluster (cluster 1, high K4me3) and one enhancer-like cluster (cluster 2, low K4me3). B. Three clusters were used to separate Δ DHS at 27 h into two promoter-like clusters (cluster 1, high K4me3; cluster 2, intermediate K4me3) and one enhancer-like cluster (cluster 3, low K4me3). Scales shown are linear intensity values calculated in deepTools.

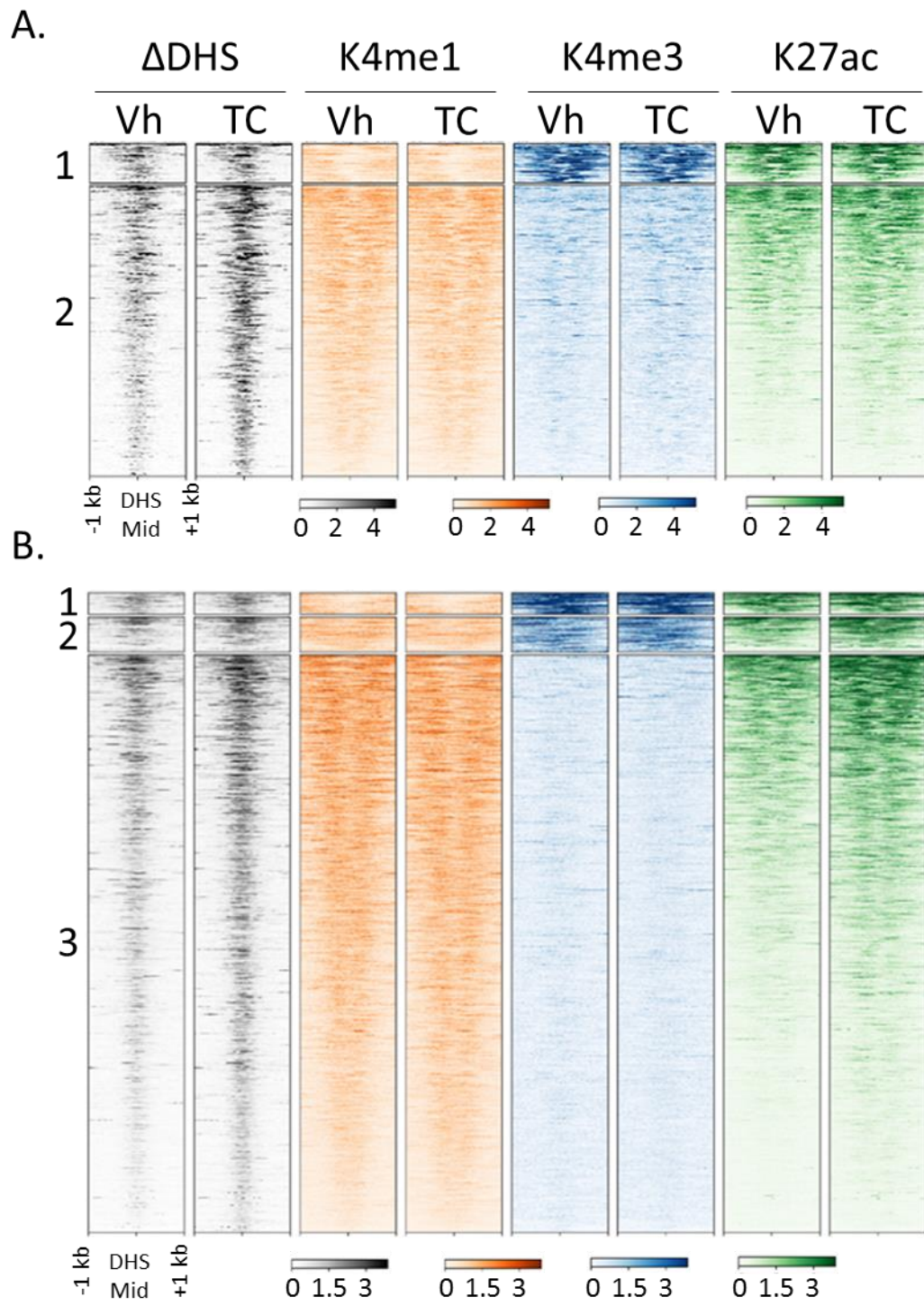


Fig. 4.4 Distance from Δ DHS to the nearest TSS. Δ DHS were mapped to the nearest gene within the same TAD. Shown are box plots of the genomic distance was determined for each Δ DHS in each promoter-like and enhancer-like cluster defined in Fig. 4.3. Values shown above each box are the median distances from the DHS within the cluster to the nearest gene TSS within the same TAD.

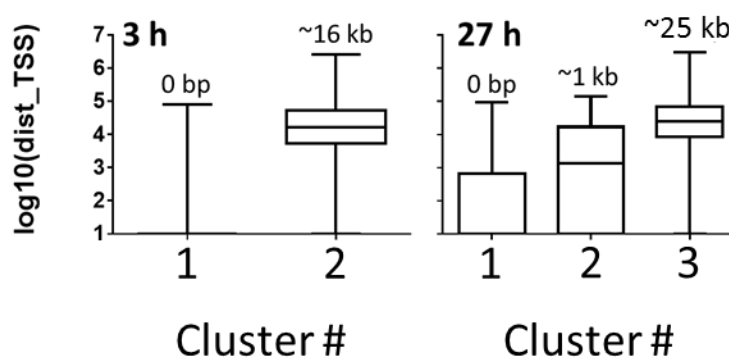


Fig 4.5 **Static active and dynamic active enhancers.** A. Shown is the number of differential K27ac peaks (Δ K27ac) that overlap with Δ DHS, static DHS (sDHS), or no DHS, determined using BEDtools. Given DHS, by their definition, lack histone proteins, DHS and K27ac peaks were considered overlapping if found within 1 kb of each other. Bar graphs show the overlap of Δ K27ac with Δ DHS (grey), sDHS (black), or no DHS (white) in male mice after TCPOBOP-treatment for 3 h or 27 h. B. Shown is the number of Δ DHS that overlap with Δ K27ac (grey), sK27ac (black), or no K27ac (white) using the same 1 kb distance metric as in A. C. Number of static active enhancers and dynamic active regions were defined in male liver following 3 h or 27 h TCPOBOP exposure. D-E Number of dynamic active enhancers and static active enhancers were counted in TADs that contained TCPOBOP-responsive genes at 3 h or 27 h. Genes that were within TADs that only contained static active enhancers (orange) or genes that were within TADs with both static active enhancers and dynamic active enhancers (brown) were identified. No TCPOBOP-responsive genes were found within a TAD with only dynamic active enhancers. F. Enrichment scores were calculated to compare the mapping of dynamic active enhancers (Dyn. act.) to TCPOBOP-responsive genes to the mapping of static active enhancers (static act.) or inactive regions (static DHS without a K27ac mark) to TCPOBOP-responsive genes. G. Fold inductions of genes found within the same TAD as dynamic active enhancers vs inductions of genes found in TADs with only static active enhancers.

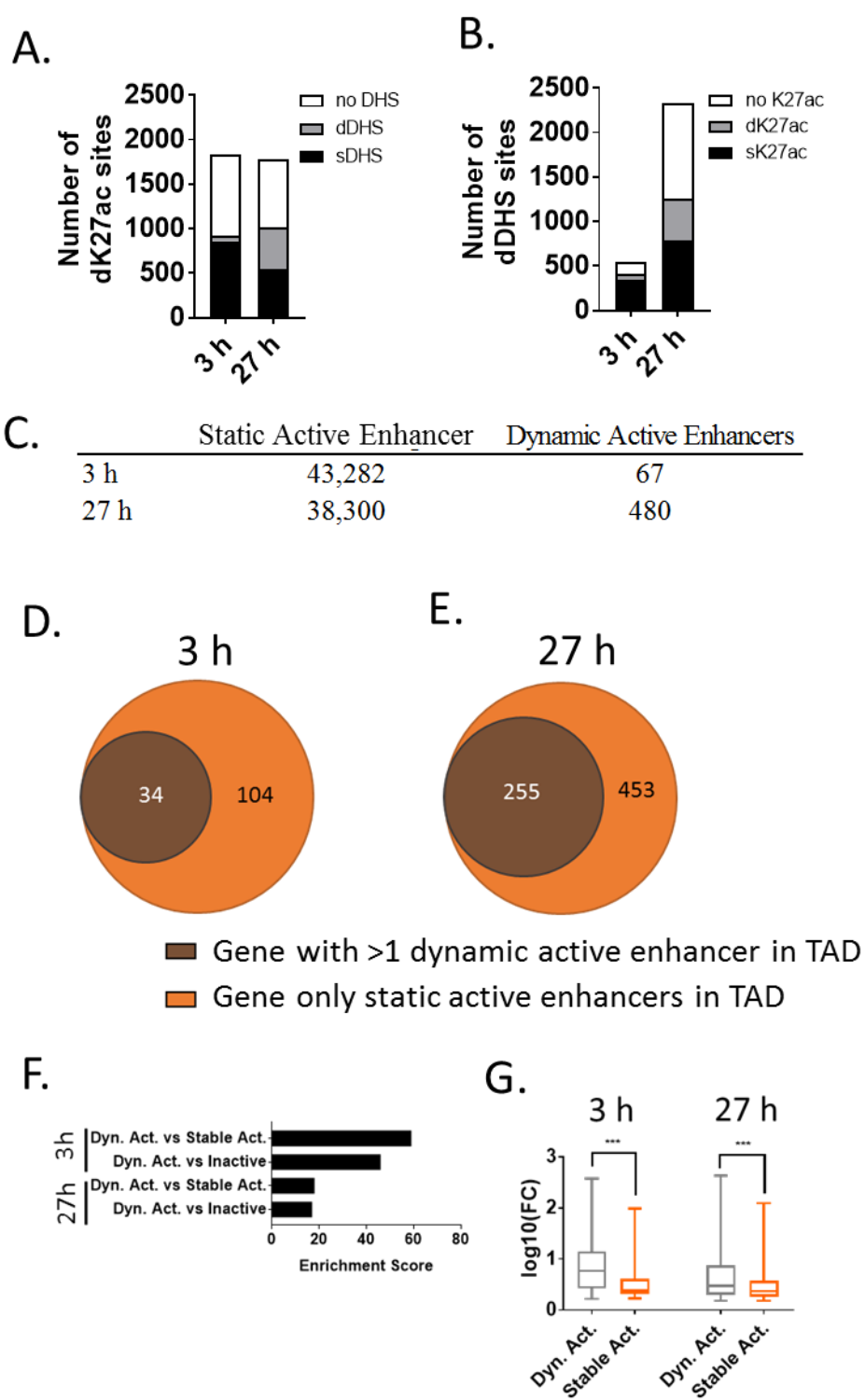
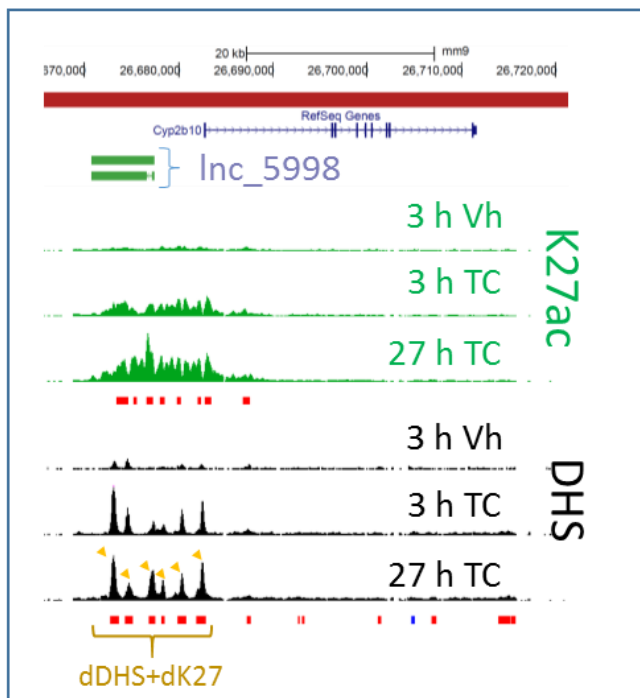


Fig. 4.6 **Dynamic active enhancers near *Cyp2b10* and *Cyp3a11*.** DHS and K27ac peaks were visualized around the *Cyp2b10* and *Cyp3a11* loci. Differential peaks at 27 h, as defined by the overlap of a diffReps region and a MACS2 peak (see Methods) are denoted by red bars under the K27ac tracks and the DHS tracks. Static K27ac or DHS are marked by blue bars. A. Six dynamic active enhancers (Δ DHS and Δ K27ac, yellow arrow heads) are found upstream of *Cyp2b10*, three of which are within the gene body of *Inc_5998*. B. Two dynamic active enhancers (Δ DHS and Δ K27ac, yellow arrow heads) are found near the *Cyp3a11* TSS, while one static active enhancers (static DHS and static K27ac, blue arrow head) is found ~10 kb upstream. Two static DHS with flanking Δ K27ac (purple arrow heads) are also found upstream of *Cyp3a11*.

A.



B.

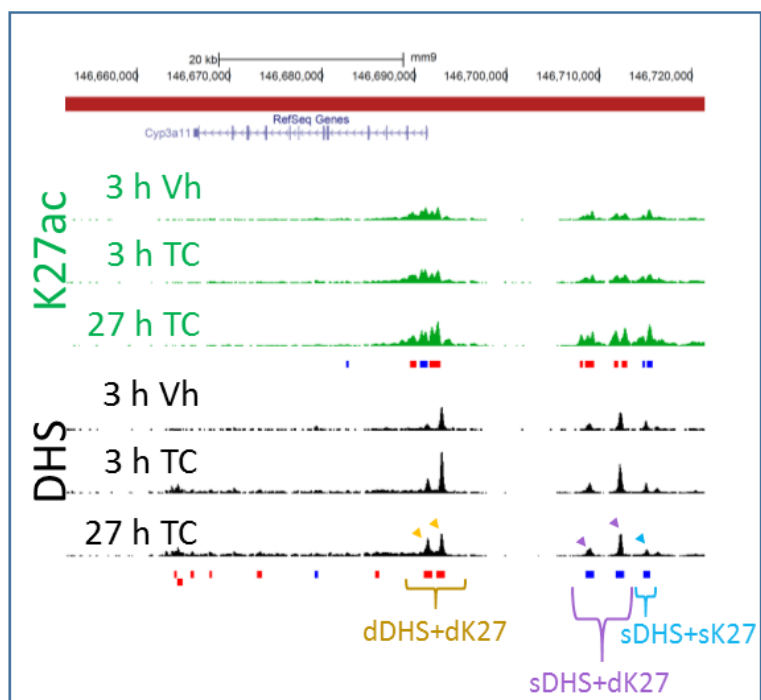


Fig. 4.7 Gene induction precedes dynamic active enhancer formation. A. Shown is the number of genes that respond to TCPOBOP at 3 h that were within TADs that only contained static active enhancer (orange striped) at 27 h, and genes that were within TADs with both static and dynamic active enhancers (grey striped). B. Example of a gene whose induction by TCPOBOP precedes dynamic active enhancer formation (*Gadd45b*). Differential peaks at 3 h or 27 h, as defined by the overlap of a diffReps region and a MACS2 peak (see methods) are denoted by red bars under the corresponding K4me1, K4me3, K27ac, and DHS tracks. Static K4me1, K4me3, K27ac, and DHS are marked by blue bars. K27ac is stable at 3 h and several static K27ac peaks are found downstream of *Gadd45b* and within the gene body of *Gng7*, which is unresponsive to TCPOBOP (blue arrow heads). At 27 h, several dynamic active enhancer regions are seen within the same cluster of enhancers (green arrow head). A promoter-like region that contains a Δ DHS and Δ K27ac is found at the *Gadd45b* TSS. C. Induction of *Gadd45b*, as measured by RNA-seq reported in Chapter 3. FPKM (fragments per kilobase length per million sequenced reads) values for vehicle-treated and TCPOBOP-treated male mice are presented.

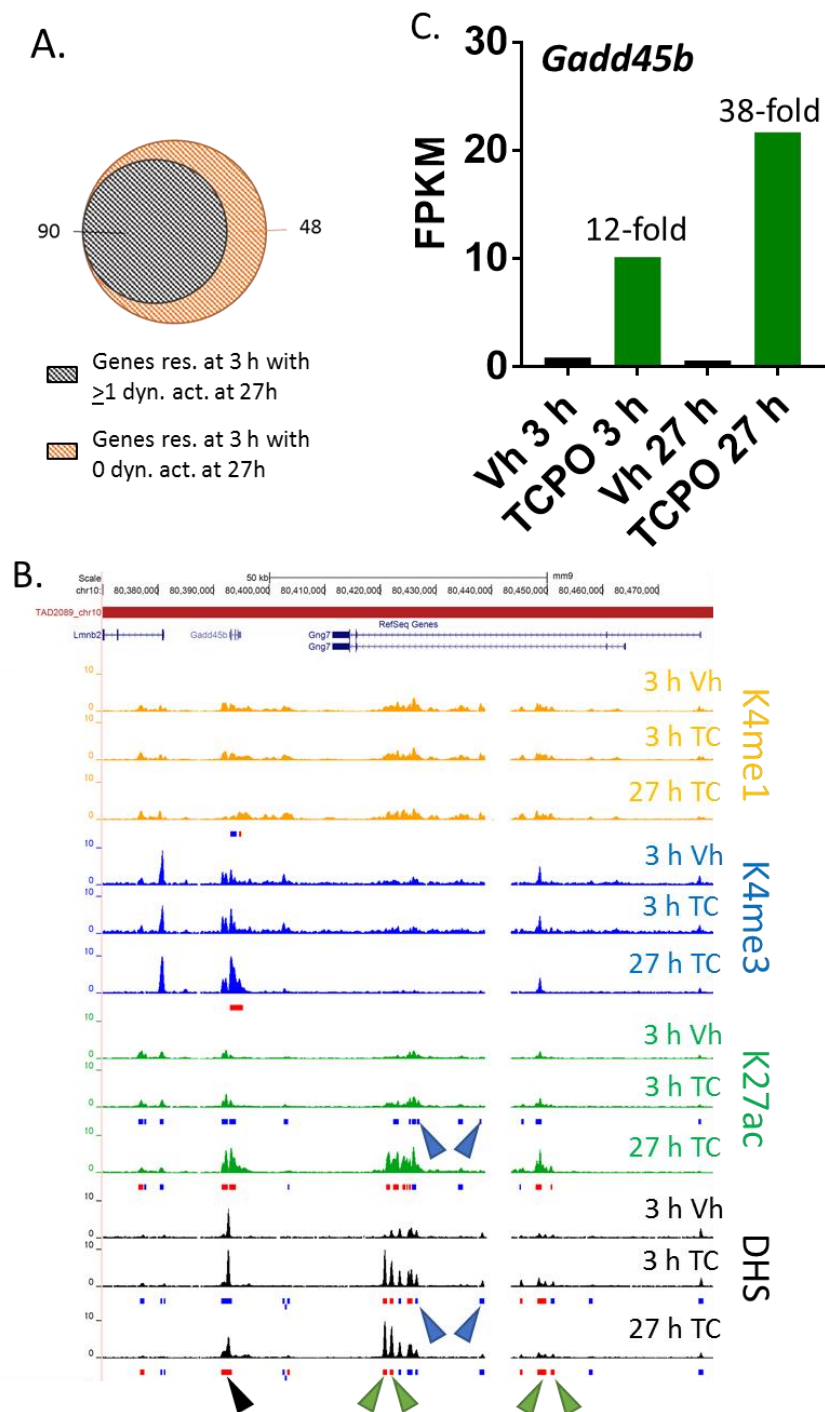


Table 4.1 Sequencing reads obtained and peaks called. Shown are the number of raw sequenced reads (TOTAL_READ_COUNT) obtained for DNase-seq in male and female mouse liver and for ChIP-seq in male liver for K27ac, K4me1, and K4me3. Number of mapped reads (MAPPED_READ_COUNT), ratio of mapped to unmapped reads (MAPPED_READ_RATIO), MACS2 peaks called (MACS2_PEAK_COUNT, see Methods), number of reads in the MACS2 peaks called (READ_IN_PEAK_COUNT), and the ratio of reads in peaks (READ_IN_PEAK_RATIO) are also shown.

Experiment Type	SAMPLE_ID	Description	TOTAL_READ_COUNT	MAPPED_READ_COUNT	MAPPED_READ_RATIO	MACS2_READ_COUNT	READ_IN_PEAK_COUNT	READ_IN_PEAK_RATIO
DHS males 3 h	G98_M1M2	male_vehicles_3hr_combined	44,029,336	32,736,945	0.74	39,547	5,024,662	0.15
	G98_M3M7	male TCPOBOP_3hr_combined	59,729,373	43,689,373	0.73	45,734	8,032,236	0.18
DHS males 27 h	G115_M1M2	male_vehicles_27hr_combined	107,139,390	79,135,269	0.74	53,043	18,433,066	0.23
	G115_M3M4	male TCPOBOP_27hr_combined	87,267,307	64,625,816	0.74	51,702	16,745,098	0.26
DHS females 3 h	G91_M1M2	female_vehicles_3hr_combined	44,575,595	33,019,632	0.74	38,854	4,968,449	0.15
	G91_M3M4	female TCPOBOP_3hr_combined	55,319,193	40,477,181	0.73	41,617	6,445,752	0.16
DHS females 27 h	G144_M7M8	Female 27h Control DHS combined	66,536,526	46,555,482	0.70	43,613	10,022,903	0.21
	G144_M9M10	Female 27h TCPOBOP_DHS_combined	79,499,612	55,292,324	0.70	49,644	13,053,221	0.24
DHS PEAK UNION	-	All DHS samples combined	-	-	-	60,739	-	-
K4me1 3 h	G121_M1M2M3	K4me1_It_600bp_Male_Vehicle_3hr_Combined	165,556,694	125,496,835	0.76	123,834	22,927,799	0.37
	G121_M4M5M6	K4me1_It_600bp_Male_TCPOBOP_3hr_Combined	159,605,552	118,327,618	0.74	124,626	20,268,865	0.34
K4me1 3 h PEAK UNION	-	All K4me1 3 h samples combined	-	-	-	124,811	-	-
K4me3 3 h	G143_M7M8M9	Male_3hr_Control_K4me3_Combined	172,416,906	110,488,841	0.64	46,931	7,057,991	0.13
	G143_M10M11M12	Male_3hr_TCPOBOP_K4me3_Combined	142,288,766	91,012,556	0.64	40,491	4,451,992	0.10
K4me3 3 h PEAK UNION	-		-	-	-	41,637	-	-
K4me1 27 h	G150_K4me1_TC	male_K4me1_TCPOBOP_27h	185,284,642	135,766,154	0.73	124,995	16,143,901	0.24
	G150_K4me1_Cont	male_K4me1_Control_27h	139,524,466	103,278,559	0.74	112,389	11,961,865	0.23
K4me1 27 h PEAK UNION	-		-	-	-	108,255	-	-
K4me3 27 h	G150_K4me3_TC	male_K4me3_TCPOBOP_27h	180,273,390	103,748,215	0.58	25,021	6,012,621	0.12
	G150_K4me3_Cont	male_K4me3_control_27h	135,284,850	76,675,947	0.57	21,573	4,699,481	0.12
K4me3 27 h PEAK UNION	-		-	-	-	23,536	-	-
K27ac 27 h	G150_K27ac_TC	male_K27ac_TCPOBOP_27h	155,589,128	116,444,141	0.75	58,832	17,140,784	0.29
	G150_K27ac_Cont	male_K27ac_control_27h	122,610,576	94,797,094	0.77	59,676	15,346,328	0.32
K27ac 27 h PEAK UNION	-		-	-	-	59,432	-	-

Table 4.2 Genes cluster in TADs. Analysis of TADs with a cluster of regulated genes (≥ 2 genes) in male or female liver following 3 h or 27 h TCPOBOP exposure. Responsive TADs (i.e. a TAD with ≥ 2 genes) were classified by the response pattern of the dysregulated genes within the TAD. Up Only TADs contain at least 2 dysregulated genes that are up regulated but do not contain any down regulated genes. Down Only TADs contain at least 2 dysregulated genes that are down regulated but do not contain any up regulated genes. Mixed TADs contain genes that are up regulated and genes that are down regulated. Percentage of TADs and dysregulated genes for the Up Only, Down Only and Mixed designation are based on the number of TADs or genes that show a clustered response. Total number of TADs that showed a clustered response and the percentage of all responsive TADs, is shown as is the total number of genes and percentage of all responsive genes. See Supplemental Table S4.5 for a full listing of responsive TADs and the corresponding number of up and down regulated genes in each experimental group.

TAD Group	Male 3 h		Male 27 h		Female 3 h		Female 27 h	
	TADS (%)	Genes (%)	TADS (%)	Genes (%)	TADS (%)	Genes (%)	TADS (%)	Genes (%)
Total	26	77	206	432	43	127	149	413
<i>Up Only</i>	20 (76.9)	61 (79.2)	94 (45.6)	246 (56.9)	21 (48.8)	64 (50.4)	69 (46.3)	196 (47.5)
<i>Down Only</i>	1 (3.8)	2 (2.6)	38 (18.4)	38 (8.8)	11 (25.6)	28 (22.0)	45 (30.2)	108 (26.2)
<i>Mixed</i>	5 (19.2)	14 (18.2)	74 (35.9)	148 (34.3)	11 (25.6)	35 (27.6)	35 (23.5)	109 (26.4)

Table 4.3 **Δ DHS map to responsive genes.** Δ DHS that open (Group_1 and Group_2), Δ DHS that close (Group_3 and Group_4), and static DHS (sDHS; Group_5) found in male or female mouse liver following TCPOBOP exposure for 3 h or 27 h were discovered using a combination of MACS2 and diffReps (See Methods). Δ DHS were mapped to specific TADs within the mouse genome. Number of dysregulated genes and the direction of their regulation were examined at each TAD that contained a Δ DHS. Δ DHS that are in a TAD with ≥ 1 upregulated gene but no down regulated gene (Group_1A, Group_3A), Δ DHS that are in a TAD with ≥ 1 down regulated gene but no upregulated gene (Group_1B, Group_3B), and Δ DHS that were in a TAD with both up and down regulated genes (Group_1C, Group_3C) were counted. Δ DHS that are in a TAD with no regulated gene(s) were also counted (Group_2, Group_4).

	Male 3h	Male 27h	Female 3h	Female 27h
All Δ DHS	544	2,331	613	3,236
Δ DHS open	472	1,767	512	2,357
ΔDHS open; in TAD with ≥ 1 regulated genes	106	801	154	944
<i>ΔDHS open; in TAD with up regulated genes only</i>	95	611	129	734
<i>ΔDHS open; in TAD with down regulated genes only</i>	4	62	5	105
<i>ΔDHS open; in TAD with up and down regulated genes</i>	7	128	20	105
ΔDHS open; in TAD with no regulated genes	386	966	358	1,413
Δ DHS close	72	564	101	879
ΔDHS close; in TAD with ≥ 1 regulated genes	2	222	14	345
<i>ΔDHS close; in TAD with up regulated genes only</i>	0	57	7	66
<i>ΔDHS close; in TAD with down regulated genes only</i>	1	108	5	237
<i>ΔDHS close; in TAD with up and down regulated genes</i>	1	57	2	42
ΔDHS close; in TAD with no regulated genes	70	342	87	534
sDHS	60,195	58,408	60,126	57,503

Table 4.4 Highly active TADS. Five examples of highly active TADs after TCPOBOP exposure. Number of Δ DHS and regulated genes per TAD per experiment are reported.

	Δ DHS				Regulated Genes				Annotation
	Male 3 h	Male 27 h	Female 3 h	Female 27 h	Male 3 h	Male 27 h	Female 3 h	Female 27 h	
TAD3479 chr19	7	35	14	38	11	12	9	9	Cyp2c locus
TAD1421 chr7	6	16	8	15	3	3	3	4	Cyp2b10 and 2 lncRNAs locus
TAD1156 chr5	1	9	4	10	4	4	3	9	Cyp3a locus
TAD110 chr1	1	2	3	1	1	2	1	2	Ugt1a1 locus
TAD694 chr3	1	8	0	11	1	4	1	3	Gstm locus

Table 4.5 **Δ DHS that respond in multiple data sets.** All TCPOBOP-responsive DHS is the union of all Δ DHS regions discovered in all 4 groups. Common responses in all 4 TCPOBOP datasets are those Δ DHS that respond in all 4 groups. Responds in male only (or female only) are Δ DHS that respond in males (or females) at 3 h or 27 h and do not respond in female (or males) at any time point. Early responding, both male and female are Δ DHS that respond at 3 h in either sex, independent of their responsiveness at 27 h. Late responding, both male and female are Δ DHS that only respond in either sex after 27 h.

TCPOBOP response profile	Open	Close
	Number of Δ DHS	
All TCPOBOP-responsive DHS	3,466	1,444
Common responses in all 4 TCPOBOP datasets	121	1
Responds in Male only	910	489
Responds in Female only	1,422	816
Early responding, both Male and Female	783	166
Late responding, both Male and Female	990	623

Table 4.6 Enrichment scores. All 60,739 DHS (Δ DHS and static DHS) were mapped to a single putative gene target (closest TSS within the same TAD) and enrichment scores were calculated based on the number of a given set of Δ DHS (e.g. Δ DHS that open) to a given set of regulated genes (e.g. genes up regulated) in a given treatment group (males at 3h) compared to the ratio of static DHS mapping to the same given set of regulated genes. For example, in males treated with TCPOBOP for 3 h, 70 Δ DHS that open map to TCPOBOP-induced genes and 402 Δ DHS that open map to uninduced genes ($70/402 = 0.174$), while 393 static DHS map to TCPOBOP-induced genes and 55,473 static DHS map to uninduced genes ($393/55,474 = 0.007$) for an enrichment score of 24.6 ($0.174/0.007 = 24.6$). Enrichment of common peaks to common genes was calculated based on the mapping of Δ DHS that are open in all four experimental conditions (males and females, 3 h and 27 h) and the mapping of static DHS in all four experimental conditions to genes that respond in common in all four experimental conditions.

		Enrichment Score	pval
Common Peaks to Common Genes		121.3	<E-43
Male 3 h	Open Peaks to Up genes	24.6	<E-64
	Close Peaks to Down Genes	1.0	-
Male 27 h	Open Peaks to Up genes	8.3	<E-199
	Close Peaks to Down Genes	36.5	<E-27
Female 3 h	Open Peaks to Up genes	24.3	<E-92
	Close Peaks to Down Genes	5.2	<E-2
Female 27 h	Open Peaks to Up genes	10.6	<E-277
	Close Peaks to Down Genes	8.7	<E-64

Table 4.7 Common gene targets. 19 genes that are regulated by TCPOBOP in all 4 experimental conditions that are targeted by 27 Δ DHS common to all 4 experimental conditions

Peak					Gene										
Chr	Start	End	Peak Name	TAD	Name	Strand	TAD	Male 3 h		Male 27 h		Female 3 h		Female 27 h	
								FC	FDR	FC	FDR	FC	FDR	FC	FDR
chr16	93346416	93347975	all_tcpo_peak_23672	TAD3128_chr16	1810053823Rik	-	TAD3128_chr16	19.2	3.24E-06	208.6	9.74E-59	10.5	2.55E-13	8.9	4.03E-21
chr9	15104582	15104873	all_tcpo_peak_56646	TAD1777_chr9	4931406C07Rik	-	TAD1777_chr9	4.0	2.20E-31	7.5	8.88E-83	6.1	5.82E-50	6.9	6.38E-31
chr8	107255076	107256643	all_tcpo_peak_55402	TAD1722_chr8	Ces2a	+	TAD1722_chr8	9.7	1.90E-49	15.0	3.26E-117	32.2	1.01E-143	13.1	5.19E-44
chr7	26679888	26680779	all_tcpo_peak_50362	TAD1421_chr7	Cyp2b10	+	TAD1421_chr7	111.7	8.20E-190	138.5	1.19E-145	126.9	1.04E-203	49.1	2.31E-88
chr7	26681891	26682863	all_tcpo_peak_50363	TAD1421_chr7	Cyp2b10	+	TAD1421_chr7	111.7	8.20E-190	138.5	1.19E-145	126.9	1.04E-203	49.1	2.31E-88
chr19	39286312	39288075	all_tcpo_peak_29783	TAD3479_chr19	Cyp2c53-ps	+	TAD3479_chr19	30.1	3.04E-118	254.1	1.56E-275	80.0	2.33E-23	1919.6	2.55E-142
chr19	39072665	39073872	all_tcpo_peak_29773	TAD3479_chr19	Cyp2c55	+	TAD3479_chr19	82.2	2.78E-76	282.7	2.29E-267	214.5	2.96E-134	502.1	9.03E-166
chr5	146691030	146691952	all_tcpo_peak_46011	TAD1156_chr5	Cyp3a11	-	TAD1156_chr5	3.8	6.20E-30	9.3	9.80E-92	5.6	3.98E-40	10.2	7.00E-33
chr6	67099387	67100258	all_tcpo_peak_47564	TAD1264_chr6	Gadd45a	-	TAD1264_chr6	2.8	2.76E-09	5.1	5.60E-18	2.5	2.30E-12	3.5	1.83E-11
chr10	80420504	80421154	all_tcpo_peak_5898	TAD2089_chr10	Gadd45b	+	TAD2089_chr10	11.6	1.18E-40	38.5	1.73E-57	14.8	3.82E-84	39.4	4.80E-79
chr10	80421721	80422333	all_tcpo_peak_5899	TAD2089_chr10	Gadd45b	+	TAD2089_chr10	11.6	1.18E-40	38.5	1.73E-57	14.8	3.82E-84	39.4	4.80E-79
chr10	75266568	75267610	all_tcpo_peak_5625	TAD2080_chr10	Gstt1	-	TAD2080_chr10	2.4	5.42E-06	4.4	3.03E-40	3.4	4.25E-16	2.6	1.01E-07
chr5	140679978	140680789	all_tcpo_peak_45797	TAD1142_chr5	Mad1l1	-	TAD1142_chr5	2.7	2.92E-11	6.7	7.54E-44	3.5	1.30E-16	10.2	7.62E-40
chr16	93792692	93793926	all_tcpo_peak_23691	TAD3129_chr16	nc_as_c16_13512	-	TAD3129_chr16	8.4	9.94E-13	14.6	4.95E-48	7.7	6.40E-09	8.8	2.82E-16
chr6	87163079	87164058	all_tcpo_peak_48002	TAD1291_chr6	nc_as_c6_5335	+	TAD1291_chr6	10.1	1.12E-06	340.0	1.15E-101	39.7	1.20E-11	262.4	5.64E-83
chr6	87165998	87166722	all_tcpo_peak_48003	TAD1291_chr6	nc_as_c6_5335	+	TAD1291_chr6	10.1	1.12E-06	340.0	1.15E-101	39.7	1.20E-11	262.4	5.64E-83
chr12	82030983	82031685	all_tcpo_peak_12864	TAD2480_chr12	nc_inter_c12_10715	-	TAD2480_chr12	8.2	0.000176	10.4	6.09E-15	7.1	0.007169	4.0	0.000242
chr15	88721484	88723136	all_tcpo_peak_21086	TAD2982_chr15	nc_inter_c15_12834	-	TAD2982_chr15	9.3	1.63E-06	16.8	3.52E-10	5.3	0.021415	8.8	2.35E-07
chr7	26672711	26673610	all_tcpo_peak_50358	TAD1421_chr7	nc_inter_c7_5998	-	TAD1421_chr7	376.7	4.00E-152	372.3	1.90E-279	449.0	6.73E-71	176.0	1.13E-118
chr7	26674299	26675132	all_tcpo_peak_50359	TAD1421_chr7	nc_inter_c7_5998	-	TAD1421_chr7	376.7	4.00E-152	372.3	1.90E-279	449.0	6.73E-71	176.0	1.13E-118
chr7	26676826	26677554	all_tcpo_peak_50360	TAD1421_chr7	nc_inter_c7_5998	-	TAD1421_chr7	376.7	4.00E-152	372.3	1.90E-279	449.0	6.73E-71	176.0	1.13E-118
chr7	26678218	26678518	all_tcpo_peak_50361	TAD1421_chr7	nc_inter_c7_5998	-	TAD1421_chr7	376.7	4.00E-152	372.3	1.90E-279	449.0	6.73E-71	176.0	1.13E-118
chr9	106165589	106166283	all_tcpo_peak_59213	TAD1937_chr9	nc_inter_c9_8301	+	TAD1937_chr9	4.4	4.68E-19	13.0	4.64E-29	6.4	1.67E-07	21.6	8.83E-39
chr9	106167727	106168323	all_tcpo_peak_59214	TAD1937_chr9	nc_inter_c9_8301	+	TAD1937_chr9	4.4	4.68E-19	13.0	4.64E-29	6.4	1.67E-07	21.6	8.83E-39
chr5	136158348	136159308	all_tcpo_peak_45560	TAD1132_chr5	Por	+	TAD1132_chr5	5.7	2.48E-48	4.5	1.46E-33	5.7	1.37E-46	2.6	3.54E-07
chr7	105506531	105507212	all_tcpo_peak_51907	TAD1512_chr7	Tsku	-	TAD1512_chr7	3.5	2.83E-17	11.5	8.61E-71	11.2	2.51E-27	18.3	2.87E-49
chr7	105508245	105509181	all_tcpo_peak_51908	TAD1512_chr7	Tsku	-	TAD1512_chr7	3.5	2.83E-17	11.5	8.61E-71	11.2	2.51E-27	18.3	2.87E-49

Table 4.8 Results from ChIP-Seq. Total number of peaks discovered by MACS2 and number of overlapping diffReps regions (see Methods). See Supplemental Table S4.2 for full listing K27ac, K4me1, and K4me3 peaks.

	Merged Peaks	Male 3 h		Male 27 h	
		Increase in mark	Decrease in mark	Increase in mark	Decrease in mark
K27ac	78,340	1,222	606	1,219	470
K4me1	139,460	214	110	174	192
K4me3	43,120	143	45	46	41

CHAPTER 5 Thesis summary and future directions

5.1 Chapter 2: *In utero* exposure to BPA does not permanently impact mouse testis function

5.1.1 Chapter 2 summary

In Chapter 2, we provide evidence of minimal long term endocrine disruption in male mice following an *in utero* exposure to BPA during a critical window of testis gonadogenesis. Mice were exposed to human-relevant doses of BPA during embryonic days 9 through 18 and several measurements of markers of endocrine disruption were taken during postnatal development (Fig. 2.1). BPA had no impact on overall litter size or survivability of male mice exposure to BPA (Fig. 2.2), indicating there was no toxicological effects of the exposure. BPA also had minimal impact on several markers of endocrine disruption including body weight, anogenital distances, white adipose accumulation, testis histopathology, and sperm production (Fig. 2.3 – Fig. 2.5). Microarray analysis was performed on testis from young adult (postnatal day 28; PND29) and sexually mature adult mice (PND49) following *in utero* exposure to BPA. Few genes were identified as dysregulated (Fig. 2.6) and none of the genes tested were able to be confirmed by qPCR, driven by high variance among biological replicates (Fig. 2.8). Together, these results suggest effects of BPA on male mouse development are minimal, are limited to short-term

effects that are corrected or repaired after the exposure has ceased, or the window chosen does not represent the true critical window in testis development.

5.1.2 Chapter 2 discussion and future directions

5.1.2.1 Other exposure routes or chronic exposures may result in changes to testis function

In my experiments, I was interested in the effects of oral exposure to endocrine disruption chemicals during a specific window of supposed gonadal susceptibility. This window corresponded to the time in which the developing bipotential gonads develops into embryonic testis in males or ovaries in females, and thus has been shown to be vulnerable to endocrine disruption (Ikeda et al. 2008, Golub et al. 2010). However, given the ubiquitous presence of BPA-derived plastics in the environment, human exposures to BPA are often chronic. Indeed, several studies of humans subjected to chronic BPA contact have shown exposed individuals had lower semen quality and higher instance of infertility (Meeker et al. 2010, Meeker et al. 2010).

A further complication in studying effects of BPA using rodent models and using the results to hypothesize human outcomes is the exposure is often limited to a single route of exposure in a laboratory setting while humans are exposed to environmental chemicals through multiple routes, and sometimes concurrently. For example, BPA is used in thermal paper used for printing receipts (Bernier and Vandenberg 2017), was once used to coat the

interiors of cans used for food (Lorber et al. 2015), and can be found at high levels in the air around contaminated water ways (Kassotis et al. 2015), thus, one may be exposed to BPA through dermal contact, ingestion, and inhalation simultaneously or within a short period. While studying the impact of each of these individual exposures is critical for human health and safety, multifaceted combinatorial approaches may be needed to fully understand human risks.

5.1.2.2 Limitations of microarray analysis

While microarray technology is useful for assessing genome wide changes to gene expression in some cases, there are limitations to the technology. For example, one major limitation is the inability to differentiate between individual genes within a highly homologous gene family, such as the cytochrome P450 family enzymes. Cyp enzymes, particularly those in the *Cyp11*, *Cyp17* and *Cyp19* families, are responsible for several key steps in steroid hormone biosynthesis and can be targets of endocrine disruption (Sanderson 2006). Due to the high sequence similarity in *Cyp* family genes, probes designed for a specific member can detect the presence of many closely related transcripts. Therefore, if one or a select few *Cyp* genes are highly dysregulated while others are not, the microarray signal from probes designed against these genes may not detect changes in gene expression. Conversely, if microarray analysis identifies a dysregulated gene that is a part of a large gene family, the wrong gene may be identified due to poor probe annotations,

and thus would lead to false-positive identifications and difficulty in confirming the regulation by other methods, such as qPCR.

We used microarray analysis to measure global gene expression changes in mouse testis following *in utero* BPA exposures and found (1) relatively few genes were regulated by *in utero* BPA exposure and (2) genes identified were unable to be confirmed by qPCR. Limitations discussed above may be the cause of these two issues and thus future experimentation using RNA-seq may be needed to better understand gene expression changes in this system.

5.2 Chapter 3: Male-based response of tumor promotion-associated genes and dysregulation of novel long non-coding RNAs in constitutive androstane receptor-activated mice

5.2.1 Chapter 3 summary

In Chapter 3, I presented a detailed analysis of mouse liver nuclear RNA-seq following short-term exposures (3 h and 27 h) to the mouse CAR direct agonist, TCPOBOP. First, we show a clear advantage of nuclear RNA-seq over traditional whole tissue RNA-seq as nuclear RNA is better able to detect gene induction and repression following a short activation of CAR (Fig. 3.1). This is likely due to the relatively large pool of fully mature and stable mRNA in the cytoplasm could dampen any emerging changes in gene expression. This is particularly problematic when attempting to measure repressed gene expression as

stable mRNA may persist in the cytoplasm even after extended periods of transcriptional silencing. Using nuclear RNA-seq, I discovered a strong male-bias in the activation of CAR-dependent hepatocellular carcinoma pathways after TCPOBOP exposure in mouse liver (Fig. 3.7 – Fig. 3.10). Additionally, there was a female-bias activation of the Nf- κ B pathway, which exerts a negative cross-talk with CAR gene responses, suggesting a protective role of Nf- κ B in HCC progression. CAR-induction and repression of novel long non-coding RNAs was also explored in Chapter 3. We identified as many as 530 CAR-responsive lncRNAs in mouse liver, many of which are directly adjacent or near a regulated protein-coding gene. While the exact functions of these non-coding transcripts are unknown, given the number regulated lncRNAs and the magnitude of their regulation, it is reasonable to assume a subset of them may be functioning to mediate CAR-dependent gene expression.

5.2.2 Chapter 3 discussion and future directions

5.2.2.1 Nf- κ B may protect females from HCC

Female mice have been shown to be more resilient to TCPOBOP-dependent HCC tumor promotion despite having higher basal levels of CAR protein (Kalra et al. 2008, Hernandez et al. 2009, Lu et al. 2013). We present evidence in Chapter 3 that the Nf- κ B/TNF pathway is more active in female liver than male mouse liver following TCPOBOP exposure. One possible hypothesis is Nf- κ B activity is necessary in female, but not male, liver due to the higher basal level of CAR as a mechanism to prevent low-to-moderate xenobiotic

exposures to leading to over activation of the CAR-dependent HCC tumor promotion pathway in females. A potential future experiment would be to knock down key components in the Nf- κ B pathway to see (1) if basal expression of HCC pathway genes are dysregulated in the absence of xenobiotic exposures or (2) if the male-bias activation of the CAR-dependent HCC pathway is ablated.

5.2.2.2 Role of sex hormones in CAR activation

CAR was first identified as an orphan nuclear receptor with unknown endogenous ligands and it was later discovered that several steroid hormones such as testosterone, androstanol, androstenol, progesterone, estradiol, and estrone (Forman et al. 1998, Kawamoto et al. 2000, Handschin and Meyer 2003, Maglich et al. 2003) act as ligands. Interestingly, while estradiol and estrone are agonist, testosterone, androstanol, androstenol, and progesterone are antagonist or inverse agonists. In male mice, this results in the near continuous suppression of CAR through the presences of high levels of testosterone, androstanol, and androstenol. In females, however, this results in cyclic basal activity of CAR, due to the spiking of estrone, estradiol, and progesterone during different stages of the estrus cycle. Given these differences, it would be interesting to see if performing RNA-seq on gonadectomized mice also ablates the sex differences associated with CAR activation presented in Chapter 3.

5.2.2.3 LncRNA function

LncRNA biology is an emerging field that can lead to many exciting and novel discoveries of mechanism for gene regulation in the cell. To date, several mechanisms for how a non-coding transcript can play a function role in regulating protein-coding genes have been identified and were discussed in Chapter 3. Briefly, these mechanisms include tethering of chromatin modifying enzymes to the site of lncRNA transcription, acting as molecular scaffolds to keep large protein complexes intact and guiding them to specific sequences through RNA-DNA interactions, and physical disruption of RNAPII via head-to-head collisions (Pelechano and Steinmetz 2013, Goff and Rinn 2015, Werner and Ruthenburg 2015). Given the sheer number of regulated lncRNAs we discovered in Chapter 3, it is likely some of them are functioning to mediate TCPOBOP-induced DME gene expression or CAR-dependent HCC tumor promotion.

A drawback of discovering several hundred candidates with potential function is it is difficult to perform in-depth experimentation on each individual candidate to test for functionality. However, in Chapter 3, I detailed several filters that can be applied which greatly reduce the number of candidate lncRNAs. One such filter is the identification of lncRNAs that are regulated in common across multiple data sets. By applying this filter, the list of regulated lncRNAs is reduced to 30 transcripts that are in common between the four TCPOBOP exposure conditions and only 15 of those transcripts are also found regulated in the PCN treated group. Given pathways and genes that were in common

between these groups include many DME and related genes, an initial screen perturbing the expression of these 15 or 30 lncRNAs and testing for the expression of the common DME gene targets is a reasonable approach. Other approaches to filter our lncRNAs include (1) proximity and orientation to the nearest regulated protein-coding genes, with a priority given to those lncRNAs close to inducible protein coding genes or (2) lncRNAs that show a strong sex-bias in activation and/or are in close proximity to protein-coding genes that show a strong sex-bias in activation.

Knockdowns can be achieved using the anti-sense oligonucleotides and RNAi techniques. However, a disadvantage of these techniques is RNAi is often achieved through post-transcriptional knockdown, which may provide enough of a window for the target lncRNA to perform a function thus resulting in a false negative, although some groups have been successful using this technique (Stojic et al. 2016). Targeted knockdowns of lncRNA using a CRISPR/Cas9 system also has its own obstacles not encountered when targeting protein-coding genes. For example, CRISPR/Cas9 is often used to introduce a frame-shift mutation early in the coding sequence of protein-coding gene, thus achieving an effective complete knockdown of the target protein. However, given that lncRNAs do not code for any proteins, they cannot acquire frameshift mutations, by definition. Further complicating the use of CRISPR/Cas9 is the fact that many of the strongly induced lncRNAs are antisense to induced protein-coding genes, as is the case with lnc_8460, lnc_15011, and lnc_15014, highlighted in Chapter 3, among others. Targeted genomic mutations of these lncRNAs

have the potential to also disrupt the sense transcript and thus could lead to false attribution of function.

5.3 Chapter 4: Regulation of chromatin accessibility and histone modifications by activated CAR in male mouse liver

5.3.1 Chapter 4 summary

In chapter 4, I characterize the dynamic changes in mouse liver epigenome associated with CAR activation. First, I report, in male and female mice, CAR-responsive genes cluster into topologically associating domains (TADs). Responsive genes are found with other responsive genes that are regulated in the same direction. Next, we discovered several thousand DNase-I hypersensitivity sites that open or close (Δ DHS) following TCPOBOP exposure, via DNase-seq, which cluster in TADs with induced or repressed genes, indicating they play a functional role in regulating those genes. Interestingly, we also report evidence of DHS opening or closing after 3 h TCPOBOP exposure preceding any associated gene expression as ~30% of Δ DHS 3 h that are found within a TAD without a gene regulated at 3 h but with at least 1 regulated gene at 27 h. Next, genome wide analysis in male liver of the activating chromatin marks H3K4me1 (K4me1), H3K4me3 (K4me3), and H3K27ac as well as the repressive chromatin mark H3K27me3 (K27me3) was performed via CHIP-seq. We used a combination of data from DNase-seq and CHIP-seq to analyze the various classes of DNA regulatory elements, including active promoter regions (DHS, K4me3, K27ac) and active enhancer regions (DHS, K4me1, K27ac). We identified

several dynamically activated enhancer regions that acquire a Δ DHS and Δ K27ac. These dynamically activated enhancers map to several known CAR-target genes including *Cyp2b10*, *Cyp3a11*, and interestingly, novel lncRNA genes including *lnc_5998*.

5.3.2 Chapter 4 discussion and future directions

5.3.2.1 Δ DHS precedes gene expression

We report a striking result that Δ DHS at 3 h are seen before any associated change in gene expression is measured within the same TAD region, but after 27 h, one or more gene within those TADs become dysregulated. One hypothesis for this observation is gene expression changes are dependent on the initial establishment of enhancer regions. A test of this hypothesis is to see if the same observation can be made with the \sim 1,000 Δ DHS at 27 h in male and female liver that do not have any associated regulated gene within the same TAD region by performing RNA-seq on mouse liver exposed to TCPOBOP for 52 h (48 h + 3h) or 75 h (72 h + 3 h). This experiment would provide additional data related to Chapter 3 and can be used to see if striking sex-biases occur with long term TCPOBOP exposures.

5.3.2.1 Better mapping through chromatin capture based assays

In Chapter 4, we were limited to mapping genomic regions of interest to putative gene targets by linear distances within the same TAD region. While this is a reasonable approach based on the data currently available, a more accurate view of enhancer-gene regulatory

networks can be achieved through chromatin capture technologies such as 3C, 4C, or Hi-C. By utilizing these more advanced techniques, we can better understand how CAR target genes are regulated in mouse liver and which genomic locations we identified in Chapter 4 are functional in the cell.

5.3.2.1 Additional chromatin marks may be relevant to CAR-dependent regulation of gene expression

Chromatin marks analyzed in Chapter 4 were chosen based on their common presence around DNA regulatory elements of interest, such as enhancer and promoter regions. However, there are many histone modifications found in the genome and each could potentially be used by the cell to signal different critical regions. For example, H3K9me3 is a mark of heterochromatin and is found in dense, transcriptionally silent regions of the genome. This mark may, however, be important for establishing the sex-bias activation of the HCC tumor promotion pathway observed in Chapter 3. Other marks that may be relevant to CAR activation are H3K36me2 and H3K36me3, which mark regions of the genome actively transcribed. These two marks may be relevant in determining if a lncRNA is actively targeted for transcription by the cell or if the transcription of the lncRNA is a byproduct of spurious transcription of the genome.

APPENDIX

Appendix 1 – List of supplemental tales related to Chapter 3.

Supplemental files are available upon request by email to djw@bu.edu

Table S3.1 - Primer sequences used for qPCR analysis.

Table S2 – Genes showing significant differential expression at $|\text{fold change}| > 1.5$ and $\text{FDR} < 0.001$, based on RNA-seq and EdgeR analysis of liver nuclear RNA after 3 h or 27 h of TCPOBOP treatment in male or female mice, or after 3 h of PCN treatment in male mice, when compared to time-matched and sex-matched vehicle controls (1% DMSO in corn oil). Data shown are normalized differential expression ratios, calculated as treatment/vehicle, corresponding fold change (FC) values, normalized read counts (FPKM; fragments per kilobase of region of interest per million mapped reads) for vehicle and treatment, and FDR (adjusted p-values) for each of the five comparisons. Collapsed exon regions were considered for counting regions using FeatureCounts (Liao, 2014, Bioinformatics). Also shown are the mouse genomic coordinates (genome release mm9) (Mapping Location(s)), NCBI accession number, official gene symbol, and Gene Ontology (GO) terms for each RefSeq gene. The RefSeq Gene Notes column indicates which mouse TAD the gene is located in (TADs numbered sequentially from 1 to approx. 3660, based on their location in the mouse genome), which strand the gene is transcribed from, overlapping genes and isoforms, etc. TFS number: Total Flag Sum, a numeric identifier used to denote in which of the 5 TCPOBOP or PCN exposure data sets the RefSeq gene

shows significant regulation. Each of the 5 digits to the right of the decimal place indicates one of the 5 data sets, with a value of 1 indicating up regulation and a value of 2 indicating down regulation. Examples: TFS value that indicates up regulation in Male 3h TCPOBOP only = x.10000; TFS for Male 27h TCPOBOP only = x.01000; TFS for Female 3h TCPOBOP only = x.00100; TFS for Female 27h TCPOBOP only = x.00010; and TFs for PCN only = x.00001. In addition, TFS values for up regulation in Male 3h TCPOBOP and in Male 27 h TCPOBOP but not any of the 3 other treatments = x.11000, down regulation in Female 3h TCPOBOP and Male 3h PCN = x.00202, etc.

Table S3 – Shown are differential expression data for the 530 liver-expressed lncRNA genes that show significant differential expression at $|\text{fold change}| > 4$ and $\text{FDR} < 0.05$, based on RNA-seq and EdgeR analysis of liver nuclear RNA after 3 h or 27 h of TCPOBOP treatment in male or female mice, or after 3 h of PCN treatment in male mice, when compared to time-matched and sex-matched vehicle controls (1% DMSO in corn oil). TFS values (column A) are explained in Table S2. Here, the TFS values are based on thresholds of $|\text{fold change}| > 2$ and $\text{FDR} < 0.05$. Other details are as described in Table S2. LncRNA genes are numbered sequentially from 1 to 15,558 based on their genomic location. The LncRNA Gene ID column further indicates whether the lncRNA is intergenic ('inter'), intragenic ('intra'), or antisense ('as') relative to the nearest protein coding gene. The LncRNA Notes column indicates which mouse TAD the gene is located in (TADs numbered sequentially from TAD1 to TAD3617, based on their location in the mouse

genome), which strand the gene is transcribed from, numbers of exons and RNA isoforms, the length of the longest open reading frame (ORF), and any overlapping genes. LncRNAs included in Fig. 6, Fig. 7 or in Supplemental Fig. S4 are shown in BOLD. For multi-exonic lncRNAs, column J indicates whether the lncRNA is in the same TAD as a co-expressed or opposite expressed RefSeq target gene (as listed in Table S6), or is not, in which case it is designated Distal.

Table S4 - Summary of comprehensive output from KEGG Pathway analysis using DAVID, based on individual KEGG output data shown in Tables S4A-S4E. RefSeq genes dysregulated with a $|\text{fold-change}| > 1.5$ and an adjusted p-value (FDR) < 0.001 were used for analysis. Full output from DAVID was filtered based on FDR (Benjamini-Hochberg) < 0.05 and pathways were annotated based on broad association with cell cycle or metabolic pathways, as shown in the last column. Shown in red text are pathways populated by genes are other than drug and lipid metabolizing enzymes.

Table S5 - Comprehensive output from IPA Upstream regulator analysis. Raw output was filtered to remove 'chemical' and 'biological drug' molecular types, as well as redundant terms. Upstream regulators with a minimum of 5 downstream gene targets with an $|\text{activation z-score}| > 2$ and p-value of overall < 0.001 were considered significant and are included here.

Table S6 - Genomic distance between TCPOBOP or PCN responsive multi-exonic lncRNA ($|FC| > 2$; $FDR < 0.05$) and the nearest responsive RefSeq gene ($|FC| > 1.5$; $FDR < 0.001$) in each data set. Responsive transcripts (lncRNA and RefSeq) were defined for each experiment separately and gene body-to-gene body distances were determined using BEDTools. Only those lncRNA-RefSeq gene pairs that are in the same TAD are presented. lncRNA-RefSeq gene pairs that show the opposite response to TCPOBOP or PCN treatment and highlighted. These may represent cases where the lncRNA exerts negative regulation on the RefSeq gene.

Appendix 2 – List of supplemental files related to Chapter 4.

Supplemental files are available upon request by email to djw@bu.edu

Supplemental Table S4.1- Δ DHS and static DHS mapped to genes. Merged list of DHS were generated based on the the MACS2 peaks called in each sequenced replicated (see Methods) and assigned a unique name (Peak Number, column D). Genomic position of DHS is listed in columns A-C and mouse liver TAD DHS is found in is listed in column E. Columns F-J: TFS score for each DHS in each TCPOBOP-exposed group. 3 h male- 1.1= Δ DHS that opens, 1.2= Δ DHS that closes; 27 h male- 2.01= Δ DHS that opens, 2.02= Δ DHS that closes; 3 h female- 4.001= Δ DHS that opens, 4.002= Δ DHS that closes; 27 h female- 8.0001= Δ DHS that opens, 8.0002 = Δ DHS that closes. Column J is the total TFS score (sum of columns F-J). Nearest gene within the same TAD to each DHS is listed in column N with the linear genomic distance listed in column P. Columns R-AK, results from RNA-seq, as reported in Chapter 3, in males and females at 3 h and 27 h. RNA-seq results include FPKM (fragments per kilobase per million reads) in vehicle-treated and TCPOBOP-treated animals, ratio, and adjusted pvalue (FDR). Corresponding TFS for the gene is listed in columns V, AA, AF, AK. 3 h male- 1.1= up regulated, 1.2=down regulated; 27 h male- 2.01=up regulated, 2.02=down regulated; 3 h female- 4.001=up regulated, 4.002=down regulated; 27 h female- 8.0001=up regulated, 8.0002 = down regulated.

Supplemental Table S4.2- Results from CHIP-seq analysis of K27ac, K4me1, and

K4me3. Merged lists of peaks for each individual histone mark was generated based on the MACS2 peaks called for each biological replicated sequenced (see Methods). Overlap of merged MACS2 peaks for each mark with diffReps regions discovered for each mark was determined using BEDtools. For each mark, merged peaks that overlapped diffReps regions discovered at 3 h or 27 h were annotated. 1.1=peak overlaps with diffReps region discovered at 3 h and is more abundant in TCPOBOP-treated samples. 1.2=peak overlaps with diffReps region at 27 h and is more abundant in vehicle-treated samples. 1.3=peak does not overlap with diffReps region but is MACS2 peak in both vehicle- and TCPOBOP-treated samples. 2.01=peak overlaps with diffReps region discovered at 27 h and is more abundant in TCPOBOP-treated samples. 2.02=peak overlaps with diffReps region at 27 h and is more abundant in vehicle-treated samples. 2.03=peak does not overlap with diffReps region but is MACS2 peak in both vehicle- and TCPOBOP-treated samples. A. Results from K27ac. B. Results from K4me1. C. Results from K4me3. D. DHS were mapped to the nearest annotated K27ac, K4me1, and K4me3 peak. Distance from the DHS to the given mark are found in columns H and J (K27ac at 3 h, K27ac at 27 h), N (K4me1), and R (K4me3).

Supplemental Table S4.3- Enhancer class definitions. DHS were mapped to the nearest K27ac peak found at 3 h or 27 h, as described in Supplemental Table S4.2. DHS were then classified based on the overlap of DHS and K27ac. DHS and K27ac were considered

overlapping if found within 1 kb of one another (see Methods). Dynamic active enhancers are defined as a Δ DHS that overlaps with a Δ K27ac peak while a stable active region is defined by a static DHS that overlaps with a static K27ac peak. Dynamic active enhancers at 3 h are flagged as '1' in column U while stable active regions are flagged as '1' in column V. Dynamic active enhancers at 27 h are flagged as '1' in column W while stable active regions are flagged as '1' in column X.

Supplemental Table S4.4 - DHS with K4me3 cluster definitions. Δ DHS were clustered based on the K4me3 signal in a 2 kb window (\pm 1 kb) centered on the DHS midpoint using k-means clustering in deepTools. Two clusters were used for 3 h Δ DHS and three clusters were used for 27 h Δ DHS. 3 h cluster definitions (column M): cluster 1- promoter like, cluster 2- enhancer like; 27 h cluster definitions (column N): cluster 1- promoter like, cluster 2- promoter like, cluster 3- enhancer-like. DHS definitions and further details about gene mapping found in Supplemental Table 4.1. DHS marked as #N/A are static DHS at the given time point and was therefore not used for K4me3 clustering.

Supplemental Table S4.5-Genes and DHS per TAD. Up and down regulated genes were counted for each mouse liver TAD in male or female mice treated with TCPOBOP for 3 h or 27 h (columns B-I). Δ DHS that open and close were counted for each mouse liver TAD in male or female mice treated with TCPOBOP for 3 h or 27 h (columns J-Q).

LIST OF JOURNAL ABBREVIATIONS

Acta Pharm Sin B	Acta Pharmaceutica Sinica B
Acta Pharmacol Sin	Acta Pharmacologica Sinica
Am J Pathol	The American Journal of Pathology
Am J Physiol Gastrointest Liver Physiol	American Journal of Physiology - Gastrointestinal and Liver Physiology
Am J Public Health	American Journal of Public Health
Andrology	Andrology
Annu Rev Biochem	Annual Review of Biochemistry
Annu Rev Physiol	Annual Review of Physiology
Arch Biochem Biophys	Archives of Biochemistry and Biophysics
Arch Toxicol	Archives of Toxicology
Asian J Androl	Asian Journal of Andrology
Biochem J	Biochemical Journal
Biochem Pharmacol	Biochemical Pharmacology
Biochemistry (Mosc)	Biochemistry (Moscow)
Biochim Biophys Acta	Biochimica et Biophysica Acta
Biol Chem	The Journal of Biological Chemistry

Biol Sex Differ	Biology of Sex Differences
Birth Defects Res B Dev Reprod Toxicol	Birth Defects Research. Part B, Developmental and Reproductive Toxicology
Cancer Cell	Cancer Cell
Cancer Res	Cancer Research
Carcinogenesis	Carcinogenesis
Cell	Cell
Cell Rep	Cell Reports
Chronobiol Int	Chronobiology International
Cold Spring Harb Protoc	Cold Spring Harbor Protocols
Crit Rev Toxicol	Critical Reviews in Toxicology
Curr Opin Pulm Med	Current Opinion in Pulmonary Medicine
Dev Dyn	Developmental Dynamics
Diabete	Diabetes
Drug Metab Dispos	Drug Metabolism and Disposition
Drug Metab Pharmacokinet	Drug Metabolism and Pharmacokinetics
Drug Metab Rev	Drug Metabolism Reviews

EMBO J	European Molecular Biology Organization Journal
Endocr Rev	Endocrine Reviews
Endocrinology	Endocrinology
Environ Health	The Journal of Environmental Health
Environ Health Perspect	Environmental Health Perspectives
Environ Int	Environment International
Environ Res	Environmental Research
Environ Sci Pollut Res Int	Environmental Science and Pollution Research
Environ Sci Technol	Environmental Science & Technology
Epigenetics	Epigenetics
Essays Biochem	Essays in Biochemistry
Eur J Oral Sci	European Journal of Oral Sciences
Exp Biol Med (Maywood)	Experimental Biology and Medicine
Expert Opin Drug Metab Toxicol	Expert Opinion on Drug Metabolism and Toxicology

FEBS Lett	Federation of European Biochemical Societies Letters
Food Chem Toxicol	Food and Chemical Toxicology
Gene	Gene
Genes Dev	Genes and Development
Genome Biol	Genome Biology
Genome Res	Genome Research
Gynecol Surv	Obstetrical & Gynecological Survey
Hepatology	Hepatology
Hum Reprod	Human Reproduction
Infect Disord Drug Targets	Infectious Disorders Drug Targets
Int Arch Occup Environ Health	International Archives of Occupational and Environmental Health
Int J Androl	International Journal of Andrology
Int J Exp Pathol	International Journal of Experimental Pathology
J Biol Chem	Journal of Biological Chemistry
J Cell Biol	The Journal of Cell Biology

J Clin Invest	Journal of Clinical Investigation
J Hepatol	Journal of Hepatology
J Lipid Res	The Journal of Lipid Research
J Mammary Gland Biol Neoplasia	Journal of Mammary Gland Biology and Neoplasia
J Med Chem	Journal of Medicinal Chemistry
J Pharmacol Exp Ther	Journal of Pharmacology and Experimental Therapeutics
J Psychosom Obstet Gynaecol	Journal of Psychosomatic Obstetrics and Gynecology
J Steroid Biochem Mol Biol	The Journal of Steroid Biochemistry and Molecular Biology
J Toxicol Sci	The Journal of Toxicological Sciences
J Transl Med	Journal of Translational Medicine
J Urol	Journal of Urology
Journal of Occupational Health	Journal of Occupational Health
Lab Invest	Laboratory Investigation
Life Sci	Life Sciences

Methods Mol Biol	Methods in Molecular Biology
Microsc Res Tech	Microscopy Research and Technique
Mol Biol Rep	Molecular Biology Reports
Mol Cell	Molecular Cell
Mol Cell Biol	Molecular and Cellular Biology
Mol Cell Endocrinol	Molecular and Cellular Endocrinology
Mol Endocrinol	Molecular Endocrinology
Mol Nutr Food Res	Molecular Nutrition and Food Research
Mol Pharm	Molecular Pharmaceutics
Mol Pharmacol	Molecular Pharmacology
Nat Commun	Nature Communications
Nat Genet	Nature Genetics
Nat Rev Genet	Nature Reviews Genetics
Nat Rev Mol Cell Biol	Nature Reviews Molecular Cell Biology
Nature	Nature
Naunyn Schmiedebergs Arch Exp Pathol Pharmacol	Naunyn-Schmiedeberg's Archives of Pharmacology
Nucl Recept Signal	Nuclear Receptor Signaling

Nucleic Acids Res	Nucleic Acids Research
Oncotarget	Oncotarget
Pharmacol Rev	Pharmacological Reviews
Physiol Rev	Physiological Reviews
PLoS Genet	Public Library of Science Genetics
PLoS One	Public Library of Science One
Proc Natl Acad Sci U S A	Proceedings of the National Academy of Sciences
Proc Soc Exp Biol Med	Proceedings of the Society for Experimental Biology and Medicine
Protein Cell	Protein and Cell
Reprod Toxicol	Reproductive Toxicology
Rev Environ Contam Toxicol	Reviews of Environmental Contamination and Toxicology
Sci Signal	Science Signaling
Sci Total Environ	Science of the Total Environment
Science	Science
Steroids	Steroids

Theriogenology	Theriogenology
Toxicol Appl Pharmacol	Toxicology and Applied Pharmacology
Toxicol Ind Health	Toxicology and Industrial Health
Toxicol Lett	Toxicology Letters
Toxicol Mech Methods	Toxicology Mechanisms and Methods
Toxicol Pathol	Toxicologic Pathology
Toxicol Sci	Toxicological Sciences
Toxicology	Toxicology
Trends Endocrinol Metab	Trends in Endocrinology and Metabolism
Trends Genet	Trends in Genetics
World J Gastroenterol	World Journal of Gastroenterology

REFERENCES

- Abdel-Hafiz, H. A. and K. B. Horwitz (2015). "Role of epigenetic modifications in luminal breast cancer." Epigenomics **7**(5): 847-862.
- Ahbab, M. A., N. Barlas and G. Karabulut (2017). "The toxicological effects of bisphenol A and octylphenol on the reproductive system of prepubertal male rats." Toxicol Ind Health **33**(2): 133-146.
- Al-Hiyasat, A. S., H. Darmani and A. M. Elbetieha (2002). "Effects of bisphenol A on adult male mouse fertility." Eur J Oral Sci **110**(2): 163-167.
- Aleksunes, L. M. and C. D. Klaassen (2012). "Coordinated regulation of hepatic phase I and II drug-metabolizing genes and transporters using AhR-, CAR-, PXR-, PPARalpha-, and Nrf2-null mice." Drug Metab Dispos **40**(7): 1366-1379.
- Atanassova, N. (2000). "Comparative Effects of Neonatal Exposure of Male Rats to Potent and Weak (Environmental) Estrogens on Spermatogenesis at Puberty and the Relationship to Adult Testis Size and Fertility: Evidence for Stimulatory Effects of Low Estrogen Levels." Endocrinology **141**(10): 3898-3907.
- Barski, A., S. Cuddapah, K. Cui, T. Y. Roh, D. E. Schones, Z. Wang, G. Wei, I. Chepelev and K. Zhao (2007). "High-resolution profiling of histone methylations in the human genome." Cell **129**(4): 823-837.

- Bartek, J. and J. Lukas (2011). "DNA repair: Cyclin D1 multitasks." Nature **474**(7350): 171-172.
- Bernier, M. R. and L. N. Vandenberg (2017). "Handling of thermal paper: Implications for dermal exposure to bisphenol A and its alternatives." PLoS One **12**(6): e0178449.
- Bielinska, M., A. Seehra, J. Toppari, M. Heikinheimo and D. B. Wilson (2007). "GATA-4 is required for sex steroidogenic cell development in the fetal mouse." Dev Dyn **236**(1): 203-213.
- Blizard, D., T. Sueyoshi, M. Negishi, S. S. Dehal and D. Kupfer (2001). "Mechanism of induction of cytochrome p450 enzymes by the proestrogenic endocrine disruptor pesticide-methoxychlor: interactions of methoxychlor metabolites with the constitutive androstane receptor system." Drug Metab Dispos **29**(6): 781-785.
- Bonev, B. and G. Cavalli (2016). "Organization and function of the 3D genome." Nat Rev Genet **17**(11): 661-678.
- Burd, C. J., J. M. Ward, V. J. Crusselle-Davis, G. E. Kissling, D. Phadke, R. R. Shah and T. K. Archer (2012). "Analysis of chromatin dynamics during glucocorticoid receptor activation." Mol Cell Biol **32**(10): 1805-1817.

- Calafat, A. M., Z. Kuklennyik, J. A. Reidy, S. P. Caudill, J. Ekong and L. L. Needham (2005). "Urinary concentrations of bisphenol A and 4-nonylphenol in a human reference population." Environ Health Perspect **113**(4): 391-395.
- Chang, T. K. and D. J. Waxman (2006). "Synthetic drugs and natural products as modulators of constitutive androstane receptor (CAR) and pregnane X receptor (PXR)." Drug Metab Rev **38**(1-2): 51-73.
- Chen, W. D., X. Fu, B. Dong, Y. D. Wang, S. Shiah, D. D. Moore and W. Huang (2012). "Neonatal activation of the nuclear receptor CAR results in epigenetic memory and permanent change of drug metabolism in mouse liver." Hepatology **56**(4): 1499-1509.
- Chen, X., Z. Meng, X. Wang, S. Zeng and W. Huang (2011). "The nuclear receptor CAR modulates alcohol-induced liver injury." Lab Invest **91**(8): 1136-1145.
- Chen, Y., S. S. Ferguson, M. Negishi and J. A. Goldstein (2003). "Identification of constitutive androstane receptor and glucocorticoid receptor binding sites in the CYP2C19 promoter." Mol Pharmacol **64**(2): 316-324.
- Cherian, M. T., S. C. Chai and T. Chen (2015). "Small-molecule modulators of the constitutive androstane receptor." Expert Opin Drug Metab Toxicol **11**(7): 1099-1114.

- Chitra, K. C., K. R. Rao and P. P. Mathur (2003). "Effect of bisphenol A and co-administration of bisphenol A and vitamin C on epididymis of adult rats: a histological and biochemical study." Asian J Androl **5**(3): 203-208.
- Cirillo, L. A., F. R. Lin, I. Cuesta, D. Friedman, M. Jarnik and K. S. Zaret (2002). "Opening of compacted chromatin by early developmental transcription factors HNF3 (FoxA) and GATA-4." Mol Cell **9**(2): 279-289.
- Claessens, F. and D. T. Gewirth (2004). "DNA recognition by nuclear receptors." Essays Biochem **40**: 59-72.
- Colborn, T., F. S. vom Saal and A. M. Soto (1993). "Developmental effects of endocrine-disrupting chemicals in wildlife and humans." Environ Health Perspect **101**(5): 378-384.
- Columbano, A., G. M. Ledda-Columbano, M. Pibiri, C. Cossu, M. Menegazzi, D. D. Moore, W. Huang, J. Tian and J. Locker (2005). "Gadd45beta is induced through a CAR-dependent, TNF-independent pathway in murine liver hyperplasia." Hepatology **42**(5): 1118-1126.
- Conforto, T. L. and D. J. Waxman (2012). "Sex-specific mouse liver gene expression: genome-wide analysis of developmental changes from pre-pubertal period to young adulthood." Biol Sex Differ **3**: 9.

- Connerney, J., D. Lau-Corona, A. Rampersaud and D. J. Waxman (2017). "Activation of Male Liver Chromatin Accessibility and STAT5-dependent Gene Transcription by Plasma Growth Hormone Pulses." Endocrinology **158**(4).
- Consortium, E. P. (2012). "An integrated encyclopedia of DNA elements in the human genome." Nature **489**(7414): 57-74.
- Cooke, P. S., P. A. Heine, J. A. Taylor and D. B. Lubahn (2001). "The role of estrogen and estrogen receptor-alpha in male adipose tissue." Mol Cell Endocrinol **178**(1-2): 147-154.
- Cooke, P. S. and A. Naaz (2004). "Role of estrogens in adipocyte development and function." Exp Biol Med (Maywood) **229**(11): 1127-1135.
- Creyghton, M. P., A. W. Cheng, G. G. Welstead, T. Kooistra, B. W. Carey, E. J. Steine, J. Hanna, M. A. Lodato, G. M. Frampton, P. A. Sharp, L. A. Boyer, R. A. Young and R. Jaenisch (2010). "Histone H3K27ac separates active from poised enhancers and predicts developmental state." Proc Natl Acad Sci U S A **107**(50): 21931-21936.
- Cucchiara, V., J. C. Yang, V. Mirone, A. C. Gao, M. G. Rosenfeld and C. P. Evans (2017). "Epigenomic Regulation of Androgen Receptor Signaling: Potential Role in Prostate Cancer Therapy." Cancers (Basel) **9**(1).

- Cui, J. Y., S. S. Gunewardena, C. E. Rockwell and C. D. Klaassen (2010). "ChIPing the cistrome of PXR in mouse liver." Nucleic Acids Res **38**(22): 7943-7963.
- Cui, J. Y. and C. D. Klaassen (2016). "RNA-Seq reveals common and unique PXR- and CAR-target gene signatures in the mouse liver transcriptome." Biochim Biophys Acta **1859**(9): 1198-1217.
- de Rooij, D. G. (2009). "The spermatogonial stem cell niche." Microsc Res Tech **72**(8): 580-585.
- Deane, N. G., M. A. Parker, R. Aramandla, L. Diehl, W. J. Lee, M. K. Washington, L. B. Nanney, Y. Shyr and R. D. Beauchamp (2001). "Hepatocellular carcinoma results from chronic cyclin D1 overexpression in transgenic mice." Cancer Res **61**(14): 5389-5395.
- Dixon, J. R., D. U. Gorkin and B. Ren (2016). "Chromatin Domains: The Unit of Chromosome Organization." Mol Cell **62**(5): 668-680.
- Dong, B., J. S. Lee, Y. Y. Park, F. Yang, G. Xu, W. Huang, M. J. Finegold and D. D. Moore (2015). "Activating CAR and beta-catenin induces uncontrolled liver growth and tumorigenesis." Nat Commun **6**: 5944.

- Duivenvoorden, I., B. Teusink, P. C. Rensen, J. A. Romijn, L. M. Havekes and P. J. Voshol (2005). "Apolipoprotein C3 deficiency results in diet-induced obesity and aggravated insulin resistance in mice." Diabetes **54**(3): 664-671.
- Eisenberg, M. L., T. K. Jensen, R. C. Walters, N. E. Skakkebaek and L. I. Lipshultz (2012). "The relationship between anogenital distance and reproductive hormone levels in adult men." J Urol **187**(2): 594-598.
- El-Serag, H. B. and F. Kanwal (2014). "Epidemiology of hepatocellular carcinoma in the United States: where are we? Where do we go?" Hepatology **60**(5): 1767-1775.
- Engreitz, J. M., J. E. Haines, E. M. Perez, G. Munson, J. Chen, M. Kane, P. E. McDonel, M. Guttman and E. S. Lander (2016). "Local regulation of gene expression by lncRNA promoters, transcription and splicing." Nature **539**(7629): 452-455.
- Eveillard, A., L. Mselli-Lakhal, A. Mogha, F. Lasserre, A. Polizzi, J. M. Pascussi, H. Guillou, P. G. Martin and T. Pineau (2009). "Di-(2-ethylhexyl)-phthalate (DEHP) activates the constitutive androstane receptor (CAR): a novel signalling pathway sensitive to phthalates." Biochem Pharmacol **77**(11): 1735-1746.
- Faure, A. J., D. Schmidt, S. Watt, P. C. Schwalie, M. D. Wilson, H. Xu, R. G. Ramsay, D. T. Odom and P. Flicek (2012). "Cohesin regulates tissue-specific expression by stabilizing highly occupied cis-regulatory modules." Genome Res **22**(11): 2163-2175.

- Fisher, J. S., K. J. Turner, D. Brown and R. M. Sharpe (1999). "Effect of neonatal exposure to estrogenic compounds on development of the excurrent ducts of the rat testis through puberty to adulthood." Environ Health Perspect **107**(5): 397-405.
- Forman, B. M., I. Tzamelis, H. S. Choi, J. Chen, D. Simha, W. Seol, R. M. Evans and D. D. Moore (1998). "Androstane metabolites bind to and deactivate the nuclear receptor CAR-beta." Nature **395**(6702): 612-615.
- Fraser, P. and F. Grosveld (1998). "Locus control regions, chromatin activation and transcription." Curr Opin Cell Biol **10**(3): 361-365.
- Gao, J. and W. Xie (2010). "Pregnane X receptor and constitutive androstane receptor at the crossroads of drug metabolism and energy metabolism." Drug Metab Dispos **38**(12): 2091-2095.
- Gaspar-Maia, A., A. Alajem, E. Meshorer and M. Ramalho-Santos (2011). "Open chromatin in pluripotency and reprogramming." Nat Rev Mol Cell Biol **12**(1): 36-47.
- Geter, D. R., V. S. Bhat, B. B. Gollapudi, R. Sura and S. D. Hester (2014). "Dose-response modeling of early molecular and cellular key events in the CAR-mediated hepatocarcinogenesis pathway." Toxicol Sci **138**(2): 425-445.

- Godmann, M., R. Lambrot and S. Kimmins (2009). "The dynamic epigenetic program in male germ cells: Its role in spermatogenesis, testis cancer, and its response to the environment." Microsc Res Tech **72**(8): 603-619.
- Goff, L. A. and J. L. Rinn (2015). "Linking RNA biology to lncRNAs." Genome Res **25**(10): 1456-1465.
- Goldstone, A. E., Z. Chen, M. J. Perry, K. Kannan and G. M. Louis (2015). "Urinary bisphenol A and semen quality, the LIFE Study." Reprod Toxicol **51**: 7-13.
- Golub, M. S., K. L. Wu, F. L. Kaufman, L. H. Li, F. Moran-Messen, L. Zeise, G. V. Alexeeff and J. M. Donald (2010). "Bisphenol A: developmental toxicity from early prenatal exposure." Birth Defects Res B Dev Reprod Toxicol **89**(6): 441-466.
- Gray, L. E., B. Ryan, A. Hotchkiss and K. Crofton (2010). "Rebuttal of "Flawed Experimental design Reveals the Need for Guidelines Requiring Appropriate Positive Controls in Endocrine Disruption Research" by vom Saal." Toxicol Sci **115**(2): 614-620.
- Grontved, L., S. John, S. Baek, Y. Liu, J. R. Buckley, C. Vinson, G. Aguilera and G. L. Hager (2013). "C/EBP maintains chromatin accessibility in liver and facilitates glucocorticoid receptor recruitment to steroid response elements." EMBO J **32**(11): 1568-1583.

- Gupta, C. (2000). "Reproductive malformation of the male offspring following maternal exposure to estrogenic chemicals." Proc Soc Exp Biol Med **224**(2): 61-68.
- Hanania, N. A., B. F. Dickey and R. A. Bond (2010). "Clinical implications of the intrinsic efficacy of beta-adrenoceptor drugs in asthma: full, partial and inverse agonism." Curr Opin Pulm Med **16**(1): 1-5.
- Handschin, C. and U. A. Meyer (2003). "Induction of drug metabolism: the role of nuclear receptors." Pharmacol Rev **55**(4): 649-673.
- Hanukoglu, I. (1992). "Steroidogenic enzymes: structure, function, and role in regulation of steroid hormone biosynthesis." J Steroid Biochem Mol Biol **43**(8): 779-804.
- Heindryckx, F., I. Colle and H. Van Vlierberghe (2009). "Experimental mouse models for hepatocellular carcinoma research." Int J Exp Pathol **90**(4): 367-386.
- Hernandez, J. P., W. Huang, L. M. Chapman, S. Chua, D. D. Moore and W. S. Baldwin (2007). "The environmental estrogen, nonylphenol, activates the constitutive androstane receptor." Toxicol Sci **98**(2): 416-426.
- Hernandez, J. P., L. C. Mota, W. Huang, D. D. Moore and W. S. Baldwin (2009). "Sexually dimorphic regulation and induction of P450s by the constitutive androstane receptor (CAR)." Toxicology **256**(1-2): 53-64.

- Hnisz, D., D. S. Day and R. A. Young (2016). "Insulated Neighborhoods: Structural and Functional Units of Mammalian Gene Control." Cell **167**(5): 1188-1200.
- Hobson, D. J., W. Wei, L. M. Steinmetz and J. Q. Svejstrup (2012). "RNA polymerase II collision interrupts convergent transcription." Mol Cell **48**(3): 365-374.
- Honkakoski, P. and M. Negishi (1997). "Characterization of a phenobarbital-responsive enhancer module in mouse P450 Cyp2b10 gene." J Biol Chem **272**(23): 14943-14949.
- Honkakoski, P., I. Zelko, T. Sueyoshi and M. Negishi (1998). "The nuclear orphan receptor CAR-retinoid X receptor heterodimer activates the phenobarbital-responsive enhancer module of the CYP2B gene." Mol Cell Biol **18**(10): 5652-5658.
- Honma, S., A. Suzuki, D. L. Buchanan, Y. Katsu, H. Watanabe and T. Iguchi (2002). "Low dose effect of in utero exposure to bisphenol A and diethylstilbestrol on female mouse reproduction." Reprod Toxicol **16**(2): 117-122.
- Hori, T., R. Moore and M. Negishi (2016). "p38 MAP Kinase Links CAR Activation and Inactivation in the Nucleus via Phosphorylation at Threonine 38." Drug Metab Dispos **44**(6): 871-876.

- Huang, P., V. Chandra and F. Rastinejad (2010). "Structural overview of the nuclear receptor superfamily: insights into physiology and therapeutics." Annu Rev Physiol **72**: 247-272.
- Ikeda, Y., H. Tanaka and M. Esaki (2008). "Effects of gestational diethylstilbestrol treatment on male and female gonads during early embryonic development." Endocrinology **149**(8): 3970-3979.
- Inoue, K. and M. Negishi (2009). "Early growth response 1 loops the CYP2B6 promoter for synergistic activation by the distal and proximal nuclear receptors CAR and HNF4alpha." FEBS Lett **583**(12): 2126-2130.
- Iwafuchi-Doi, M. and K. S. Zaret (2014). "Pioneer transcription factors in cell reprogramming." Genes Dev **28**(24): 2679-2692.
- Jackson, J. P., S. S. Ferguson, M. Negishi and J. A. Goldstein (2006). "Phenytoin induction of the cyp2c37 gene is mediated by the constitutive androstane receptor." Drug Metab Dispos **34**(12): 2003-2010.
- Jirawatnotai, S., Y. Hu, W. Michowski, J. E. Elias, L. Becks, F. Bienvenu, A. Zagozdzon, T. Goswami, Y. E. Wang, A. B. Clark, T. A. Kunkel, T. van Harn, B. Xia, M. Correll, J. Quackenbush, D. M. Livingston, S. P. Gygi and P. Sicinski (2011). "A function for cyclin D1 in DNA repair uncovered by protein interactome analyses in human cancers." Nature **474**(7350): 230-234.

- Kalra, M., J. Mayes, S. Assefa, A. K. Kaul and R. Kaul (2008). "Role of sex steroid receptors in pathobiology of hepatocellular carcinoma." World J Gastroenterol **14**(39): 5945-5961.
- Kang, E. R., K. Iqbal, D. A. Tran, G. E. Rivas, P. Singh, G. P. Pfeifer and P. E. Szabo (2011). "Effects of endocrine disruptors on imprinted gene expression in the mouse embryo." Epigenetics **6**(7): 937-950.
- Kanno, Y., M. Suzuki, T. Nakahama and Y. Inouye (2005). "Characterization of nuclear localization signals and cytoplasmic retention region in the nuclear receptor CAR." Biochim Biophys Acta **1745**(2): 215-222.
- Kassotis, C. D., D. A. Alvarez, J. A. Taylor, F. S. vom Saal, S. C. Nagel and D. E. Tillitt (2015). "Characterization of Missouri surface waters near point sources of pollution reveals potential novel atmospheric route of exposure for bisphenol A and wastewater hormonal activity pattern." Sci Total Environ **524-525**: 384-393.
- Kawamoto, T., S. Kakizaki, K. Yoshinari and M. Negishi (2000). "Estrogen activation of the nuclear orphan receptor CAR (constitutive active receptor) in induction of the mouse Cyp2b10 gene." Mol Endocrinol **14**(11): 1897-1905.
- Kawamoto, T., T. Sueyoshi, I. Zelko, R. Moore, K. Washburn and M. Negishi (1999). "Phenobarbital-responsive nuclear translocation of the receptor CAR in induction of the CYP2B gene." Mol Cell Biol **19**(9): 6318-6322.

- Kazantseva, Y. A., Y. A. Pustyl'nyak and V. O. Pustyl'nyak (2016). "Role of Nuclear Constitutive Androstane Receptor in Regulation of Hepatocyte Proliferation and Hepatocarcinogenesis." Biochemistry (Mosc) **81**(4): 338-347.
- Kazantseva, Y. A., A. A. Yarushkin and V. O. Pustyl'nyak (2014). "CAR-mediated repression of Foxo1 transcriptional activity regulates the cell cycle inhibitor p21 in mouse livers." Toxicology **321**: 73-79.
- Kettner, N. M., H. Voicu, M. J. Finegold, C. Coarfa, A. Sreekumar, N. Putluri, C. A. Katchy, C. Lee, D. D. Moore and L. Fu (2016). "Circadian Homeostasis of Liver Metabolism Suppresses Hepatocarcinogenesis." Cancer Cell **30**(6): 909-924.
- Kobayashi, K., M. Hashimoto, P. Honkakoski and M. Negishi (2015). "Regulation of gene expression by CAR: an update." Arch Toxicol **89**(7): 1045-1055.
- Kobayashi, K., T. Sueyoshi, K. Inoue, R. Moore and M. Negishi (2003). "Cytoplasmic accumulation of the nuclear receptor CAR by a tetratricopeptide repeat protein in HepG2 cells." Mol Pharmacol **64**(5): 1069-1075.
- Kobayashi, K., Y. Yamanaka, N. Iwazaki, I. Nakajo, M. Hosokawa, M. Negishi and K. Chiba (2005). "Identification of HMG-CoA reductase inhibitors as activators for human, mouse and rat constitutive androstane receptor." Drug Metab Dispos **33**(7): 924-929.

- Kodama, S., C. Koike, M. Negishi and Y. Yamamoto (2004). "Nuclear receptors CAR and PXR cross talk with FOXO1 to regulate genes that encode drug-metabolizing and gluconeogenic enzymes." Mol Cell Biol **24**(18): 7931-7940.
- Koh, K. H., S. Jurkovic, K. Yang, S. Y. Choi, J. W. Jung, K. P. Kim, W. Zhang and H. Jeong (2012). "Estradiol induces cytochrome P450 2B6 expression at high concentrations: implication in estrogen-mediated gene regulation in pregnancy." Biochem Pharmacol **84**(1): 93-103.
- Kohalmy, K., V. Tamasi, L. Kobori, E. Sarvary, J. M. Pascussi, P. Porrogi, D. Rozman, R. A. Prough, U. A. Meyer and K. Monostory (2007). "Dehydroepiandrosterone induces human CYP2B6 through the constitutive androstane receptor." Drug Metab Dispos **35**(9): 1495-1501.
- Konno, Y., M. Negishi and S. Kodama (2008). "The roles of nuclear receptors CAR and PXR in hepatic energy metabolism." Drug Metab Pharmacokinet **23**(1): 8-13.
- Kuno, T., H. Togawa and T. Mizutani (2008). "Induction of human UGT1A1 by a complex of dexamethasone-GR dependent on proximal site and independent of PBREM." Mol Biol Rep **35**(3): 361-367.
- Kyronlahti, A., R. Euler, M. Bielinska, E. L. Schoeller, K. H. Moley, J. Toppari, M. Heikinheimo and D. B. Wilson (2011). "GATA4 regulates Sertoli cell function and fertility in adult male mice." Mol Cell Endocrinol **333**(1): 85-95.

La Rosa, P., M. Pellegrini, P. Totta, F. Acconcia and M. Marino (2014). "Xenoestrogens alter estrogen receptor (ER) alpha intracellular levels." PLoS One **9**(2): e88961.

Langmead, B., C. Trapnell, M. Pop and S. L. Salzberg (2009). "Ultrafast and memory-efficient alignment of short DNA sequences to the human genome." Genome Biol **10**(3): R25.

LaRocca, J., A. Boyajian, C. Brown, S. D. Smith and M. Hixon (2011). "Effects of in utero exposure to Bisphenol A or diethylstilbestrol on the adult male reproductive system." Birth Defects Res B Dev Reprod Toxicol **92**(6): 526-533.

Larocca, J., A. Boyajian, C. Brown, S. D. Smith and M. Hixon (2011). "Effects of in utero exposure to Bisphenol A or diethylstilbestrol on the adult male reproductive system." Birth Defects Res B Dev Reprod Toxicol.

Latendresse, J. R., A. R. Warbritton, H. Jonassen and D. M. Creasy (2002). "Fixation of testes and eyes using a modified Davidson's fluid: comparison with Bouin's fluid and conventional Davidson's fluid." Toxicol Pathol **30**(4): 524-533.

Lau-Corona, D., A. Suvorov and D. J. Waxman (2017). "Feminization of male mouse liver by persistent growth hormone stimulation: Activation of sex-biased transcriptional networks and dynamic changes in chromatin states." Mol Cell Biol.

- Le Dily, F. and M. Beato (2015). "TADs as modular and dynamic units for gene regulation by hormones." FEBS Lett **589**(20 Pt A): 2885-2892.
- Ledda-Columbano, G. M., M. Pibiri, D. Concas, C. Cossu, M. Tripodi and A. Columbano (2002). "Loss of cyclin D1 does not inhibit the proliferative response of mouse liver to mitogenic stimuli." Hepatology **36**(5): 1098-1105.
- Ledda-Columbano, G. M., M. Pibiri, D. Concas, F. Molotzu, G. Simbula, C. Cossu and A. Columbano (2003). "Sex difference in the proliferative response of mouse hepatocytes to treatment with the CAR ligand, TCPOBOP." Carcinogenesis **24**(6): 1059-1065.
- Ledda-Columbano, G. M., M. Pibiri, R. Loi, A. Perra, H. Shinozuka and A. Columbano (2000). "Early increase in cyclin-D1 expression and accelerated entry of mouse hepatocytes into S phase after administration of the mitogen 1, 4-Bis[2-(3,5-Dichloropyridyloxy)] benzene." Am J Pathol **156**(1): 91-97.
- Lee, M. R., J. H. Kim, Y. H. Choi, S. Bae, C. Park and Y. C. Hong (2015). "Association of bisphenol A exposure with overweight in the elderly: a panel study." Environ Sci Pollut Res Int **22**(12): 9370-9377.
- Li, D., B. Mackowiak, T. G. Brayman, M. Mitchell, L. Zhang, S. M. Huang and H. Wang (2015). "Genome-wide analysis of human constitutive androstane receptor (CAR)

transcriptome in wild-type and CAR-knockout HepaRG cells." Biochem Pharmacol **98**(1): 190-202.

Li, J., R. Mao, Q. Zhou, L. Ding, J. Tao, M. M. Ran, E. S. Gao, W. Yuan, J. T. Wang and L. F. Hou (2016). "Exposure to bisphenol A (BPA) in Wistar rats reduces sperm quality with disruption of ERK signal pathway." Toxicol Mech Methods **26**(3): 180-188.

Li, Z., G. Tuteja, J. Schug and K. H. Kaestner (2012). "Foxa1 and Foxa2 are essential for sexual dimorphism in liver cancer." Cell **148**(1-2): 72-83.

Lickteig, A. J., I. L. Csanaky, M. Pratt-Hyatt and C. D. Klaassen (2016). "Activation of Constitutive Androstane Receptor (CAR) in Mice Results in Maintained Biliary Excretion of Bile Acids Despite a Marked Decrease of Bile Acids in Liver." Toxicol Sci **151**(2): 403-418.

Ling, G. and D. J. Waxman (2013). "DNase I digestion of isolated nuclei for genome-wide mapping of DNase hypersensitivity sites in chromatin." Methods Mol Biol **977**: 21-33.

Ling, G. and D. J. Waxman (2013). "Isolation of nuclei for use in genome-wide DNase hypersensitivity assays to probe chromatin structure." Methods Mol Biol **977**: 13-19.

- Liu, S. J., M. A. Horlbeck, S. W. Cho, H. S. Birk, M. Malatesta, D. He, F. J. Attenello, J. E. Villalta, M. Y. Cho, Y. Chen, M. A. Mandegar, M. P. Olvera, L. A. Gilbert, B. R. Conklin, H. Y. Chang, J. S. Weissman and D. A. Lim (2017). "CRISPRi-based genome-scale identification of functional long noncoding RNA loci in human cells." Science **355**(6320).
- Lodato, N. J., T. Melia, A. Rampersaud and D. J. Waxman (2017). "Sex-Differential Responses of Tumor Promotion-Associated Genes and Dysregulation of Novel Long Noncoding RNAs in Constitutive Androstane Receptor-Activated Mouse Liver." Toxicol Sci.
- Lodato, N. J., T. Melia, A. Rampersaud and D. J. Waxman (2017). "Sex-Differential Responses of Tumor Promotion-Associated Genes and Dysregulation of Novel Long Noncoding RNAs in Constitutive Androstane Receptor-Activated Mouse Liver." Toxicological Sciences.
- Lorber, M., A. Schechter, O. Paepke, W. Shropshire, K. Christensen and L. Birnbaum (2015). "Exposure assessment of adult intake of bisphenol A (BPA) with emphasis on canned food dietary exposures." Environ Int **77**: 55-62.
- Lu, Y. F., T. Jin, Y. Xu, D. Zhang, Q. Wu, Y. K. Zhang and J. Liu (2013). "Sex differences in the circadian variation of cytochrome p450 genes and

corresponding nuclear receptors in mouse liver." Chronobiol Int **30**(9): 1135-1143.

Luisier, R., H. Lempiainen, N. Scherbichler, A. Braeuning, M. Geissler, V. Dubost, A. Muller, N. Scheer, S. D. Chibout, H. Hara, F. Picard, D. Theil, P. Couttet, A. Vitobello, O. Grenet, B. Grasl-Kraupp, H. Ellinger-Ziegelbauer, J. P. Thomson, R. R. Meehan, C. R. Elcombe, C. J. Henderson, C. R. Wolf, M. Schwarz, P. Moulin, R. Terranova and J. G. Moggs (2014). "Phenobarbital induces cell cycle transcriptional responses in mouse liver humanized for constitutive androstane and pregnane x receptors." Toxicol Sci **139**(2): 501-511.

Madsen, M. S., R. Siersbaek, M. Boergesen, R. Nielsen and S. Mandrup (2014).

"Peroxisome proliferator-activated receptor gamma and C/EBPalpha synergistically activate key metabolic adipocyte genes by assisted loading." Mol Cell Biol **34**(6): 939-954.

Maglich, J. M., D. C. Lobe and J. T. Moore (2009). "The nuclear receptor CAR (NR113) regulates serum triglyceride levels under conditions of metabolic stress." J Lipid Res **50**(3): 439-445.

Maglich, J. M., D. J. Parks, L. B. Moore, J. L. Collins, B. Goodwin, A. N. Billin, C. A.

Stoltz, S. A. Kliewer, M. H. Lambert, T. M. Willson and J. T. Moore (2003).

"Identification of a novel human constitutive androstane receptor (CAR) agonist

and its use in the identification of CAR target genes." J Biol Chem **278**(19): 17277-17283.

Manfo, F. P., R. Jubendradass, E. A. Nantia, P. F. Moundipa and P. P. Mathur (2014). "Adverse effects of bisphenol A on male reproductive function." Rev Environ Contam Toxicol **228**: 57-82.

Mann, M., V. Cortez and R. K. Vadlamudi (2011). "Epigenetics of estrogen receptor signaling: role in hormonal cancer progression and therapy." Cancers (Basel) **3**(3): 1691-1707.

Meeker, J. D., A. M. Calafat and R. Hauser (2010). "Urinary bisphenol A concentrations in relation to serum thyroid and reproductive hormone levels in men from an infertility clinic." Environ Sci Technol **44**(4): 1458-1463.

Meeker, J. D., S. Ehrlich, T. L. Toth, D. L. Wright, A. M. Calafat, A. T. Trisini, X. Ye and R. Hauser (2010). "Semen quality and sperm DNA damage in relation to urinary bisphenol A among men from an infertility clinic." Reprod Toxicol **30**(4): 532-539.

Melia, T., P. Hao, F. Yilmaz and D. J. Waxman (2016). "Hepatic Long Intergenic Noncoding RNAs: High Promoter Conservation and Dynamic, Sex-Dependent Transcriptional Regulation by Growth Hormone." Mol Cell Biol **36**(1): 50-69.

- Mellor, C. L., F. P. Steinmetz and M. T. Cronin (2016). "The identification of nuclear receptors associated with hepatic steatosis to develop and extend adverse outcome pathways." Crit Rev Toxicol **46**(2): 138-152.
- Mendonca, K., R. Hauser, A. M. Calafat, T. E. Arbuckle and S. M. Duty (2014). "Bisphenol A concentrations in maternal breast milk and infant urine." Int Arch Occup Environ Health **87**(1): 13-20.
- Meshorer, E. and T. Misteli (2006). "Chromatin in pluripotent embryonic stem cells and differentiation." Nat Rev Mol Cell Biol **7**(7): 540-546.
- Meyer, S. A. and R. L. Jirtle (2013). "Old dance with a new partner: EGF receptor as the phenobarbital receptor mediating Cyp2B expression." Sci Signal **6**(274): pe16.
- Montes-Grajales, D. and J. Olivero-Verbel (2013). "Computer-aided identification of novel protein targets of bisphenol A." Toxicol Lett **222**(3): 312-320.
- Moreau, A., M. J. Vilarem, P. Maurel and J. M. Pascussi (2008). "Xenoreceptors CAR and PXR activation and consequences on lipid metabolism, glucose homeostasis, and inflammatory response." Mol Pharm **5**(1): 35-41.
- Myers, J. P., F. S. vom Saal, B. T. Akingbemi, K. Arizono, S. Belcher, T. Colborn, I. Chahoud, D. A. Crain, F. Farabollini, L. J. Guillette, Jr., T. Hassold, S. M. Ho, P. A. Hunt, T. Iguchi, S. Jobling, J. Kanno, H. Laufer, M. Marcus, J. A. McLachlan,

A. Nadal, J. Oehlmann, N. Olea, P. Palanza, S. Parmigiani, B. S. Rubin, G. Schoenfelder, C. Sonnenschein, A. M. Soto, C. E. Talsness, J. A. Taylor, L. N. Vandenberg, J. G. Vandenberg, S. Vogel, C. S. Watson, W. V. Welshons and R. T. Zoeller (2009). "Why public health agencies cannot depend on good laboratory practices as a criterion for selecting data: the case of bisphenol A." Environ Health Perspect **117**(3): 309-315.

Naciff, J. M., K. A. Hess, G. J. Overmann, S. M. Torontali, G. J. Carr, J. P. Tiesman, L. M. Foertsch, B. D. Richardson, J. E. Martinez and G. P. Daston (2005). "Gene expression changes induced in the testis by transplacental exposure to high and low doses of 17 α -ethynyl estradiol, genistein, or bisphenol A." Toxicol Sci **86**(2): 396-416.

Nagaich, A. K., D. A. Walker, R. Wolford and G. L. Hager (2004). "Rapid periodic binding and displacement of the glucocorticoid receptor during chromatin remodeling." Mol Cell **14**(2): 163-174.

Nahar, M. S., A. S. Soliman, J. A. Colacino, A. M. Calafat, K. Battige, A. Hablas, I. A. Seifeldin, D. C. Dolinoy and L. S. Rozek (2012). "Urinary bisphenol A concentrations in girls from rural and urban Egypt: a pilot study." Environ Health **11**: 20.

- Nakamura, D., Y. Yanagiba, Z. Duan, Y. Ito, A. Okamura, N. Asaeda, Y. Tagawa, C. Li, K. Taya, S. Y. Zhang, H. Naito, D. H. Ramdhan, M. Kamijima and T. Nakajima (2010). "Bisphenol A may cause testosterone reduction by adversely affecting both testis and pituitary systems similar to estradiol." Toxicol Lett **194**(1-2): 16-25.
- Newbold, R. R., B. C. Bullock and J. A. McLachlan (1985). "Lesions of the rete testis in mice exposed prenatally to diethylstilbestrol." Cancer Res **45**(10): 5145-5150.
- Newbold, R. R., E. Padilla-Banks, R. J. Snyder and W. N. Jefferson (2007). "Perinatal exposure to environmental estrogens and the development of obesity." Mol Nutr Food Res **51**(7): 912-917.
- Nikaido, Y., K. Yoshizawa, N. Danbara, M. Tsujita-Kyutoku, T. Yuri, N. Uehara and A. Tsubura (2004). "Effects of maternal xenoestrogen exposure on development of the reproductive tract and mammary gland in female CD-1 mouse offspring." Reprod Toxicol **18**(6): 803-811.
- Nora, E. P., A. Goloborodko, A. L. Valton, J. H. Gibcus, A. Uebersohn, N. Abdennur, J. Dekker, L. A. Mirny and B. G. Bruneau (2017). "Targeted Degradation of CTCF Decouples Local Insulation of Chromosome Domains from Genomic Compartmentalization." Cell **169**(5): 930-944 e922.

- Orrenius, S. and J. L. Ericsson (1966). "Enzyme-membrane relationship in phenobarbital induction of synthesis of drug-metabolizing enzyme system and proliferation of endoplasmic membranes." J Cell Biol **28**(2): 181-198.
- Osabe, M. and M. Negishi (2011). "Active ERK1/2 protein interacts with the phosphorylated nuclear constitutive active/androstane receptor (CAR; NR1I3), repressing dephosphorylation and sequestering CAR in the cytoplasm." J Biol Chem **286**(41): 35763-35769.
- Oshida, K., N. Vasani, C. Jones, T. Moore, S. Hester, S. Nesnow, S. Auerbach, D. R. Geter, L. M. Aleksunes, R. S. Thomas, D. Applegate, C. D. Klaassen and J. C. Corton (2015). "Identification of chemical modulators of the constitutive activated receptor (CAR) in a gene expression compendium." Nucl Recept Signal **13**: e002.
- Ostuni, R., V. Piccolo, I. Barozzi, S. Polletti, A. Termanini, S. Bonifacio, A. Curina, E. Prosperini, S. Ghisletti and G. Natoli (2013). "Latent enhancers activated by stimulation in differentiated cells." Cell **152**(1-2): 157-171.
- Oti, M., J. Falck, M. A. Huynen and H. Zhou (2016). "CTCF-mediated chromatin loops enclose inducible gene regulatory domains." BMC Genomics **17**: 252.

- Pallottini, V., P. Bulzomi, P. Galluzzo, C. Martini and M. Marino (2008). "Estrogen regulation of adipose tissue functions: involvement of estrogen receptor isoforms." Infect Disord Drug Targets **8**(1): 52-60.
- Palmlund, I. (1996). "Exposure to a xenoestrogen before birth: the diethylstilbestrol experience." J Psychosom Obstet Gynaecol **17**(2): 71-84.
- Park, Y., H. Li and B. Kemper (1996). "Phenobarbital induction mediated by a distal CYP2B2 sequence in rat liver transiently transfected in situ." J Biol Chem **271**(39): 23725-23728.
- Pelechano, V. and L. M. Steinmetz (2013). "Gene regulation by antisense transcription." Nat Rev Genet **14**(12): 880-893.
- Peretz, J. and J. A. Flaws (2013). "Bisphenol A down-regulates rate-limiting Cyp11a1 to acutely inhibit steroidogenesis in cultured mouse antral follicles." Toxicol Appl Pharmacol **271**(2): 249-256.
- Petrick, J. S. and C. D. Klaassen (2007). "Importance of hepatic induction of constitutive androstane receptor and other transcription factors that regulate xenobiotic metabolism and transport." Drug Metab Dispos **35**(10): 1806-1815.

- Poland, A., I. Mak and E. Glover (1981). "Species differences in responsiveness to 1,4-bis[2-(3,5-dichloropyridyloxy)]-benzene, a potent phenobarbital-like inducer of microsomal monooxygenase activity." Mol Pharmacol **20**(2): 442-450.
- Poland, A., I. Mak, E. Glover, R. J. Boatman, F. H. Ebetino and A. S. Kende (1980). "1,4-Bis[2-(3,5-dichloropyridyloxy)]benzene, a potent phenobarbital-like inducer of microsomal monooxygenase activity." Mol Pharmacol **18**(3): 571-580.
- Pradeepa, M. M., G. R. Grimes, Y. Kumar, G. Olley, G. C. Taylor, R. Schneider and W. A. Bickmore (2016). "Histone H3 globular domain acetylation identifies a new class of enhancers." Nat Genet **48**(6): 681-686.
- Quinlan, A. R. and I. M. Hall (2010). "BEDTools: a flexible suite of utilities for comparing genomic features." Bioinformatics **26**(6): 841-842.
- Rao, S. S., M. H. Huntley, N. C. Durand, E. K. Stamenova, I. D. Bochkov, J. T. Robinson, A. L. Sanborn, I. Machol, A. D. Omer, E. S. Lander and E. L. Aiden (2014). "A 3D map of the human genome at kilobase resolution reveals principles of chromatin looping." Cell **159**(7): 1665-1680.
- Remmer, H. (1959). "[The accelerated decomposition of drugs in the liver microsomes under the effect of luminal]." Naunyn Schmiedebergs Arch Exp Pathol Pharmacol **235**(4): 279-290.

- Repo, S., J. Jyrkkarinne, J. T. Pulkkinen, R. Laatikainen, P. Honkakoski and M. S. Johnson (2008). "Ligand specificity of constitutive androstane receptor as probed by induced-fit docking and mutagenesis." J Med Chem **51**(22): 7119-7131.
- Rinn, J. L., M. Kertesz, J. K. Wang, S. L. Squazzo, X. Xu, S. A. Brugmann, L. H. Goodnough, J. A. Helms, P. J. Farnham, E. Segal and H. Y. Chang (2007). "Functional demarcation of active and silent chromatin domains in human HOX loci by noncoding RNAs." Cell **129**(7): 1311-1323.
- Rolland, M., J. Le Moal, V. Wagner, D. Royere and J. De Mouzon (2013). "Decline in semen concentration and morphology in a sample of 26,609 men close to general population between 1989 and 2005 in France." Hum Reprod **28**(2): 462-470.
- Ross, P. K., C. G. Woods, B. U. Bradford, O. Kosyk, D. M. Gatti, M. L. Cunningham and I. Rusyn (2009). "Time-course comparison of xenobiotic activators of CAR and PPARalpha in mouse liver." Toxicol Appl Pharmacol **235**(2): 199-207.
- Rousseaux, S., C. Caron, J. Govin, C. Lestrat, A. K. Faure and S. Khochbin (2005). "Establishment of male-specific epigenetic information." Gene **345**(2): 139-153.
- Rubin, B. S. (2011). "Bisphenol A: An endocrine disruptor with widespread exposure and multiple effects." J Steroid Biochem Mol Biol.

- Rubin, B. S. (2011). "Bisphenol A: an endocrine disruptor with widespread exposure and multiple effects." J Steroid Biochem Mol Biol **127**(1-2): 27-34.
- Rubin, M. M. (2007). "Antenatal exposure to DES: lessons learned...future concerns." Obstet Gynecol Surv **62**(8): 548-555.
- Ryan, K. K., A. M. Haller, J. E. Sorrell, S. C. Woods, R. J. Jandacek and R. J. Seeley (2010). "Perinatal exposure to bisphenol-a and the development of metabolic syndrome in CD-1 mice." Endocrinology **151**(6): 2603-2612.
- Saito, K., R. Moore and M. Negishi (2013). "Nuclear receptor CAR specifically activates the two-pore K⁺ channel Kcnk1 gene in male mouse livers, which attenuates phenobarbital-induced hepatic hyperplasia." Toxicol Sci **132**(1): 151-161.
- Sakaue, M., S. Oshako, R. Ishimua, S. Kurosawa, M. MKurahmaru, Y. Hayashi, Y. Aoki, J. Yonemoto and C. Tohyama (2001). "Bisphenol A Affects Spermatogenesis in the Adult Rat Even at a Low Dose." Journal of Occupational Health **43**: 185-190.
- Salian, S., T. Doshi and G. Vanage (2009). "Neonatal exposure of male rats to Bisphenol A impairs fertility and expression of sertoli cell junctional proteins in the testis." Toxicology **265**(1-2): 56-67.
- Salian, S., T. Doshi and G. Vanage (2009). "Perinatal exposure of rats to Bisphenol A affects the fertility of male offspring." Life Sci **85**(21-22): 742-752.

- Salian, S., T. Doshi and G. Vanage (2011). "Perinatal exposure of rats to Bisphenol A affects fertility of male offspring--an overview." Reprod Toxicol **31**(3): 359-362.
- Sanderson, J. T. (2006). "The steroid hormone biosynthesis pathway as a target for endocrine-disrupting chemicals." Toxicol Sci **94**(1): 3-21.
- Sekido, R. and R. Lovell-Badge (2009). "Sex determination and SRY: down to a wink and a nudge?" Trends Genet **25**(1): 19-29.
- Selwyn, F. P., J. Y. Cui and C. D. Klaassen (2015). "RNA-Seq Quantification of Hepatic Drug Processing Genes in Germ-Free Mice." Drug Metab Dispos **43**(10): 1572-1580.
- Shen, L., N. Y. Shao, X. Liu, I. Maze, J. Feng and E. J. Nestler (2013). "diffReps: detecting differential chromatin modification sites from ChIP-seq data with biological replicates." PLoS One **8**(6): e65598.
- Shizu, R., S. Benoki, Y. Numakura, S. Kodama, M. Miyata, Y. Yamazoe and K. Yoshinari (2013). "Xenobiotic-induced hepatocyte proliferation associated with constitutive active/androstane receptor (CAR) or peroxisome proliferator-activated receptor alpha (PPARalpha) is enhanced by pregnane X receptor (PXR) activation in mice." PLoS One **8**(4): e61802.

- Shlyueva, D., G. Stampfel and A. Stark (2014). "Transcriptional enhancers: from properties to genome-wide predictions." Nat Rev Genet **15**(4): 272-286.
- Siersbaek, R., R. Nielsen, S. John, M. H. Sung, S. Baek, A. Loft, G. L. Hager and S. Mandrup (2011). "Extensive chromatin remodelling and establishment of transcription factor 'hotspots' during early adipogenesis." EMBO J **30**(8): 1459-1472.
- Song, L. and G. E. Crawford (2010). "DNase-seq: a high-resolution technique for mapping active gene regulatory elements across the genome from mammalian cells." Cold Spring Harb Protoc **2010**(2): pdb prot5384.
- Soto, A. M., C. Brisken, C. Schaeberle and C. Sonnenschein (2013). "Does cancer start in the womb? altered mammary gland development and predisposition to breast cancer due to in utero exposure to endocrine disruptors." J Mammary Gland Biol Neoplasia **18**(2): 199-208.
- Soufi, A., M. F. Garcia, A. Jaroszewicz, N. Osman, M. Pellegrini and K. S. Zaret (2015). "Pioneer transcription factors target partial DNA motifs on nucleosomes to initiate reprogramming." Cell **161**(3): 555-568.
- Stojic, L., M. Niemczyk, A. Orjalo, Y. Ito, A. E. Ruijter, S. Uribe-Lewis, N. Joseph, S. Weston, S. Menon, D. T. Odom, J. Rinn, F. Gergely and A. Murrell (2016).

"Transcriptional silencing of long noncoding RNA GNG12-AS1 uncouples its transcriptional and product-related functions." Nat Commun **7**: 10406.

Sueyoshi, T., T. Kawamoto, I. Zelko, P. Honkakoski and M. Negishi (1999). "The repressed nuclear receptor CAR responds to phenobarbital in activating the human CYP2B6 gene." J Biol Chem **274**(10): 6043-6046.

Sugatani, J., H. Kojima, A. Ueda, S. Kakizaki, K. Yoshinari, Q. H. Gong, I. S. Owens, M. Negishi and T. Sueyoshi (2001). "The phenobarbital response enhancer module in the human bilirubin UDP-glucuronosyltransferase UGT1A1 gene and regulation by the nuclear receptor CAR." Hepatology **33**(5): 1232-1238.

Sugathan, A. and D. J. Waxman (2013). "Genome-wide analysis of chromatin states reveals distinct mechanisms of sex-dependent gene regulation in male and female mouse liver." Mol Cell Biol **33**(18): 3594-3610.

Suino, K., L. Peng, R. Reynolds, Y. Li, J. Y. Cha, J. J. Repa, S. A. Kliewer and H. E. Xu (2004). "The nuclear xenobiotic receptor CAR: structural determinants of constitutive activation and heterodimerization." Mol Cell **16**(6): 893-905.

Sun, M. and W. L. Kraus (2015). "From discovery to function: the expanding roles of long noncoding RNAs in physiology and disease." Endocr Rev **36**(1): 25-64.

- Takahashi, K. and S. Yamanaka (2006). "Induction of pluripotent stem cells from mouse embryonic and adult fibroblast cultures by defined factors." Cell **126**(4): 663-676.
- Takahashi, O. and S. Oishi (2000). "Disposition of orally administered 2,2-Bis(4-hydroxyphenyl)propane (Bisphenol A) in pregnant rats and the placental transfer to fetuses." Environ Health Perspect **108**(10): 931-935.
- Takahashi, O. and S. Oishi (2003). "Testicular toxicity of dietarily or parenterally administered bisphenol A in rats and mice." Food Chem Toxicol **41**(7): 1035-1044.
- Takizawa, D., S. Kakizaki, N. Horiguchi, Y. Yamazaki, H. Tojima and M. Mori (2011). "Constitutive active/androstane receptor promotes hepatocarcinogenesis in a mouse model of non-alcoholic steatohepatitis." Carcinogenesis **32**(4): 576-583.
- Tang, L., E. Nogales and C. Ciferri (2010). "Structure and function of SWI/SNF chromatin remodeling complexes and mechanistic implications for transcription." Prog Biophys Mol Biol **102**(2-3): 122-128.
- Thankamony, A., V. Pasterski, K. K. Ong, C. L. Acerini and I. A. Hughes (2016). "Anogenital distance as a marker of androgen exposure in humans." Andrology **4**(4): 616-625.

- Thurman, R. E., E. Rynes, R. Humbert, J. Vierstra, M. T. Maurano, E. Haugen, N. C. Sheffield, A. B. Stergachis, H. Wang, B. Vernot, K. Garg, S. John, R. Sandstrom, D. Bates, L. Boatman, T. K. Canfield, M. Diegel, D. Dunn, A. K. Ebersol, T. Frum, E. Giste, A. K. Johnson, E. M. Johnson, T. Kutuyavin, B. Lajoie, B. K. Lee, K. Lee, D. London, D. Lotakis, S. Neph, F. Neri, E. D. Nguyen, H. Qu, A. P. Reynolds, V. Roach, A. Safi, M. E. Sanchez, A. Sanyal, A. Shafer, J. M. Simon, L. Song, S. Vong, M. Weaver, Y. Yan, Z. Zhang, Z. Zhang, B. Lenhard, M. Tewari, M. O. Dorschner, R. S. Hansen, P. A. Navas, G. Stamatoyannopoulos, V. R. Iyer, J. D. Lieb, S. R. Sunyaev, J. M. Akey, P. J. Sabo, R. Kaul, T. S. Furey, J. Dekker, G. E. Crawford and J. A. Stamatoyannopoulos (2012). "The accessible chromatin landscape of the human genome." Nature **489**(7414): 75-82.
- Tian, J., H. Huang, B. Hoffman, D. A. Liebermann, G. M. Ledda-Columbano, A. Columbano and J. Locker (2011). "Gadd45beta is an inducible coactivator of transcription that facilitates rapid liver growth in mice." J Clin Invest **121**(11): 4491-4502.
- Timsit, Y. E. and M. Negishi (2007). "CAR and PXR: the xenobiotic-sensing receptors." Steroids **72**(3): 231-246.
- Timsit, Y. E. and M. Negishi (2014). "Coordinated regulation of nuclear receptor CAR by CCRP/DNAJC7, HSP70 and the ubiquitin-proteasome system." PLoS One **9**(5): e96092.

- Tojima, H., S. Kakizaki, Y. Yamazaki, D. Takizawa, N. Horiguchi, K. Sato and M. Mori (2012). "Ligand dependent hepatic gene expression profiles of nuclear receptors CAR and PXR." Toxicol Lett **212**(3): 288-297.
- Toyama, Y. and S. Yuasa (2004). "Effects of neonatal administration of 17beta-estradiol, beta-estradiol 3-benzoate, or bisphenol A on mouse and rat spermatogenesis." Reprod Toxicol **19**(2): 181-188.
- Tyl, R. W. (2009). "The presence (or not) of effects from low oral doses of BPA." J Toxicol Sci **34**(5): 587-588.
- Tyl, R. W., C. B. Myers, M. C. Marr, C. S. Sloan, N. P. Castillo, M. M. Veselica, J. C. Seely, S. S. Dimond, J. P. Van Miller, R. N. Shiotsuka, D. Beyer, S. G. Hentges and J. M. Waechter, Jr. (2008). "Two-generation reproductive toxicity study of dietary bisphenol A in CD-1 (Swiss) mice." Toxicol Sci **104**(2): 362-384.
- Tyl, R. W., C. B. Myers, M. C. Marr, B. F. Thomas, A. R. Keimowitz, D. R. Brine, M. M. Veselica, P. A. Fail, T. Y. Chang, J. C. Seely, R. L. Joiner, J. H. Butala, S. S. Dimond, S. Z. Cagen, R. N. Shiotsuka, G. D. Stropp and J. M. Waechter (2002). "Three-generation reproductive toxicity study of dietary bisphenol A in CD Sprague-Dawley rats." Toxicol Sci **68**(1): 121-146.

- Tzameli, I., P. Pissios, E. G. Schuetz and D. D. Moore (2000). "The xenobiotic compound 1,4-bis[2-(3,5-dichloropyridyloxy)]benzene is an agonist ligand for the nuclear receptor CAR." Mol Cell Biol **20**(9): 2951-2958.
- Ueda, A., H. K. Hamadeh, H. K. Webb, Y. Yamamoto, T. Sueyoshi, C. A. Afshari, J. M. Lehmann and M. Negishi (2002). "Diverse roles of the nuclear orphan receptor CAR in regulating hepatic genes in response to phenobarbital." Mol Pharmacol **61**(1): 1-6.
- Umweltbundesamt (2010). "Bisphenol A: An industrial chemical with adverse effects."
- Van Ess, P. J., M. P. Mattson and R. A. Blouin (2002). "Enhanced induction of cytochrome P450 enzymes and CAR binding in TNF (p55(-/-)/p75(-/-)) double receptor knockout mice following phenobarbital treatment." J Pharmacol Exp Ther **300**(3): 824-830.
- Vandenberg, L. N., M. V. Maffini, C. Sonnenschein, B. S. Rubin and A. M. Soto (2009). "Bisphenol-A and the great divide: a review of controversies in the field of endocrine disruption." Endocr Rev **30**(1): 75-95.
- Varney, D. R., L. A. Varney, R. W. Hemken, P. M. Zavos and M. R. Siegel (1991). "Onset of puberty in CD-1 mouse pups exposed prenatally through weaning to endophyte-infected tall fescue seed." Theriogenology **35**(5): 883-892.

- Vietri Rudan, M., C. Barrington, S. Henderson, C. Ernst, D. T. Odom, A. Tanay and S. Hadjur (2015). "Comparative Hi-C reveals that CTCF underlies evolution of chromosomal domain architecture." Cell Rep **10**(8): 1297-1309.
- Vitku, J., J. Heracek, L. Sosvorova, R. Hampl, T. Chlupacova, M. Hill, V. Sobotka, M. Bicikova and L. Starka (2016). "Associations of bisphenol A and polychlorinated biphenyls with spermatogenesis and steroidogenesis in two biological fluids from men attending an infertility clinic." Environ Int **89-90**: 166-173.
- Vogel, S. A. (2009). "The politics of plastics: the making and unmaking of bisphenol a "safety"." Am J Public Health **99 Suppl 3**: S559-566.
- vom Saal, F. S., B. T. Akingbemi, S. M. Belcher, D. A. Crain, D. Crews, L. C. Guidice, P. A. Hunt, C. LERANTH, J. P. Myers, A. Nadal, N. Olea, V. Padmanabhan, C. S. Rosenfeld, A. Schneyer, G. Schoenfelder, C. Sonnenschein, A. M. Soto, R. W. Stahlhut, S. H. Swan, L. N. Vandenberg, H. S. Wang, C. S. Watson, W. V. Welshons and R. T. Zoeller (2010). "Flawed experimental design reveals the need for guidelines requiring appropriate positive controls in endocrine disruption research." Toxicol Sci **115**(2): 612-613; author reply 614-620.
- vom Saal, F. S., P. S. Cooke, D. L. Buchanan, P. Palanza, K. A. Thayer, S. C. Nagel, S. Parmigiani and W. V. Welshons (1998). "A physiologically based approach to the study of bisphenol A and other estrogenic chemicals on the size of reproductive

organs, daily sperm production, and behavior." Toxicol Ind Health **14**(1-2): 239-260.

vom Saal, F. S. and C. Hughes (2005). "An extensive new literature concerning low-dose effects of bisphenol A shows the need for a new risk assessment." Environ Health Perspect **113**(8): 926-933.

vom Saal, F. S. and W. V. Welshons (2006). "Large effects from small exposures. II. The importance of positive controls in low-dose research on bisphenol A." Environ Res **100**(1): 50-76.

Voss, T. C., R. L. Schiltz, M. H. Sung, P. M. Yen, J. A. Stamatoyannopoulos, S. C. Biddie, T. A. Johnson, T. B. Miranda, S. John and G. L. Hager (2011). "Dynamic exchange at regulatory elements during chromatin remodeling underlies assisted loading mechanism." Cell **146**(4): 544-554.

Vrooman, L. A., J. M. Oatley, J. E. Griswold, T. J. Hassold and P. A. Hunt (2015). "Estrogenic exposure alters the spermatogonial stem cells in the developing testis, permanently reducing crossover levels in the adult." PLoS Genet **11**(1): e1004949.

Wada, T., J. Gao and W. Xie (2009). "PXR and CAR in energy metabolism." Trends Endocrinol Metab **20**(6): 273-279.

- Wadia, P. R., L. N. Vandenberg, C. M. Schaeberle, B. S. Rubin, C. Sonnenschein and A. M. Soto (2007). "Perinatal bisphenol A exposure increases estrogen sensitivity of the mammary gland in diverse mouse strains." Environ Health Perspect **115**(4): 592-598.
- Wauthier, V. and D. J. Waxman (2008). "Sex-specific early growth hormone response genes in rat liver." Mol Endocrinol **22**(8): 1962-1974.
- Waxman, D. J. (1999). "P450 gene induction by structurally diverse xenochemicals: central role of nuclear receptors CAR, PXR, and PPAR." Arch Biochem Biophys **369**(1): 11-23.
- Waxman, D. J. and L. Azaroff (1992). "Phenobarbital induction of cytochrome P-450 gene expression." Biochem J **281 (Pt 3)**: 577-592.
- Waxman, D. J. and M. G. Holloway (2009). "Sex differences in the expression of hepatic drug metabolizing enzymes." Mol Pharmacol **76**(2): 215-228.
- Waxman, D. J., N. A. Pampori, P. A. Ram, A. K. Agrawal and B. H. Shapiro (1991). "Interpulse interval in circulating growth hormone patterns regulates sexually dimorphic expression of hepatic cytochrome P450." Proc Natl Acad Sci U S A **88**(15): 6868-6872.

- Welsh, M., D. J. MacLeod, M. Walker, L. B. Smith and R. M. Sharpe (2010). "Critical androgen-sensitive periods of rat penis and clitoris development." Int J Androl **33**(1): e144-152.
- Werner, M. S. and A. J. Ruthenburg (2015). "Nuclear Fractionation Reveals Thousands of Chromatin-Tethered Noncoding RNAs Adjacent to Active Genes." Cell Rep **12**(7): 1089-1098.
- Wilhelm, D., S. Palmer and P. Koopman (2007). "Sex determination and gonadal development in mammals." Physiol Rev **87**(1): 1-28.
- Wisniewski, P., R. M. Romano, M. M. Kizys, K. C. Oliveira, T. Kasamatsu, G. Giannocco, M. I. Chiamolera, M. R. Dias-da-Silva and M. A. Romano (2015). "Adult exposure to bisphenol A (BPA) in Wistar rats reduces sperm quality with disruption of the hypothalamic-pituitary-testicular axis." Toxicology **329**: 1-9.
- Xi, W., C. K. Lee, W. S. Yeung, J. P. Giesy, M. H. Wong, X. Zhang, M. Hecker and C. K. Wong (2011). "Effect of perinatal and postnatal bisphenol A exposure to the regulatory circuits at the hypothalamus-pituitary-gonadal axis of CD-1 mice." Reprod Toxicol **31**(4): 409-417.
- Xie, M., P. Bu, F. Li, S. Lan, H. Wu, L. Yuan and Y. Wang (2016). "Neonatal bisphenol A exposure induces meiotic arrest and apoptosis of spermatogenic cells." Oncotarget **7**(9): 10606-10615.

Xiong, Y., G. J. Hannon, H. Zhang, D. Casso, R. Kobayashi and D. Beach (1993). "p21 is a universal inhibitor of cyclin kinases." Nature **366**(6456): 701-704.

Xu, R. X., M. H. Lambert, B. B. Wisely, E. N. Warren, E. E. Weinert, G. M. Waitt, J. D. Williams, J. L. Collins, L. B. Moore, T. M. Willson and J. T. Moore (2004). "A structural basis for constitutive activity in the human CAR/RXRalpha heterodimer." Mol Cell **16**(6): 919-928.

Yamamoto, Y., R. Moore, T. L. Goldsworthy, M. Negishi and R. R. Maronpot (2004). "The orphan nuclear receptor constitutive active/androstane receptor is essential for liver tumor promotion by phenobarbital in mice." Cancer Res **64**(20): 7197-7200.

Yamamoto, Y., R. Moore, T. L. Goldsworthy, M. Negishi and R. R. Maronpot (2004). "The orphan nuclear receptor constitutive active/androstane receptor is essential for liver tumor promotion by phenobarbital in mice." Cancer research **64**(20): 7197-7200.

Yamazaki, Y., R. Moore and M. Negishi (2011). "Nuclear receptor CAR (NR1I3) is essential for DDC-induced liver injury and oval cell proliferation in mouse liver." Lab Invest **91**(11): 1624-1633.

Yan, J., B. Chen, J. Lu and W. Xie (2015). "Deciphering the roles of the constitutive androstane receptor in energy metabolism." Acta Pharmacol Sin **36**(1): 62-70.

- Yan, L., Y. Wang, J. Liu, Y. Nie, X. Zhong, Q. Kan and L. Zhang (2017). "Alterations of Histone Modifications Contribute to Pregnane X Receptor-mediated Induction of CYP3A4 by Rifampicin." Mol Pharmacol.
- Yang, H. and H. Wang (2014). "Signaling control of the constitutive androstane receptor (CAR)." Protein Cell **5**(2): 113-123.
- Ye, L., B. Zhao, G. Hu, Y. Chu and R. S. Ge (2011). "Inhibition of human and rat testicular steroidogenic enzyme activities by bisphenol A." Toxicol Lett **207**(2): 137-142.
- Yiu, K. W., C. K. Lee, K. C. Kwok and N. H. Cheung (2014). "Measuring the kinetics of the binding of xenoestrogens and estrogen receptor alpha by fluorescence polarization." Environ Sci Technol **48**(19): 11591-11599.
- Yue, F., Y. Cheng, A. Breschi, J. Vierstra, W. Wu, T. Ryba, R. Sandstrom, Z. Ma, C. Davis, B. D. Pope, Y. Shen, D. D. Pervouchine, S. Djebali, R. E. Thurman, R. Kaul, E. Rynes, A. Kirilusha, G. K. Marinov, B. A. Williams, D. Trout, H. Amrhein, K. Fisher-Aylor, I. Antoshechkin, G. DeSalvo, L. H. See, M. Fastuca, J. Drenkow, C. Zaleski, A. Dobin, P. Prieto, J. Lagarde, G. Bussotti, A. Tanzer, O. Denas, K. Li, M. A. Bender, M. Zhang, R. Byron, M. T. Groudine, D. McCleary, L. Pham, Z. Ye, S. Kuan, L. Edsall, Y. C. Wu, M. D. Rasmussen, M. S. Bansal, M. Kellis, C. A. Keller, C. S. Morrissey, T. Mishra, D. Jain, N. Dogan, R. S.

Harris, P. Cayting, T. Kawli, A. P. Boyle, G. Euskirchen, A. Kundaje, S. Lin, Y. Lin, C. Jansen, V. S. Malladi, M. S. Cline, D. T. Erickson, V. M. Kirkup, K. Learned, C. A. Sloan, K. R. Rosenbloom, B. Lacerda de Sousa, K. Beal, M. Pignatelli, P. Flicek, J. Lian, T. Kahveci, D. Lee, W. J. Kent, M. Ramalho Santos, J. Herrero, C. Notredame, A. Johnson, S. Vong, K. Lee, D. Bates, F. Neri, M. Diegel, T. Canfield, P. J. Sabo, M. S. Wilken, T. A. Reh, E. Giste, A. Shafer, T. Kutuyavin, E. Haugen, D. Dunn, A. P. Reynolds, S. Neph, R. Humbert, R. S. Hansen, M. De Bruijn, L. Selleri, A. Rudensky, S. Josefowicz, R. Samstein, E. E. Eichler, S. H. Orkin, D. Levasseur, T. Papayannopoulou, K. H. Chang, A. Skoultschi, S. Gosh, C. Disteché, P. Treuting, Y. Wang, M. J. Weiss, G. A. Blobel, X. Cao, S. Zhong, T. Wang, P. J. Good, R. F. Lowdon, L. B. Adams, X. Q. Zhou, M. J. Pazin, E. A. Feingold, B. Wold, J. Taylor, A. Mortazavi, S. M. Weissman, J. A. Stamatoyannopoulos, M. P. Snyder, R. Guigo, T. R. Gingeras, D. M. Gilbert, R. C. Hardison, M. A. Beer, B. Ren and E. C. Mouse (2014). "A comparative encyclopedia of DNA elements in the mouse genome." *Nature* **515**(7527): 355-364.

Zaret, K. S. and J. S. Carroll (2011). "Pioneer transcription factors: establishing competence for gene expression." *Genes Dev* **25**(21): 2227-2241.

Zhang, M. F., Z. Y. Zhang, J. Fu, Y. F. Yang and J. P. Yun (2009). "Correlation between expression of p53, p21/WAF1, and MDM2 proteins and their prognostic significance in primary hepatocellular carcinoma." J Transl Med 7: 110.

Zhang, Y., T. Liu, C. A. Meyer, J. Eeckhoute, D. S. Johnson, B. E. Bernstein, C. Nusbaum, R. M. Myers, M. Brown, W. Li and X. S. Liu (2008). "Model-based analysis of ChIP-Seq (MACS)." Genome Biol 9(9): R137.

Zhou, M., J. Luo, M. Chen, H. Yang, R. M. Learned, A. M. DePaoli, H. Tian and L. Ling (2017). "Mouse species-specific control of hepatocarcinogenesis and metabolism by FGF19/FGF15." J Hepatol.

CURRICULUM VITAE

